UNIVERSITEIT GENT

FACULTY OF SCIENCES
DEPARTMENT GEOLOGY AND SOIL SCIENCE

HYDRO-METEOROLOGICAL INFLUENCES ON THE BEHAVIOUR AND NATURE OF SEDIMENT SUSPENSIONS IN THE BELGIAN-DUTCH COASTAL ZONE

MATTHIAS BAEYE

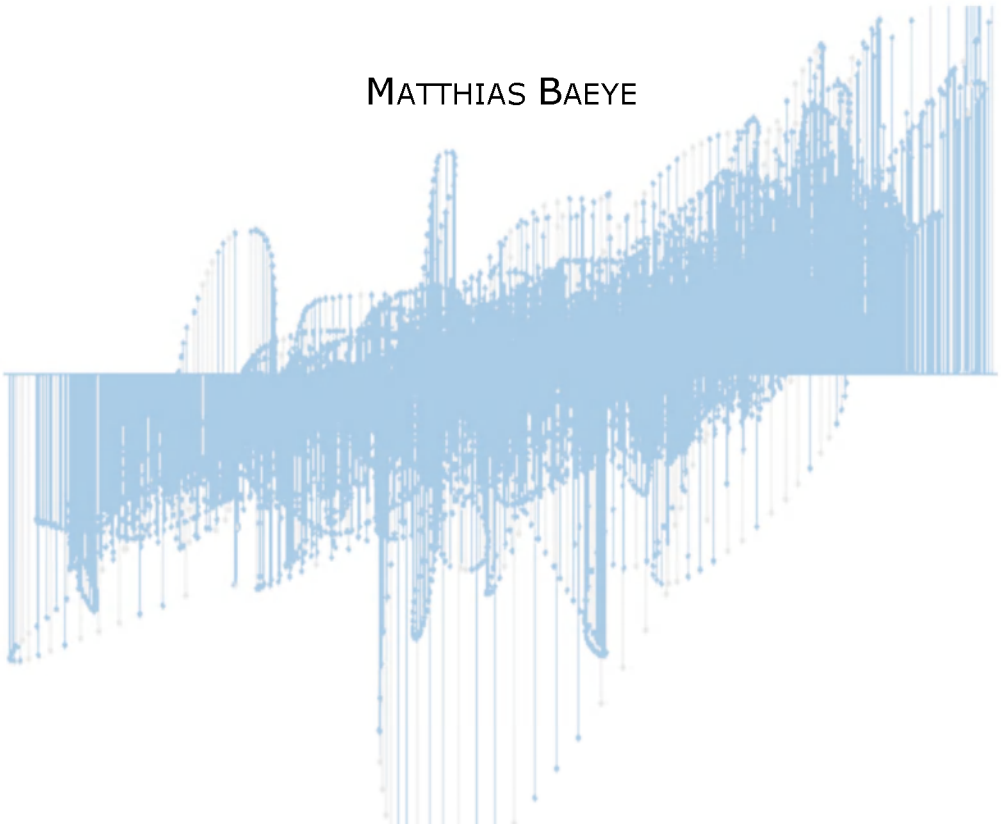

Thesis submitted in partial fulfilment of the requirements for the degree of Doctor in Sciences, Geology

Academic Year 2011-2012

RCMG

UNIVERSITEIT GENT

FACULTY OF SCIENCES
DEPARTMENT GEOLOGY AND SOIL SCIENCE

HYDRO-METEOROLOGICAL INFLUENCES ON THE BEHAVIOUR AND NATURE OF SEDIMENT SUSPENSIONS IN THE BELGIAN-DUTCH COASTAL ZONE

HYDRO-METEOROLOGISCHE EFFECTEN OP HET GEDRAG EN SAMENSTELLING VAN SEDIMENTSUSPENSIES IN DE BELGISCH-NEDERLANDSE KUSTZONE

MATTHIAS BAEYE

Promoter: Prof. Dr. Marc De Batist

Co-promoter: Prof. Dr. Vera Van Lancker, Dr. Michael Fettweis

Faculty of Sciences

Department of Geology and Soil Science

Research Unit Renard Centre of Marine Geology

RCMG

To refer to this thesis:

Baeye M. 2012. Hydro-meteorological influences on the behaviour and nature of sediment suspensions in the Belgian-Dutch coastal zone, Ph.D. thesis, Ghent University, Ghent, Belgium.

Reading Committee

Prof. Dr. Vera Van Lancker (Ghent University/
Management Unit of the North Sea Mathematical Models, Belgium): co-promoter

Dr. Michael Fettweis (Management Unit of the North Sea
Mathematical Models, Belgium): co-promoter

Prof. Dr. Robert Lafite (University of Rouen, France)

Prof. Dr. Ir. Jaak Monbaliu (KU Leuven, Belgium)

Examination Committee

Prof. Dr. Jacques Verniers
(Ghent University, Belgium): chairman

Prof. Dr. Marc De Batist
(Ghent University, Belgium): promoter, secretary

Prof. Dr. Vera Van Lancker (Ghent University/
Management Unit North Sea Mathematical Models, Belgium): co-promoter

Dr. Michael Fettweis (Management Unit North Sea
Mathematical Models, Belgium): co-promoter

Prof. Dr. Robert Lafite (University of Rouen, France)

Prof. Dr. Ir. Jaak Monbaliu (KU Leuven, Belgium)

Prof. Dr. Frank Mostaert (Ghent University, Belgium)

Prof. Dr. Ir. Renaat Desutter (Ghent University, Belgium)

Table of contents

Melissa

Prof. Dr. Marc De Batist, Vera Van Lancker, Michael Fettweis, George Pichot

My parents Luc and Jenny, family and friends

Marc, Sonia, Maarten, Mario, Koen, David, Lies, Andres, Prof. Em. Dr. Jean-Pierre Henriet, Tine, Thomas, Prof. Dr. David Van Rooij, Sébastien, Willem, Philipp (Ugent-RCMG)

Prof. Dr. George Voulgaris, Mary, Gwen, Nirnimesh, Tim (CPSD lab, University of South Carolina)

André, Lieven, Joan, Jean-Pierre, Kevin, Bieke, Brigitte, Dries, Fritz, Sébastien, Griet, Katrijn, Jean-Sebastien, Ruth, Bouchra, Karien, Yolande, Quinten (MUMM)

Hans, Dré, Wim, Michiel, Roeland (VLIZ)

Yves Dupont (CPF IMM PDOST)

Thomas, Ralf (BWB – FWG)

Jeroen, Isabelle, Peter, Katrien, Rindert, Stijn, Dries, Jasper, Kristien, Maarten, Ann

ABS: Acoustic Backscatter Strength
ADCP: Acoustic Doppler Current Profiler (RDInstruments®)
ADP: Acoustic Doppler Profiler
ADV: Acoustic Doppler Velocimeter

BM-ADCP: Bottom Mounted Acoustic Doppler Current Profiler
BRM: Burial Registration Mines

CT: Conductivity, Temperature
CTD: Conductivity, Temperature and Depth
CTM: Coastal Turbidity Maximum
CV: Coefficient of Variance

D50: Median Grainsize
doy: day of year

ETM: Estuarine Turbidity Maximum

HCMS: High-Concentrated Mud Suspension
H_s: Significant Waveheight
HW: High Water

LED: Light Emitting Diodes
LISST: Laser In-situ Scattering and Transmissometer
LW: Low Water

mab: meter above bed
MLLWS: Mean Lowest Low Water at Spring tide
MODIS: Moderate Resolution Imaging Spectroradiometer
MOW: Ministerie van Openbare Werken

NAO: North Atlantic Oscillation
NAOwi: North Atlantic Oscillation Winter Index
NTU: Nephelometric Turbidity Units

OBS: Optical Backscatter Sensor
OM: Organic Matter

PP: Primary Particles
PSD: Particle Size Distribution

sonar: sound navigation and ranging
SPM: Suspended Particulate Matter

tdm: ton dry matter
TKE: Turbulent Kinetic Energy
TMZ: Turbidity Maximum Zone
T_{XXX}: True North

Context

In the southern Bight of the North Sea, the Belgian coastal zone corresponds largely to a coastal turbidity maximum (CTM) zone, extending between Ostend and the Westerscheldt estuary. Suspended particulate matter (SPM), mainly originating from input through the Strait of Dover, settles off the Belgian coast before leaving Belgian waters towards the northeast. Some of the fine material is buffered into the Westerschelde. The so-called coastal turbidity maximum is present permanently, and is due to congestion in the residual transport along the Belgian coast. SPM from local erosion of the seabed contributes further to the increased turbidity levels in the CTM zone. SPM is continuously deposited and re-suspended; though significant variations occur during tidal (semi-diurnal) cycles and during neap-spring cycles (lunar). Also, seasons and meteorological conditions have an influence on SPM behaviour.
The seabed in the CTM zone consists mainly of sand- and clay-dominated cohesive sediments. The large reservoir of soft- to medium-consolidated Holocene mud is partly covered with sands and freshly deposited mud and/or high-concentrated mud suspensions (HCMS). Significant amounts of fluid mud and HCMS are also found in the navigational channels; as such significant siltation is expected. Navigation accessibility is ensured through intensive dredging of fine material in these areas.
Besides the economical aspect, water turbidity and HCMS and/or fluid mud occurrences will also affect the ecological system: SPM controls the underwater light field, hence, the primary production and development of phytoplankton; SPM and HCMS can smother benthic organisms and habitats, resulting in a reduction in the production and diversity of species.

Objectives

Main objectives were: (1) increase in knowledge on temporal variability of SPM within the CTM zone; (2) increased understanding in the spatial variability of the extent of the CTM zone; (3) gaining new insights in the dynamic behaviour of HCMS, and its influence on near-bed processes; (4) evaluating the use of optical and acoustic sensor measurements in revealing the varying SPM nature within the CTM zone; and (5) distinguishing anthropogenic contributions to SPM concentration from the natural SPM variability through time.

Conclusions

see 9.1

Keywords: Suspended particulate matter; coastal turbidity maximum; natural variability; advection; wind climate; storminess; NAO; particle size distribution; high-concentrated mud suspensions; mud disposal; mine burial

Context

De Belgische kustzone bevindt zich in de zuidelijke bocht van de Noordzee, en is gekenmerkt door de aanwezigheid van een turbiditeitsmaximum gelegen tussen Oostende en het mondingsgebied van de Westerschelde. De deeltjes in suspensie zijn hoofdzakelijk afkomstig van aanvoer door de Straat van Dover, en vooraleer ze verder noordelijk getransporteerd worden, blijven ze een tijd voor de kust aanwezig. Een fractie van deze fijne sedimenten zijn ook aanwezig in de Westerschelde. Het zogenoemde turbiditeitsmaximum aan de kust is permanent aanwezig, en is gerelateerd aan een opstoppingseffect in het residueel transport langsheen de Belgische kust. De deeltjes in suspensie vinden hun oorsprong ook terug in lokale erosie van de zeebodem, want ze zijn continu onderhevig aan bezinking en re-suspensie; echter, significante variaties in hun concentraties komen voor tijdens eb-vloed cycli, alsook tijdens dood-springtij cycli. Het gedrag van suspensiemateriaal wordt ook nog beinvloed door seizoenen en meteorologische omstandigheden.
In de turbiditeitsmaximumzone bestaat de zeebodem hoofdzakelijk uit cohesieve sedimenten met een bepaald gehalte aan zand en/of klei. Het grote reservoir aan zacht tot medium geconsolideerde klei, van Holocene ouderdom, is grotendeels bedekt met zand en recent slib en/of hooggeconcentreerde slibsuspensies. Significante hoeveelheden aan vloeibaar slib en hooggeconcentreerde slibsuspensies worden ook teruggevonden in de navigatiekanalen, met een belangrijke verslibbing als gevolg. De toegang tot de havens wordt verzekerd door het intensief baggeren van slib.
Afgezien van het economisch belang, is er ook een ecologisch aspect, namelijk: troebelheid van water en het voorkomen van hooggeconcentreerde slibsuspensies en/of vloeibaar slib beïnvloeden het onderwaterlichtregime en bijgevolg ook de primaire groei en de ontwikkeling van fytoplankton. Verder zullen bodemorganismen en habitats verstoord worden, met een reductie in de groei en diversiteit van specifieke species als resultaat.

Objectieven

Hoofdobjectieven van het onderzoek omvatten: (1) een belangrijke toename in de kennis omtrent de variabiliteit van het suspensiemateriaal gerelateerd aan het turbiditeitsmaximum doorheen de tijd; (2) onderzoek naar de ruimtelijke variabiliteit van het turbiditeitsmaximum langsheen de Belgische kust; (3) verwerven van nieuwe inzichten omtrent het dynamische karakter van hooggeconcentreerde slibsuspensies en de invloed op bodemprocessen; (4) evalueren van het gebruik van optische en akoestische sensormetingen naar aanleiding van variaties in de samenstelling van het suspensiemateriaal gerelateerd aan het turbiditeitsmaximum; en (5) onderscheiden van menselijke invloeden op de concentraties aan suspensiemateriaal van de natuurlijke variaties, doorheen de tijd.

Conclusies

Data verkregen door bijna-continue multi-sensor bodemmetingen op drie locaties aan de Belgische kust hebben bijgedragen tot een betere kennis omtrent de natuurlijke variaties en processen van suspensiemateriaal. Ruimtelijke distributiepatronen van concentraties aan suspensiemateriaal, nabij het wateroppervlakte, werden verkregen via een satelliet-sensor (MODIS-Aqua). Analyse van deze kaarten leidde tot betere inzichten in de ruimtelijke variatie in grootte en positie van het turbiditeitsmaximum. Deze informatie werd dan vervolgens geanalyseerd, in combinatie met hydro-meteorologische data. De volgende conclusies werden verkregen:

De residuele stromingen, evenwijdig aan de kustlijn, werden in beschouwing genomen om twee stromingsregimes te definieren. Een heersende wind met noordelijke component induceert een stroming langsheen de kust richting het SW (Frankrijk). Deze windsector komt 15% van de tijd voor, en bedraagt gemiddeld 7.1 m s^{-1} (± 3.3 m s^{-1}). Het tegengestelde residuele stromingsveld (richting Nederland) wordt gestuurd door krachtigere winden vanuit het W-SW (23% van de tijd), namelijk 9.5 m s^{-1} ± 4.3 m s^{-1}.

Tijdens het noordoostwaartse stromingsregime wordt er in het studiegebied een toename in saliniteit en een afname in de concentratie aan suspensiemateriaal geobserveerd. Dit wordt verklaard door advectie van helder, maar zoutig, Atlantisch water doorheen het Engelse Kanaal en de Straat van Dover dat zich mengt met de kustwateren. Als deze windcondities krachtig zijn, dan gaan deze ook gepaard met golfwerking (gemiddelde golfhoogte van 0.85 m). Dat draagt op zijn beurt bij aan een sterkere bodemwrijvingsspanning die de zachte slibafzettingen zullen eroderen. Bovendien, werd er besloten dat onder deze omstandigheden het turbiditeitsmaximum zich uitstrekt tot in de Nederlandse wateren (Walcheren) zoals afgeleid uit de kaarten van concentratie aan suspensiemateriaal nabij het wateroppervlakte. Hierbij wordt de zoetwaterrivierpluim (Westerschelde) ook beïnvloed door deze windcondities met als resultaat dat de uitbreiding van de pluim zeer beperkt wordt. Dit verklaart waarom er geen relatie kon worden afgeleid tussen het turbiditeitsmaximum en de zoetwaterpluim. De Westerschelde vertoont bijgevolg geen typische turbiditeitspluim, zoals deze voorkomt in vele mondingsgebieden (Humber, Thames, Elbe etc.) in de zuidelijke Noordzee. Stroomopwaarts transport van marien suspensiemateriaal in de Westerschelde wordt gesuggereerd.
Er werd verder geobserveerd en geconcludeerd dat tijdens zeer krachtige west-zuidwest wind- en stormcondities de samenstelling van het suspensiemateriaal verandert. Namelijk, de kleine primaire deeltjes, en flocculi (grotere vlokken zijn opgebroken), m.a.w. cohesieve sedimenten, worden weggetransporteerd naar het NE en worden vervangen door een partikelverdeling dat werd gedomineerd door fijn zand. Dit resulteerde ongetwijfeld in implicaties van de gebruikte sensoren: de OBS (optical backscatter sensor) vertoonde systematisch sterk gereduceeerde concentraties aan suspensiemateriaal tijdens deze omstandigheden; terwijl de akoestische sensoren (acoustic Doppler profiler/velocimeter) verhoogde concentraties registreerden. Het laatste type sensoren vertoont een betere performantie wanneer de verdeling van suspensiedeeltjes (eerder partikelkorrels dan vlokken) unimodaal is, en zich in de grof silt – fijn zandfractie bevindt.

De kustwateren zijn minder geaffecteerd door de Atlantische wateren tijdens het regime van residuele stroming naar het zuidwesten, en zijn dan bijgevolg minder salien. De zoetwaterpluim van de Westerschelde (+ Rijn-Maas systeem) breidt zich zeewaarts uit, alsook naar het zuidwesten. Het turbiditeitsmaximum komt opnieuw niet overeen met de zoetwaterpluim, aangezien de kern van troebelheid zich geisoleerd bevindt tussen Oostende en Zeebrugge, dus zonder duidelijke verbinding met de Westerschelderivier. In vergelijking met het vorige stromingsregime zijn de concentraties aan suspensiemateriaal hoger. Ook werden multi-modale partikelverdelingen (primaire deeltjes, flocculi, microflocs, macroflocs) waargenomen die de dynamica van cohesieve sedimenten, namelijk vlokkenvorming en ontbinding, verklaren. Omwille van de voorkomens van deze fijne suspensiematerialen, en van de afwezigheid van zandig materiaal zullen de optische sensoren algemeen een goede benadering van de concentratie geven. Wanneer echter de fractie aan macrovlokken toeneemt, dan zal de optische sensor de concentratie aan suspensiemateriaal minder nauwkeurig meten.
Er werd dus besloten dat elk stromingsregime, tengevolge van de verschillende hydro-meteorologische factoren, overeenkomt met een typische aard van suspensiemateriaal. De concentratie aan suspensiemateriaal is hoofdzakelijk in verband te brengen met de advectie en dus de verdeling van watermassa's. De saliniteit, geassocieerd met de watermassa's, zal daarom goed correleren met de concentratie aan suspensiemateriaal.

Stormen komen het meeste voor in het seizoen met sterke hydrodynamische condities (winters), en de daarmee gepaardgaande windgolven zullen de bodem in het relatief ondiepe studiegebied affecteren. De grootste golven zijn typisch gerelateerd aan winden uit het noorden, dat door een relatief grote *fetch* een langere golfperiode vertonen. Zoals eerder vermeld, genereren de krachtige winden uit het SW ook golven met een periode rond de 4 s. De langere periodegolven uit het noorden vertonen vanzelfsprekend grotere golf-orbitale snelheden die een verhoogde re-suspensie van bodemmaterial zal teweegbrengen. Dit heeft als gevolg dat het turbiditeitsmaximum zeer omvangrijk wordt, en bovendien de hoogste concentraties aan suspensiemateriaal

wordt vertoond. Er werd gesuggegereerd dat de grote slibplaat in de kustzone, en de zachte slibafzettingen in de navigatiekanalen geërodeerd worden tijdens deze meteorologische condities.

Een zeer significante uitbreiding van het turbiditeitsmaximum langsheen de kust en in de richting van de Nederlandse wateren werd geobserveerd in de wintermaanden die overeenkomen met talrijke en krachtige winden uit het SW. Winterperiodes met aanzienlijk minder SW winden resulteren bijgevolg in een duidelijk verschillende spreiding van het turbiditeitsmaximum. Deze analyse werd gerealiseerd door een classificatie van kaarten van concentraties aan oppervlaktesuspensiemateriaal, op basis van de klimatologische index – Noord-Atlantische oscillatie, met dus een belangrijke invloed op de spreiding van het turbiditeitsmaximum voor een periode van 4 maanden.
Met betrekking tot bodemprocessen heeft deze studie bijgedragen tot de voorkomens en het belang van hooggeconcentreerde slibsuspensies aan de bodem. Deze laatste vertonen concentraties aan suspensiemateriaal tot een paar g l^{-1}, en vertonen verschillende condities en tijdsperiodes waarin ze voorkomen:

- intra-tidaal (tijkentering)
- gerelateerd aan stormen
- doodtij

Het eerste type is kenmerkend voor het turbiditeitsmaximum en werd geobserveerd op regelmatige basis (4 keer per dag). De hydrodynamica is gekenmerkt door een getijdenellips dat uitgesproken plat is (typisch voor ondiep water); dus de lange (paar uren) fasen van tijkentering, en dus fasen van verminderde turbulente energie laten gravitationele bezinking toe van het suspensiemateriaal uit de waterkolom. Dit wordt verder ook bewerkstelligd door vlokkenvorming, waarbij grote vlokken sneller kunnen bezinken. Het tweede type wordt gerelateerd aan de impact van een storm waarbij golfwerking de cohesieve slibbodem vloeibaar maakt. Zoals eerder aangehaald zijn de concentraties aan suspensiemateriaal tijdens stormen typisch toegenomen, mede door erosie van slibsedimenten uit de navigatiekanalen. Ook na de passage van stormen kan veel suspensiemateriaal gaan bezinken en dus hooggeconcentreerde slibsuspensies veroorzaken. Het laatste type wordt geassocieerd aan een rustige periode van verminderde turbulente energie tijdens doodtij, waarbij het suspensiemateriaal massaal bezinkt en de zeebodem bedekt wordt met hooggeconcentreerde slibsuspensies, en eventueel met vloeibaar slib. De duur van voorkomen wordt hydrodynamisch gestuurd door stormwerking en/of door het opeenvolgende springtij.

Wereldwijd lijden havens en navigatiekanalen onder de toeslibbing door hooggeconcentreerde slibsuspensies, en zijn er intensieve bagger-stort programma's nodig om de toegankelijkheid van en naar de havens te garanderen. Een experiment met betrekking tot (alternatief) storten van slib over de strekdam van de haven van Zeebrugge werd uitgevoerd, en er werd daarbij statistisch aangetoond dat stortactiviteiten ook bijdragen tot de vorming van hooggeconcentreerde slibsuspensies en/of vloeibaar slib op 5 km afstand van de stortplaats. Door een statistische benadering werd eerst de natuurlijke variaties in het complexe gedrag van suspensiemateriaal onderzocht, om vervolgens de door de mens geïnduceerde impact te evalueren. Naar aanleiding hiervan werd de concentratie aan suspensiemateriaal en de voorkomens van hooggeconcentreerde slibsuspensies voorgesteld als indicator voor veranderingen in het fysische milieu, zowel door menselijke ingrepen, als door natuurlijke veranderingen (bijvoorbeeld de trend van het windklimaat).

Tenslotte werd, in het turbiditeitsmaximum, de kans op begraving van zeemijnen onderzocht door hooggeconcentreerde slibsuspensies; dit met betrekking tot detectie van zeemijnen en andere objecten op de zeebodem. Een testmijn, uitgerust met optische sensoren, registreerde gedurende 3 maanden het dynamische karakter van deze slibsuspensies. De bevindingen werden teruggekoppeld aan metingen van de multi-sensor tripode waardoor nieuwe inzichten zijn verworven met betrekking tot het onderzoek naar het gedrag van deze slibsuspensies. Alle types van munitie

(onafhankelijk van vorm, densiteit, oriëntatie) kunnen, bij hoge concentraties aan suspensiemateriaal, door dit mechanisme periodisch worden begraven en blootgesteld. Het gevaar dreigt dat munitie niet gevonden wordt bij het opsporen in gebieden waar hooggeconcentreerde slibsuspensies aanhoudend voorkomen, en daarom is het aangewezen dat deze gebieden verder opgevolgd en geanalyseerd worden. Aan de Belgische kust wordt het risico hoog ingeschat in het turbiditeitsmaximum tijdens doodtij, aangezien dan begraving langdurig wordt ingeschat.

Trefwoorden: Suspensiemateriaal; turbiditeitsmaximum; natuurlijke variabiliteit; advectie; windklimaat; stormen; North Atlantic Oscillation; partikelgrootteverdeling; hooggeconcentreerde slibsuspensies; baggerstortplaatsen; zeemijnbegraving

Introduction, aims and thesis structure

1. Introduction

1.1. Socio-economic relevance of fine-grained sediment dynamics

Because of (rapid) sedimentation of suspended particulate matter (SPM) and the presence of fluid mud (Verlaan and Spahnhof 2000, Winterwerp 2005, PIANC 2008, van Maren et al. 2009, Manning et al. 2011), shoaling of maritime access routes and harbour basins in coastal or estuarine turbidity maximum environments is detrimental for their accessibility. Deposition of mud in the dredging areas can be seen as a temporarily storage of (fluid) mud (Kineke et al. 1996, Le Hir 1997, Winterwerp and van Kesteren 2004, Schrottke et al. 2006, Uncles et al. 2006). Mud is here referred to as water-rich sediment typically with a considerable amount of clay-silt particles (also sand). The harbours of Zeebrugge (Fig.1.1), Ostend and the marinas of Blankenberge and Nieuwpoort, and their navigation channels need very regular maintenance dredging in order to guarantee accessibility. Maintenance dredging amounts up to about 10 million tons of dry matter per year for Zeebrugge and the major shipping lanes (Lauwaert et al. 2009).

Figure 1.1 *Sediment transport in the vicinity of the harbour of Zeebrugge. Blue areas are masked areas*

The dredged material, which consists of pure mud in the harbour or of sandy mud in the navigation channels, is disposed of at dedicated disposal grounds at sea. The OSPAR convention (1992; Convention for the Protection of the Marine Environment of the North-East Atlantic) aimed at preventing and eliminating pollution and at protecting the maritime area against the adverse effects of human activities. Although disposing of dredged material at sea is allowed, a risk remains that toxic substances (organic micro-pollutants and heavy metals) associated with the disposal of dredged material over large areas are present. Detailed knowledge of SPM dynamics, including its temporal and geographical variability, is therefore needed.
Several research programmes have been carried out or are ongoing that have investigated the human impact caused by dredging and disposal in the Belgian nearshore area: MOCHA (BelSPO) (Fettweis et al. 2007), MAREBASSE (BelSPO) (Van Lancker et al. 2007), QUEST4D (BelSPO) (Van Lancker et al. 2011), HCBS-Zeebrugge (IMDC 2010); and MOMO (Flemish Authorities) (Lauwaert et al. 2009, Fettweis et al. 2011a).
Several techniques have been proposed to minimize harbour siltation of which an overview is presented in PIANC (2008) and Kirby (2011). In Belgium the focus is on optimizing the disposal of dredged material (Fettweis et al. 2011b), on optimizing dredging methods (Berlamont et al. 1985, Berlamont 1989, Fettweis et al. 2011c) and

on decreasing the sedimentation in the dredging areas. The latter requires infrastructural adaptations (e.g current-deflecting-wall) in order to decrease the water exchange and thus the mud input between the harbour basin and its environment (Fettweis and Sas 1998, Hofland et al. 2001, Kuijper et al. 2005, van Maren et al. 2009, 2011). The efficiency of disposal grounds is defined by physical, economical and ecological aspects. In other words, an efficient disposal ground implies a minimal recirculation of the disposed matter towards the dredged areas. As such, a minimal distance between the dredged area and disposal ground is preferred, however, under the assumption that the impact on the marine environment is negligible. Consequently, there is no disposal ground that covers all three aspects. Efficiently disposing of dredged material then requires a more dynamic strategy that allows choosing the best location, as a function of the (predicted) physical impacts or conditions. Potential disposal grounds may be chosen in the coastal turbidity maximum, when it can be argued that the disposal activities do not increase significantly the turbidity levels, compared to the natural background in turbidity (Fettweis and Van den Eynde 2003).

1.2. High-turbidity areas in the southern North Sea

The southern North Sea region is composed of the Southern Bight, the German Bight and also part of UK waters; 56° north latitude is the northward boundary. The overall distribution of salinity, and hence water masses determine the distribution of turbidity (e.g. Lee and Folkard 1969). Since 1997, measuring physical oceanographic characteristics from space (ocean colour remote sensors; MODIS-Aqua, SeaWiFs; MERIS) has become common practice to derive mean patterns of e.g. surface SPM in shelf seas such as the North Sea (Ruddick et al. 2000, van der Woerd and Pasterkamp 2004, Eleveld et al. 2004, Staneva et al. 2009, Neukermans et al. 2009, Nechad et al. 2010, Pietrzak et al. 2011). The southern North Sea SPM system is characterized by different spatial structures of turbidity (Fig. 1.2): (1) the 'classical' river plumes such as the Tees, Humber, Thames estuary, Wash, Meuse-Rhine, Elbe, Weser and Ems. In the northern hemisphere, the freshwater-turbidity plumes turn right due to Coriolis forcing. Exception is the Thames river plume that turns left due to residual circulation (e.g. Pietrzak et al. 2011). In the German Bight, the coastal waters are affected by mainly the Elbe, Weser and Ems. (2) The East Anglian Plume (Prandtl et al. 1993, Dyer and Moffat 1998) representing offshore deflecting buoyant coastal waters. It originates from the Thames river plume and crosses the southern North Sea (Holt and James 1999) towards the German Bight (Dyer and Moffat 1998). (3) The turbidity area in the Belgian-Dutch coastal waters which is best described as a coastal turbidity maximum zone.

1.3. Coastal turbidity maximum along the Belgian-Dutch coast

The term coastal turbidity maximum (CTM) refers to the persistent high surface SPM concentrations (up to 100 mg l^{-1}) in the Belgian-Dutch coastal zone (Bastin et al. 1984, Ruddick et al. 2000, Eleveld et al. 2004, Fettweis et al. 2010), with a main spatial extension between about Ostend and the Westerscheldt estuary. Geographically, the mouth of the estuary is situated at Vlissingen, although geo-morphologically the area between Zeebrugge and Walcheren is part of the mouth. The term 'coastal turbidity maximum' is not frequently used in literature (Lee and Folkard 1969, Fettweis et al. 2010), and corresponds roughly with an 'estuarine turbidity maximum' (ETM) in the sense that one or more trapping mechanisms for SPM occur. These are not due to salinity (ETM), but rather due to e.g. congestion in the residual SPM transport (Fettweis and Van den Eynde 2003). In the shallow Belgian-Dutch CTM zone, where water depths range between 0 and 16 m MLLWS (Mean Lower Low Water Springs), the main morphological entities are sandbanks and swales, as also navigational channels e.g. towards Zeebrugge and the Westerscheldt. These channels are maintained at a water depth of minimum 15 m MLLWS.

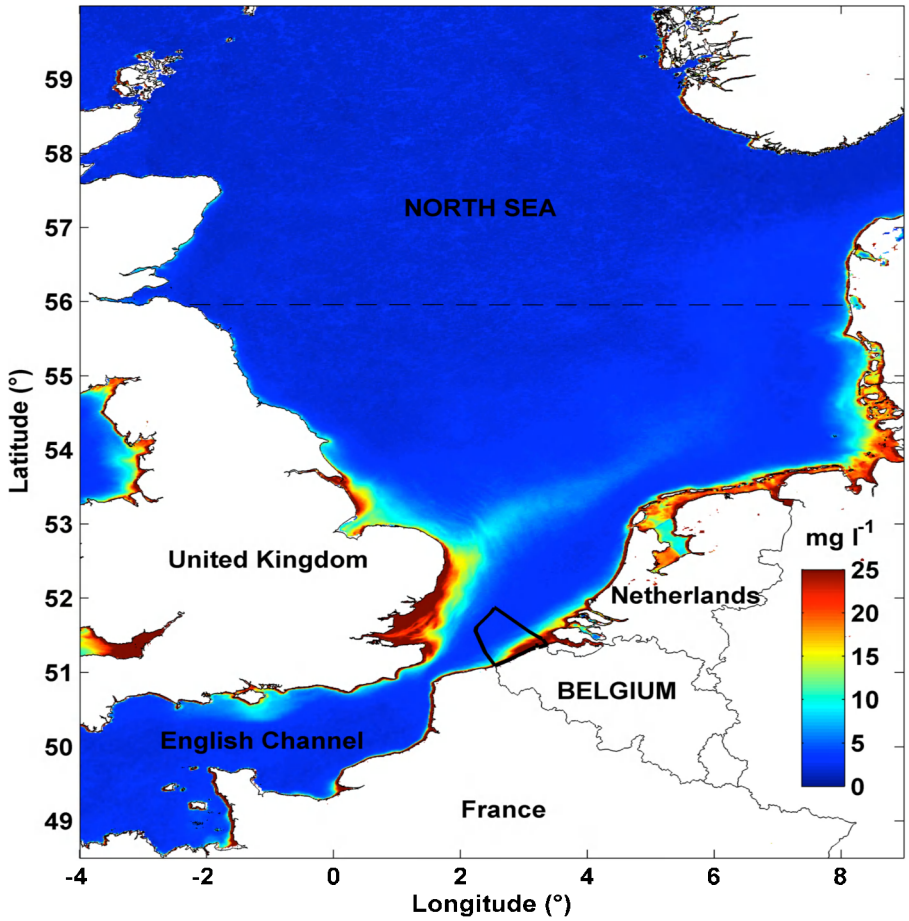

Figure 1.2 *Emerging patterns of turbidity as observed (derived from MODIS-Aqua imagery) at the water surface in the southern North Sea*

1.4. Coastal hydrodynamics

The macro-tidal regime is the main control of the hydrodynamics along the Belgian-Dutch coast. Tides are semi-diurnal and slightly asymmetric with a mean tidal range of 4.3 m at Zeebrugge during spring tide and 2.8 m during neap tide. Tidal current velocities are of the order of 0.6 to 1.2 m s^{-1} in the coastal zone, with maximum velocities of 1.5 m s^{-1} around the port of Zeebrugge. As a consequence, the bottom shear stresses (frictional force exerted by the flow per unit area of the seabed) are the largest there. The residual (subtidal) circulation is known to contribute to the long-term transport of fine sediments (mainly clay-silt particles and fine sands), and is governed by different forcings:

- wind forcing
- tides (through non-linear effects)
- vertical density gradients (temperature, salinity)

The wind climate may affect the residual current vectors resulting in significant flows in the surface layer diminishing with increasing water depth (Yang 1998, Lentz et al. 1999). Winds originate mainly from west-southwest, when Atlantic depressions are moving from west to east above the Belgian coast (Fig. 1.3).

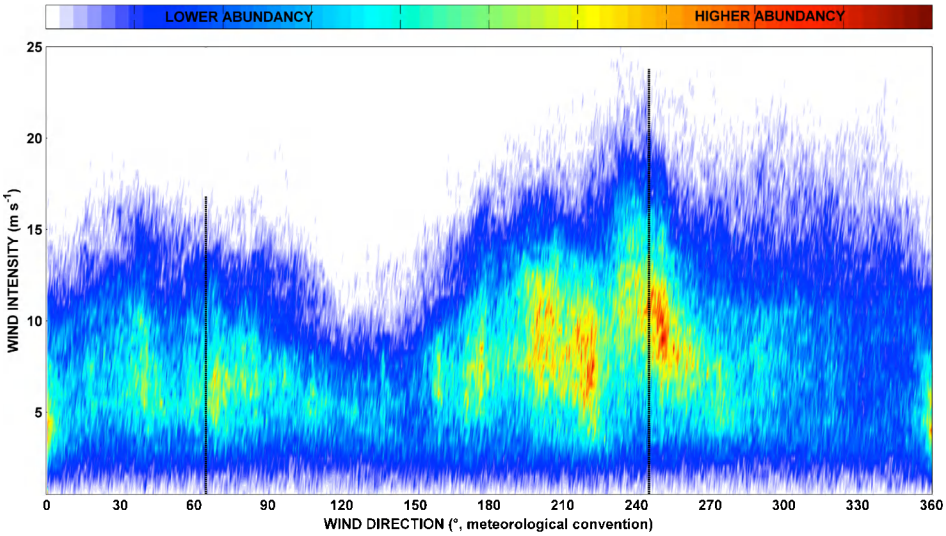

Figure 1.3 *Wind climate along the Belgian coastal zone, based on measurements between 2000 and 2010 at Zeebrugge harbour station (data from Ministery of the Flemish Community, Maritime Services, Coastal Division/Hydrography)*

The second frequent wind sector is northeast, as a result of the development of a high pressure field (between two Atlantic depressions) that moves from the UK towards Central Europe or Scandinavia. Other wind directions are less abundant, since they are transitional directions between the two main wind regimes. Since the coastline (as indicated by the vertical lines in Fig. 1.3) is oriented about 65° true north, strong wind-forced flows are present alongshore (Verlaan and Groenendijk 1993, Yang 1998). Response time of the North Sea to changes in wind speed generally varies between 6 and 34 h (Ishiguro 1983). In literature, the existence of the CTM zone has been correlated with residual flow circulation. On a regional scale, the mechanism of SPM entering the North Sea through the Dover Strait open boundary and settling off the Belgian-Dutch coast has been widely discussed in literature (Eisma and Kalf 1987, Van Alphen 1990, Lafite et al. 1993, 2000, Gerritsen et al. 2000, Fettweis et al. 2007). However, the fate of fine-grained sediments in the coastal zone is still controversial. In some studies residual current patterns with large gyres (Nihoul 1975, Gullentops et al. 1976, Delhez and Carabin 2001) and flow convergences (Van Veen 1936) are hypothesized; these authors plead for a closed system to explain the presence of cohesive sediments (Fig. 1.4). In other studies, detailed hydrodynamic and sediment transport modelling (Fettweis and Van den Eynde 2003), ground-truthed with tracer tests (Van den Eynde 2004) have been used to argue against the existence of residual eddies, or the closed system concept. It was shown that most of the mud from the Dover Strait is actually leaving the study area towards the northeast, being controlled by tides and meteorological forcing. Because of the decreasing magnitude of the northeast-directed residual transport and the presence of the island of Walcheren (the Netherlands), a kind of congestion occurs in the sediment transport. In combination with the nature of seabed sediments (see 1.5), this would explain the presence of the turbidity zone.

Influence of vertical density gradients on the CTM formation, hence the potential of "thermo-haline circulation" is negligible. The water column is generally well mixed throughout the entire year (e.g. de Ruijter et al. 1987) due to the high tidal amplitudes, the strong tidal currents and the low freshwater discharge of the River Scheldt (yearly average is 100 $m^3\ s^{-1}$, with a minimum of 20 $m^3\ s^{-1}$ during summer and a maximum of 600 $m^3\ s^{-1}$ during winter). Horizontal density gradients occur in the coastal zone and are influenced by the freshwater outflow of the Westerscheldt estuary, mainly (Lacroix et al. 2004). They are caused by tidal- and wind-driven advection and are generally low (salinity difference during a tide is <1; salinity difference of 2 occurs in 10% of the tides).

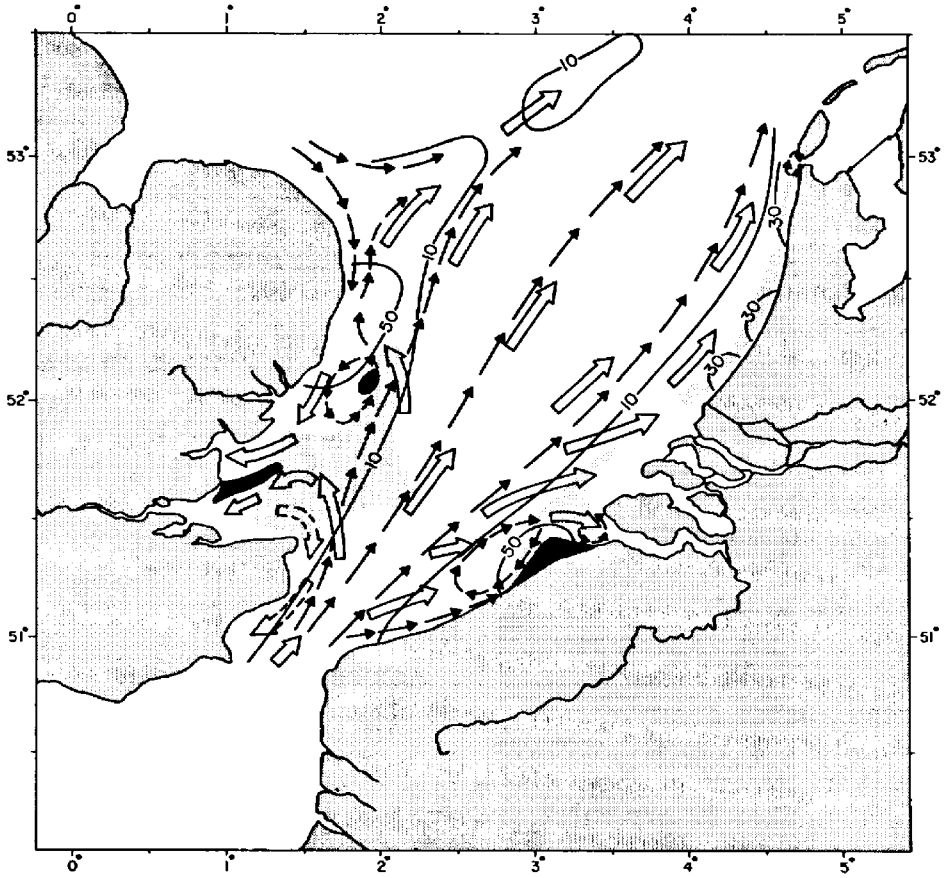

Figure 1.4 *Overview of SPM transport in the southern Bight of the North Sea (adopted from Eisma and Kalf 1979); SPM concentration in mg l^{-1}; small arrows are residual current patterns (Nihoul and Ronday 1975, Prandle 1978 in Eisma and Kalf 1979); contour arrows indicate transport pathways of SPM; interrupted contour arrows (Ramster et al. 1976 in Eisma and Kalf 1979)are indicative of flow of water and SPM from the Thames estuary to the English Channel under strong northerly winds; black areas are mud deposits consisting of >50% of particles smaller than 50 µm (Bastin 1974, Jarke 1956 in Eisma and Kalf 1979); dotted areas are deposits consisting of >2% of particles smaller than 50 µm (Eisma 1966, McCave 1979 in Eisma and Kalf 1979)*

1.5. Heterogeneous sedimentary environment

Both the geological and sedimentological situation in the Belgian-Dutch coastal zone is complex. The Palaeozoic basement was flooded during Late Cretaceous times (Le Bot et al. 2003), and the present Tertiary sequence coincides with slightly, northeast dipping deposits. These, from mid-Eocene to upper-Pliocene, deposits exhibit a varying sedimentology (sandy clay, clay, clayey sand, and sand) with thickness between 10 and 30 m (De Batist 1989, Ebbing et al. 1992). Further, Quaternary sediments mainly include the Pleistocene backfilled scour hollows in Palaeogene shelf strata (Mostaert et al. 1989, Liu 1990), and the Holocene tidal sandbanks. Thicknesses of the Quaternary deposits in the coastal zone vary between 0 and 10 m, mainly (besides the Ostend valley deposits). More resistant Tertiary layers, such as Boom clay and Asse clay, outcrop in the navigational channel towards the Westerscheldt where the Quaternary cover is absent. The Quaternary deposits are typically sands with sporadic strata of shells (or shell fragments); though near the Zeebrugge harbour and the Vlakte van de

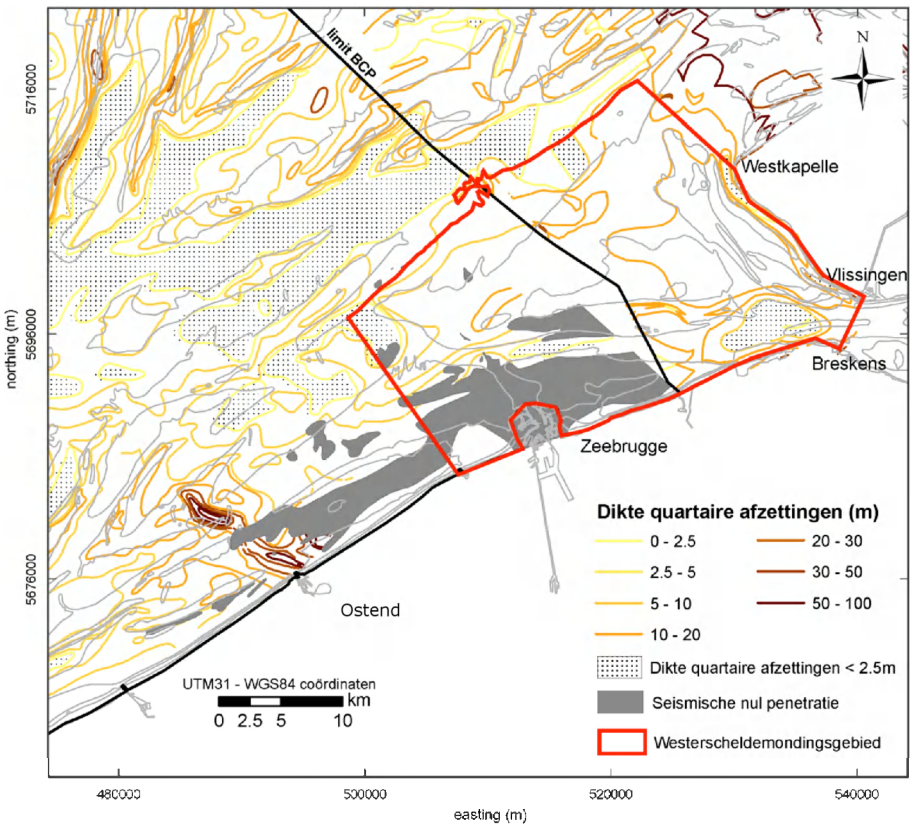

Figure 1.5 *Thickness (m) of Quaternary sediments (Liu 1990, Ebbing et al. 1992); dotted areas are less than 2.5 m thick; the red polyline corresponds to the Westerscheldt estuary; very poor seismic penetration is found in the grey filled region (from Du Four et al. 2006)*

Raan, clay, clay-sand alternations and peat layers are mostly present (Le Bot et al. 2003, 2005).
The Holocene (interglacial period beginning at the end of the Pleistocene, i.e. ~11700 years ago) is characterized with a sea level rise because of melting glaciers. The shallow parts of the inundated coastal area allowed the development of marshes and peat formation (Baeteman and Van Strijdonck 1989). In addition, the Pleistocene deposits are largely eroded (Baeteman and Van Strijdonck 1997) and reworked as tidally-induced mudflat deposits, estuarine sand plates and beach deposits. Finally, during the last period of the Holocene, a continuous displacement and reworking of sediments under tidal hydrodynamics resulted in the present-day seafloor morphology (planar, small and large bed forms) (Eisma and Kalf 1979, Mathys 2009).
The composition of bottom sediments in the Belgian-Dutch coastal zone is not uniform; it varies from pure clays to very coarse sands (Verfaillie et al. 2006). The heterogeneous character of the seabed is natural, but also partly because of human impact, such as dredging-disposal activities (see 1.1). The sand fraction is partly relict and partly in transport, dependent on the prevalent bottom shear stresses. Grain-sizes become typically coarser in the offshore direction (Lanckneus et al. 2001). Clay and silt size bottom sediments are also abundant between Ostend and the River Scheldt mouth (Van Lancker et al. 2007 a, b). In the last years, several techniques have been used to characterize the nature of the muddy seabed in the CTM zone: seismic surveys (Missiaen et al. 2002, Mathys 2009), seabed mapping (Van Lancker et al. 2004) and intensive seabed box coring (Van Lancker et al. 2004, Fettweis et al. 2010).
The bed structure, wet bulk density and consolidation of the cohesive sediments have been investigated with erosion behaviour measurements (Fettweis et al. 2005,

Fettweis et al. 2010), and allowed establishing the presence of the following bed layers: fluffy / fluid mud layers (0.5-1 Pa; 1100-1200 kg m^{-3}); freshly (recently) deposited mud (1-4 Pa; 1300-1500 kg m^{-3}); soft to medium consolidated Holocene mud (up to 13 Pa; 1500-1800 kg m^{-3}) with intercalations of thin sand layers (~1 Pa). From the geophysical surveys in the CTM zone, a mud plate has been identified as a distinct unit of Holocene age partly covered by sands (Mathys 2009). The presence of the mud plate confirmed earlier observations (Stessels 1866, Van Mierlo 1899, Gilson 1900, Bastin 1974, Gullentops 1976); for Mathys (2009) it is a deposit formed within the last 450 years. This deposit is basically seen as a reworked (Holocene) back barrier deposit. The very poor seismic penetration of the unit is because of methane gas formation in shallow peat layers (Missiaen et al. 2002). The thickness is on average less than 1 m, but may reach 5 m in the eastern part. It forms the largest reservoir of fine-grained sediments in the nearshore area (Fettweis et al. 2009); it contributes as a source of SPM, mainly during storm events (Fettweis et al. 2010). However, the physical behaviour of the outcropping consolidated mud (swelling, mass erosion, resuspension, weakening) in the area is quantitatively not known yet.

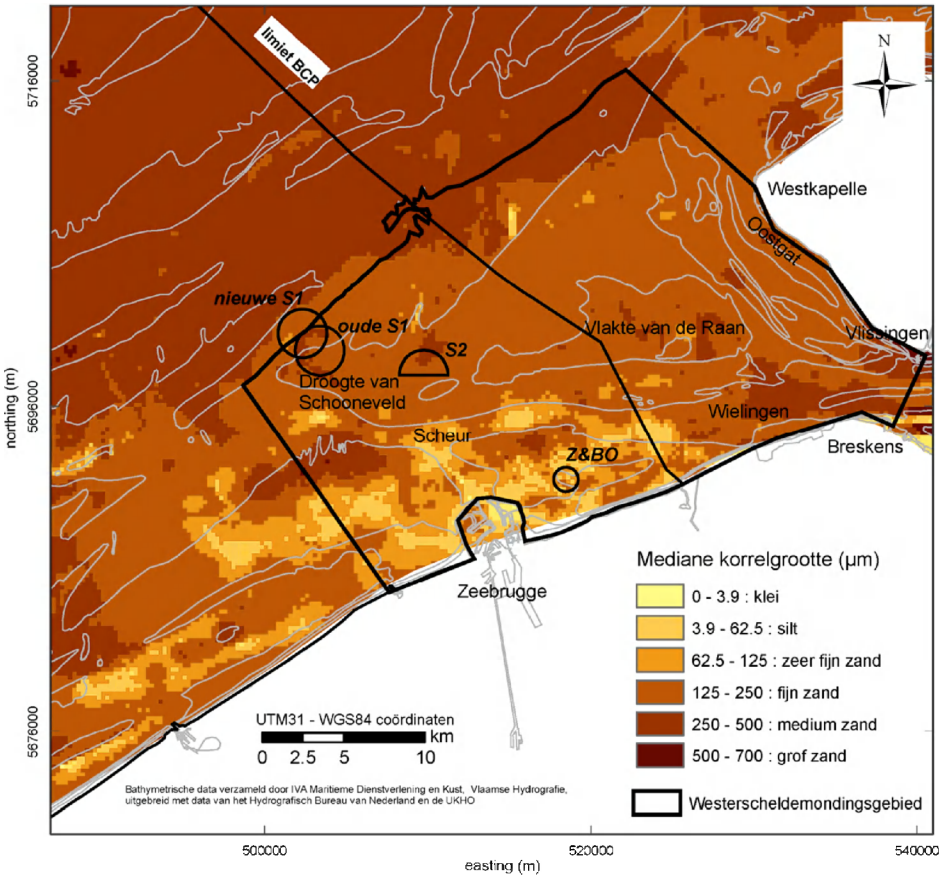

Figure 1.6 *Map of median grain size (based on sedisurf@database (Van Lancker et al. 2007 a), and sediment data from TNO (NL); black (semi-) circles are disposal grounds of dredged material (from Du Four et al. 2006)*

1.6. SPM characteristics

Ocean colour satellite sensors derive SPM concentration for the near-surface layer from optical properties of the sea (e.g. Doerffer et al. 1994). The degree of turbidity (water clarity) is an optical property of the water and is influenced by (1) coloured dissolved organic matter (CDOM; e.g. humic substances) and (2) suspended

particulate matter (SPM). The latter consists of fine-grained materials (clay, silt and sand) and is composed of minerals (clay minerals, quartz, carbonates), organic matter (OM) and water (Eisma 1986, Berlamont et al. 1993). OM consists of micro-organisms, their metabolic products, residuals from dead organisms and faecal pellets (Hamm 2002, Bhaskar et al. 2005). OM content in the water column will determine the flocculation dynamics (Fettweis et al. 2006, see 1.7), as with higher OM content the SPM flocs become larger. Flocculation is caused mainly by the clay minerals interacting with each other, with other minerals and with the organic matter resulting in increased cohesiveness of the SPM (Kranenburg 1994, Dyer and Manning 1999, Son and Hsu 2009). Regarding the Belgian coastal zone, the SPM consists of a clay to silt ratio of ~1:4, median grain size of the primary particles (building stones of flocs) of <3µm, 7.5% organic matter, and 40% $CaCO_3$ (Fettweis et al. 2007 b). These figures must be regarded with caution since measurements were realised at different sample stations and under different hydrodynamical conditions. Density of primary particles takes into account the different fractions (OM, $CaCO_3$ and clays and non-clay minerals) and the corresponding densities, and was found to be 2580 kg m^{-3} for the Belgian coastal zone. From a mineralogical point of view (Zeelmaekers 2011), the consolidated mud deposits, as well as the freshly deposited mud, share the same clay-composition as the SPM found in the CTM. Therefore, he suggested that constant reworking of the older mudplate deposits contributes significantly more towards the SPM than previously thought. More distant sources of SPM considered in literature are the erosion of the coastal cliffs in the English Channel (Eisma and Kalf 1987, Lafite et al. 1993, Irion and Zöllmer 1999, Velegrakis et al. 1999, Gerritsen et al. 2000, Fettweis and Van den Eynde 2003), the erosion of outcropping Tertiary (Paleogene) clay (Fettweis et al. 2009) and the River Scheldt (Gullentops et al. 1976, Nechad et al. 2003).

1.7. SPM dynamics

Generally, SPM particles undergo various cycles of re-suspension, settling and advection before being deposited more offshore and forming fine-grained sediment deposits (e.g. Gerritsen et al. 2000). SPM dynamics are controlled by several forcings: tides, wind, mean sea level, ocean currents, sources of sediment, thermohaline fields, freshwater flux (Stanev et al. 2009); as well as by biological processes (e.g. Nowell et al. 1981, Arndt et al. 2007, März 2009) and human impact (dredging-disposal cycles), typically for the study area.

The most significant time-scale for SPM dynamics are the tides; the alteration of high current velocities and slack water inducing a continuous change in re-suspension, mixing, settling and deposition. Tidal ellipses are more elongated towards the shore and thus the difference between maximum and minimum currents increases. During the periods with minimum currents, the so-called slack waters (or slack tides), SPM aggregates into larger flocs with higher settling velocities and thus an enhanced settling and sedimentation occurs (e.g. Dyer 1989, van Leusen 1994). The cohesive sediments (predominantly clayey particulate matter) are re-suspended when current velocities increase again. A schematic overview is given by Maggi (2005, Fig. 1.7) showing the complexity and coupling between aforementioned processes.

From cohesive sediment transport (modelling) studies, and chemical engineering applications (i.e. water purification), flocculation is very well known to be controlled by turbulent shear and time (Toorman 2001). SPM flocs will start breaking up during increased turbulence. In the subtidal time-domain, neap tidal phases are characterized by higher accumulation rate, deposition of thicker (fluid) mud layers, consolidation of these layers and a decrease of SPM concentrations (Fettweis and Van den Eynde 2003). The subsequent spring tide conditions will re-suspend these temporal mud deposits.

Floc size (distribution) and hence settling velocity may considerably vary over the tidal cycle, as well as for spring and neap tide (Winterwerp et al. 2002, Fettweis et al. 2006). Also, seasons have an influence on SPM concentration, which are mainly explained by the higher frequency of storms during winter (Visser 1969, Cacchione and Drake 1982, Williams et al. 1999, Ferré et al. 2005, Guillen et al. 2006). Higher river discharges in spring, and hence high plankton growth are expected (Terwindt 1967, Lancelot and Mathot 1987, Lacroix et al. 2007) implying change in SPM composition and floc characteristics (van der Lee 2001, März et al. 2010).

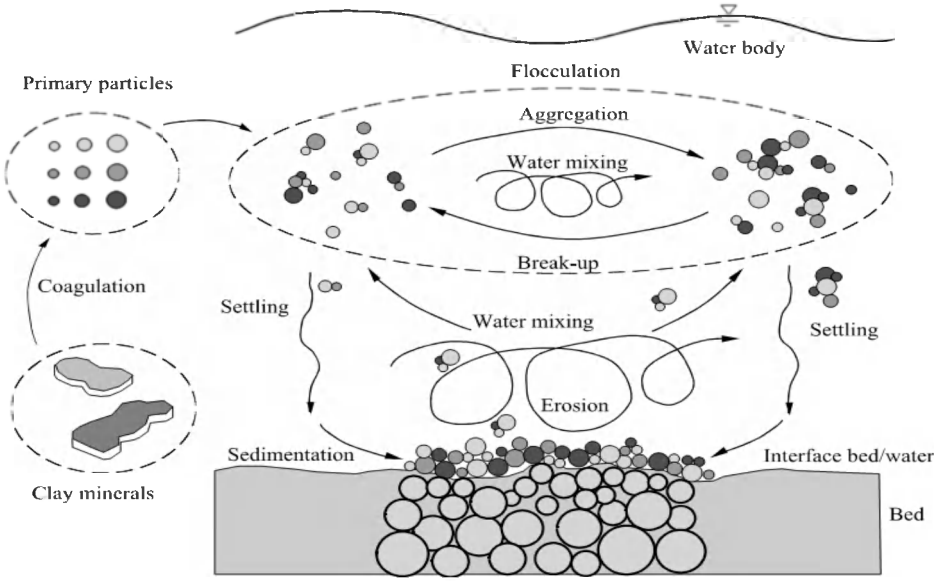

Figure 1.7 *Cycle of deposition and resuspension of cohesive sediment (from Maggi 2005)*

1.8. High-concentration mud suspensions (HCMS) and fluid mud

During periods of decreased turbulent kinetic energy (neap and slack tides), SPM flocs settle out of the water column resulting in high near-bed SPM concentrations. Suspensions with concentrations of a few 100 mg l^{-1} to a few g l^{-1} are defined as high-concentration mud suspensions (Winterwerp 1999). They interact with the turbulent flow field, behave Newtonian (with some increased viscosity), and are in transport with the main flow. A strong vertical, sediment-induced, density gradient (lutocline) in the water column (near-bed) is often associated with HCMS. Related to ETMs, HCMS have been described extensively (Inglis and Allen 1957, Allen et al. 1980, Faas and Wartel 1985, Odd 1988, van Leussen 1994). HCMS occurrences are also associated with current-driven sediment gravity flows off high-load rivers (Friedrichs and Wright 2006); however high-load river discharges in the Belgian coastal area are not expected (Fettweis et al. 2007). Fluid mud is a suspension of cohesive sediment above the gelling point (between 10 to 100 g l^{-1}); the gelling point refers to the concentration that is favourable for flocs to structure a network (Winterwerp and van Kesteren 2004). The rheology of fluid mud exhibits non-Newtonian behaviour, and can be either stationary or mobile. Both HCMS and fluid mud give rise to large siltation rates, as found in harbour basins and navigational channels (Winterwerp 2002). Another mechanism, responsible for the occurrence of HCMS in the marine environment, is due to wave action (de Wit and Kranenburg 1997, Li and Mehta 2000, Winterwerp et al. 2001, Fettweis et al. 2010).

1.9. Influence of SPM on the structure and function of eco-systems

The ecological functioning of the coastal system is amongst other controlled by the water clarity and thus by the amount of fine-grained material in the water column. In addition, SPM may control the transport, re-activity and biological impacts of substances in the marine environment (Turner and Millward 2002). For example, SPM has a crucial impact on the underwater light field by reducing the available light for primary production (Behrenfeld and Falkowski 1997, Arndt et al. 2011). Additionally, SPM controls the development of phytoplankton biomass and hence the dissolved nutrients in the water column (Cloern 1987, Monbet 1992). Further, SPM dynamics control the functioning of benthic communities (Murray et al. 2002) since SPM carries a major part of the food resources for the benthos. Frequent HCMS and fluid mud

formation may affect bioturbation or bio-irrigation modes, both important ecosystem functions of soft substrata macrobenthos. Bioturbation and bio-irrigation are of paramount importance for ecosystem functioning in fine sandy sediments receiving high loadings of organic matter (OM). A decrease in density of bioturbators entails a decrease in OM burial, whereas a decline in bio-irrigators implies less oxygenation of the sediment and denitrification, an important nitrogen-eutrophication counteracting process in shallow coastal seas. Bioturbation and bio-irrigation are therefore key transport mechanisms in carbon and nitrogen cycling in shallow seas (Braeckman 2011).

1.10. Aims

The overall aim of this PhD dissertation was to increase knowledge on the dynamics of suspended particulate matter (SPM) in the Belgian coastal zone. High amounts of SPM are associated with the occurrence of a coastal turbidity maximum (CTM), present within the Belgian-Dutch coastal zone. The seabed is composed of a mixture of sand and mud; both are re-suspended under various hydro-meteorological conditions. Within the CTM, the formation of high-concentrated mud suspensions (HCMS) is a particular phenomenon, though its dynamics and occurrence has up to now, only occasionally been investigated. Further the dissertation aimed at increasing the understanding of human impacts on SPM dynamics. This requires dedicated instrumentation, preferably measuring on a quasi-continuous basis. The choice of instrumentation is critical in determining the processes occurring in the water column, as well as near-bed.

Main questions posed were:

(1) What drives the temporal variability of SPM within the CTM zone?

(2) How does (1) influence the spatial variability of the extent of the CTM zone?

(3) What is the dynamic behaviour of HCMS, and their influence on near-bed processes?

(4) How will mixed sediments within the CTM zone influence optical and acoustic sensor measurements?

(5) Can anthropogenic contributions to SPM concentration be distinguished from the natural variability through time?

1.11. Thesis structure

Research results are divided over the following "paper chapters":

In Chapter 2 in-situ measurements are described at a single-point location in the Belgian nearshore area. The effect of wind on the advection of the fine-grained sediments and the dynamics of high-concentrated mud suspensions are investigated aiming at obtaining new insights into fine-grained sediment transport. Different techniques have been used, including acoustic methods for sediment transport and ensemble-averaging of data. In a next chapter, general findings from the single-point location described in Chapter 2 are tested against the SPM concentration field results in the Belgian-Dutch coastal zone as measured from space (Chapter 3). Satellite images are used to study the geographical variability of the turbidity maximum, based on meteorology- and climate-based classification schemes. In Chapter 4, the near-surface satellite and near-bed tripod findings are combined to study the behaviour of sediment suspensions, aiming at determining the full-water column characteristics (sediment re-suspension, advection, fluxes and vertical mixing degree) by means of acoustic Doppler profiler datasets. Implications towards used instrumentation for measuring SPM concentration result from particle size differentiation over time. Chapter 5 deals with multi-modal suspended particle size distributions under different hydro-meteorological influences, based on several statistical techniques (Chapter 2

treats only the median value of the particle size spectrum). Chapters 6 and 7 are combined since both represent applied research. They deal with the formation and erosion of high-concentrated mud suspensions in the coastal turbidity maximum zone with relevance to mine burial, and to disposal (of dredged mud) activities, respectively. The synthesis (with discussion) chapter (8) is followed by conclusions and future research perspectives (Chapter 9).

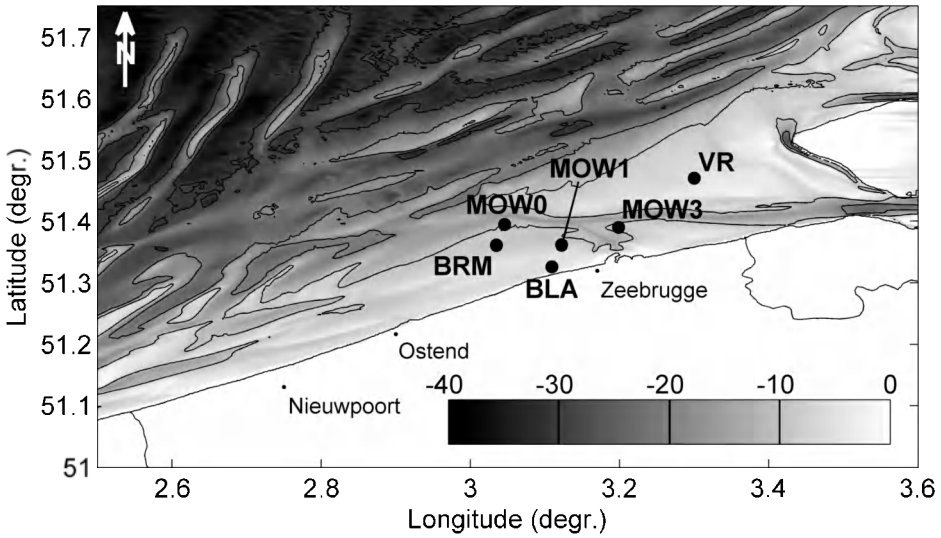

Figure 1.8 *Overview of observatory and study locations used in the study area. Extent map coincides with MODIS-Aqua SPM concentration maps (Chapter 3). Bathymetry (in meters) with MLLWS as reference*

Fig. 1.8 shows all measurement locations (MOW1, MOW0, BRM, BLA, VR, and MOW3) used in this study; all of them are shallow (< 10 m). All chapters are published or accepted/submitted for publication, resulting in inevitable overlap regarding introductions and study area descriptions; though, each chapter can be consulted independently from the others.

For the dissertation, in-situ data and research results were made available from the following research projects:

- **MOMO (Flemish Authorities, Maritime Access)**: *Monitoring and modelling of cohesive sediment transport and evaluation of the effects of dredging and dumping operations on the marine ecosystem (**Management Unit of the North Sea Mathematical Models-MUMM**)*

The "MOMO" project is part of the general and permanent duties of monitoring and evaluation of the effects of all human activities on the marine ecosystem to which Belgium is committed following the OSPAR convention (1992). The goal of the project is to study the cohesive sediments on the Belgian Continental Shelf (BCS) using numerical models as well as by carrying out measurements. Through this, data will be provided on the transport processes, which are essential in order to answer questions on the composition, origin and residence of these sediments on the BCS, the alterations of sediment characteristics due to dredging and disposal operations, natural variability, the impact on the marine ecosystem, the estimation of the net input of hazardous substances and the possibilities to decrease this impact as well as this input.

Fettweis M, Baeye M, Lee BJ, Van den Eynde D, Van Lancker VRM (2011). Monitoring en modellering van het cohesieve sedimenttransport en evaluatie van de effecten op

het mariene ecosysteem ten gevolge van bagger- en stortoperatie (MOMO): activiteitsrapport (1 juli 2010 - 31 december 2010). BMM/MUMM: Brussel. 44 pp. + appendices.

- **QUEST4D (Belgian Science Policy)**: *QUantification of Erosion/Sedimentation patterns to Trace naturalyl versus anthropogenically-induced sediment dynamics (**Ugent**, **MUMM**, **KUL**, **WL**)*

Quest4D targets the Belgian part of the North Sea to investigate the seabed ecosystem over the past 100 years. Main objectives include: (1) Increase in knowledge on natural variability of seabed nature and processes; (2) Establish historic baselines, as reference situations for impact studies; (3) Quantification of ecosystem changes, on the medium- to long-term; (4) Demonstration of human impact, with case studies relating seabed changes to both naturally and anthropogenically induced sediment dynamics; (5) Assessing climate change scenarios and their effect on seabed management; and (6) Development of more sustainable exploitation strategies of non-living seabed resources.

Van Lancker V, Baeye M, Du Four I, Janssens R, Degraer S, Fettweis M, Francken F, Houziaux JS, Luyten P, Van den Eynde D, Devolder M, De Cauwer K, Monbaliu J, Toorman E, Portilla J, Ullman A, Liste Muñoz M, Fernandez L, Komijani H, Verwaest T, Delgado R, De Schutter J, Janssens J, Levy Y, Vanlede J, Vincx M, Rabaut M, Vandenberghe H, Zeelmaekers E, Goffin A (2011). QUantification of Erosion/Sedimentation patterns to Trace the natural versus anthropogenic sediment dynamics (QUEST4D). Final Report. Science for Sustainable Development. Brussels: Belgian Science Policy, 97 pp. + Annexes.

- **MINE BURIAL** *(Mine Warfare Data Centre group): Belgian Naval Defence, Direction Générale Material Resources (**DGMR**) Mine Counter Measure, and in co-operation with Bundesamt für Wehrtechnik und Beschaffung - Forschungsanstalt der Bundeswehr für Wasserschall und Geophysik (**BWB - FWG**, Germany) and Ghent University (**Renard Centre of Marine Geology RCMG**)*

The "Mine Burial" project aims to evaluate the time necessary for partial or total burial of objects in shallow water (<40m depth) by studying the sand dynamics on the Belgian Continental Shelf in both time and space domain. Several techniques are used to reach this goal: time-series of side scan sonar measurements, box-cores for validation of acoustic images, and instrumented mines at strategic locations to investigate small-scale variability of sand dynamics for over several months. The areas of analysis are chosen following scientific, economical and societal criteria. The research is used for military and civil applications regarding the safety at sea.

1.12. References

Allen GP, Salomon JC, Bassoullet P, Du Penhoat Y, De Grandpre C. (1980). Effects of tides on mixing and suspended sediment transport in macrotidal estuaries. Sedimentary Geology 26, 69–90.

Arndt S, Lacroix G, Gypens N, Regnier P, Lancelot C (2011). Nutrient dynamics and phytoplankton development along an estuary-coastal zone continuum: A model study. Journal of Marine Systems 84 (3-4), 49-66.

Arndt S, Vanderborght J-P, Regnier P (2007). Diatom growth response to physical forcing in a macrotidal estuary: coupling hydrodynamics, sediment transport, and biogeochemistry. Journal of Geophysical Research 112 C05045.

Baeteman C, Van Strijdonck M (1989). Radiocarbon dates on peat from the Holocene coastal deposits in West Belgium. p. 59-91. In: Quaternary sea-level investigations from Belgium. Baeteman C. (Ed.). Ministerie van Economische Zaken, Geologische Dienst van België, Brussel, België.

Baeteman C, Denys L (1997). Holocene shoreline and sea-level data from the Belgian coast. Paleoclimate Research. 21, 49-74.

Bastin A (1974). Regionale sedimentologie en morfologie van de zuidelijke Noordzee en van het Schelde estuarium. Onuitgegeven doktoraatsthesis Thesis, Katholieke Universiteit Leuven, 91 pp.
Bastin A, Caillot A, Malherbe B (1984). Sediment transport measurements on and off the Belgium coast by means of tracers. 8th International Harbour Congress, KVIV, Royal Flemish Society of Engineers. Antwerp, Belgium.
Behrenfeld MJ, Falkowski PG (1997a). Photosynthetic rates derived from satellite-based chlorophyll concentration. Limnology and Oceanography 42, 1-20.
Berlamont J, Ockenden M, Toorman E, Winterwerp J (1993). The characterisation of cohesive sediment properties. Coastal Engineering 21, 105–128.
Berlamont J, van Goethem J, Berleur E, van Bruwaene A (1985). A permanent mud pumping installation as an alternative for local maintenance dredging. 21st IAHR Congress, Melbourne, Australia. Barton: Institution of Engineers, 4, 100-105.
Berlamont J (1989). Pumping fluid mud: Theoretical and experimental considerations. Journal of Coastal Research, 5, p 195-205.
Bhaskar PV, Grossart H-P, Bhosle NB, Simon M (2005). Production of macroaggregates from dissolved exopolymeric substances (EPS) of bacterial and diatom origin. FEMS Microbiology Ecolology 53, 255–264.
Braeckman U (2011). Macrobenthos structuring the sea floor: importance of its functional biodiversity for the benthic ecosystem. Ghent University (UGent), 239 pp.
Cacchione D, Drake D (1982). Measurements of storm-generated bottom stresses on the continental shelf. Journal of Geophysical Research, 87(C3).
Cloern JE (1987). Turbidity as a control on phytoplankton biomass and productivity in estuaries. Continental Shelf Research 7(11/12), 1367-1381.
De Batist M (1989). Seismo-stratigrafie en struktuur van het Paleogeen in de Zuidelijke Noordzee. Ph.D.Thesis, UGent, België. 107 pp.
Delhez EJM, Carabin G (2001). Integrated modelling of the Belgian coastal zone Estuarine, Coastal and Shelf Sciences 53(4), 477-491.
de Ruijter WPM, Postma L, Kok JMD (1987). Transport Atlas of the Southern North Sea Rijkswaterstaat, The Hague. 33 pp.
de Wit PJ, Kranenburg C (1997). The wave-induced liquefaction of cohesive sediment beds. Estuarine, Coastal and Shelf Science 45, 261-271.
Doerffer R, Fischer J (1994). Concentrations of chlorophyll, suspended matter and gelbstoff in case II waters derived from satellite coastal zone colour scanner data with inverse modelling methods. Journal of Geophysical Research 99, 7457–7466.
Du Four I, Schelfaut K, Vanheteren S, Van Dijk T, Van Lancker VRM (2006). Geologie en sedimentologie van het Westerscheldemondingsgebied, in: Coosen J et al. (Ed.) (2006). Studiedag: De Vlakte van de Raan van onder het stof gehaald, Oostende, 13 oktober 2006. pp. 16-29.
Dyer KR, Moffat TJ (1998). Fluxes of suspended matter in the East Anglian plume Southern North Sea. Continental Shelf Research 18, 1311–1331.
Dyer KR, Manning AJ (1999). Observation of the size, settling velocity and effective density of flocs, and their fractal dimensions. Journal Sea Research 41, 87-95.
Dyer KR (1989). Sediment processes in estuaries: future research requirements. Journal of Geophysical Research 94 (C10), 14327-14339.
Ebbing JHJ, Laban C, Frantsen PJ, Nederhof HP (1992). Kaartblad Rabsbank, concessieblokken voor olie en gas S7, S8, S10 en S11 (51°20′ N.B. – 3°00′ O.L.). Rijks Geologische Dienst, Nederland.
Eisma D, Kalf J (1987). Dispersal, concentration and deposition of suspended matter in the North Sea. Journal of Geological Society. London 144, 161-178.
Eisma D (1986). Flocculation and de-flocculation of suspended matter in estuaries. Netherlands Journal of Sea Research 20, 183-199.
Eisma D, Kalf J (1979). Distribution and particle size of suspended matter in the southern Bight of the North Sea. Journal of Sea Research 13, 298-324.
Eleveld MA, Pasterkamp R, van der Woerd HJ (2004). A survey of total suspended matter in the southern North Sea based on the 2001 SeaWiFS data. EARSeL eProceeding 3(2), 166-178.

Faas RW, Wartel S (1985). Resuspension potential of fluid mud and its significance to sediment transport in the Scheldt estuary, Belgium Estuaries 8, 113A.
Ferre B, Guizien K, Durrieudemadron X, Palanques A, Guillen J, Gremare A (2005). Fine-grained sediment dynamics during a strong storm event in the inner-shelf of the Gulf of Lion (NW Mediterranean). Continental Shelf Research 25 (19-20), 2410-2427.
Fettweis M, Sas M (1998). Antwerp tidal dock, summary of Expert Meeting, 4-5 June 1998.
Fettweis M, Van den Eynde D (2003). The mud deposits and the high turbidity in the Belgian-Dutch coastal zone, Southern bight of the North Sea. Continental Shelf Research 23, 669-691.
Fettweis M, Francken F, Van den Eynde D, Houziaux J-S, Vandenbergh N, Fontaine K, Deleu S, Van Lancker VRM, Van Rooij D (2005). Mud Origin, Characterisation and Human Activities (MOCHA): Characteristics of cohesive sediments on the Belgian Continental Shelf. Scientific Report Year 1 (01/04/2004-31/03/2005). Belgian Science Policy: Brussel. 70 + app. pp.
Fettweis M, Du Four I, Zeelmaeker E, Baeteman C, Francken F, Houziaux J-S, Mathys M, Nechad B, Pison V, Vandenberghe N, Van den Eynde D, Van Lancker V, Wartel S (2007). Mud Origin, Characterisation and Human Activities (MOCHA). Final Scientific Report, D/2007/1191/28. Belgian Science Policy Office, 59 pp.
Fettweis M, Francken F, Pison V, Van den Eynde D (2006). Suspended particulate matter dynamics and aggregate sizes in a high turbidity area. Marine Geology 235, 63–74.
Fettweis M, Francken F, Van den Eynde D, Verwaest T, Janssens J, Van Lancker V (2010). Storm influence on SPM concentrations in a coastal turbidity maximum area with high anthropogenic impact (southern North Sea). Continental Shelf Research 30, 1417-1427.
Fettweis M, Baeye M, Lee BJ, Van den Eynde D, Francken F, Van Lancker V (2011a). MOMO activiteitsrapport 2 (1 juli 2010 – 31 december 2010). BMM-rapport MOMO/5/ MF/201102/NL/AR/2, 44pp + app.
Fettweis M, Houziaux J-S, Du Four I, Van Lancker V, Baeteman C, Mathys M, Van den Eynde D, Francken F, Wartel S (2009). Long-term influence of maritime access works on the distribution of cohesive sediments: analysis of historical and recent data from the Belgian nearshore area (Southern North Sea). Geo-marine Letters 29(5), 321-330.
Fettweis M, Van den Eynde D, Martens C (2011b). Optimalisatie stortbeleid: Voorstel voor een terreinproef. MOMO-aMT rapport, 22pp.
Fettweis M, Baeye M, Francken F, Lauwaert B, Van den Eynde D, Van Lancker V, Martens C, Michielsen T (2011c). Monitoring the effects of disposal of fine sediments from maintenance dredging on suspended particulate matter concentration in the Belgian nearshore area (southern North Sea). Marine Pollution Bulletin 62, 258-269.
Friedrichs CT, Wright LD (2006). Gravity driven sediment transport on continental shelves: Recent advances in understanding. 2006 AGU Fall Meeting, San Francisco, CA, 11-15 December.
Gerritsen HG, Vos RJ, van der Kaaij Th, Lane A, Boon JG (2000). Suspended sediment modelling in a shelf sea (North Sea). Coastal Engineering 41, 317-352.
Gilson G (1900). Exploration de la mer sur les côtes de la Belgique en 1899. Mémoires du Musée Royal d'Histoire Naturelle de Belgique. Verhandelingen van het Koninklijk Natuurhistorisch Museum van België, I(2). Polleunis & Ceuterick: Bruxelles. 81 pp.
Guillén J, Bourrin F, Palanques A, Durrieu de Madron X, Puig P, Buscail R (2006). Sediment dynamics during wet and dry storm events on the Têt inner shelf (SW Gulf of Lion). Marine Geology 234, 129-142.
Gullentops F, Moens M, Ringele A, Sengier R (1976). Geologische kenmerken van de suspensie en de sedimenten. In: Nihoul, J., Gullentops, F. (Eds.), Project Zee-Projet Mer., vol. 4. Science Policy Office, Brussels, Belgium, pp. 1–137.
Hamm CE (2002). Interactive aggregation and sedimentation of diatoms and clay-sized lithogenic material. Limnology Oceanography 47, 1790–1795.

Hofland B, Christiansen H, Crowder RA, Kirby R, van Leeuwen CW, Winterwerp JC (2001). The current deflecting wall in an estuarine harbour. Proceedings of the XXIV IAHR Congress, Beijing, 242-250.

Holt JT, James ID (1999). A simulation of the southern North Sea in comparison with measurements from the North Sea Project Part 2 Suspended Particulate Matter. Continental Shelf Research 19, 1617-1642.

IMDC (2010). Langdurige monitoring van zout/zoet-verdeling in de haven van Zeebrugge en monitoring van zoutconcentratie, slibconcentratie en hooggeconcentreerde slibsuspensies in de Belgische kustzone. Deelrapport 8: Rapport over de aanwezigheid van HCBS lagen in de Belgische kustzone. I/RA/11292/07.038/JME, 192 pp.

IMDC (2011). Project Externe Effecten Deurganckdok. Deelrapport 1: Syntheserapport van het Current Deflecting Wall Onderzoek. I/RA/11354/10.063/MBO.

Inglis CC, Allen FH (1957). The regimen of the Thames Estuary as affected by currents, salinities, and river flow. Proceedings Institution Civil Engineering 7, 827–878.

Irion G, Zöllmer V (1999). Clay mineral associations in fine-grained surface sediments of the North Sea. Journal of Sea Research 41, 119–128.

Ishiguro S (1983). Storm surge prediction for the North Sea by the quasi uniform wind pressure field method. In North Sea dynamics: Edited by Sundermann J and Lenz W. Springer, Berlin, pp. 318–339.

Kineke GC, Sternberg RW, Trowbridge JH, Geyer WR (1996). Fluid mud processes of the Amazon continental shelf. Continental shelf research 16, 667-696.

Kirby R (2011). Minimising harbour siltation - findings of PIANC WorkingGroup 43. Ocean Dynamics 61, 233-244.

Kranenburg C (1994). On the fractal structure of cohesive sediment aggregates. Estuarine, Coastal and Shelf Sciences 39, 451-460.

Kuijper C, Christiansen H, Cornelisse J, Winterwerp JC (2005). Reducing harbour siltation. Part II: application to Parkhafen, Hamburg. ASCE Journal of Waterways, Ports, Coastal and Ocean Engineering 131, 267–276.

Lacroix G, Ruddick KG, Ozer J, Lancelot C (2004). Modelling the impact of the Scheldt and Rhine/Meuse plumes on the salinity distribution in Belgian waters (southern North Sea). Journal of Sea Research 52, 149-163.

Lacroix G, Ruddick K, Park Y, Gypens N, Lancelot C (2007). Validation of the 3D biogeochemical model MIRO&CO with field nutrient and phytoplankton data and MERIS-derived surface chlorophyll a images Journal of Marine Systems 64(1-4), 66-88.

Lafite R, Shimwell S, Grochowski N, Dupont J-P, Nash L, Salomon J-C, Cabioch L, Collins M, Gao S (2000). Suspended particulate matter fluxes through the Strait of Dover, English Channel: observations and modelling. Oceanologica Acta 23, 687–700.

Lafite R, Shimwell SJ, Nash LA, Dupont JP, Huault MF, Grochowski NTL, Lamboy, JM, Collins MB (1993). Sub-Task S1: Suspended material fluxes through the Strait of Dover, Hydrodynamics and Biogeo-chemical Fluxes in the Eastern Channel: Fluxes into the North Sea. FLUXMANCHE I Second annual report, MAST 0053-C (EDB), pp. 81-106.

Lancelot C, Mathot S (1987). Dynamics of a Phaeocystis-dominated spring bloom in Belgian coastal waters: 1. Phytoplanktonic activities and related parameters Marine Ecology Progress Series 37, 238-248.

Lanckneus J, Van Lancker V, Moerkerke G, Van den Eynde D, Fettweis M, De Batist M, Jacobs P (2001). Investigation of the natural sand transport on the Belgian continental shelf (BUDGET). Final report. Belgian federal public planning service Science policy (PPS Science policy), 104 pp. + Annex 87 pp.

Lauwaert B, Bekaert K, Berteloot M, De Backer A, Derweduwen J, Dujardin A, Fettweis M, Hillewaert H, Hoffman S, Hostens K, Ides S, Janssens J, Martens C, Michielsen T, Parmentier K, Van Hoey G, Verwaest T (2009). Synthesis report on the effects of dredged material disposal on the marine environment (licensing period 2008-2009). Report by BMM, ILVO, CD, aMT and WL BL/2009/01. 73 pp.

Le Bot S, Van Lancker V, Deleu S, De Batist M, Henriet JP (2003). Tertiary and quaternary geology of the Belgian Continental Shelf. Science Policy Office, Brussel, België. 75 pp.
Le Bot S, Van Lancker V, Deleu S, De Batist M, Henriet JP, Haegeman W (2005). Geological characteristics and geotechnical properties of Eocene and Quaternary deposits on the Belgian Continental Shelf: synthesis in the context of offshore wind farming Geologie Mijnbouw 84(2), 147-160.
Lee A J and Folkard A R 1969; Factors affecting turbidity in the southern North Sea. J. Cons. perm. int. Explor. Mer. 32(3), 291-302. in Eisma D and Kalf J (1979). Distribution and particle size of suspended matter in the southern Bight of the North Sea and the Eastern Channel. Netherlands Journal of Sea Research 13 (2), 298-324.
Le Hir P (1997). Fluid and sediment integrated modelling application to fluid mud flows in estuaries. Cohesive Sediments, proceedings INTERCOH '94.
Lentz SJ, Guza RT, Elgar S., Feddersen F, Herbers THC (1999). Momentum balances on the North Carolina inner shelf, Journal Geophysical Research 104, 18205–18226.
Li Y, Mehta AJ (2000). Fluid mud in the wave-dominated environment revisited. In: Coastal and Estuarine Fine Sediment Dynamics. (McAnally WH, Mehta AJ, eds.), Proceedings in Marine Science 3, 79-93.
Liu AC (1990). A seismic and geomorphological study of the erosion surface at the top of the Tertiary in the Southern North Sea (Belgian and Northern French sectors). Unpublished doctoral thesis Thesis, Gent University, vol. 1: 119 pp. + vol. 2: 97 fig. pp.
Maggi F (2005). Flocculation dynamics of cohesive sediment, PhD Thesis, University of Technology, Delft, 136 pp.
Manning AJ, Van Kessel T, Melotte J, Sas M, Winterwerp H, Pidduck EL (2011). On the consequence of a new tidal dock on the sedimentation regime in the Antwerpen area of the Lower Sea Scheldt. Continental Shelf Research 31, 150-164.
März J, Wirtz K (2009). Resolving physically and biologically driven suspended particulate matter dynamics in a tidal basin with a distribution based model. Estuarine, Coastal and Shelf Science 84 (1), 128 – 138.
März J, Verney R, Wirtz K, Feudel U (2010). Modeling flocculation processes: intercomparison of a size class-based model and a distribution-based model. Special Issue INTERCOH 2007.
Mathys M (2009). De Quartaire geologische evolutie van het Belgisch Continentaal Plat, zuidelijke Noordzee. The Quaternary geological evolution of the Belgian Continental Shelf, southern North Sea. PhD Thesis. Universiteit Gent. Faculteit Wetenschappen: Gent. xxiv, 382, annexes pp.
Missiaen T, Murphy S, Loncke L, Henriet J-P (2002). Very high-resolution seismic mapping of shallow gas in the Belgian coastal zone. Continental Shelf Research 22(16), 2291-2301.
Monbet Y (1992). Control of phytoplankton biomass in estuaries: A comparative analysis of microtidal and macrotidal estuaries. Estuaries 15(4), 563-571.
Mostaert F, Auffret JP, De Batist M, Henriet JP, Moons A, Sevens E, Van Den Broeke I, Verschuren M (1989). Quaternary shelf deposits and drainage patterns off the French and Belgian coasts. In: J.P. Henriet and G. De Moor (Editors), The Quaternary and Tertiary Geology of the Southern Bight, North Sea. Belgian Geological Survey, pp. 111-118.
Murray JMH, Meadows A, Meadows PS (2002). Biogeochemical implications of micro-scale interactions between sediment geotechniques and marine benthos: a review. Geomorphology 47, 15–30.
Nechad B, Van den Eynde D, Fettweis M, Francken F (2003). Suspended particulate matter mapping from multi-temporal SeaWiFS imagery over the southern North Sea - SEBAB project, in: Smits PC et al. (Ed.) (2004). Analysis of multi-temporal remote sensing images: Proceedings of the second international workshop on the Joint Research Centre Ispra, Italy 16-18 July 2003. pp. 357-367.

Nechad B, Ruddick KG, Park Y (2010). Calibration and validation of a generic multisensor algorithm for mapping of Total Suspended Matter in turbid waters. Remote Sensing of Environment 114 (4), 854-866.
Neukermans G, Ruddick K, Bernard E, Ramon D, Nechad B, Deschamps P-Y (2009). Mapping total suspended matter from geostationary satellites: a feasibility study with SEVIRI in the Southern North Sea Optics Express. International Electronic Journal of Optics 17(16), 14029-14052.
Nihoul J (1975). Effect of tidal stress on residual circulation and mud deposition in the Southern Bight of the North Sea. Review of Pure and Applied Geophysics 113, 577–591.
Nowell AR, Jumars PA, Eckman JE (1981). Effects of biological activity on the entrainment of marine sediments. Marine Geology 42, 133-153.
Odd NVM (1988). Mathematical modelling of mud transport in estuaries. In: Dronkers, J., van Leussen, W. (Eds.), Physical Processes in Estuaries. Springer-Verlog, Berlin, pp. 503–531.
PIANC 2008. Minimising harbour siltation, Report No 102, 75 pp.
Pietrzak J, de Boer G, Eleveld M (2011). Mechanisms controlling the intra-annual mesoscale variability of SST and SPM in the southern North Sea. Continental Shelf Research 31(6), 594-610.
Prandle D, Player R (1993). Residual currents through the Dover Strait measured by H.F. radar. Estuarine, Coastal and Shelf Science 37(6), 635-653.
Ruddick KG, Ovidio F, Rijkeboer M (2000). Atmospheric correction of SeaWiFS imagery for turbid coastal and inland waters Applied Optics 39(6), 897-912.
Schrottke K, Becker M, Bartholoma A, Flemming BW, Hebbeln D (2006). Fluid mud dynamics in the Weser estuary turbidity zone tracked by high resolution side-scan sonar and parametric sub – bottom profiler. Geo-marine Letters 26, 185-198.
Son M, Hsu T-J (2009). The effect of variable yield strength and variable fractal dimension on flocculation of cohesive sediment. Water Research 43, 3582-3592.
Stanev EV, Dobrynin M, Pleskachevsky A, Grayek S, Günther H (2009). Bed shear stress in the southern North Sea as an important driver for suspended sediment dynamics. Ocean Dynamics 59(2), 183-194.
Staneva J, Stanev EV, Wolff J-O, Badewien T, Reuter R, Flemming B, Bartholomä A, Bolding K (2009). Hydroynamics and sediment dynamics in the German bight. A focus on observations and numerical modelling in the East Frisian Wadden Sea. Continental Shelf Research 29, 302-319.
Stessels (1866). Carte générale des bancs de Flandre compris entr Gravelines et l'embouchure de l'Escaut. Ministre des affaires étrangères, Anvers, Belgium.
Terwindt JHJ (1967). Mud transport in the Dutch Delta area and along the adjacent coastline. Journal of Sea Research Netherlands, 3 (4) 505-531.
Toorman EA (2001). Cohesive sediment transport modeling: European perspective. Coastal and Estuarine Fine Sediment Processes, (McAnally WH & Mehta AJ, eds.), pp. 1-18, Proceedings in Marine Science Vol.3, Elsevier Science, Amsterdam.
Turner A, Millward GE (2002). Suspended particles: Their role in estuarine biogeochemical cycles. Estuarine, Coastal and Shelf Science 55, 857-883.
Uncles RJ, Stephens JA, Law DJ (2006). Turbidity maximum in the macrotidal, highly turbid Humber Estuary, UK: flocs, fluid mud, stationary suspensions and tidal bores. Estuarine, Coast and Shelf Sciences 67, 30–52.
Van Alphen JS (1990). A mud balance for Belgian–Dutch coastal waters between 1969 and 1986. Netherlands Journal of Sea Research 25, 19–30.
Van den Eynde D (2004). Interpretation of tracer experiments with fine-grained dredging material at the Belgian Continental Shelf by the use of numerical models. Journal of Marine Systems 48, 171-189.
van der Lee WTB (2001). Parameters affecting mud floc size on a seasonal time scale: the impact of a phytoplankton bloom in the Dollard estuary, The Netherlands, in: McAnally WH et al. (Ed.) (2001). Coastal and estuarine fine sediment processes. Proceedings in Marine Science 3, 403-421.

Van der Woerd H, Pasterkamp R (2004). Mapping of the North Sea Turbid Coastal Waters Using SeaWiFS data. Canadian Journal of Remote Sensing 30 (1), 44-53.

Van Lancker V, Deleu S, Bellec V, Du Four I, Schelfaut K, Verfaillie E, Fettweis M, Van den Eynde D, Francken F, Monbaliu J, Giardino A, Portilla J, Lanckneus J, Moerkerke G, Degraer S (2007). MAREBASSE: Bridging gaps with other disciplines and end-users. In: Science and sustainable management of the North Sea: Belgian case studies (Calewaert J-B, Maes F, eds.). Academia Press. 83-136.

Van Lancker V, Du Four I, Degraer S, Fettweis M, Francken F, Van den Eynde D, Devolder M, Luyten P, Monbaliu J, Toorman E, Portilla J, Ullmann A, Verwaest, T, Janssens J, Vanlede J, Vincx M, Rabaut M, Houziaux J-S, Mallaerts T, Vandenberghe N, Zeelmaekers E, Goffin A (2009). QUantification of Erosion /Sedimentation patterns to Trace the natural versus anthropogenic sediment dynamics (QUEST4D). Final Report Phase 1. Science for Sustainable Development, Belgian Science Policy, 135 pp.

Van Lancker V, Du Four I, Verfaillie E, Deleu S, Schelfaut K, Fettweis M, Van den Eynde D, Francken F, Monbaliu J, Giardino A, Portilla J, Lanckneus J, Moerkerke G, Degraer S (2007). Management, Research and Budgetting of Aggregates in Shelf Seas related to End-users (Marebasse). Belgian Science Policy: Brussel. 139 pp.

Van Lancker VRM, Deleu S, Bellec V, Le Bot S, Verfaillie E, Fettweis M, Van den Eynde D, Francken F, Pison V, Wartel S, Monbaliu J, Portilla J, Lanckneus J, Moerkerke G, Degraer S (2004). Management, Research and Budgeting of Aggregates in Shelf Seas related to End-users (Marebasse): Scientific Report Year 2 (01/04/2003 - 31/03/2004). Belgian Science Policy: Belgium. 144 pp.

van Leussen W (1994). Estuarine macroflocs and their role in fine-grained sediment transport. PhD thesis, Universiteit Utrecht, 488 pp.

van Maren DS, Winterwerp JC, Sas M, Vanlede J (2009). The effect of dock length on harbour siltation. Continental Shelf Research 29, 1410-1425.

van Maren DS, Winterwerp JC, Decrop B, Wang ZB, Vanlede J. 2011. Predicting the effect of a current deflecting wall on harbour siltation. Continental Shelf Research 31, 182-198.

Van Mierlo CJ (1899). La carte lithologique de la partie méridionale de la Mer du Nord. Bulletin de la Société Belge de Géologie, t., XIII.

Van Veen J (1936). Onderzoekingen in de Hoofden in verband met de gesteldheid der Nederlandse Kust, Nieuwe Verhandelingen van het Bataafse Genootschap voor Proefondervindelijke Wijsbegeerte te Rotterdam, 2e reeks, IIe deel. 252 pp.

Velegrakis AF, Michel D, Collins MD, Lafite R, Oikonomou EK, Dupont JP, Huault MF, Lecouturier M, Salomon JC, Bishop C (1999). Sources, sinks and resuspension of suspended particulate matter in the eastern English Channel. Continental Shelf Research 19(15-16), 1933-1957.

Verfaillie E, Van Lancker V, Van Meirvenne M (2006). Multivariate geostatistics for the predictive modelling of the surficial sand distribution in shelf seas. Continental Shelf Research 26(19), 2454-2468.

Verlaan PAJ, Groenendijk FC (1993). Long term pressure gradients along the Belgian and Dutch coast. MAST G8M report DGW-93.045, Rijkswaterstaat Tidal Waters Division.

Verlaan PAJ, Spanhoff R (2000). Massive sedimentation events at the mouth of the Rotterdam waterway. Journal of Coastal Research 16, 458-469.

Visser MP (1969). The turbidity of the Southern North Sea. Dtsch. hydrogr. Z. 23, 97-117.

Williams JJ, Rose CP, Rijn LC (1999). Suspended sediment concentration profiles in wave-current flows. Journal of Hydraulic Engineering 125 (9), 906-911.

Winterwerp JC (1999). On the dynamics of high-concentrated mud suspensions. PhD-thesis, Delft University of Technology, Faculty of Civil Engineering and Geosciences, Communications on Hydraulic and Geotechnical Engineering, Report No 99-3.

Winterwerp JC, Van Kesteren WGM (2004). Introduction to the physics of cohesive sediment in the marine environment. Developments in Sedimentology 56 (Elsevier, Amsterdam).
Winterwerp JC (2001). Stratification effects by cohesive and non-cohesive sediment. Journal of Geophysical Research 106 (C10), 22559-22574.
Winterwerp JC (2005). Reducing harbour siltation I: methodology. Journal of Waterway, Port and Coastal Ocean Engineering 131, 258–266.
Winterwerp JC, Bruens AW, Gratiot N, Kranenburg C, Mory M, Toorman EA (2002). Dynamics of concentrated benthic suspension layers, in: Winterwerp, JC et al. (Ed.) (2002). Fine sediment dynamics in the marine environment. Proceedings in Marine Science 5, 41-55.
Yang L (1998). Modelling of hydrodynamic processes in the Belgian Coastal Zone, Applied Mathematics. Catholic University of Louvain, Leuven, pp. 204.
Zeelmaekers E (2011). Computerized qualitative and quantitative clay mineralogy: introduction and application to known geological cases. PhD Thesis. Katholieke Universiteit Leuven. Groep Wetenschap en Technologie: Heverlee. ISBN 978-90-8649-414-9. XII, 397 pp.

Sediment mobility in response to tidal and wind-driven flows along the Belgian shelf, southern North Sea*

Matthias Baeye[1], Michael Fettweis[2], George Voulgaris[3], Vera Van Lancker[2]

[1]*Department of Geology and Soil Science, Renard Centre of Marine Geology (RCMG), Ghent University, Ghent, B-9000, Belgium*

[2]*Management Unit of the North Sea Mathematical Models (MUMM), Royal Belgian Institute of Natural Sciences, Brussels, B-1200, Belgium*

[3]*Department of Earth and Ocean Sciences, University of South Carolina, Columbia, SC 29208, USA*

*published in Ocean Dynamics (Springer)

M. Baeye processed and interpreted the datasets, wrote the manuscript and made all figures. Co-authors helped by reviewing the manuscript and/or providing the datasets. For the methodology of processing the datasets, assistance was given by G. Voulgaris.

Abstract

The effect of hydro-meteorological forcings (tidally- and wind-induced flows) on the transport of suspended particulate matter (SPM), on the formation of high-concentrated mud suspensions and on the occurrence of sand-mud suspensions has been studied using long-term multi-parametric observations. Data have been collected in a coastal turbidity maximum area (southern North Sea) where a mixture of sandy and muddy sediments prevails. Data have been classified according to variations in sub-tidal alongshore currents, with the direction of sub-tidal flow depending on wind direction. This influences the position of the turbidity maximum; as such also the origin of SPM. Winds blowing from the NE will increase SPM concentration, whilst SW winds will induce a decrease. The latter is related to advection of less turbid English Channel water, inducing a shift of the turbidity maximum towards the NE and the Westerscheldt estuary. Under these conditions, marine mud will be imported and buffered in the estuary. Under persistent NE winds, high-concentrated mud suspensions are formed and remain present during several tidal cycles. Data show that SPM consists of a mixture of flocs and locally eroded sand grains during high currents. This has implications towards used instrumentation: SPM concentration estimates from optical backscatter sensors will only be reliable when SPM consists of cohesive sediments only; with mixtures of cohesive and non-cohesive sediments, a combination of both optical and acoustic sensors are needed to get an accurate estimate of the total SPM concentration.

Keywords: Suspended particulate matter; mixed sediments; high-concentrated mud suspensions; alongshore sediment transport; acoustic and optical backscattering; southern North Sea

2.1. *Introduction*

In coastal areas benthic sediments generally consist of sand and mud mixtures. The mud:sand ratio influences the transition between cohesive and non-cohesive sediments and has a major influence on the erosion behaviour, on suspended particulate matter (SPM) concentration and on the benthic ecological properties (Williamson and Torfs 1996, Torfs et al. 1996, Panagiotopulos et al. 1997, Wallbridge et al. 1999, Flemming and Delafontaine 2000, van Ledden et al. 2004, Waeles et al. 2007, Van Hoey et al. 2007). Frequently, mixed sediments occur as an alternation of sand and mud layers. Fan et al. (2004) describe storm-induced waves as randomly occurring erosive forces on the sediment bed, producing intense sediment mobilization leading to the deposition of sand-dominated layers. This type of vertical segregation within the sedimentary record can only occur, if cohesive SPM concentration is relatively low. In case of high SPM concentration the segregation in sand/mud suspensions occurs when the initial mud concentration is smaller than its gelling point (Torfs et al. 1996). Cohesive SPM dynamics are complex and are affected by hydrodynamics, waves, wind, local and remote sediment availability (i.e. SPM sources), bed composition, biological processes, and human impact (Le Bot et al. 2010, Van Lancker et al. 2010). Further, in high-turbidity areas fluid mud layers may be formed. Fluid mud is a high-concentration suspension of fine-grained sediment in which settling is substantially hindered. Fluid mud consists of water, clay-sized particles, and organic materials; it displays a variety of rheological behaviours ranging from elastic to pseudo-plastic (McAnally et al. 2007). Massive sedimentation of fine-grained sediments in harbours and navigational channels is often related with the occurrence of fluid mud layers (Verlaan and Spanhoff 2000, Winterwerp 2005, PIANC 2008).
The inner shelf of the Belgian coast, located in the southern North Sea, is an example of an area where bed sediment composition varies from pure sand to pure mud (Verfaillie et al. 2006). It is characterized by elevated SPM concentrations (Fettweis et al. 2006) and has been the subject of high anthropogenic stresses due to harbour extension, dredging and disposal works, deepening of navigational channels and aggregate extraction (Du Four and Van Lancker 2008, Lauwaert et al. 2009, Van Lancker et al. 2010). Understanding of sediment distribution and mobility in such areas requires the use of multi-parametric observations. These should account for the mutual interaction of sand-mud mixtures as a function of bed armouring, size fraction, sheltering and exposure effects (Wiberg et al. 1994, Wallbridge et al. 1999, Wu et al. 2003).
With this scope in mind, in-situ measurements of SPM concentration and characteristics, as also of currents have been carried out, using optical and acoustic sensors. This approach has already been successfully adopted in various mixed sediment environments (e.g. Thorne and Hanes 2002, Fugate and Friedrichs 2002, Voulgaris and Meyers 2004). The objective of this contribution is to identify the effects of the various hydrodynamic forcings (tidal and wind-induced flows) on suspended sediment transport and on the formation of high-concentrated mud suspensions (HCMS) and fluid mud layers. Furthermore, the forcing and sedimentary responses are analyzed in terms of climatological parameters for the study site; as such the findings can be used for developing an understanding of the long-term evolution of the system, and potentially for inclusion in future morphodynamic models.

2.2. *Methodology*

2.2.1. *Study site*

Situated in the southern North Sea (Fig. 2.1 a), the Belgian nearshore is characterized by high-turbidity waters (Fig. 2.1 b). Nearshore SPM concentration ranges between 20–70 mg l^{-1} and reaches 100 to >3.000 mg l^{-1} near-bed; lower values (<10 mg l^{-1}) occur offshore (Fettweis et al. 2010). The measurement station BLA

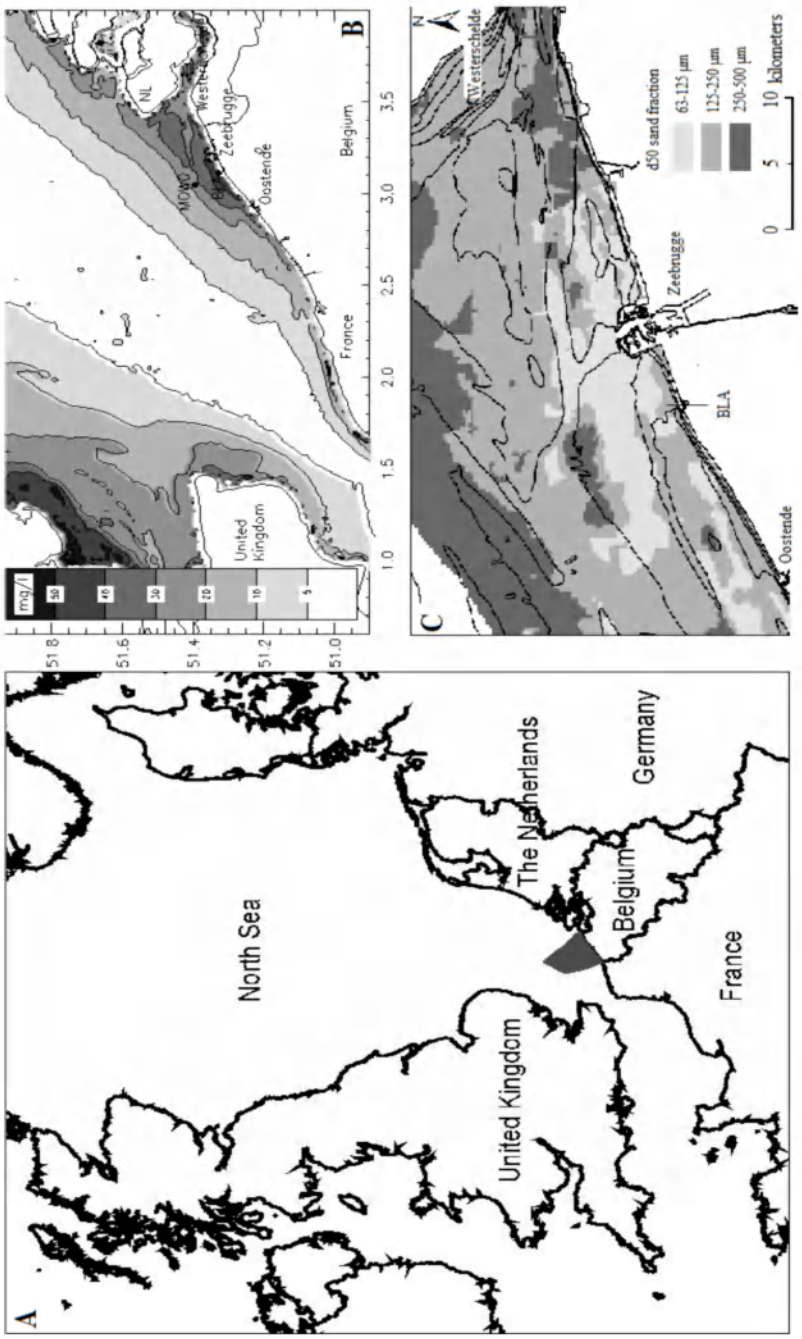

Figure 2.1 a *Map of southern North Sea, neighbouring countries and Belgian continental shelf (grey area);* ***b*** *map of the southern North Sea with the in-situ SM concentration measurement situation BLA and the meteorological station MOW0. The background consists of the yearly averaged surface SPM concentration (mg* l^{-1}*) from MODIS images (2003-2008);* ***c*** *map of d50 sand grain size (µm) in the region of interest (high-turbidity area between Ostend and the Westerscheldt*

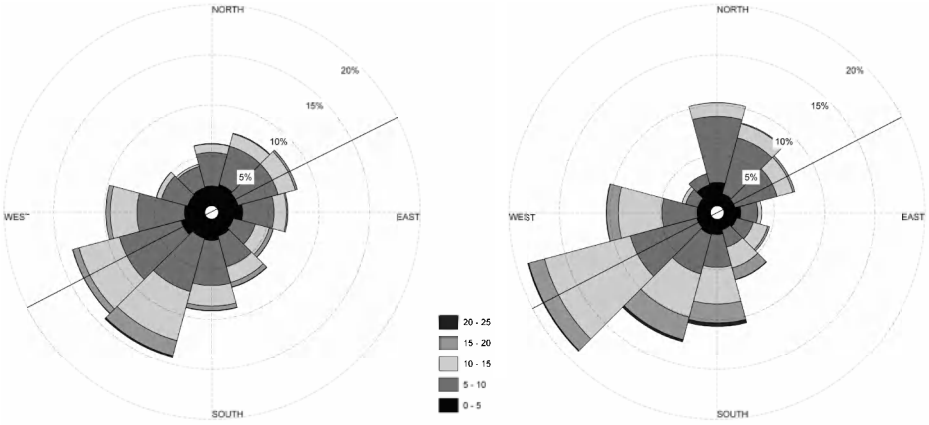

Figure 2.2 *Wind rose diagrams showing wind data over for 10 years (**left**) and wind data for the period of measurements (**right**). Values in m s^{-1}. Black line indicates coastline orientation at the measurement location (BLA)*

(Blankenberge) is situated about 5 km SW of the port of Zeebrugge and is located on the eastern part of a shoreface-connected sand ridge (Fig. 2.1 c). A coastal turbidity maximum zone (CTM) is present between Ostend and the mouth of the Westerscheldt (Fettweis et al. 2007). The BLA station is positioned in the TMZ. Sediment samples near BLA show variable sediment characteristics (fine sand, silt/clay), with a median grain size of the sand fraction of about 150 µm (Fig. 2.1 c). Tidal regime is semi-diurnal and the mean tidal range at Zeebrugge is 4.3 and 2.8 m at spring and neap tide, respectively. A wind rose diagram (Fig. 2.2, left diagram) shows data over a 10-years period, collected at station MOW0 (3.5 km away from BLA). Southwesterly winds dominate the overall wind climate, followed by winds from the N-NE sector. Maximum wind speeds coincide with the southwesterly winds; still, highest waves are generated under northwesterly winds.

2.2.2. Instrumentation

An instrumented tripod was deployed at a water depth of 5 m (location BLA, Fig. 2.1) to collect current, salinity and suspended sediment data. The instrumentation suite consisted of a 5 MHz SonTek^{R} Acoustic Doppler Velocimeter (ADVOcean-Hydra), a 3 MHz SonTek^{R} Acoustic Doppler Profiler (ADP), two DandA^{R} optical backscatter point sensors (OBS), Sea-bird^{R} SBE37 CT and a Sequoia Scientific^{R} Laser In-Situ Scattering and Transmissometer 100-X (LISST-100X, Type-C). All data (except LISST) were stored in two SonTek^{R} Hydra data logging systems. The OBS's were mounted at 0.2 and 2 meters above the bed (hereafter referred to as mab). The ADV velocities were measured at 0.2 mab, while the ADP profiler was attached at 2.3 mab and down-looking, measuring current and acoustic intensity profiles with a bin resolution of 0.25 m. Range of blank zone under ADP is 0.2 m. Mean values were obtained once every 10 min for the OBS, LISST, and ADV, while the ADP was set to record a profile every 1 min; later on averaging was performed to a 10 min interval to match the sampling interval of the other sensors. A total of 198 days of data have been collected, during 5 deployments, spanning autumn-winter 2006-07, winter 2008 and spring 2008 (Table 2.1). The long deployments have ensured accurate sampling of conditions that include complete periods of neap and spring tides, as well as the occurrence of a variety of meteorological events.

The voltage of the OBS was converted to SPM concentration by calibration against filtered water samples during several field campaigns (Fettweis et al. 2006). A linear regression between all OBS signals and SPM concentrations from filtration was assumed. Data from the LISST 100C (2 mab) have been analyzed only for the sediment grain size information.

Table 2.1 *Tripod deployments at BLA site and the median and maximum significant wave height (Hs) during the measurement period*

Start (dd/mm/yyyy hh:mm)	End ((dd/mm/yyyy hh:mm)	Duration (days)	Median (max) H_s (m)
8/11/2006 14:30	15/12/2006 08:30	36.7	0.83 (2.76)
18/12/2006 10:47	7/2/2007 13:17	50.1	0.79 (2.96)
28/01/2008 15:38	24/02/2008 13:18	26.9	0.44 (2.82)
6/3/2008 9:09	8/4/2008 15:29	33.7	0.76 (3.03)
15/04/2008 08:58	5/6/2008 7:48	51	0.46 (1.69)

Besides time-series of current velocities and acoustic amplitude, the ADV was configured to also measure and store the distance between sensor and boundary (i.e., seabed). The altimetry of the ADV was used to detect variation in bed level, as also for the identification of deposition and re-suspension of fine-grained sediments. For the study site, decreasing distance between probe and bed boundary can correspond to the presence of HCMS acting as an acoustic reflector. However, the boundary detection may fail, due to attenuation of the signal (Velasco and Huhta, App. Note).

2.2.3. Analysis of data

Current time-series (ADV and ADP) were filtered for the tidal signal using a low-pass filter for periods less than 33 hours (Rosenfeld 1983, Beardsley et al. 1985). Following, the velocity components were projected onto an along/cross-shore orthogonal coordinate system, with the positive alongshore axis oriented to the northeast (65°) and the positive cross-shore axis directed onshore, towards the southeast (155°).
The backscattered acoustic signal strength, from ADP, was also used to estimate SPM concentrations. After conversion to decibels, the signal strength was corrected for geometric spreading and water attenuation. Furthermore, an iterative approach (Kim et al. 2004) was used to also correct for sediment attenuation. The upper OBS-derived SPM concentration estimates were used to empirically calibrate the ADP's first bin. In general, the backscattering is affected by sediment type, size and composition. All are difficult to quantify by single-frequency backscatter sensors (Hamilton et al. 1998). Limitations associated with optical and acoustic instruments have been addressed in literature (Thorne et al. 1991, Hamilton et al. 1998, Bunt et al. 1999, Fugate and Friedrichs 2002, Vincent et al. 2003, Voulgaris and Meyers 2004). Briefly, the optical sensors tend to underestimate the coarser particles present in the water column. Acoustic devices produce better estimates of mass concentration than optical for the coarser fraction (Fugate and Friedrichs 2002).

Table 2.2 *Data grouping in terms of wind forcing cases 0, SWW and NEW and tidal range (neap and spring) for each wind forcing case*

Case	Subtidal flow (u_T)	Number of tidal cycles/%	Tidal range	Number of tidal cycles/%
Case 0 (tidal flow, no wind forcing)	$-0.05<u_t<0.05$ m s^{-1}	173/46	Neap	79/20.8
			Spring	94/24.7
Case SWW: (NE wind forcing)	$u_T<-0.05$ m s^{-1}	100/26	Neap	32/8.4
			Spring	68/17.9
Case NEW: (SW wind forcing)	$u_T>0.05$ m s^{-1}	107/28	Neap	58/15.3
			Spring	49/12.9
Total		380/100		380/100

The flow data have been used to separate the records in different groups corresponding to different hydrodynamic forcing. All records collected correspond to a total of 380 full semi-diurnal tidal cycles. For each tidal cycle the average value of the alongshore low-passed flow was estimated and subsequently used to characterize the tidal cycle in terms of wind-driven flow (Table 2.2). All tidal cycles with an alongshore low-passed flow ranging from -0.05 to 0.05 m s^{-1} are considered to represent purely

tidal forcing conditions; these are hereafter referred to as Case 0 conditions (total of 173 tidal cycles, 46% of data). All remaining tidal cycles (203 cycles) with a low passed alongshelf flow speed, in excess of 0.05 m s^{-1}, are assumed to correspond to periods with significant influence of wind-driven flows. Negative values correspond to flows towards the SW, driven by N-NE winds (Case SWW, total of 100 cycles), while positive subtidal flows, in excess of 0.05 m s^{-1} (107 cycles), are directed to the NE, corresponding to wind forcing from the SW (Case NEW). In addition to the above classification, each tidal cycle was classified as neap or spring, in terms of the tidal range of the particular cycle. Cycles with a tidal range greater than the mean range (3.6 m) are classified as spring tidal cycles, while cycles with a range less that 3.6 m as considered neap tidal ranges. This classification has resulted in a total of 6 categories of tidal cycles where each category represents both tidal and wind forcing. Tidal cycles, from each category, were ensemble-averaged to create a "typical" representative tidal cycle for each case. Following the methodology described in Murphy and Voulgaris (2006), the time of data collection from each tidal cycle was converted from absolute time to tidal phase within the cycle, using the local high water slack time as a reference time. Then data from each case, falling within the same bin (width of 10 min) of the tidal phase, were averaged and a mean cycle and associated standard error were calculated.

2.3. Results

2.3.1. Wind and tidal circulation data

Wind and wave data were collected by a buoy (Flemish Government, Maritime Services, Coastal Division), located at 4 km from the BLA measurement location. The overall wind conditions over a period of 10 years and during the period of data collection is shown in Fig. 2.2. Wind analyses clearly show that winds from the SW are the strongest and most commonly occurring for 33 % of the year. Cross-correlation with wave data, recorded by the buoy at water depth of 8 m MLLWS, indicates that these dominant winds from the SW coincide with an average wave height of 0.85 m and period of 4 s (Fig. 2.3).

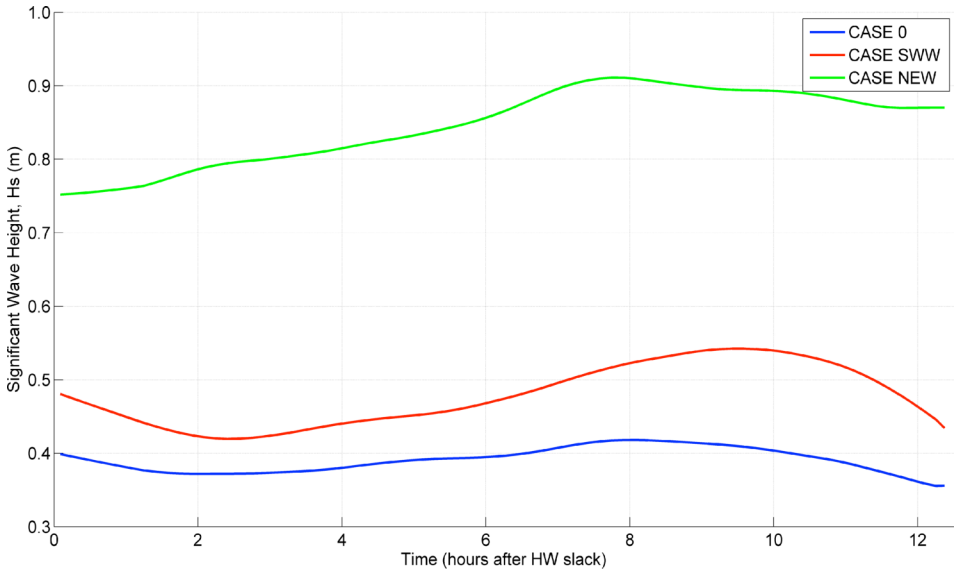

Figure 2.3 *Average significant wave height for the three cases under spring conditions. Highest waves occur in case NEW meteorological conditions*

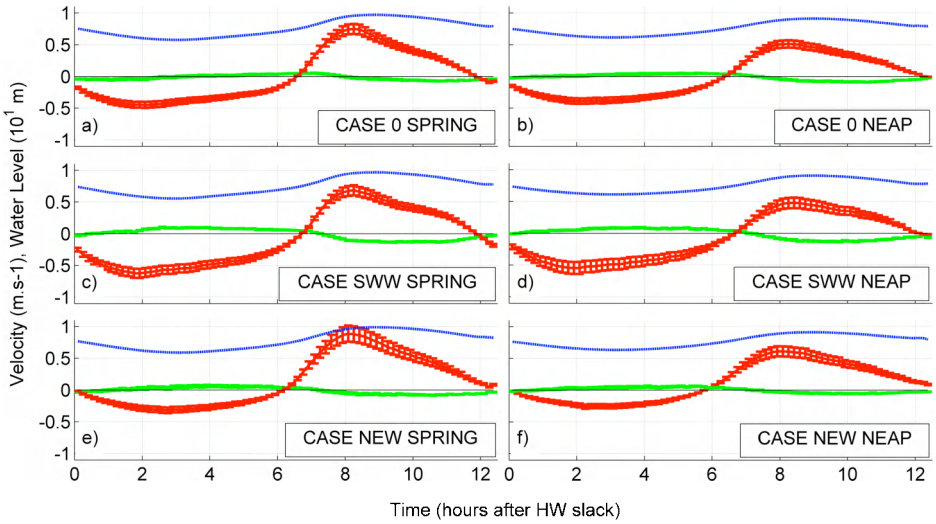

Figure 2.4 *Ensemble-averages of sea surface elevation (blue), alongshore (red) and cross-shore (green) currents derived from the ADP observations at 1.25 mab (m s^{-1}) for cases 0 (**a** and **b**), SWW (**c** and **d**) and NEW (**e** and **f**) and for spring (**left**) and neap (**right**) tidal range within each case. The error bars indicate standard error*

For the three cases, the spring–neap tidal cycles for the near-bed (1.25 mab) alongshore and cross-shore currents are shown in Fig. 2.4 a-f.
Overall, the cross-shore components are negligible, indicating a highly rectilinear current ellipse, aligned with the coastline. Tidal forcing in the study area (Case 0) is characterized by an asymmetry between ebb and flood. The maximum flood current is approximately 0.75 m s^{-1} and of short duration, while the ebb current peaks at 0.45 m s^{-1}, but persists longer in time; this is typical of asymmetrical tidal condition. Neap conditions show similar patterns in terms of asymmetry, but with reduced magnitudes. Although, wind forcing was defined in terms of tidally-averaged subtidal flow strength, the correlation between this flow and alongshore wind speed is used to check the assumption that these flows are predominantly (R^2=0.76) driven by the wind and not by baroclinic processes (Fig. 2.5). Case NEW corresponds with stronger winds than Case SWW, something expected given the wind patterns in this area (Fig. 2.2).

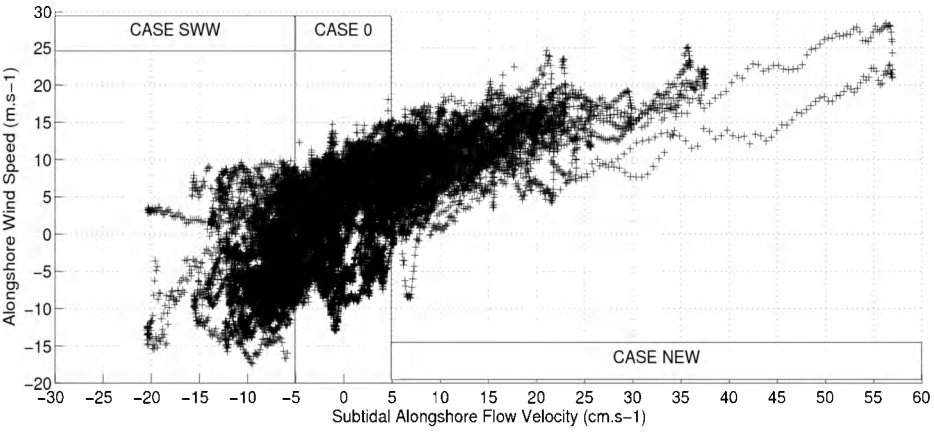

Figure 2.5 *Relationship between wind-induced flow in the alongshore direction and the alongshore wind component*

Examination of the tidal variability of the salinity records for each case reveals that overall salinity is highest (33) for Case NEW and lowest (30.5) for Case SWW (30.5); this indicates a higher riverine influence (Westerscheldt) in the latter case (Fig. 2.6 a-b). Steady winds bias the tidal forcing, because of the introduction of a wind-induced flow component. Fig. 2.4 (Case SWW) shows that prevailing northeasterly winds result in increased ebb (33%) and slightly reduced flood current (15%), compared with the tidal forcing (Case 0). These effects are most pronounced during spring tidal conditions. Southwesterly winds are the most common (Case NEW) and tend to bias the ebb-flood current pattern significantly (Fig. 2.4 e, f). Under spring conditions, the ebb current is reduced by 33 %, whereas the flood current is enhanced by 13 %.

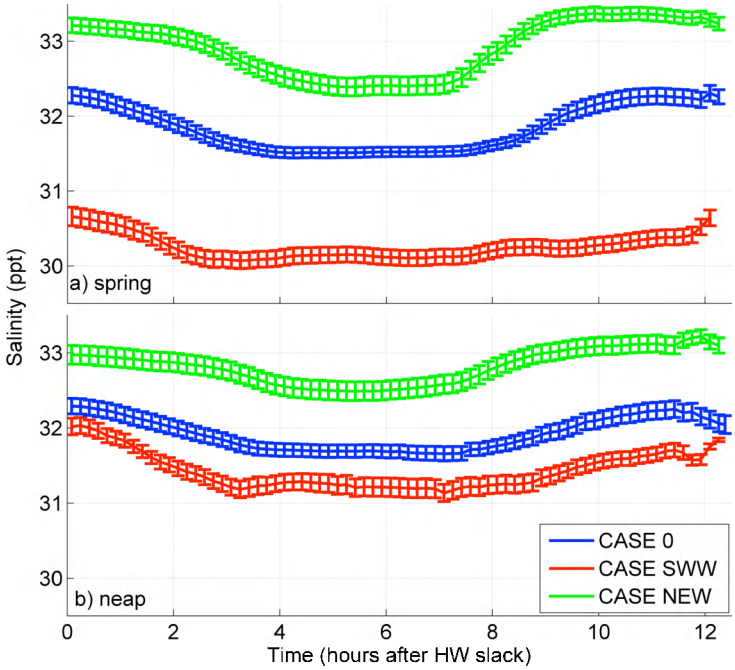

Figure 2.6 *Ensemble-averaged tidal variability of salinity measured at 1 mab for the three cases and for spring (upper) and neap (lower). The error bars indicate standard error*

2.3.2. SPM concentration and particle size

For the upper OBS (2 mab), the qualitative variation in SPM concentration is very similar for all cases (0, SWW, NEW). Generally, tidal variability is characterized by two local maxima, corresponding with ebb and flood flows, respectively, with the ebb maximum being lower than the one during flood (Fig. 2.7 a-f). The flood is characterized by a pronounced maximum, occurring at the beginning of the flood during spring tide and is due to re-suspension. This maximum is firstly detected at 0.2 mab and only later at 2 mab. The occurrence of such a time lag is well known and is related to the time necessary for vertical mixing (e.g. Bass et al. 2002).
In Cases 0 (Fig. 2.7 a, b) and NEW (Fig. 2.7 e, f) one can observe that around 2-3 hr and 9 hr, when current strength is high, a vertical stratification of SPM concentration, according the two measuring levels, is limited. Vertical stratification remains always significant in Case SWW (Fig. 2.7 c, d), with permanently higher SPM concentrations present in the lower level than in the upper level.
The three cases show distinct differences in SPM concentration at 0.2 mab. Case SWW exhibits different maxima in SPM concentration during ebb as well as flood, indicating multiple re-suspension events; whereas for Case NEW the SPM concentration maximum

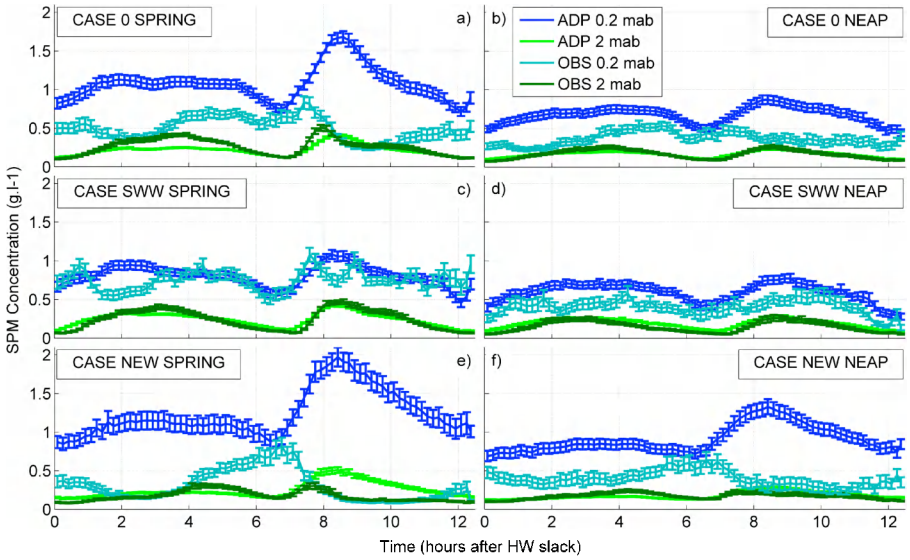

Figure 2.7 *Ensemble-averages of tidally varying SPM estimates from OBS and ADP at 0.2 (blue) and 2 mab (green). The error bars indicate standard error*

occurs at the end of the ebb and during slack water. The remaining time SPM concentration is relatively low.
SPM concentrations, derived from ADP, are also plotted in Fig. 2.7. SPM concentration at 2 mab is very similar to the concentration derived from OBS, except during flood in Case NEW. At 0.2 mab significant differences occur for Case 0 and NEW (spring tides), where the ADP signal gives significantly higher SPM concentrations than the OBS. Under neap conditions, the OBS and ADP SPM data coincide well. Case SWW shows for both spring and neap conditions similar SPM concentrations at 0.2 mab for the OBS and ADP. These differences between optical and acoustic sensors are suggesting variability in sediment size composition that leads to different responses by the different sensors, something we will discuss later.
In-situ particle sizes from LISST were classified and averaged per case (Fig. 2.8 a-f). Overall, the median particle size varies between 40 and 130 µm. The fact that highest particle sizes occur during slack water and lowest during maximum velocities indicate that the main part of the particles consists of flocs. The median floc size in Case SWW (Fig. 2.8 c, d) is reduced during slack water (about 70 µm vs. 100 µm in Case 0). Case NEW (Fig. 2.8 e, f) shows a distinct pattern with less pronounced particle size maxima. Higher standard error bars are because of more variable wave conditions occurring during Case NEW.

2.3.3. Seabed altimetry

Seabed level variations have been derived from ADV altimetry. Besides the general procedure of averaging and grouping, a reference level has also been introduced in order to obtain normalised altimetry data from the 5 different tripod moorings taking into account the tripod movement (pitch and roll) and the dilute settling of the tripod into the sediment right after deployment and during high-energy meteorological events. The data per Case (0, SWW, NEW) and per spring or neap condition are presented in Fig. 2.9 (a-f). The seabed level, on which the ADV acoustic signal reflects, might either consist of sandy material or strong SPM gradient when fluid mud or even HCMS is present.
For all cases (0, SWW, NEW), vertical bed level rises are associated with slack waters. Seabed rise is on average 5 cm, under spring conditions, whereas during neap tides only a few cm. Case SWW (Fig. 2.9 c, d) shows a clear seabed rise during the HW slack (around 12 hours).

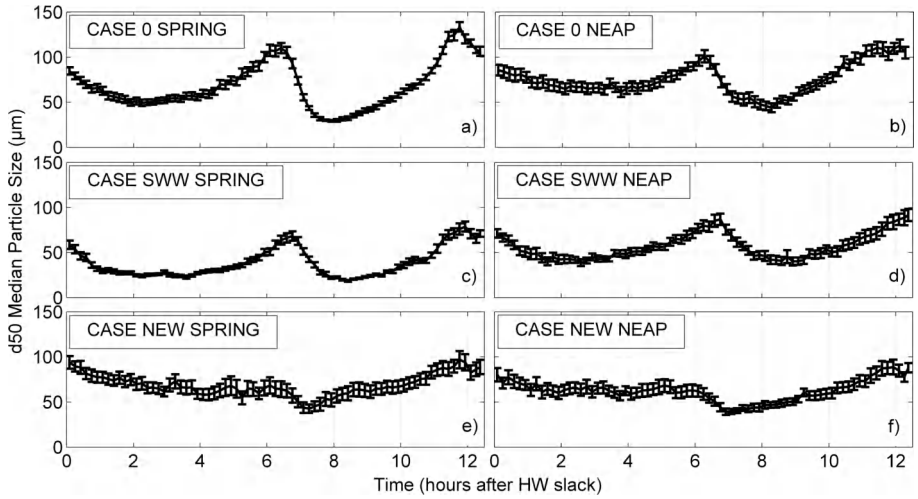

Figure 2.8 *Averaged median particle size as measured by the LISST 100X-type C. The error bars indicate standard error*

2.4. Discussion

Measurements show that near-bed hydrodynamics and sediment dynamics, although dominated by the tidal forcing, are significantly modified by wind-induced flows with different effects, depending on the wind direction. Below the effects of wind and tidally-driven circulation, as well as the distinct optical and acoustic response on varying SPM concentration and composition, are discussed in more detail. Further a conceptual sediment transport model is proposed for the area.

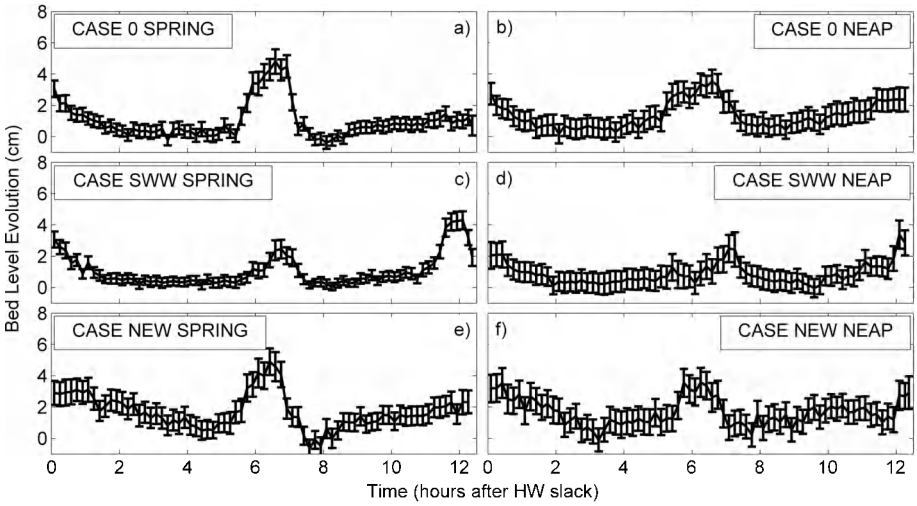

Figure 2.9 *Averaged seabed level variation derived from ADV altimetry with standard error bars*

2.4.1. General tidal and wind-driven circulation in the study area

The wind climate in the study area is characterized by mainly SW and NE winds (Fig. 2.2 left-right) affecting the direction and strength of alongshore water mass transport. Salinity records are used as a proxy to identify the source of water masses (Fig. 2.6 a-b). The salinity at the study site is mainly influenced by the Scheldt, Rhine and Seine

rivers (Lacroix et al. 2004) and has an overall tidally and seasonally averaged mean of 32.2, with a standard deviation of 1.1. This salinity varies as a function of the tidal cycle. For periods of limited wind forcing (Case 0) the mean salinity during ebb and flood amounts to 31.5 and 32.3, respectively. The mean salinity during periods associated with southwesterly winds (Case NEW) is about 33, indicating advection of oceanic water masses from the English Channel towards the study site. On the other hand, during periods of NE wind activity (Case SWW) the mean salinity reduces to 30.5, suggesting the influence of freshwater input, from mainly the Scheldt River, approximately 30 km away from the study site (Fig. 2.1).
SPM measurements, under tidal forcing only, show concentration maxima occurring at the end of ebb (5 hr) and at the beginning of flood (8hr). The latter is a result of re-suspension during maximum flood currents. The ebb-maxima are explained by the fact that the centre of the turbidity maximum is usually situated in ebb direction of the measurements. Hence, the maxima during ebb occur when, SPM concentrations advected from the centre of the turbidity maximum, have reached the measuring location. Neap tidal conditions show similar patterns, but with lower SPM concentrations. SPM measurements, from OBS, show that Cases SWW (flow from NE) and NEW (flow from SW) correspond with high and lower SPM concentrations, respectively, and show that the wind-driven alongshore advection has a significant influence on SPM concentration. Indeed, ocean water masses, advected into the coastal area (Case SWW), have generally lower SPM concentrations than the nearshore waters (Fettweis et al. 2010).
The ebb-flood tidal cycle is typically characterized by an increase and decrease in SPM concentration, driven by accelerating and decelerating currents, respectively. However, measurements indicate strikingly different SPM concentration behaviour near the bed (0.2 mab) between the three cases (Fig. 2.7 a-f). The water column in the Cases 0 (no wind-driven advection) and SWW (SW advection) is characterized by good vertical mixing, as can be seen in Fig. 2.7 (a, b, e, f) at about 2 and 9 hours, when SPM concentration at 0.2 and 2 mab are very similar. However, in Case NEW (advection from the SW) vertical mixing is sustained for a longer time interval (Fig. 2.7 e, f). The vertical mixing during wind-driven advection from the NE (Case SWW, Fig. 2.7 c, d) is limited during both spring and neap tidal conditions; this is probably the result of higher mud concentrations and the occurrence of HCMS (see also below); the latter functioning as a bigger reservoir of sediment to be re-suspended and thus maintaining a strong vertical gradient. The decreasing flows around 4 and 10 hours favour settling of particles and results in a decrease of SPM concentration at 2 mab. However, a continuous increase in SPM concentration at 0.2 mab is only present in Case NEW, where the maximum SPM concentration at 0.2 mab occurs around slack water. In Cases 0 and SWW, the SPM concentration decreases around LW slack and HW slack, indicating the formation of HCMS near the bed. An extract (doy 130 - 144) from the time-series (tripod mooring no. 5) of vertical distance between ADV sensor and seabed boundary is shown in Fig. 2.10. Quarter-diurnal peaks of bed level change occur during slack water and consist of HCMS. They easily reach 10 cm with maxima of 15 cm, and last for at least 50 minutes (maximum of 3 hours). The general seabed level on which these changes are superimposed is also changing in time. Around doy 136 – 140, a seabed level change occurs under Case SWW, spring conditions and persists over 4 days (~8 tidal cycles). This increase in bed level occurs during high vertical SPM concentration gradients and corresponds with the formation of HCMS.
In Case NEW the SPM concentration is lower and wave conditions on average higher, resulting thus in less favourable conditions for deposition. Depending on how much sediment was deposited during slack water, a SPM concentration peak in both OBS's is shown during Cases 0 and SWW (Fig. 2.7 c, d).

2.4.2. Nature of sediment in re-suspension

The nearshore area is characterized by the occurrence of fine sands (d50: 150 µm) and muds (Fettweis and Van den Eynde 2003), suggesting that mixed sediment transport occurs. The wind-driven sub-tidal flow towards the NE (Case NEW) increases the flood current on average by 13 % and decreases ebb currents by 33 %, compared to Case 0 (Fig. 2.4 a, b, e, f). The enhanced flood current is strong enough for

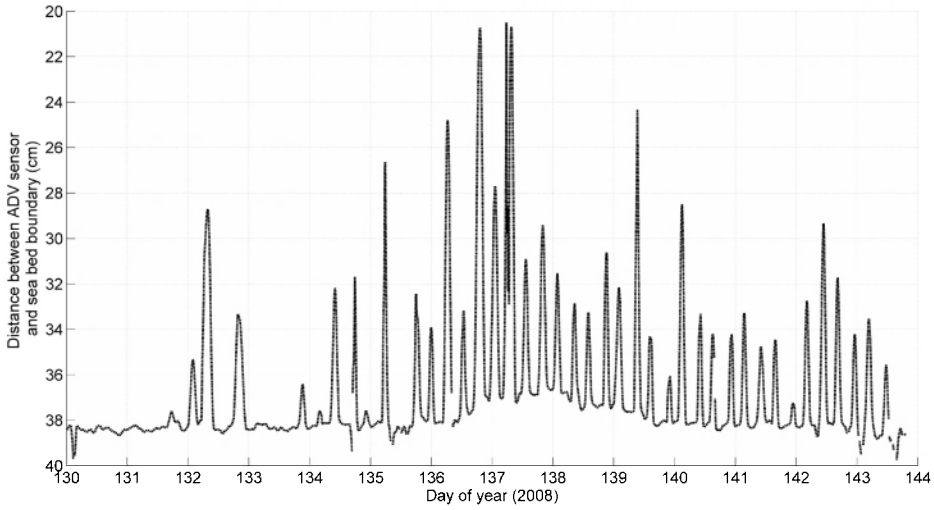

Figure 2.10 *Time-series of distance between ADV sensor and seabed boundary (centimetre). Peaks indicate periodic deposits (quarter-diurnal). Around 136–140, a longer persisting HCMS/mud layer is present*

re-suspension of the in-situ bed material. The measurements show that the OBS- and ADP-derived SPM concentrations are different, mostly during flood. Highest differences occur for Case NEW (Fig. 2.7 e, f), when flood currents are highest and reveal that SPM concentration, measured by the acoustic devices is significantly higher than by OBS. It is well known from literature that the OBS tends to underestimate the coarser particles in suspension (Bunt et al. 1999, Fugate and Friedrichs 2002, Vincent et al. 2003, Voulgaris and Meyers 2004, Downing 2006). This suggests that the higher SPM concentration, detected during flood, in the ADP is formed by the presence of fine sand in suspension. This is confirmed by the particle size data from the LISST (at 2 mab), showing a bimodal size distribution during maximum flood (Fig. 2.11).

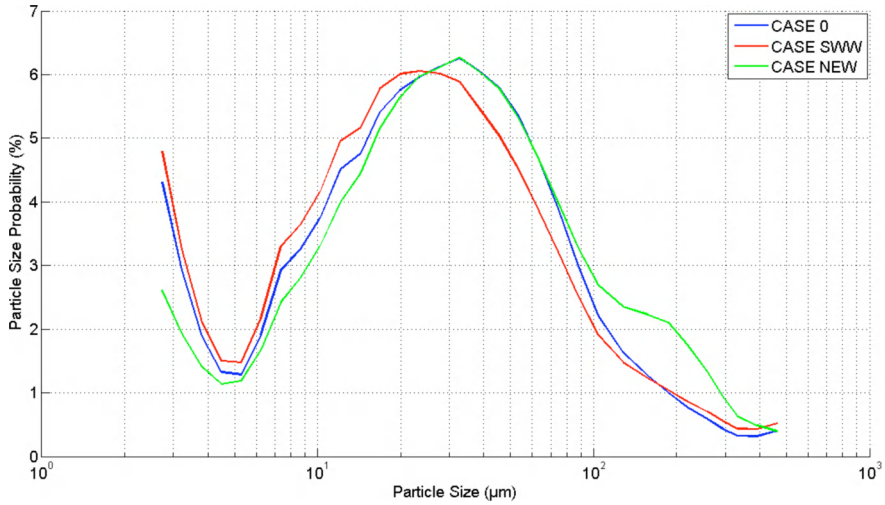

Figure 2.11 *Averaged particle size distributions around maximum flood current under spring conditions (8 h after HW slack, see Fig. 2.7). Remark the bimodal distribution in case NEW, with one maximum around 45 µm and another one around 150–200 µm. The latter is caused by the re-suspension of fine sand during strong flood currents*

The first mode is situated around 35 µm and corresponds with the typical size of flocs (Fettweis et al. 2006), whereas the second mode corresponds with the median grain size of the sand (150 µm). The rising tail at fine particle sizes is due to the presence of particles finer than the measuring range of the instruments (Agrawal and Pottsmith 2000). The fact that flood currents are higher, that SPM concentrations are lower, and that the water column is well-mixed during Case NEW, suggest that the parent bed (sand) is exposed and not covered with mud. The fact that the LISST does not detect sand-sized particles at 2 mab in the other cases suggests most probably that sand re-suspension is lower; this is confirmed by the generally lower peak currents and the fact that the bed is during longer periods covered by mud (see below). As such, the data suggest the occurrence of an 'inverse' bed armouring, where a layer of fine sediments prevents the erosion of coarser material. Sand transport in the turbidity maximum area is therefore mainly directed in flood direction, with the highest sand transport rates during a wind-driven advection towards the NE.

2.4.3. Conceptual SPM transport system

Altimetry data (Fig. 2.9 a-f and 2.10) show bed level variations that can be explained by the formation of HCMS. In Case 0 and NEW (Fig. 2.9 a, e) their occurrence is limited to slack water periods. The corresponding neap condition cases (Fig. 2.9 b, f) show a similar, however, reduced pattern, as re-suspension is lower. In Case SWW (Fig. 2.9 c, d and Fig. 2.10), the corresponding altimetry pattern suggests the occurrence of HCMS layers, persistent over several tides. Lower flood currents, together with higher SPM concentrations, a generally lower wave activity and a reduced vertical mixing strengthen the argument that a semi-permanent HCMS or mud layer is formed. The damping of turbulence by HCMS layers is a major mechanism maintaining these layers during longer time periods (Sheremet et al. 2005, Reed et al. 2009). Our data show that semi-permanent HCMS occur when the sub-tidal flow is directed towards the SW, mainly under NE wind forcing. These winds are not very frequent and their wind speeds are rather reduced. However, we believe that this type of benthic sediment transport is very important and has implications for object burial and sediment recirculation in and around the port (Fig. 2.1). In Case 0 and NEW, HCMS corresponds with deposition during slack water and re-suspension by ebb-flood currents. We conclude that the variability in HCMS and SPM concentration is also influenced by shifts in the location of the high turbidity maximum zone, which is controlled by the wind climate and thus alongshore advection. During Case NEW, the TMZ is situated more towards the northeast and corresponds with SW winds (most frequent wind sector). For these conditions, no continuous HCMS was found. The parent bed consisting of fine sands will be exposed and re-suspension of the parent bed can occur. Under these conditions, more marine fine-grained sediments are entering the Westerscheldt estuary. Indeed, the Westerscheldt cohesive sediments show a very strong marine signature (>80 %) (Van Alphen 1990, Verlaan 1998, 2000), suggesting that the estuary serves as a buffer of marine fine-grained matter (van der Wal et al. 2010). Part of these fine-grained sediments is permanently deposited in inter-tidal areas (Temmerman et al. 2003). The fact that under SW-directed sub-tidal flow, higher SPM concentrations are measured, suggests the outflow of marine sediments from the Westerscheldt. Fettweis and Van den Eynde (2003) proposed that the turbidity maximum was formed by congestion in the sediment transport along the coast. Our data suggest also that the River Scheldt functions as storage area of marine sediments, which are released into the sea under specific hydro-meteorological conditions (SWW flow).

2.5. Conclusions

A total of 198 days of in-situ data on SPM and currents have been collected in the coastal turbidity maximum area of the Belgian inner shelf. The measurements, made in autumn-winter 2006-2007 and winter-spring 2008, were averaged and classified into three cases, based on the direction and strength of subtidal advection. The main conclusions are:

1) Near bed hydrodynamics and SPM dynamics are predominantly dominated by tidal forcing. Generally, SPM concentration is significantly influenced by advection during ebb, whereas during flood local re-suspension is more important.
2) A significant modification of the tidal forcing results from alongshore advection due to wind-induced flows and influences the position of the turbidity maximum; as such also the origin of SPM. Winds persistently blowing from the NE will increase SPM concentration, due to an increased SPM outflow from the Westerscheldt estuary. SW winds will decrease SPM concentrations. The latter is related to the advection of less turbid English Channel water to the measuring location, inducing a shift of the turbidity maximum towards the NE and the Westerscheldt estuary. Under these conditions, marine mud will be imported and buffered in the estuary.
3) With prevailing NE winds, the increase in SPM concentration results in the formation of persistent HCMS. The results have indicated that these layers mostly remain present throughout the tidal cycle. Inverse armouring occurs, as the sandy bed is sheltered from erosion. SPM consists of cohesive sediments only.
4) In case of tidal influence and SW prevailing winds, HCMS occur only around slack water. SPM consists of a mixture of cohesive sediments (flocs) and locally eroded sand grains during high currents.
5) Regarding instrumentation, it is shown that SPM estimates from OBS are only reliable when SPM consists of cohesive sediments only; with mixtures of cohesive and non-cohesive sediments, a combination of optical (OBS) and acoustic sensors (ADP, ADV) are needed to get an accurate estimate of the total SPM concentration.

2.6. *Acknowledgements*

The study was partly funded by Belgian Science Policy (Science for a Sustainable Development, QUEST4D, SD/NS/06A) and partly by the Maritime Access Division of the Ministery of the Flemish Community (MOMO project). G. Dumon (Ministery of the Flemish Community, Maritime Services, Coastal Division/Hydrography) made available wind and wave measurement data. We want to acknowledge the crew of RV Belgica, Zeearend and Zeehond for their skilful mooring and recuperation of the tripod. Measurements would not have been possible without technical assistance of A. Pollentier, J.-P. De Blauwe, and J. Backers (Measuring service of MUMM, Oostende). The first author acknowledges a specialisation grant from IWT (Agency for Innovation by Science and Technology, Flanders).

2.7. *References*

Bass SJ, Aldridge JN, McCave IN, Vincent CE (2002). Phase relationships between fine sedimens suspensions and tidal currents in coastal seas. Journal of Geophysical Research 107, C10-3146.

Bunt JAC, Larcombe P, Jago CF (1999). Quantifying the response of optical backscatter devices and transmissometers to variations in suspended particulate matter. Continental Shelf Research 19, 1199-1220.

Downing J (2006). Twenty-five years with OBS sensors: The good, the bad, and the ugly. Continental Shelf Research 26, 2299-2318.

Du Four I, Van Lancker V (2008). Changes of sedimentological patterns and morphological features due to the disposal of dredge spoil and the regeneration after cessation of the disposal activities. Marine Geology 255, 15-29.

Fan D, Li C, Wang P (2004). Influences of storm erosion and deposition on rhythmites of the upper Wenchang Formation (Upper Ordovician) around Tonglu, Zhejiang province, China. Journal Sedimentary Research 74, 527-536.

Fettweis M, Van den Eynde D (2003). The mud deposits and the high turbidity in the Belgian-Dutch coastal zone, Southern bight of the North Sea. Continental Shelf Research 23, 669-691.
Fettweis M, Francken F, Pison V, Van den Eynde D (2006). Suspended particulate matter dynamics and aggregate sizes in a high turbidity area. Marine Geology 235, 63-74.
Fettweis M, Nechad B, Van den Eynde D (2007). An estimate of the suspended particulate matter (SPM) transport in the southern North Sea using SeaWiFS images, in-situ measurements and numerical model results. Continental Shelf Research 27, 1568-1583.
Fettweis M, Francken F, Van den Eynde D, Verwaest T, Janssens J, Van Lancker V (2010). Storm influence on SPM concentrations in a coastal turbidity maximum area with high anthropogenic impact (southern North Sea). Cont Shelf Res 30, 1417-1427.
Flemming BW, Delafontaine MT (2000). Mass physical properties of muddy intertidal sediments: some applications, misapplications and non-applications. Continental Shelf Research 20, 1179-1197.
Fugate DC, Friedrichs CT (2002) Determining concentration and fall velocity of estuarine particle populations using ADV, OBS and LISST. Continental Shelf Research 22, 1867-1886.
Hamilton LJ, Shi Z, Zhang SY (1998). Acoustic backscatter measurements of estuarine suspended cohesive sediment concentration profiles. Journal of Coastal Research 14, 1213-1224.
Lacroix G, Ruddick K, Ozer J, Lancelot C (2004). Modelling the impact of the Scheldt and Rhine/Meuse plumes on the salinity distribution in Belgian waters (southern North Sea). Journal of Sea Research 52, 149–163.
Lauwaert B, Bekaert K, Berteloot M, De Backer A, Derweduwen J, Dujardin A, Fettweis M, Hillewaert H, Hoffman S, Hostens K, Ides S, Janssens J, Martens C, Michielsen T, Parmentier K, Van Hoey G, Verwaest T (2009). Synthesis report on the effects of dredged material disposal on the marine environment (licensing period 2008-2009). MUMM, ILVO, CD, aMT, WL report BL/2009/01, 73 pp.
Kim HY, Gutierrez B, Nelson T, Dumars A, Maza M, Perales H, Voulgaris G (2004). Using the acoustic Doppler current profiler (ADCP) to estimate suspended sediment concentration. Technical Report CPSD #04-01.
Le Bot S, Lafite R, Fournier M, Baltzer A, Desprez M (2010). Morphological and sedimentary impacts and recovery on a mixed sandy to pebbly seabed exposed to marine aggregate extraction (eastern English Channel, France). Estuarine, Coastal and Shelf Sciences 89, 221-233.
McAnally WH, Friedrichs C, Hamilton D, Hayter EJ, Shrestha P, Rodriguez H, Sheremet A, Teeter A (2007). Management of fluid mud in estuaries, bays, and lakes. Present state of understanding on character and behavior. Journal of Hydraulic Engineering 133, 9-22.
Murphy S, Voulgaris G (2006). Identifying the role of tides, rainfall and seasonality in marsh sedimentation using long-ter, suspended sediment concentration data. Marine Geology 227, 31-50.
Panagiotopoulos I, Voulgaris G, Collins MB (1997). The influence of clay on the threshold of movement of fine sandy beds. Coastal Engineering 32, 19-43.
PIANC (2008). Minimising harbour siltation, Report No 102, 75 pp.
Reed AH, Faas RW, Allison MA, Calliari LJ, Holland KT, O'Reilly SE, Vaughan WC, Alves A (2009). Characterization of a mud deposit offshore of the Patos Lagoon, southern Brazil. Continental Shelf Research 29, 597-608.
Sheremet A, Mehta AJ, Liu B, Stone GW (2005). Wave-sediment interaction on a muddy inner shelf during Hurricane Claudette. Estuarine, Coastal and Shelf Science 63, 225-233.
Temmerman S, Govers G, Meire P,Wartel S (2003). Modelling long-term tidal marsh growth under changing tidal conditions and suspended sediment concentrations, Scheldt estuary, Belgium. Marine Geology 193, 151-169.
Torfs H, Mitchener H, Huysentruyt H, Toorman E (1996). Settling and consolidation of mud/sand mixtures. Coastal Engineering 29, 27-45.

Thorne PD, Hanes DM (2002). A review of acoustic measurement of small-scale sediment processes. Continental Shelf Research 22, 603-632.
Thorne PD, Vincent CE, Hardcastle PJ, Rehman S, Pearson ND (1991). Measuring suspended sediment concentrations using acoustic backscatter devices. Marine Geology 98, 7-16.
van der Wal D, van Kessel T, Eleveld MA, Vanlede J (2010). Spatial heterogeneity in estuarine mud dynamics. Ocean Dynamics 60, 519-533.
Van Hoey G, Vincx M, Degraer S (2007). Temporal variability in the Abra alba community determined by global and local events. Journal of Sea Research 58, 144-155.
Van Lancker VRM, Bonne W, Bellec V, Degrendele K, Garel E, Brière C, Van den Eynde D, Collins MB, Velegrakis AF (2010). Recommendations for the sustainable exploitation of tidal sandbanks. Journal of Coastal Research 51, 151-164.
Van den Eynde D (2004). Interpretation of tracer experiments with fine-grained dredging material at the Belgian Continental Shelf by the use of numerical models. Journal of Marine Systems 48, 171-189.
van Ledden M, van Kesteren WGM, Winterwerp J (2004). A conceptual framework for the erosion behaviour of sand-mud mixtures. Continental Shelf Research 24, 1-11.
Velasco DW, Huhta CA. Experimental verification of acoustic Doppler velocimeter (ADV) performance in fine-grained, high sediment concentration fluids. App Note SonTek/YSI.
Verfaillie E, Van Meirvenne M, Van Lancker V (2006). Multivariate geostatistics for the predictive modelling of the surficial sand distribution in shelf seas. Continental Shelf Research 26, 2454-2468.

Verlaan PAJ, Spanhoff R (2000). Massive sedimentation events at the mouth of the Rotterdam waterway. Journal of Coastal Research 16, 458-469.
Vincent CE, Bass SJ, Rees JJ (2003). Uncertainties in suspended sediment concentration and transport due to variations in sediment size. Proc Coastal Sediments, Clearwater FL, May 2002, 10 pp.
Voulgaris G, Meyers S (2004). Temporal variability of hydrodynamics, sediment concentration and sediment settling velocity in a tidal creek. Continental Shelf Research 24, 1659-1683.
Waeles B, Le Hir P, Lesueur P, Delsinne N (2007). Modelling sand/mud transport and morphodynamics in the Seine river mouth (France): an attempt using a process-based approach. Hydrobiology 588, 69-82.
Wallbridge S, Voulgaris G, Tomlinson BN, Collins MB (1999). Initial motion and pivoting characteristics of sand partlicles in uniform and heterogeneous beds: experiments and modeling. Sedimentology 46, 17-32.
Wiberg PL, Drake DE, Cacchione DA (1994). Sediment re-suspension and bed armoring during high bottom stress events on the northern California inner continental shelf: measurements and predictions. Continental Shelf Research 14, 1191-1219.
Williamson H, Torfs H (1996) Erosion of mud/sand mixtures. Coast Engineering 29, 1-25.
Winterwerp JC (2005). Reducing harbour siltation I: methodology. Journal of Waterway, Port, Coastal and Ocean Engineering 131, 258–266.
Wu B, Molinas A, Shu A (2003). Fractional transport of sediment mixtures. International Journal of Sedimentary Research 18, 232-247.

Spatio-temporal variation of surface suspended particulate matter concentration in the Belgian-Dutch coastal zone*

Matthias Baeye[1], Michael Fettweis[2], Bouchra Nechad[2], Vera Van Lancker[2]

[1] Ghent University, Renard Centre of Marine Geology, Krijgslaan 281 (S8), 9000 Gent, Belgium

[2] Royal Belgian Institute of Natural Science, Management Unit of the North Sea Mathematical Models, Gulledelle 100, 1200 Brussels, Belgium

*submitted for publication in Estuaries and Coasts (Springer)

M. Baeye handled and interpreted the datasets (SPM maps and time-series), wrote the manuscript and made all figures. Co-authors helped by reviewing the manuscript and/or providing the datasets (MODIS-SPM maps were made available by MUMM/REMSEM team). M. Fettweis carried out entropy analysis of MODIS-SPM spatial data.

Abstract

Suspended particulate matter (SPM) concentration maps, derived from satellite remote sensing (MODIS-Aqua) data, were evaluated for their use in the assessment of coastal turbidity maximum (CTM) dynamics in Belgian coastal waters. The CTM is a dynamic coastal feature of which the geographic position and extent varies under different meteorological, astronomical and climatological conditions. Analyses were based on grouping-averaging of SPM concentration maps, using different classification schemes. To better spatially depict the CTM, entropy grouping was introduced. This technique analyses, per pixel, the total information contained within the probability distribution of SPM concentration. Results revealed wind-induced variations in position and extent of the CTM, with southwesterly winds inducing a largest CTM extent, in contrast to a strong reduction under northeasterly winds. Climate-induced variations were assessed contrasting 2 winters with opposing indices of the North Atlantic Oscillation (NAO). In a winter with a positive NAO index, hence stronger-than-average southwesterly winds, the CTM was extended to the Dutch waters, whereas the opposite occurred in winters with a negative NAO index, hence less-than-average southwesterly winds. To evaluate astronomical forcing (tides) grouping-averaging was performed of SPM concentration maps over a tidal cycle, and spring-neap conditions. Although, only part of the tidal cycle can be analysed, due to the sun-synchronicity of the MODIS-Aqua satellite, comparison of the results with in-situ data from a single observatory station showed good resemblance. It is concluded that MODIS-Aqua satellite data can be used to assess SPM concentration variability related to tides, neap-spring cycles, meteorological and climatological events.

Keywords: Coastal turbidity maximum; MODIS-Aqua; wind climate; tides; entropy analysis; NAO

3.1. Introduction

Mapping of suspended particulate matter (SPM) concentration from satellite imagery has become a valuable source of data to assess and monitor SPM concentration distribution (Trisakti et al. 2005, Nechad et al., 2010). These satellite data have been used in various ways and have been combined with in-situ measurements (van Raaphorst et al. 1998, Ruhl et al. 2001, Fettweis et al., 2007), sediment transport models (Vos and Gerritsen 1997, Pleskachevsky et al. 2005, Blaas et al., 2007), or have been used in the light forcing of ecosystem models (Lacroix et al., 2007). SPM dynamics control processes such as sediment transport, deposition, re-suspension and primary production and the functioning of benthic communities (McCandliss et al. 2002, Murray et al. 2002). It varies as a function of harmonic forcings such as tides, spring-neap tidal cycles and seasons, and random events such as storms or human activities. The interaction of cohesive and non-cohesive sediments, biological activity, remote or local availability of fine sediments and advective processes further influences SPM concentration (Velegrakis et al. 1997, Bass et al. 2002, Schoellhamer 2002, Le Hir et al. 2007, Fettweis et al. 2010).
The inner shelf of the Belgian coast, located in the southern North Sea, is an example of an area where bed sediment composition varies from pure sand to pure mud (Verfaillie et al. 2006). It is characterized by elevated SPM concentrations (Fettweis et al. 2010) and has been subject of high anthropogenic stresses due to harbour extension, dredging and disposal works and deepening of navigation channels (Du Four and Van Lancker 2008). Effects of various hydrodynamic forcings (tidal and wind-induced flows) on suspended sediment transport has been investigated, based on in-situ data; these indicated that a modification of the hydrodynamic forcing and thus SPM concentration results from alongshore advection, due to wind-induced flows (Baeye et al. 2011, see also Chapter 4). Such Eulerian in-situ measurements indicated that the position of the coastal turbidity maximum, and as such also the origin of SPM changed according to predominant wind directions. Variations in horizontal gradients should ideally be measured with techniques having a high geographical and temporal coverage, hitherto not or only partially available (Neukermans et al. 2009, Sirjacobs et al. 2011).
Wide swath polar-orbiting ocean colour remote sensors such as MODIS-Aqua have been used successfully to assess seasonal and intra-annual SPM concentration variability (Fettweis et al. 2007, Eleveld et al. 2008, Pietrzak et al. 2011). The long term time-series of MODIS-data for some locations in the southern North Sea reveal clearly the dominant seasonal signal (Nechad et al. 2010). However, irregular and shorter-term variations, not directly linked to seasons, can also be identified in these time-series. The aim of this paper is to investigate these random variations by linking them to typical meteorological, climatological and tidal conditions in the time and spatial domain. Such findings allow a separation and recognition of processes that control their variability and can be used for understanding the long-term evolution of the system, and potentially for prediction of future (climate-induced) changes. Further, the possible use of MODIS-Aqua imagery to assess SPM concentration variability related to tides, neap-spring cycles, and meteorological and climatological events is evaluated and compared to in-situ measurements of SPM concentration.

3.2. Environmental setting

3.2.1. Coastal turbidity maximum

The study area is located in the southern North Sea, comprising the Belgian-Dutch coastal waters and the mouth of the Westerscheldt estuary (Fig. 3.1). Water depths vary between 3 and 15 m MLLWS (Mean Lowest Low Water Spring) with shallow sand ridges, gullies and navigation channels that result in an overall complex, and irregular bathymetry (Fig. 3.1). The seabed consists of sands mainly; however, a Holocene mud plate exists between Zeebrugge and Ostend (Mathys 2009). The coastal environment is not associated with an aggradational shelf from river output; the most important sources of SPM are the erosion of nearshore Holocene and recent mud deposits, the French rivers discharging into the English Channel, and the coastal erosion of the

Cretaceous cliffs at Cap Gris-Nez and Cap Blanc-Nez (France) (Fettweis et al. 2007, Zeelmaekers 2011). The Westerscheldt estuary is considered a storage for mud, rather than a source of SPM (Van Maldegem et al. 1993, Verlaan et al. 1998, see also Chapter 2). Cohesive sediments are trapped in the coastal turbidity maximum (CTM), due to tidal forcing and flocculation of SPM. Hydrodynamic and meteorological forcings cause a congestion of the residual transport in the area. Elongated tidal ellipses, with strong tidal currents and relatively long slack waters (about 1 hour), stimulate flocculation and break-up and thus settling and re-suspension of fine-grained material.

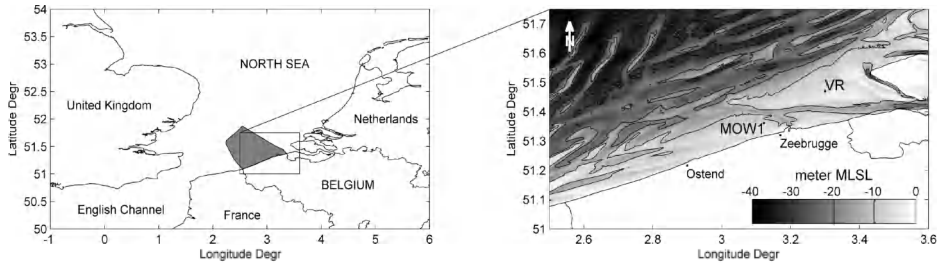

Figure 3.1 *Study area location in the southern Bight of the North Sea (**left**). Depths (every 10 m) in meters Mean Low Sea Level, and the location of the in-situ observatory station (MOW1) and the Westerscheldt estuary mouth (VR) (**right**)*

The astronomical tides are semi-diurnal with an average range of 4.3 m (2.8 m) at spring (neap) tide at Zeebrugge. Overall, residual water transport is from southwest to northeast. Further, the complex, irregular bathymetry, together with the freshwater discharges, also influences the mean circulation, the residual transport field and the spreading of the freshwater in the coastal zone (Arndt et al., 2011). Strong tidal currents (up to 1 $m.s^{-1}$) lead to a relatively well-mixed water column in the coastal zone, with salinity varying between 28 and 34, due to wind-induced advection of water masses and river discharges (Yang 1998, Lacroix et al. 2004).

3.2.2. Weather and climate

The continental coasts in the southern North Sea are subjected to a large scale west to east circulation of depressions, and to the development or weakening of high pressure systems. These fluctuations of the wind field occur at time scales of a few days to one week (Wieringa and Rijkoort 1983, Delhez and Carabin 2001). Onshore NW winds are associated with mid-latitude low-pressure systems causing high sea surges, mainly during winter periods (Ulman and Monbaliu 2010). Southwesterly winds dominate the wind regime for the decade 2001-2010, followed by northeasterly winds (Fig. 3.2 a). An increase in the frequency of west-southwesterly winds over the last decades is observed (Siegismund and Schrum 2001, Van den Eynde et al. 2011). On a global scale, the North Atlantic Oscillation (NAO) is responsible for much of the observed weather and climate variability, especially during winter months (December through March) (Hurrell 1995, Hurrell and Deser 2009). This wintertime NAO exhibits significant multi-decadal variability with positive values indicating anomalously strong westerly winds and wet conditions over northwestern Europe, whereas negative values exhibit weaker westerly flow and less precipitation (Hurrell 1995, Chelliah and Bell 2004).

3.3. Methodology

3.3.1. MODIS SPM concentration

The Moderate Resolution Imaging Spectro-radiometer (MODIS) onboard the Aqua satellite, part of the NASA Earth Observation System (EOS), provides 1 to 2 daily images over the North Sea area. These data are used to build up daily maps of SPM concentration. 2539 MODIS images, covering 9 year between July 2002 and December 2009, have been processed from Level 1A (NASA/Ocean Biology Processing Group

website, http://oceancolor.gsfc.nasa.gov/cgi/browse.pl?sen=am) to Level 2, using the SeaDAS software (available at http://oceancolor.gsfc.nasa.gov/seadas/). This consists of 2 steps: producing the Level 1B data by geo-referencing Level 1A data, and subtracting the atmospheric contributions by air molecules and aerosols from the radiances measured by the sensor at the top of the atmosphere; these yield the L2 data, where marine reflectances, ρ_w ("$_w$" referring to water), at MODIS bands may be obtained. Surface SPM concentration (further referred to as "SPM concentration") is then retrieved from Rrs (remote sensing reflectance) at MODIS central band wavelength 667 nm, using the algorithm of Nechad et al. (2010): SPM = 362.1 * ρ_w / (1 - ρ_w / 0.17). Finally, Level 2 processing flags (Patt et al. 2003) are used to mask out the land and cloud pixels and any bad quality pixel (e.g. due to atmospheric correction failure, negative reflectance neighbouring clouds, adjacency effects).

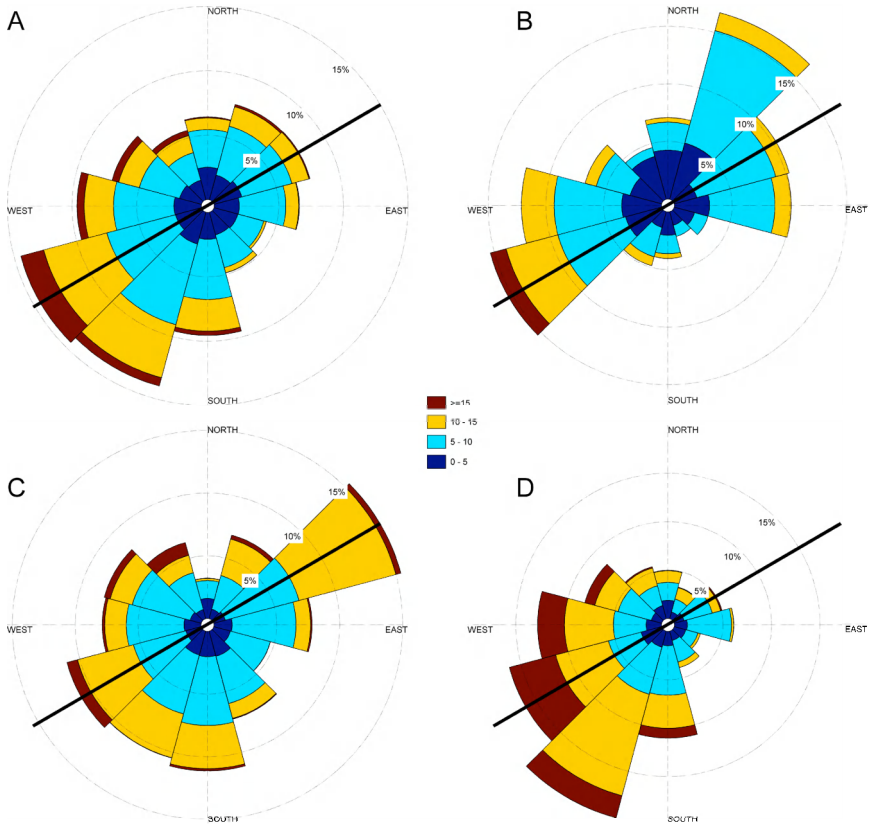

Figure 3.2 a *Wind rose diagrams (meteorological convention "wind blowing from") with coastline orientation for the period 2001-2010.* ***b*** *Idem, for MODIS-Aqua cloud-free data images, at time of satellite overpass.* ***c*** *Idem, for negative NAO winter 2005/6 and* ***d*** *for positive NAO winter 2006/7. Wind speed in m* s^{-1}

3.3.2. Classification and statistics of SPM concentration maps

To assess tidal, neap-spring cycles, meteorological and climatological effects on SPM concentration, different classification of SPM concentration maps have been carried out. The 2539 MODIS SPM concentration maps have been classified according to neap and spring tide, and each map was assigned to its corresponding intra-tidal phase, based on the time of MODIS-Aqua overpass (12:00-13:00 GMT). This was achieved through 3 steps:

a. The tidal cycles were equally divided in 12 time intervals (~1 hour interval),
b. Each tidal cycle was classified as neap or spring, based on the mean tidal range at Zeebrugge (3.6 m).

Cycles with tidal range greater than the mean range are classified as spring tides, whereas cycles with range less than 3.6 m are considered as neap tides. The SPM concentration maps were assigned neap or spring maps, based on the corresponding tidal cycles. Therefore, this classification scheme has resulted in 24 categories of SPM concentration maps, where each category represents both the semi-diurnal and fortnight tidal forcing. Per category, all maps were averaged to create a representative SPM concentration map for each case.
Meteorological effects have been addressed by classifying the satellite maps according to the wind regime, recorded at the meteorological station at Zeebrugge at the moment of MODIS-Aqua overpass. This classification was performed following four wind sectors which were defined, based on the overall wind climate measured over a decade (Fig. 3.2 a):

a. sector around SSW is the most abundant wind sector (here after referred to as SSW case),
b. the second wind sector comprises winds blowing from the NNE (NNE case),
c. the third wind sector encompasses winds from mainly the WNW (WNW case),
d. and finally land winds being the less abundant (ESE case).

Further, climatological impact has been investigated using the North Atlantic Oscillation (NAO) indices for winter SPM concentration maps. The NAO Index Data were provided by the Climate Analysis Section, NCAR, Boulder, USA, Hurrell (1995). The NAOWI (December through March) time-series exhibits two consecutive winters with opposite NAOWI index within the period of MODIS-Aqua data collection: -1.09 in winter 2005/6; and 2.79 in winter 2006/7.
For each ensemble of SPM concentration maps, an average SPM concentration map was obtained. As a result, the coastal turbidity maximum and its position along the coast are evaluated, based on the highest SPM concentration occurrences. More enhanced statistical approaches were introduced by means of entropy analysis, allowing better spatial characterization of the turbidity maximum. Entropy analysis is a statistically robust technique for grouping geographic data (Johnston and Semple 1983). Here, entropy groupings are used to categorize surface SPM concentration data ensembles (wind and NAO winter cases), taking into account the total information contained within the probability distribution curve of SPM concentration at every pixel (at which at least 100 data points exist; if not pixel is left blank). This analysis was carried out with the routine of Johnston and Semple (1983). Seven entropy groups of minimum relative entropy are used to characterize SPM concentration distribution for the entire study area; entropy groups 1 to 5 are distributions that are skewed towards lower concentrations, group 6 is intermediate, and the 7th entropy grouping (with highest median SPM concentration, and a rather normal distribution) defines the geographical extension of the coastal turbidity maximum (see 3.4.1). The entropy analysis defines the CTM area based on statistical properties rather than on absolute values; this allows comparing the geographical extension of the CTM for different wind or climatological situations.

3.3.3. In-situ SPM measurements

SPM concentration distribution in the water column was measured, in-situ, with Optical Backscatter Sensors (OBS), mounted on a water sampler and CTD (conductivity, temperature, depth) frame and on a benthic tripod. The latter was deployed in water depths of 9 m MLLWS at MOW1 station (Fig. 3.1, right). Time-series of SPM concentration were recorded at 2 m (OBS-SPM1) above the seabed (mab) for a total of ~260 days. At the MOW1 location, 16 ship-borne measurements (e.g. water and CTD profiling) were carried out during 1 tidal cycle (about 13 h). Water samples were filtered and residues were weighted in order to calibrate the OBS's of both the benthic and the CTD frame (OBS-SPM2). In-situ SPM concentrations were grouped similarly as the satellite images: per tidal phase and per spring or neap cycle. These were compared with the tidal phase averaged surface SPM concentrations, derived from MODIS at the measuring station MOW1.

3.4. Results

3.4.1. Average SPM concentration

In Fig. 3.3 a, an average SPM concentration map, based on all SPM concentration images, showed a CTM between Zeebrugge and Ostend with a maximum SPM concentration of about 50 mg l^{-1}. Offshore, SPM concentrations were reduced (<10 mg l^{-1}). The entropy CTM group (7, black coloured region in Fig. 3.3 b) defined the CTM as an area that stretches from Ostend to the Dutch-Belgian border (about 40 km), with a median SPM concentration of 33 mg l^{-1} (Table 3.1); the corresponding probability distribution of the SPM concentration was normally distributed, unlike the other groups (Fig. 3.3 c). Probability distributions of SPM concentration for the 6 other groups were skewed towards the smaller SPM concentrations.
Only 20% of all SPM concentration maps corresponded with cloud-free conditions at MOW1 pixel. The wind under these conditions (Fig. 3.2 b) was compared to the overall wind rose over the last decade (Fig. 3.2 a) showing globally weaker winds, with more NE and less NW and SSW winds. Therefore, the average surface SPM concentration map (based on all SPM concentration images) is more biased towards this weather regime.

3.4.2. Average surface SPM concentration under different meteorological forcings

SPM concentration maps for the 4 wind cases (SSW, NNE, WNW and ESE) had different spatial extensions of the CTM (Fig. 3.4). SSW wind case corresponded with the largest CTM, including the mouth of the Westerscheldt estuary. This contrasted to the NNE wind case where the coastal turbidity maximum was reduced to a small area between Zeebrugge and Ostend. The ESE wind case corresponded with a maximal alongshore extent of the CTM towards France. Median SPM concentrations of entropy group 7, for each wind case, are given in Table 3.1; they indicate that SPM concentration in the CTM is the lowest for wind case WNW.

Table 3.1 *SPM concentrations (mg l^{-1}) for the entropy group 7 (CTM), for each case*

CASE	MEDIAN SPM mg l^{-1}
ALL	33
SSW	29
WNW	25
NNE	31
ESE	32
$NAOWI^-$	43
$NAOWI^+$	35

3.4.3. Average surface SPM concentration for contrasting winter situations

The winter of 2006/7 ($NAOWI^+$) corresponded to significant SW winds, whereas the winter of 2005/6 ($NAOWI^-$) was characterized by abundant NE winds (Fig. 3.2 c, d). This is reflected in the geographical distribution of the CTM shown in the associated SPM concentration, and entropy grouping maps (Fig. 3.5). The CTM during positive NAO winter conditions had shifted significantly towards the NE and was absent in front of Ostend. A negative NAO winter coincided with a CTM extending over nearly all the Belgian coast, up to the mouth of the Westerscheldt. Median SPM concentrations during $NAOWI^-$ were higher (43 mg l^{-1}) than during $NAOWI^+$ (35 mg l^{-1}) (Table 3.1).

3.4.4. Average surface SPM concentration for different hydrodynamic conditions

The influence of tides and neap-spring cycles on surface SPM concentration is shown in Fig. 3.6. Remark that during neap and spring tide only 7 of the 12 cases are represented. Data are centered around low water (LW) during neap tide and around high water (HW) during spring tide. SPM concentration was generally higher during

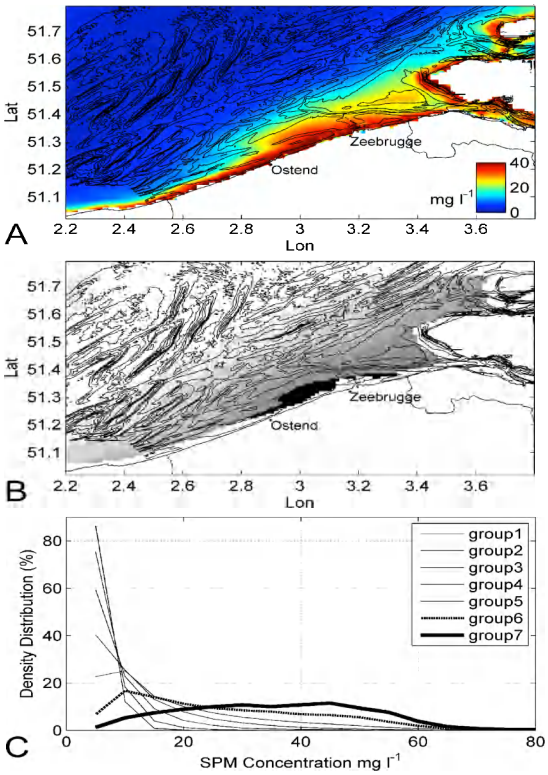

Figure 3.3 a *Surface SPM map, as an average of all MODIS-Aqua data images.* ***b*** *Surface SPM map, obtained from entropy analysis grouping SPM concentrations in 7 classes. Black coloured class (group 7) corresponds to the actual CTM and* ***c*** *Corresponding probability distribution curves of SPM concentration*

spring tide than neap tide. Highest SPM concentrations occurred at 4 hours before HW (HW-4, i.e. 2-3 hours after LW). During flood the CTM shifted towards the mouth of the Westerscheldt estuary.
The tide-induced variation in the MODIS images has been compared with in-situ data at MOW1, measured at 2 meters above bottom (mab) and near the surface (Fig. 3.7 a, c). A tidal ellipse at MOW1 (Fig. 3.7 b, d) shows that maximum ebb and flood currents occurred at LW and HW, respectively. A peak in SPM concentration at 2 mab occurred around HW and LW, with the highest SPM concentration (600 mg l^{-1}) around LW. Lowest SPM concentrations at 2 mab (100 mg l^{-1}) were observed around slack water (HW-3 and HW+3). Surface maxima and minima in SPM concentration (in-situ and MODIS) occurred later than the maxima and minima at 2 mab, due to a settling and re-suspension time lag. Although the MODIS SPM concentration curves were incomplete for both neap and spring conditions, in-situ minima/maxima in SPM concentration correlated well with near-surface data.

3.5. *Discussion*

3.5.1. *Evaluation of the use of MODIS*

Satellite data reveal variations in surface SPM concentration in the CTM resulting from tidal, neap-spring tidal cycle, meteorological and climatological forcings. The most pronounced cycle is related to seasonal variations and is well described in literature (Fettweis et al. 2007, Van den Eynde et al. 2007, Pietrzak et al. 2011). Winter SPM concentrations are a factor 2 higher than summer concentrations; although SPM concentration can vary during different winter periods, depending on climatological conditions. Influences of spring-neap cycles are clearly identified in both the in-situ

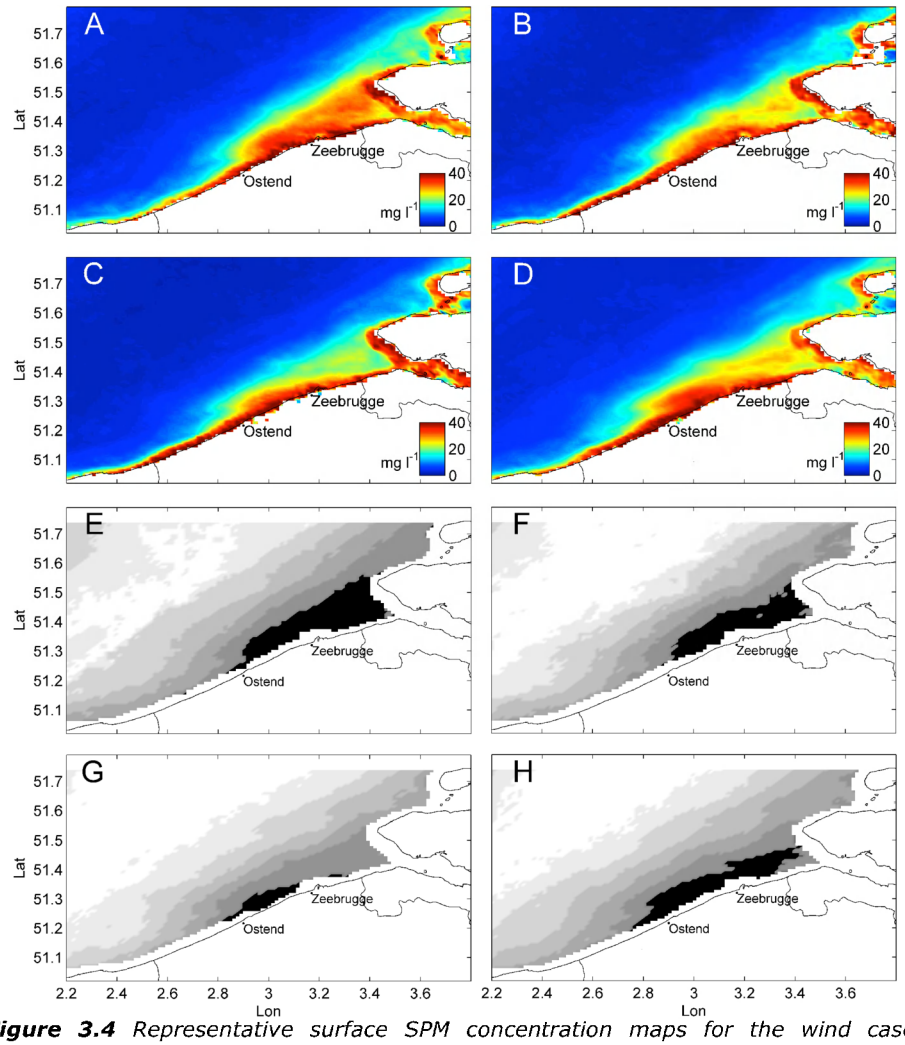

Figure 3.4 *Representative surface SPM concentration maps for the wind cases obtained from grouping-averaging MODIS-Aqua data images: SSW (**A**), WNW (**B**), NNE (**C**), ESE (**D**). Entropy grouping maps for the wind cases: SSW (**E**), WNW (**F**), NNE (**G**), ESE (**H**)*

data (Chapter 2; Baeye et al. 2011), and MODIS data. SPM concentration measured at the surface corresponds to events of re-suspension, mixing, settling and deposition.
For the relative shallow MOW1 location, a time lag of about 1 hour was identified between maximum SPM concentration near the bed (in-situ data) and at the surface (satellite), which corresponds well with literature (Bass et al. 2002). In deeper water the time lag is longer, which is also reflected in the general lower surface SPM concentration in the deeper areas, such as the navigation channel towards the Westerscheldt, situated in the CTM.
MODIS-Aqua cannot be used to gather data during a whole tidal cycle for spring and neap tides (Doxaran et al. 2009, van der Wal et al. 2010). This is a result of the 24 h sampling interval of the MODIS-Aqua which is 0.84 h shorter than the 24.84 h period of the diurnal tide. Every 15 days the same phase of the tide is sampled, corresponding to the periodicity of the spring – neap cycles. As a result, parts of the tidal cycle in relation to spring-neap tides are not captured by sun-synchronous satellites, such as MODIS-Aqua. Therefore, when grouping SPM concentration maps (per season, per wind case, per month etc.) followed by ensemble-averaging, the resulting SPM concentration maps inherently incorporate under-sampling. In-situ data

show that SPM concentration is highest during LW at spring tides; a tidal phase that is never measured by MODIS-Aqua in the study area. The latter, together with the fact that satellite images consist of a subset of the population, biased towards good weather condition or spring–summer seasons (Fettweis and Nechad 2011), explain also the lower SPM concentrations found in the satellite images when comparing to in-situ data. Surface sediment transport or light infiltration in turbid waters, based on these data, will thus always underestimate reality.

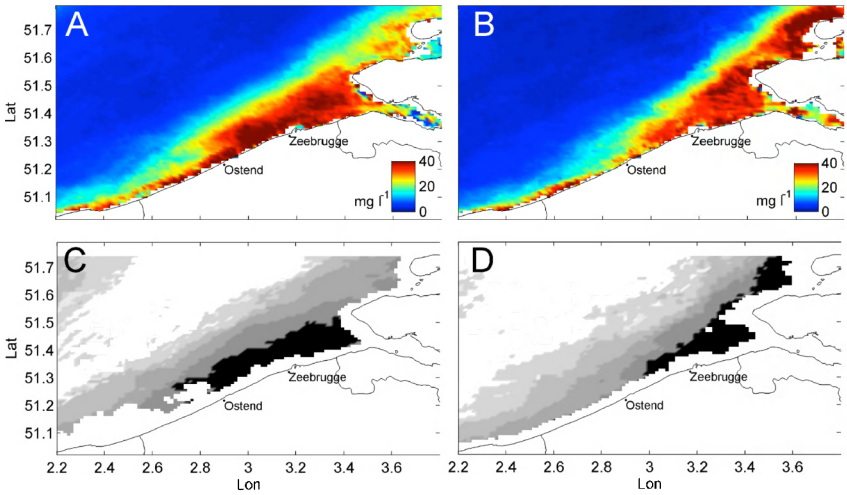

Figure 3.5 *Representative surface SPM concentration maps for two contrasting winters: NAOWI- (2005/6) (**A**) and NAOWI+ (2006/7) (**B**) and the corresponding entropy grouping maps (**C**) and (**D**), respectively*

3.5.2. Wind-induced CTM dynamics

Variability of SPM concentration is evaluated using the coefficient of variations (CV), which is calculated from the ratio of the standard deviation of SPM divided by SPM concentration (Fig. 3.8 a). Lower CV is associated to areas with a rather low relative SPM concentration variability, such as the CTM zone. Two areas can be identified: one with a slightly higher CV, corresponding to the mouth of the Westerscheldt and the Vlakte van de Raan and the other with slightly lower CV situated between Ostend and Zeebrugge. The latter area shows high SPM concentrations more often than the former area. This was already pointed out by Nechad et al. (2003) and Van den Eynde et al. (2007); however, without providing a convincing explanation. Current analyses relate this different behaviour to wind-induced alongshore advection of the CTM zone. For instance, the area of the mouth of the Westerscheldt estuary and the Vlakte van de Raan has, e.g. lower SPM concentrations during NE-E wind conditions (Fig. 3.4 c, g).
Fig. 3.3 shows also that the area between Ostend and Zeebrugge has high SPM concentrations during all wind conditions. The role of alongshore advection of water masses has been investigated, based on near-bed in-situ data from a station near Zeebrugge (Baeye et al., 2011). Data have shown that winds blowing from the SW are inducing a subtidal alongshore flow towards the NE bringing less turbid and more saline waters originating from the Strait of Dover towards the CTM. Higher SPM concentration waters are extending more towards the NE up to the mouth of the Westerscheldt (Fig. 3.4 a, f). Prevailing NE winds reverse the subtidal alongshore flow resulting in a decrease of salinity near Zeebrugge, due to an enhanced outflow of the Scheldt estuary (Arndt et al. 2011). The latter is associated with an increase of SPM concentration near Zeebrugge and the formation of high concentrated mud suspensions (HCMS) near the bed (Baeye et al. 2011). This is in contrast with the satellite images, which have on average lower surface SPM concentrations in the area between Zeebrugge and the mouth of the Westerscheldt under NNE winds. Differences between remote sensing and in-situ datasets underline that near bed SPM concentration dynamics is partially uncoupled from processes higher up in the water

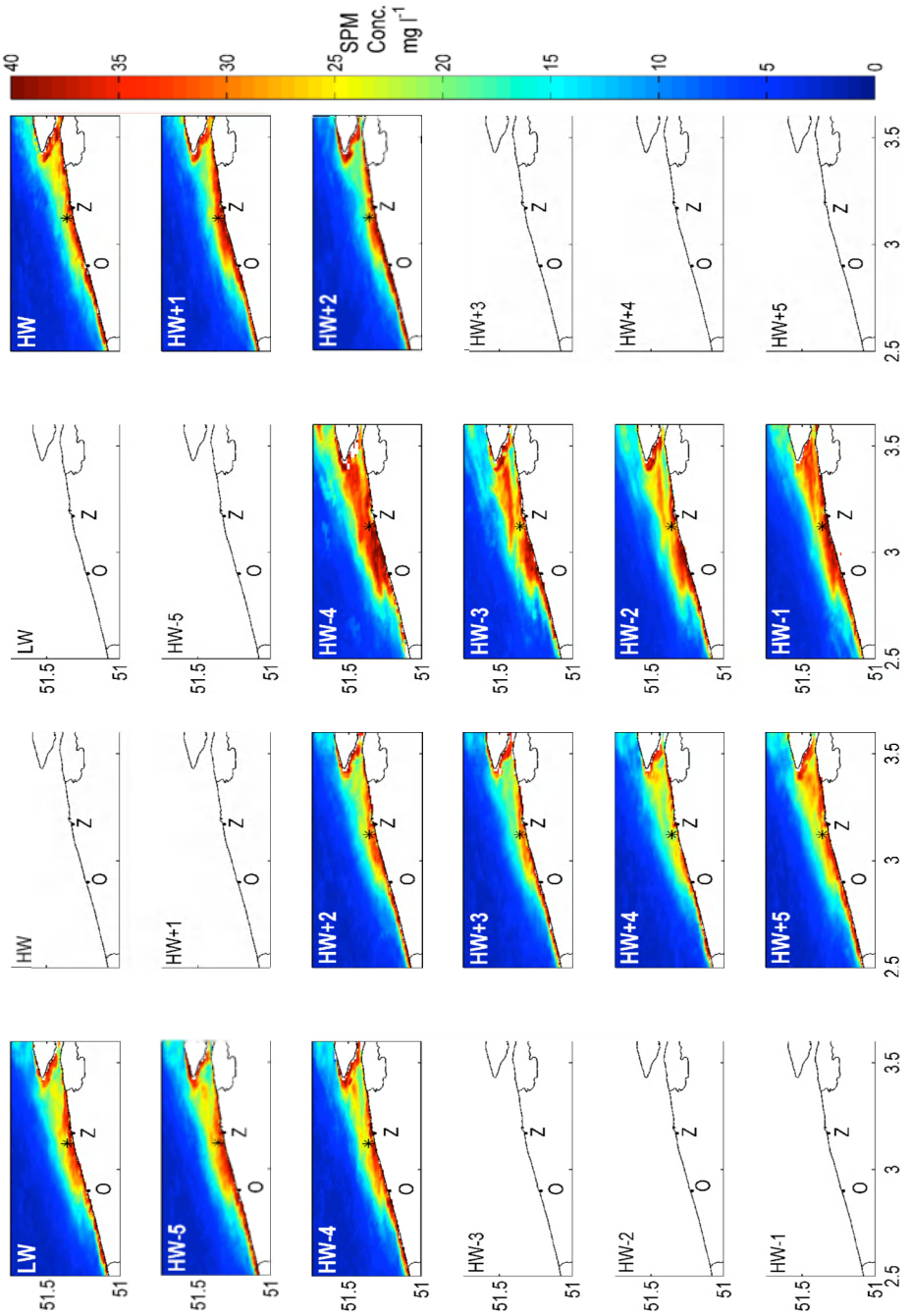

Figure 3.6 *Surface SPM concentration maps for intra-tidal phases (phase interval of about 1 hour) for neap (**left**) and spring (**right**) tidal conditions. Phases with blank maps correspond with no or not enough data. Consequently, low water phases of MODIS imagery occur only under neap tide; high water phases only during spring tide*

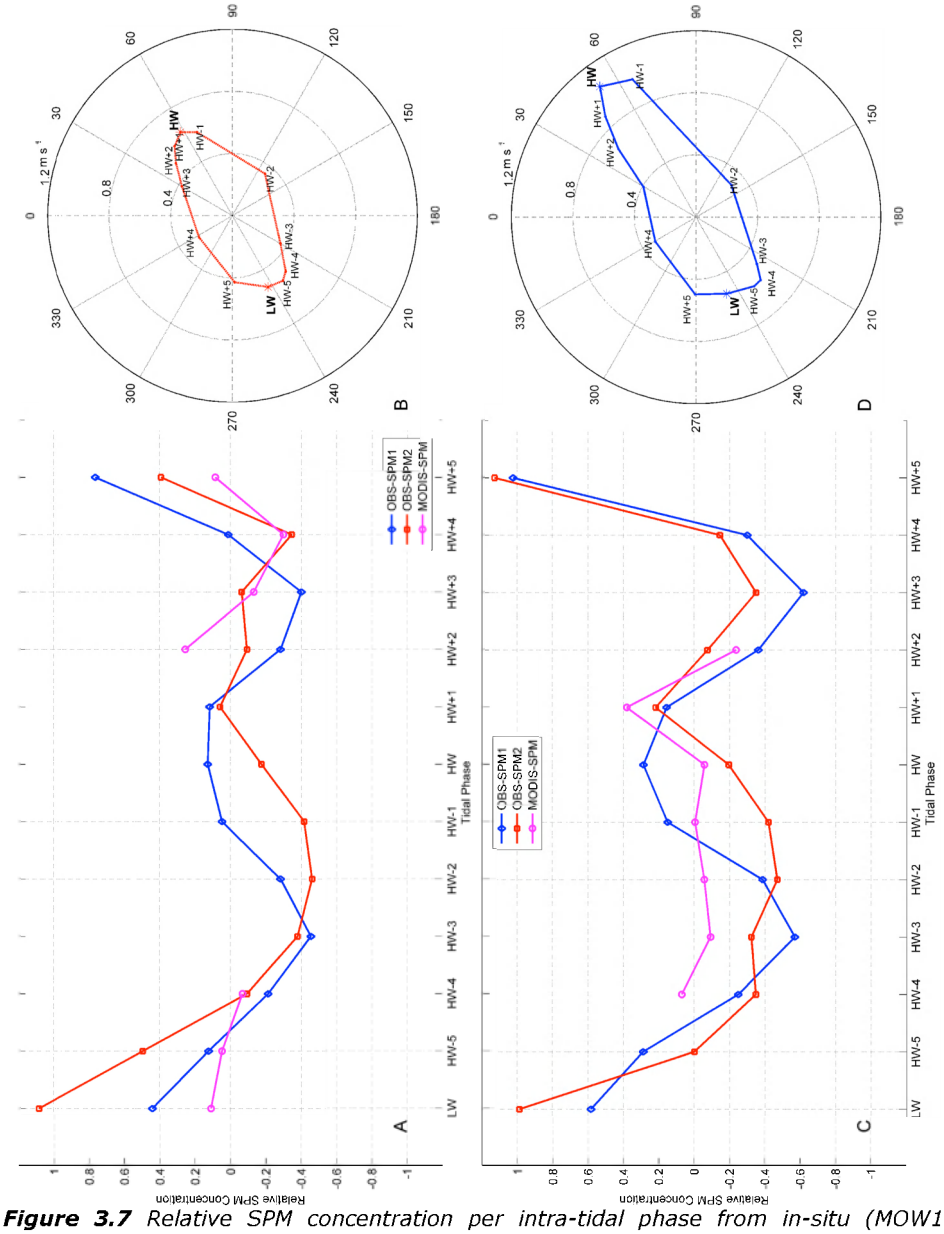

Figure 3.7 *Relative SPM concentration per intra-tidal phase from in-situ (MOW1 station) measurements (at 2 m above bed (SPM-OBS1), near surface (SPM OBS2)) for neap (**A**) and spring (**C**) tidal conditions, together with MODIS-Aqua intra-tidal phase averages at MOW1. Tidal ellipse representative for the coastal zone between Ostend and Zeebrugge for neap tide (**B**) and spring tide (**D**) conditions*

column (Fettweis and Nechad 2011).
The CTM for the ESE wind case is slightly more extended towards France, which is caused by a strong subtidal alongshore flow towards the SW and an enhanced outflow of the Westerscheldt estuary. The CTM entropy class 7 is not connected with the Westerscheldt estuary (Fig. 3.4 d, h) confirming earlier studies that considered the estuary as not an important source of SPM (Van Maldegem et al. 1993, Verlaan et al. 1998). Further, the ESE and the WNW wind cases generate cross-shore winds inducing coastal set-up and set-down, respectively. This will change the overall water depth and consequently the overall SPM concentrations in the coastal zone (e.g. Hommersom et

al. 2010). The higher median SPM concentrations for entropy class 7 under ESE winds, and the lower median SPM concentration associated with the NW winds (WNW wind case) is thus possibly also influenced by coastal set-down (-0.5 m) and set-up (+0.5 m), respectively.
The grouping-averaging of SPM concentration images per wind case is seasonally biased as winds are not equally distributed during a year (Jones et al. 1994). Wind climates per season, based on local wind field data during MODIS overpass, show that: (1) wind case SSW is well-represented throughout the year; (2) wind case N-NE is representative for all seasons, except for winter; and (3) NNW and ESE wind cases are more abundant during winter and autumn, than during summer and spring. A simple averaging of all MODIS images (Fig. 3.2 a) is therefore not a good representation of an average SPM concentration. In Fig. 3.8 (b) an unbiased averaging was carried out, based on the weighted averages of the different wind cases (percentage of occurrence and linear scale). Comparison between Fig. 3.3 (a) and Fig. 3.8 (b) shows that the CTM is more positioned towards the Westerscheldt estuary mouth (Fig. 3.8 c).

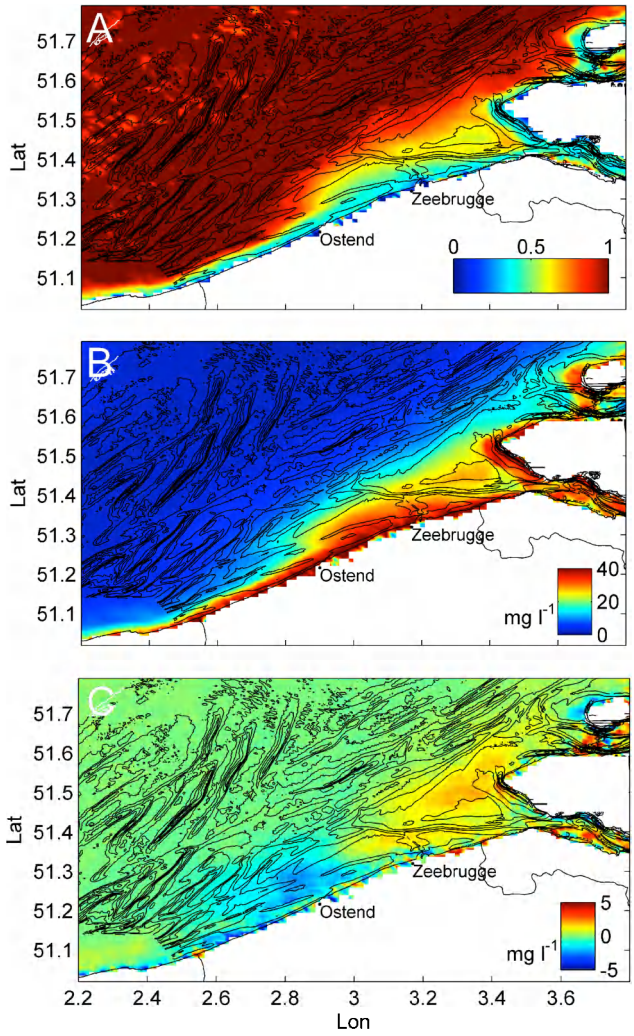

Figure 3.8 *Map of coefficient of variation (standard deviation map divided by average map) with "0" referring to low surface SPM variability, and "1" to high variability, based on all MODIS-Aqua images (**A**). Unbiased average surface SPM map based on the weighted averages of the different wind cases (**B**). Map of difference in surface SPM between A and B (**C**)*

3.5.3. *Weather, climate and environmental changes*

Changes in weather patterns affect the coastal hydrodynamics, and consequently the sediment transport of fine-grained, cohesive sediments. The influence of contrasting NAO conditions during two winters has a striking effect on the spatial extension of the CTM zone (Fig. 3.5). Over the last decades, trend analysis of wind directions shows an increase of southwesterly winds (Siegismund and Schrum 2001, Van den Eynde et al. 2011). The geographical extension of the CTM during the last decades was thus more often spreading towards the mouth of the Westerscheldt estuary as before, similarly to wind case SSW (Fig. 3.4). Houziaux et al. (2011) formulated similar remarks, based on a comparison of historical (100 year) and recent bed samples. These authors have related the changes to mainly port and dredging works that have severely altered the fine-grained sediment dynamics; hence also the turbidity levels in the coastal zone. Our data suggest that the spatial extension of the CTM, and thus SPM concentration is further influenced by natural changes.
The consequences of variations in spatial extension of the CTM zone which has occurred during the last decades must now be completed with specific analyses, e.g. have changes in macrobenthic species communities occurred since they are influenced by SPM availability, as SPM carries a major part of the food resources for the benthos; however, it might turn into an environmental stressor when SPM concentrations interfere with species filtering and respiratory systems (Rodriguez-Palma 2011). As a result, changes in benthos will likely reflect both the natural and anthropogenic disturbances in coastal environments (Dauer et al. 2000, Dauvin et al. 2007).

3.6. *Conclusions*

The coastal turbidity maximum along the Belgian-Dutch coast is not a static feature. The seasonality in the SPM concentration map time-series is superimposed by SPM concentration variations acting on shorter time scales. The paper addresses the variations that are induced mainly by meteorological forcing. Wind direction plays a significant role in the position and extent of the CTM, as observed at the sea surface. Wind field fluctuations occur over several days and as a consequence, the residual transport of fine sediments will vary, as well as the position of the CTM. Southwesterly winds typically correspond to a largest spatial extent of the CTM, whereas northeasterly winds impose a reduction. More significant alongshore displacement in CTM position towards the Dutch coastal waters is seen in winter months with stronger-than-average southwesterly winds. Winter periods also exist in which SW winds are less abundant, resulting in different CTM spatial patterns. The latter is based on the climatological index, North Atlantic Oscillation, even substantially influencing CTM position for longer periods (4 months). Astronomical forcing (tides) was evaluated also. The group-averaged, intra-tidal SPM concentration maps showed good similarities with in-situ data. It is concluded that MODIS-Aqua satellite data can be used to assess SPM concentration variability related to tides, neap-spring cycles, and meteorological and climatological events.

3.7. *Acknowledgements*

The study was partly funded by Belgian Science Policy (Science for a Sustainable Development, QUEST4D, SD/NS/06A; STEREO programme; Belcolour-2 project, SR/00/104) and partly by the Maritime Access Division of the Flemish Authorities (MOMO project). G. Dumon (Flemish Authorities, Maritime Services, Coastal Division/Hydrography) made available wind data. We want to acknowledge the crew of RV Belgica, Zeearend and Zeehond for their skilful mooring and recuperation of the tripod. Measurements would not have been possible without technical assistance of A. Pollentier, J.-P. De Blauwe and J. Backers (Measuring Service of MUMM, Oostende). The first author acknowledges a specialisation grant from IWT (Agency for Innovation by Science and Technology, Flanders).

3.8. References

Arndt S, Lacroix G, Gypens N, Regnier P, Lancelot C (2011). Nutrient dynamics and phytoplankton development along an estuary-coastal zone continuum: A model study. Journal of Marine Systems 84 (3-4), 49-66.

Baeye M, Fettweis M, Voulgaris G, Van Lancker V (2011). Sediment mobility in response to tidal and wind- driven flows along the Belgian inner shelf, southern North Sea. Ocean Dynamics 61(5), 611-622.

Bass SJ, Aldridge JN, McCave IN, Vincent CE (2002). Phase relationships between fine sediment suspensions and tidal currents in coastal seas. Journal of Geophysical Research 107(C10), 1-14.

Blaas M, El Serafy GYH, van Kessel T, de Boer GJ, Eleveld MA, van der Woerd HJ (2007). Data model integration of SPM transport in the Dutch coastal zone. Proceedings of the Joint 2007 EUMETSAT/AMS Conference, 1–8.

Chelliah M, Bell GD (2004). Tropical multi-decadal and interannual climate variations in the NCEP/ NCAR Reanalysis. *Journal of Climate* 17**,** 1777-1803.

Dauer DM, Ranasinghe JA, Weisberg SB (2000). Relationships between benthic community condition, water quality, sediment quality, nutrient loads, and land use patterns in Chesapeake Bay. Estuaries 23, 80-96.

Dauvin J-C, Ruellet T, Thiebaut E, Gentil F, Desroy N, Janson A-L, Duhamel S, Jourde J, Simon S (2007). The presence of Melinna palmata (Annelida: Polychaeta) and Ensis directus (Mollusca: Bivalvia) related to sedimentary changes in the Bay of Seine (English Channel, France). Cahiers Biologie Marine 48, 391-401.

Delhez EJM, Carabin G (2001). Integrated modeling of the Belgian coastal zone. Estuarine, coastal and shelf science 53(4), 477-491.

Doxaran D, Froidefond JM, Castaing P, Babin M (2009). Dynamics of the turbidity maximum zone in a macrotidal estuary (the Gironde, France): observations from field and MODIS satellite data. Estuarine, Coastal and Shelf Science 81, 321–332.

Du Four I, Van Lancker V (2008). Changes of sedimentological patterns and morphological features due to the disposal of dredge spoil and the regeneration after cessation of the disposal activities. Marine Geology 255(1-2), 15-29.

Eleveld MA, Pasterkamp R, van der Woerd HJ, Pietrzak JD (2008). Remotely sensed seasonality in the spatial distribution of sea-surface suspended particulate matter in the southern North Sea. Estuarine, Coastal and Shelf Science 80, 103-113.

Fettweis M, Nechad B, Van den Eynde D (2007). An estimate of the suspended particulate matter (SPM) transport in the southern North Sea using SeaWiFS images, in-situ measurements and numerical model results. Continental Shelf Research 27, 1568-1583.

Fettweis M, Francken F, Van den Eynde D, Verwaest T, Janssens J, Van Lancker V (2010). Storm influence on SPM concentrations in a coastal turbidity maximum area with high anthropogenic impact (southern North Sea). Continental Shelf Research 30, 1417-1427.

Fettweis M, Nechad B (2011). Evaluation of in-situ and remote sensing sampling methods for SPM concentrations, Belgian continental shelf (southern North Sea). Ocean Dynamics 61, 157–171.

Fettweis M, Baeye M, Francken F, Lauwaert B, Van den Eynde D, Van Lancker V, Martens C, Michielsen T (2011). Monitoring the effects of disposal of fine sediments from maintenance dredging on suspended particulate matter concentration in the Belgian nearshore area (southern North Sea). Marine Pollution Bulletin 62, 258-269.

Hommersom A, Wernad MR, Peters S, de Boer J (2010). A review on substance and processes relevant for optical remote sensing of extremely turbid marine areas, with a focus on the Wadden Sea. Helgoland Marine Research 64, 75-92.

Houziaux J-S, Fettweis M, Francken F, Van Lancker V (2011). Historic (1900) seafloor composition in the Belgian-Dutch part of the North Sea: A reconstruction based on calibrated visual sediment descriptions. Continental Shelf Research 31(10), 1043-1056.

Hurrell JW (1995). Decadal Trends in the North Atlantic Oscillation: Regional Temperatures and Precipitation. Science 269, 676-679.
Hurrell JW, Deser C (2009). North Atlantic climate variability: The role of the North Atlantic Oscillation. Journal of Marine Systems 78(1), 28-41.
Johnston RJ, Semple RK (1983). Classification using information statistics: Concepts and techniques in Modern Geography 46. Geobooks, Norwich, 157-160.
Jones SE, Jago CF, Prandtl D, Flatt D (1994). Suspended sediment dynamics: measurements and modelling in the Dover Strait. In: Beven, K.J., Chatwin, P.C., Milbank, J.H. (Eds.), Mixing and transport in the environment. Wiley, 183-201.
Lacroix G, Ruddick K, Ozer J, Lancelot C (2004). Modelling the impact of the Scheldt and Rhine/Meuse plumes on the salinity distribution in Belgian waters (southern North Sea). Journal of Sea Research 52(3), 149-163.
Lacroix G, Ruddick K, Park Y, Gypens N, Lancelot C (2007). Validation of the 3D biogeochemical model MIRO&CO with field nutrient and phytoplankton data and MERIS-derived surface chlorophyll a images. Journal of Marine Systems 64, 66–88.
Le Hir P, Monbet Y, Orvain F (2007). Sediment erodability in sediment transport modelling: can we account for biota effects? Continental Shelf Research 27, 1116–1142.
Mathys M (2009). The Quaternary geological evolution of the Belgian Continental Shelf, southern North Sea. PhD Thesis. Universiteit Gent. Faculteit Wetenschappen: Gent. xxiv, pp. 382.
McCandliss RR, Jones SE, Hearn MR, Latter RJ, Jago CF (2002). Dynamics of suspended particles in coastal waters (southern North Sea) during a spring bloom. Journal of Sea Research 47, 285-302.
Murray JMH, Meadows A, Meadows PS (2002). Biogeochemical implications of microscale interactions between sediment geotechnics and marine benthos: A review. Geomorphology 47, 15-30.
Nechad B, Ruddick KG, Park Y (2010). Calibration and validation of a generic multisensor algorithm for mapping of Total Suspended Matter in turbid waters. Remote Sensing of Environment 114, 854-866.
Nechad B, Van den Eynde D, Fettweis M, Francken F (2003). Suspended particulate matter mapping from multitemporal SeaWiFS imagery over the southern North Sea - SEBAB project, in: Smits, P.C. et al. (Ed.) (2004). Analysis Of Multi-Temporal Remote Sensing Images: Proceedings Of The Second International Workshop on the Joint Research Centre Ispra, Italy 16-18 July 2003. pp. 357-367.
Neukermans G, Ruddick K, Bernard E, Ramon D, Nechad B, Deschamps, P-Y (2009). Mapping total suspended matter from geostationary satellites: a feasibility study with SEVIRI in the Southern North Sea. Optics Express: the international electronic journal of optics 17(16), 14029-14052.
Patt FS, Barnes RA, Eplee RE, Franz BA, Robinson WD (2003). Algorithm updates for the Fourth SeaWiFS data reprocessing, NASA.
Pietrzak JD, de Boer GJ, Eleveld MA (2011). Mechanisms controlling the intra-annual mesoscale variability of SST and SPM in the southern North Sea. Continental Shelf Research 31(6), 594-610.
Pleskachevsky A, Gayer G, Horstmann J, Rosenthal W (2005). Synergy of satellite remote sensing and numerical modeling for monitoring of suspended particulate matter. Ocean Dynamics 55, 2-9.
Rodriguez-Palma O (2011). The role of suspended particulate matter in the distribution and structure of macrobenthic communities in the Belgian part of the North Sea. MSc Thesis. University Brussels. pp. 56.
Ruhl CA, Schoellhamer DH, Stumpf RP, Lindsay CL (2001). Combined use of remote sensing and continuous monitoring to analyse the variability of suspended-sediment concentrations in San Francisco Bay, California. Estuarine, Coastal and Shelf Science 53, 801-812.
Schoellhamer DA (2002). Variability of suspended-sediment concentration at tidal to annual time scales in San Francisco Bay, USA. Continental Shelf Research 22, 1857–1866.

Siegismund F, Schrum C (2001). Decadal changes in the wind forcing over the North Sea. Climate Research 18, 39-45.
Sirjacobs D, Alvera Azcárate A, Barth A, Lacroix G, Park Y, Nechad B, Ruddick K, Beckers J-M (2011). Cloud filling of ocean colour and sea surface temperature remote sensing products over the Southern North Sea by the Data Interpolating Empirical Orthogonal Functions methodology. Journal of Sea Research 65(1), 114-130.
Trisakti B, Parwati Budhiman S (2005). Study of MODIS-AQUA data for mapping total suspended matter (TSM) in coastal waters. Remote Sensing and Earth Sciences 2, 19-31.
Ullmann A, Monbaliu J (2010). Changes in atmospheric circulation over the North Atlantic and sea surge variations along the Belgian coast during the 20th century. International Journal of Climatology 30, 558-568.
Van Maldegem DC, Mulder HPJ, Langerak A (1993). A cohesive sediment balance for the Scheldt estuary. Netherlands Journal of Aquatic Ecology 27 (2–4), 247–256.
van Raaphorst W, Philippart CJM, Smit JPC, Dijkstra EJ, Malschaert JEP (1998). Distribution of suspended particulate matter in the North Sea as inferred from NOAA/ AVHRR reflectance images and in-situ observations. Journal of Sea Research 39, 197−215.
van der Wal D, Wielemaker-Van den Dool A, Herman P (2010). Spatial synchrony in intertidal benthic algal biomass in temperate coastal and estuarine ecosystems. Ecosystems 13, 338-351.
Van den Eynde D, Nechad B, Fettweis F, Francken F (2007). Seasonal variability of suspended particulate matter observed from SEAWiFS images near the Belgian coast. Estuarine and Coastal Fine Sediments Dynamics. In: Maa, JP-Y, Sanford LP, Schoellhamer DH (eds.), Estuarine and Coastal Fine Sediments Dynamics. Elsevier, pp. 291-311.
Van den Eynde D, De Sutter R, De Smet L, Francken F, Haelters J, Maes F, Malfait E, Ozer J, Polet H, Ponsar S, Reyns J, Van der Biest K, Vanderperren E, Verwaest T, Volckaert A, Willekens M (2011). Evaluation of climate change impacts and adaptation responses for marine activities. Final Report - Draft. Brussels : Belgian Science Policy, pp. 114.
Velegrakis AF, Gao S, Lafite R, Dupont JP, Huault MF, Nash LA, Collins MB (1997). Re-suspension and advection processes affecting suspended particulate matter
concentrations in the central English Channel. Journal of Sea Research 38, 17-34.
Verfaillie E, Van Lancker V, Van Meirvenne M (2006). Multivariate geostatistics for the predictive modelling of the surficial sand distribution in shelf seas. Continental Shelf Research 26(19), 2454-2468.
Verlaan PAJ, Donze M, Kuik P (1998). Marine vs. fluvial suspended matter in the Scheldt estuary. Estuarine, Coastal and Shelf Science 46 (6), 873-883.
Vos RJ, Gerritsen H (1997). Use of NOAA/AVHRR satellite remote sensing data for modelling of suspended sediment transport in the North Sea: approach in the PROMISE project. WL rapport Z2025, januari 1997. I.o.v. CEC - DGXII – MAST-3.
Wieringa J, Rijkoort PJ (1983). Windklimaat van Nederland. Staatsuitgeverij, Den Haag, pp. 263 (in Dutch).
Zeelmaekers E (2011). Computerized qualitative and quantitative clay mineralogy: introduction and application to known geological cases. PhD Thesis. Katholieke Universiteit Leuven. Groep Wetenschap en Technologie: Heverlee. ISBN 978-90-8649-414-9. XII, pp. 397.
Yang L (1998). Modelling of hydrodynamic processes in the Belgian coastal zone. PhD Thesis. Katholieke Universiteit Leuven, Belgium. pp. 214.

Sediment re-suspension and advection associated with residual flows in the Belgian coastal zone*

*to be submitted for publication in Journal of Marine Systems (Elsevier)

M. Baeye processed and interpreted the datasets, wrote the manuscript and made all figures. N. Kumar (Coastal Processes – Sediment Dynamics lab, University of South Carolina, USA) helped in processing and interpreting the BM-ADCP datasets. V. Van Lancker and M. Fettweis are thanked for their constructive comments.

Abstract

Residual (e.g. wind-driven) sediment fluxes have been studied using a combination of in-situ bottom-mounted sensors (ADCP, tripod) allowing measuring over the entire water column. Flow profiles, SPM concentration and near-bed sediment dynamics are discussed, and a vertical mixing parameter is introduced in order to evaluate when suspended sediments are well-mixed in the water column. The northeast-directed flow regime exhibits strong hydrodynamics, resulting in a good mixing. Although the southwest-directed regime is also characterized by a good mixing, there is no real link with bed shear stresses (hydrodynamics). Therefore, it is suggested that the nature of particles in suspension also must be regarded. The finer, soft (cohesive) sediments are likely to be suspended more or longer compared to the more sandy sediments, which will settle more easily. These results allowed a separation and recognition of processes that control the variability of SPM concentration and that can be used as an attempt for understanding the long-term evolution of the system.

Keywords: SPM Fluxes; bottom-ADCP; benthic tripod; vertical mixing

4.1. *Introduction*

Wind stress is an important forcing mechanism for generation of flows in the inner-shelf, while in oceans, where the Coriolis acceleration dominates over other acceleration terms, geostrophic flows occur (Lentz et al. 1999, Guttierez et al. 2006, Fewings and Lentz 2009). Besides tides and density gradients, flows on the continental shelf can also be generated from bathymetric variations (Sanay et al. 2007) or from pressure gradients associated with cape-attached shoals (McNinch and Luettich 2000). Wind induced currents will change the residual transport of water masses and the residual currents (Verlaan and Groenendijk 1993, Yang 1998); they have a significant influence on the transport of particulate and dissolved substances in the water column. The importance of wind forcing on sediment transport has been discussed in various studies (e.g. Grant and Madsen 1986, Lentz 1995, Gutierrez et al. 2005).
The fine-grained sediment dynamics in the southern North Sea and especially the occurrence of a turbidity maximum zone in the Belgian-Dutch coastal zone have been subject to many studies (Van Veen 1936, Nihoul 1975, Gullentops et al. 1976, Delhez and Carabin 2001, Van den Eynde 2004). The mud in the Belgian part of the North Sea partly owes its origin to the import of suspended particulate matter (SPM) from through the Dover Strait and partly to the erosion of local Holocene mud deposits (Fettweis et al. 2007, Zeelmaeckers 2011). Based on hydrodynamic data, Fettweis and Van den Eynde (2003) concluded that the decreasing residual water transport, the shallowness of the area and the difference in magnitude between neap and spring tidal currents and their effect on the erosion and transport capacity are responsible for the presence of the turbidity maximum area. The geographical variability of the turbidity maximum was investigated in Chapter 3 using satellite images and could be linked to wind forcing and direction. Measuring mean patterns of surface SPM concentration from space has become common practice (Stanev et al. 2009, Pietrzak et al. 2011). However, SPM concentration from satellite images represents a data set biased towards good weather conditions (Fettweis and Nechad 2011) and provides only near surface data. The aim of the present study is therefore to identify residual (e.g. wind-driven) sediment fluxes using in-situ bottom-mounted sensors (ADCP, tripod) that can measure over the entire water column. ADCP and multi-parametric tripods have been successfully used to measure current profiles, SPM concentration and/or near-bed sediment dynamics in shelf seas (e.g. Lynch et al. 1997, Hoitink and Hoekstra 2005). The results allow a separation and recognition of processes that control the variability of SPM concentration and can be used for understanding the long-term evolution of the system.

4.2. *Study area background*

The measuring site MOW1 is located in the Belgian near-shore area in the vicinity of the port of Zeebrugge (Z, Fig 4.1). At this location, acoustic and optical instruments have been deployed at a water depth of about 9 m MLLWS (mean lowest low water at spring tide) (Fettweis et al. 2010, Van Lancker et al. 2007). The area is characterised by a bottom sediment composition varying from pure sand to pure mud (Verfaillie et al. 2006) and the presence of a coastal turbidity maximum (CTM) extending between Ostend (O) and the mouth of the Westerscheldt. Near-shore SPM concentration ranges between 0.02–0.07 g l^{-1} and reaches 0.1 to >3 g l^{-1} near the bed (Fettweis et al. 2010). Anthropogenic activities such as dredging and disposal influence the bed composition and the SPM concentration in the water column (Du Four and Van Lancker 2008, Lauwaert et al. 2009).
The tidal regime is semi-diurnal, and the mean tidal range at Zeebrugge is 4.3 and 2.8 m at spring and neap tide, respectively. The tidal current ellipses are elongated in the near-shore area and become gradually more semi-circular towards the offshore. The current velocities near Zeebrugge (near-shore) vary from 0.2–1.5 m s^{-1} during spring tide and 0.2–0.6 m s^{-1} during neap tide. Ebb currents are directed towards the southwest and flood currents towards the northeast. The water is well mixed throughout the entire year and stratification due to salinity or temperature gradients is not occurring (de Ruijter et al. 1987). The freshwater discharge of the Westerscheldt is low (long-term annual mean is about 100 m^3 s^{-1}) and as a consequence, residual flows are mainly governed by tidal asymmetry and wind forcing (Yang 1998). Dominant wind

patterns include winds blowing from the southwest, and from the northeast. Prevailing winds from the north are often associated with (prolonged) stormy periods. Generally, the residual transport of the water masses is northeast directed (Yang 1998, Van Lancker et al. 2007); though fluctuations exist under the influence of changing meteorological conditions.

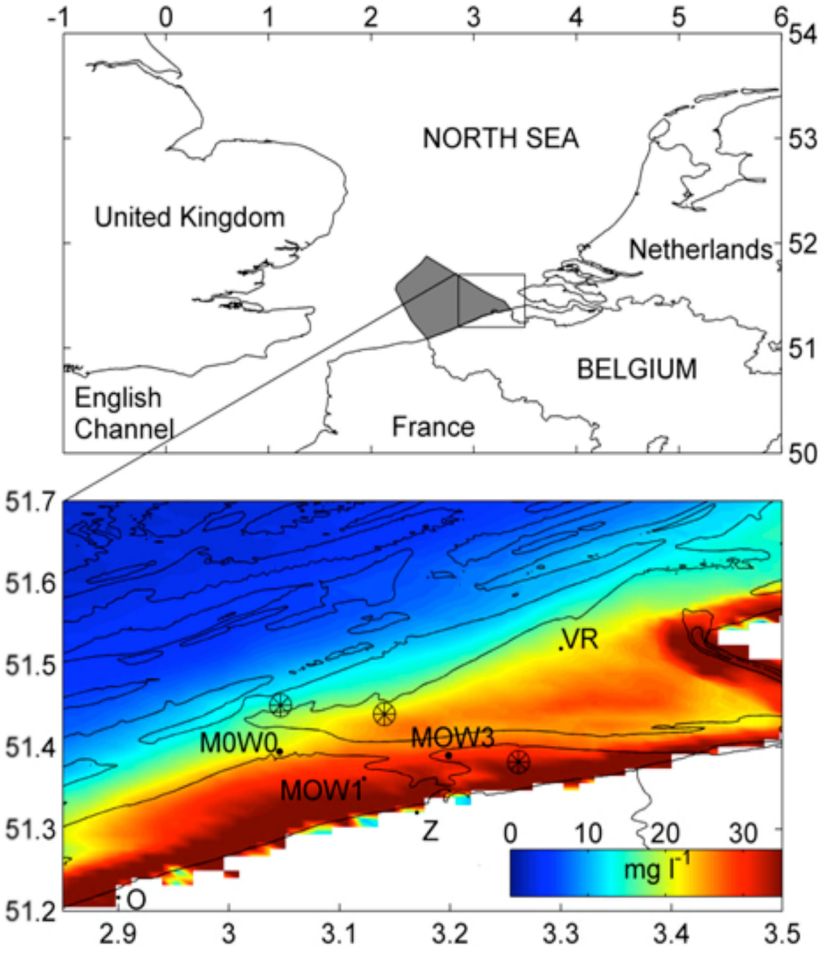

Figure 4.1 *Study area with locations of interest (MOW1, MOW3, MOW0, VR) and surface SPM concentration in mg l^{-1} (weighted mean based on wind climate) derived from Aqua MODIS satellite data; wheel symbols are disposal sites near Zeebrugge harbour (Z)*

4.3. Methodology

4.3.1. Bottom-mounted acoustic Doppler current profiler (BM-ADCP)

A 1200 kHz RDI® ADCP was bottom-mounted at MOW1 for logging vertical profiles of currents and echo intensity. Detailed information regarding the deployments is provided in Table 4.1. A total of 215 days of collected data have been used in this study. The time-series were averaged to a 1-hour interval, and the currents were decomposed into an along- and cross-shore component. The along-shore current component is positive oriented to the northeast (True North 65°, T065), and the positive cross-shore component directed onshore (T155).

Table 4.1 *Details of the BM-ADCP deployments*

year	days	time per ping	freq	pings per ensemble	time per ensemble	average ensemble interval	n° BINS	bin size	mab 1st bin
2006	134-165	3 sec	~0.33 Hz	100	5 min	5min=continuously	30	0.5	1
2007	295-331	0.26 sec	~4 Hz	50	13secs	5min	60	0.2	0.72
2008	28-97	0.26 sec	~4 Hz	50	13secs	10min	50	0.25	0.81
2010	85-125	6 sec	~0.2 Hz	50	5 min	10 min	51	0.25	0.81
2010	151-185	6 sec	~0.2 Hz	50	5 min	10 min	51	0.25	0.81

Data processing of the BM-ADCP data included the removal of the last bin from the ADCP profile closest to the water surface. Dependent on the sampling scheme (and blanking distance) the first data bin is about 0.7 to 1 meter above the bed. Further, all time-series were low-pass filtered (33 hours) using a digital tidal filter in order to remove the semi-diurnal tidal signal from the original data (Beardsley et al. 1985). As the tidal range observed is between 2.8-4.3 m, it is sensible to normalize the vertical distance of BM-ADCP measurements from the seabed by the total water depth; as such, the filtering algorithm successfully identifies the high-frequency oscillations close to the sea-surface. The echo intensity received by the ADCP is able to serve as a proxy for SPM concentration in the water column. Based on the general sonar equation (Urick 1983, Medwin and Clay 1998), the signal is corrected for beam spreading and water attenuation (due to water molecule relaxation effects):

Target Strength = Received Sound Level + 2×Transmission Loss – Source Level Power

Changes of the internal battery voltage over time will result in variations in the ADCP transmit power (Deines 1999). As a consequence of the battery decline, compensational corrections were applied. Another correction of the echo backscatter for the bins in the transducer near-field (1-3 bins) was applied to account for departure from spherical spreading or spreading loss (Downing et al. 1995). Particles in the water column are characterized by a particle size distribution which influences the received echo intensity. From acoustic theory, the range of particle sizes that can be detected by the ADCP is directly related to the ratio of the particle circumference to acoustic wave length, set between 1 and 0.1. For the 1200 kHz ADCP, particle sizes (diameters) must range between 40 and 400 µm to meet this condition. A short deployment of the bottom-mounted ADCP, together with a bottom-framed Sequoia® Laser In-Situ Scattering and Transmissometer, LISST 100X-typeC at 2 m above bed (mab) was performed at MOW1. These simultaneous recordings allowed determining the ADCP sensitivity towards particle size. Correlation coefficients were obtained between the corrected ADCP backscatter, measured for the 2 mab bin, and 32 LISST particle size classes (range of 1.25 and 500 µm) (Fig. 4.2). The highest correlation (R^2>0.8) corresponded with a particle size range between 40 and 150 µm. For flocs larger than 150 µm, ADCP acoustics and LISST optics may react differently, because of the particle shape and density (e.g. Creed et al. 2001).

4.3.2. Tripod benthic observatory

At a distance of 50 meters from the BM-ADCP, a benthic tripod system measured SPM concentration with an Optical Backscatter Sensor (D&A Instruments® OBS-3) at 2 mab, and currents in the lower 2 meter of the water column with a Sontek® Acoustic Doppler Profiler (ADP). The latter is a 3 MHz Sontek® system, also storing acoustic backscatter information. The OBS voltages were converted to SPM concentration using a laboratory calibration. On its turn, OBS SPM concentrations were used to calibrate both the upward-looking ADCP and down-ward looking ADP. This approach allows estimating the sediment flux for the total water column. Also mounted on the tripod system is a Sontek® Acoustic Doppler Velocimeter (ADV) set to record currents and bed evolution (altimetry). The latter was corrected for pitch and roll by the ADV (benthic tripod). Salinity was recorded by the Sea-bird® SBE37 CT, except for time-series conducted in 2007. During that particular deployment, salinity data were provided from a station (VR) 20 km away from the BM-ADCP measuring location, by Hydro Meteo Centrum Zeeland-HMCZ (www.hmcz.nl).

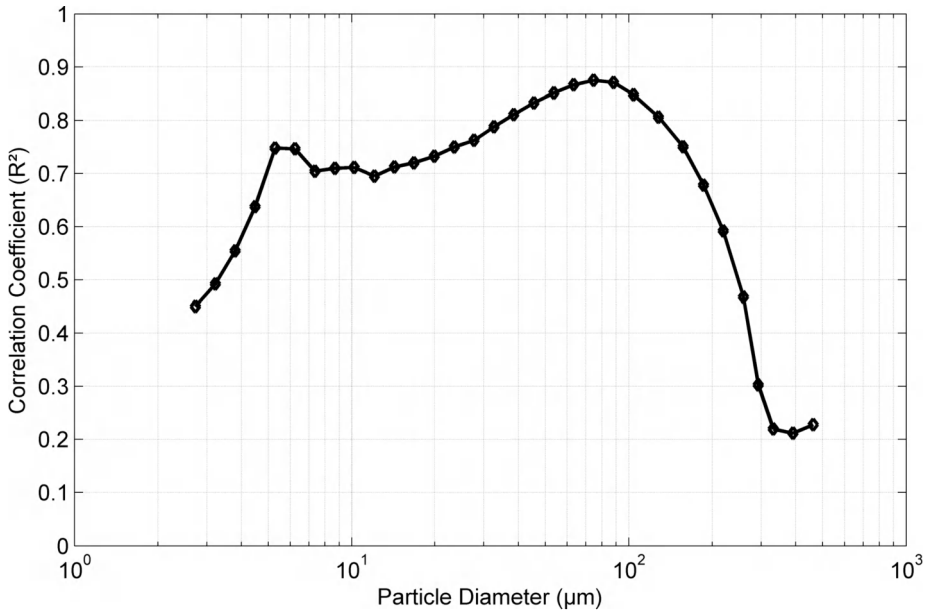

Figure 4.2 *Correlation between ADCP acoustic backscatter and LISST volume concentration in each particle size class*

Table 4.2 *Percentages of the variance explained by tides at MOW0 (MP0) and MOW3 (MP3); a, years 2005-2010; b, years 2009-2010; c, years 2009-2011*

Sampling station	MP0 (%)	MP3 (%)
Alongshore velocity	94.8[a]	97.2[b]
Cross-shore velocity	94.1[a]	93.6[b]
Total velocity	96.4[a]	93.3[b]
Sea-surface elevation	94.7[c]	94.2[c]

4.3.3. Meteorological-oceanographic station and wave buoy

Hydro-meteorological data were provided by the Agency for Maritime and Coastal Services - Hydrography (Flemish Authorities). Wind data measured at MOW0 at 25 meter above sea-surface (Fig. 4.1), logarithmically converted to the standard height of 10 m (U_{10}), have been used to estimate wind stress components by introducing a neutral (dimensionless) drag coefficient (C_{DN}) (Large and Pond 1981):

$$C_{DN} = 1.2\times10^{-3}, \text{ for } 4\ \text{ms}^{-1} \le U_{10} \le 11\ \text{ms}^{-1},$$
$$C_{DN} = \left(0.49 + 0.065\cdot U_{10}\right)\times10^{-3}, \text{ for } 11\ \text{ms}^{-1} < U_{10} \le 25\ \text{ms}^{-1}$$

Currents were measured with the Aanderaa DCM-12 at MOW0 and MOW3 (Fig. 4.1) over several years, and were treated similarly as the BM-ADCP currents. Wave characteristics were obtained recorded in the vicinity of the measuring site (MOW1 and MOW3, Fig. 4.1). MOW3 buoy is a directional wave rider sensor recording frequency-directional wave spectrum data. The other wave rider buoy measures only the frequency-wave spectrum from which the significant wave height (H33), mean wave period (TM2) are derived.

4.3.4. *Bottom shear stress estimates*

BM-ADCP currents were also used for estimating bottom shear stress in the constant stress layer. This can be obtained using the law of the wall. A hydraulic bed roughness length (z_o) of 0.2 mm for muddy seabeds and the ADCP first bin height (z) were used in the following logarithmic relationship (Soulsby 1983, Wright 1989): $u = \frac{u_*}{\kappa} \cdot \ln\left(\frac{z_0}{z}\right)$ with k, Von Karman's constant (~0.4); u, current measured in ADCP's first bin. Further, u_*, shear velocity is related to the current-induced bottom stress, τ_c, by: $\tau_c = \rho \cdot u_*^2$ (p=1030 kg m^{-3} is the density of seawater). The combined shear stress was further calculated taking into account the wave oscillatory motion. Orbital velocities were obtained through solution of the linear dispersion relationship for surface gravity waves using friction factor, f_w (for sediment grain size of 65 μm) in order to obtain the wave induced shear stress: $\tau_w = \frac{\rho f_w}{8} \cdot u_b^2$ (Grasmeijer and Kleinhans 2004). The combined or total (current and waves) shear stress was calculated as follows (Nielsen 1986): $\tau_{cw} = \sqrt{\left(\tau_m + \tau_w \cdot \cos\phi\right)^2 + \left(\tau_w \cdot \sin\phi\right)^2}$ taking into account, Φ, the angle between wave propagation and current direction, and maximum shear stress, τ_m (following Soulsby 1997): $\tau_m = \tau_c \cdot \left[1 + 1.2 \cdot \left(\frac{\tau_w}{\tau_c + \tau_w}\right)^{3.2}\right]$.

4.4. *Results*

4.4.1. *Tidally- and wind-driven flows*

Harmonic analysis of multi-year time-series of currents and sea-surface elevation at MOW0 and MOW3 (Fig. 4.1) was conducted using MATLAB®'s T-Tide (Pawlowizc et al. 2002) that allows identifying tidal constituents. This analysis also reveals that tidal variability accounts for 93-97% and 94% of total variance in the current and sea-surface elevation time series, respectively (Table 4.2). The tidal constituents - M2, S2, N2, K2, L2, O1, M4, NU2, MU2 - account for 75% of the tidal variability of the sea-surface elevation. The same percentage of the total tidal variability in the currents observations is explained by these constituents, together with the constituents: M6, 2MS6, MS4. The three largest constituents (M2, S2, and N2) are semi-diurnal and the major axes of the corresponding tidal ellipses are well aligned in the alongshore direction for the locations MOW0 (T073) and MOW3 (T082). Magnitudes of the tidal components reveal flat ellipses, rather than circular.

Time-series of low-pass filtered, depth-averaged alongshore currents, measured for each BM-ADCP deployment at MOW1 were correlated to alongshore wind stress (Tables 4.3 and 4.4). A strong correlation (R^2=0.70) was obtained for all periods, except for 2007. The weaker correlation (R^2=0.28) in 2007 is explained by the absence of alongshore wind stress during that particular deployment. Depth-averaged BM-ADCP flow components are plotted together with wind stress and salinity in Figs. 4.3 (2006), 4.4 (2007) and 4.5 (2010). Southwest winds (2006 - day of year (doy) 137-147; 2010 doy 89) with shear stresses (>0.1 N m^{-2}), acting on the sea-surface generate a northeastward flow that is associated with an increase in salinity (34). On the other hand, winds blowing from the north enhance a southwestward directed subtidal flow (2006 doy 149-150 and 164; 2007 doy 309, 312, 315 and 317; 2010 doy 122-123).

These meteorological conditions correspond with lower salinity ranging between 30 and 32. Further, periods with reduced wind stress (<0.1 N m^{-2}), regardless the wind direction, exhibit a rather weak negative (southwestward) flow (2006 doy 152-165; 2007 doy 302-308 and 320-325; 2010 doy 92-100).

Table 4.3 *Relation between wind and currents at M0W0 station, R^2*

	Cross-shore wind stress	Alongshore wind stress	Cross-shore current	Alongshore current
Cross-shore wind stress	1	-0.21	0.10	-0.51
Alongshore wind stress		1	-0.23	0.67
Cross-shore current			1	-0.06
Alongshore current				1

Table 4.4 *Relation between wind and currents for the BM-ADCP deployments, R^2*

	Alongshore flow				
	2006	2007	2008	2010	2010
Alongshore wind stress	0.74	0.28	0.73	0.63	0.70
Cross-shore wind stress	-0.52	-0.56	-0.26	-0.65	-0.71

4.4.2. SPM transport (Figs. 4.3, 4.4, 4.5, 4.6)

Acoustic Backscatter Signal (ABS) measured by acoustic current meters can be used as a proxy for SPM concentration. During spring tide conditions, strong tidal currents increase mixing and turbulence, leading to an increase in ABS. Superimposed on the spring-neap variation, significant meteorological events (e.g. southwesterly winds) have also an impact on the ABS due to increase of the SPM concentration. On the other hand, phases of increased ABS also exist without any relation to hydro-meteorological forcing (2006 doy 136, 157; 2010 doy 95, 111).
The SPM concentration profiles derived from ADCP and ADP ABS have been combined in order to obtain profiles covering almost the entire water column (this was only done for times-series 2006) for which it was attempted to calculate the SPM fluxes (Fig. 4.6). The low-pass filtered SPM concentration exhibits low-frequency (wind-induced and spring-neap) variations. Maximum near-bed (between 0 and 1.5 mab) residual concentrations are about 0.6 g l^{-1}. Depth-averaged SPM concentrations vary between 0.2 and 0.3 g l^{-1} (Fig. 4.7 a). The figures show that alongshore SPM fluxes, at that location, coincide with southwestern or northern wind events. The total SPM flux is shown in Fig. 4.7 e; one can clearly see the lower flux during neap tides (2006 doy 152-158), and the higher one (about twice) during spring tide (2006 doy 159-165). The spring-neap tidal variation in the first half (2006 doy 135-150) of the deployment is generally characterized by strong positive alongshore flows alternating with short periods of reduced or negative alongshore flow due to the prevailing meteorological conditions. Maximum depth-averaged SPM transport of 0.15 kg m^{-2} s^{-1} occurs during spring tides. On average, the lower 1.5 m of the water column accounts for 35 % of the total sediment flux (Fig. 4.7 g).

4.4.3. Wind sea waves and sediment re-suspension

Wave characteristics were available during the entire time span of MODIS data image collection (about 7.5 years between 2002 and 2009; MODIS-Aqua SPM Retrieval: see Chapter 4), and each variable was assigned to each MODIS overpass (12:00-13:00 GMT) resulting in a time series of 2539 data points (i.e. number of processed MODIS SPM images). The wave population of waves travelling from the north (T315-T360 and T000-T045) and with heights >1.5m was involved for group-averaging MODIS SPM concentration maps. This resulted in a data set of 76 MODIS-SPM images. Wind direction, measured at the meteorological station MOW0, was gathered based on the time of MODIS-Aqua overpass. Waves start to become important in re-suspension of bed sediments when significant wave heights exceed 1.5 m at the measuring site (Fettweis and Nechad 2011). The increase in SPM concentration is visible along the coast, see Fig. 4.8 where the SPM concentration in the area is shown derived from

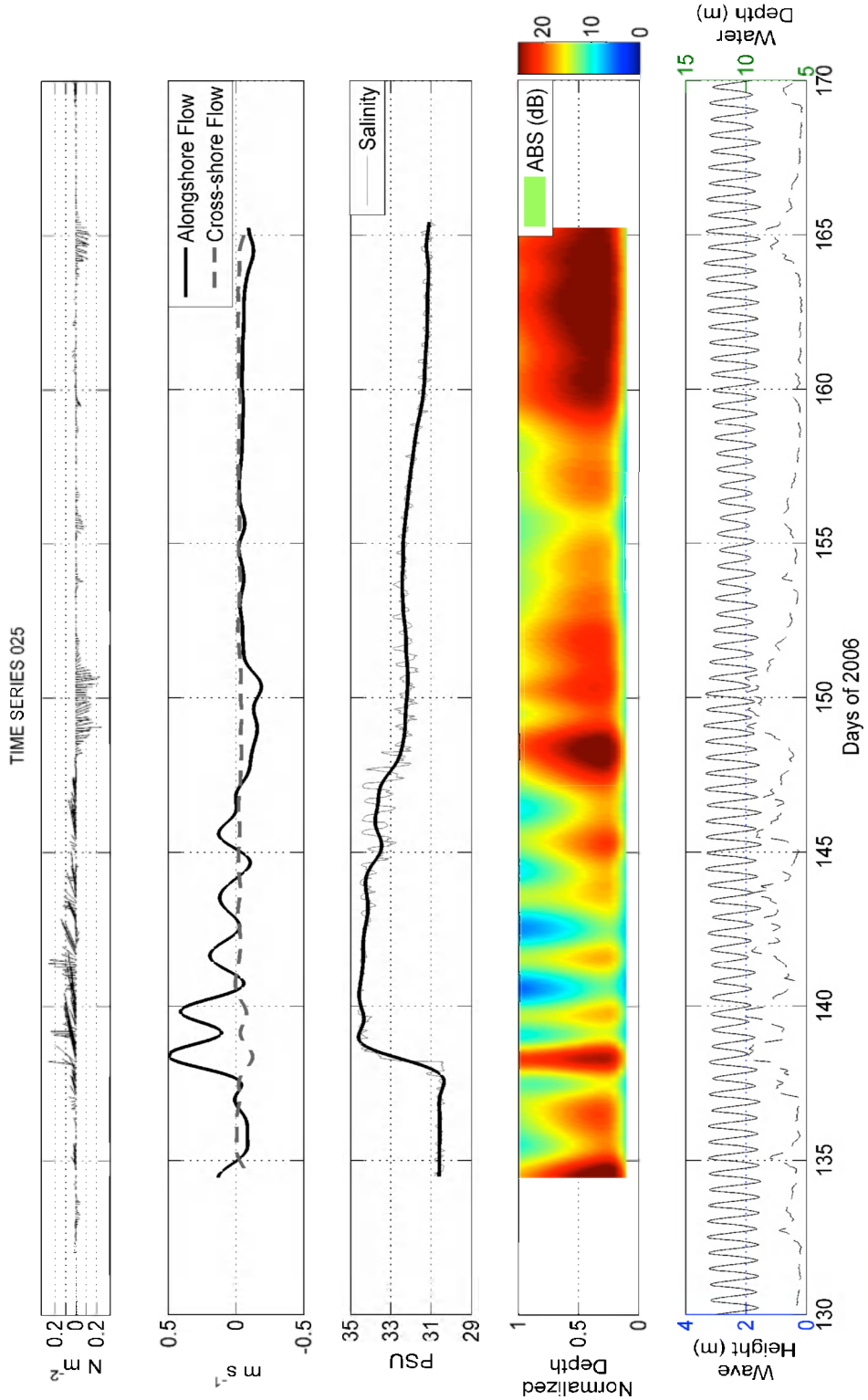

Figure 4.3 *Time-series of wind, flow, salinity, ABS, wave and tidal elevation parameters in 2006*

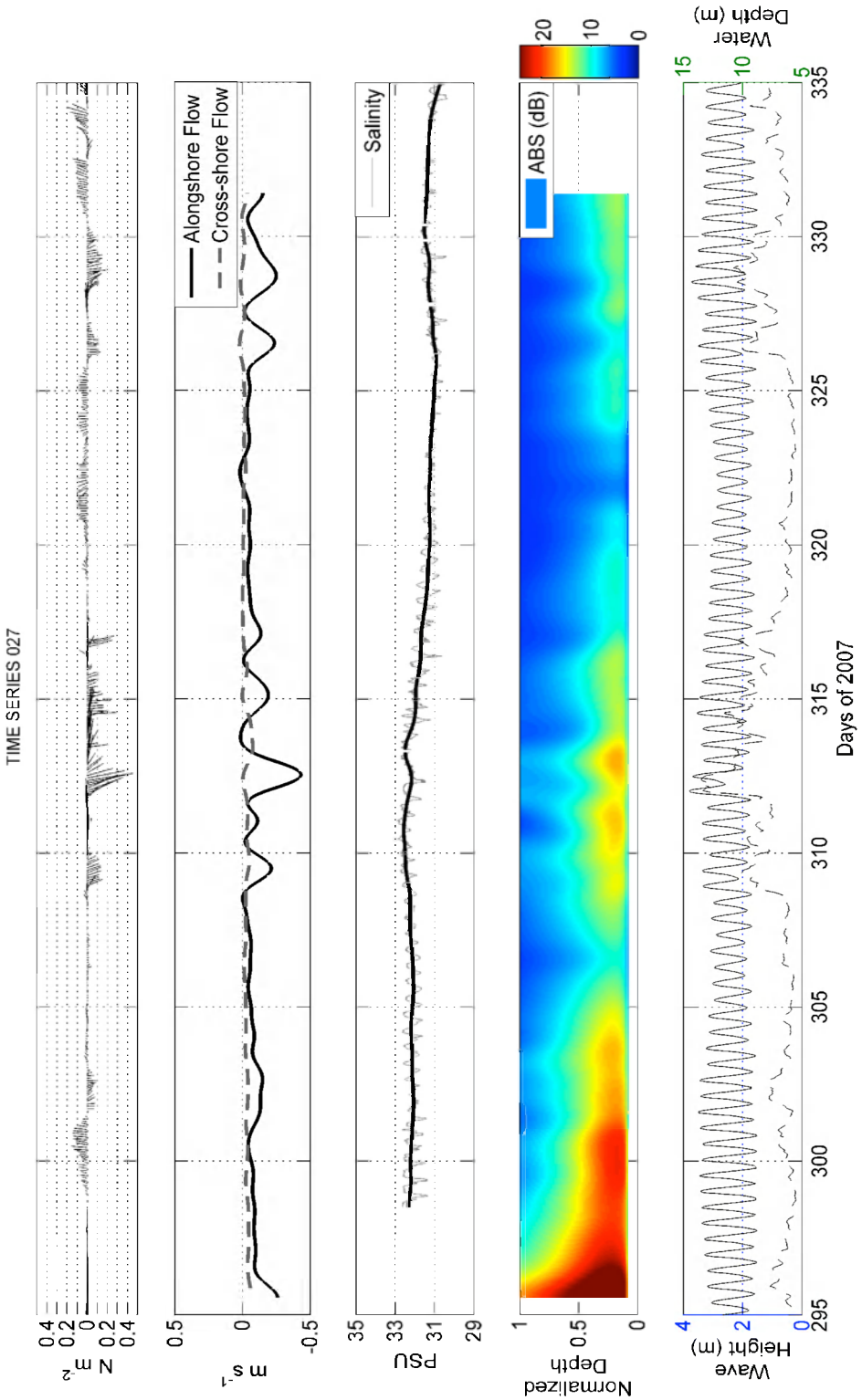

Figure 4.4 *Time-series of wind, flow, salinity, ABS, wave and tidal elevation parameters in 2007*

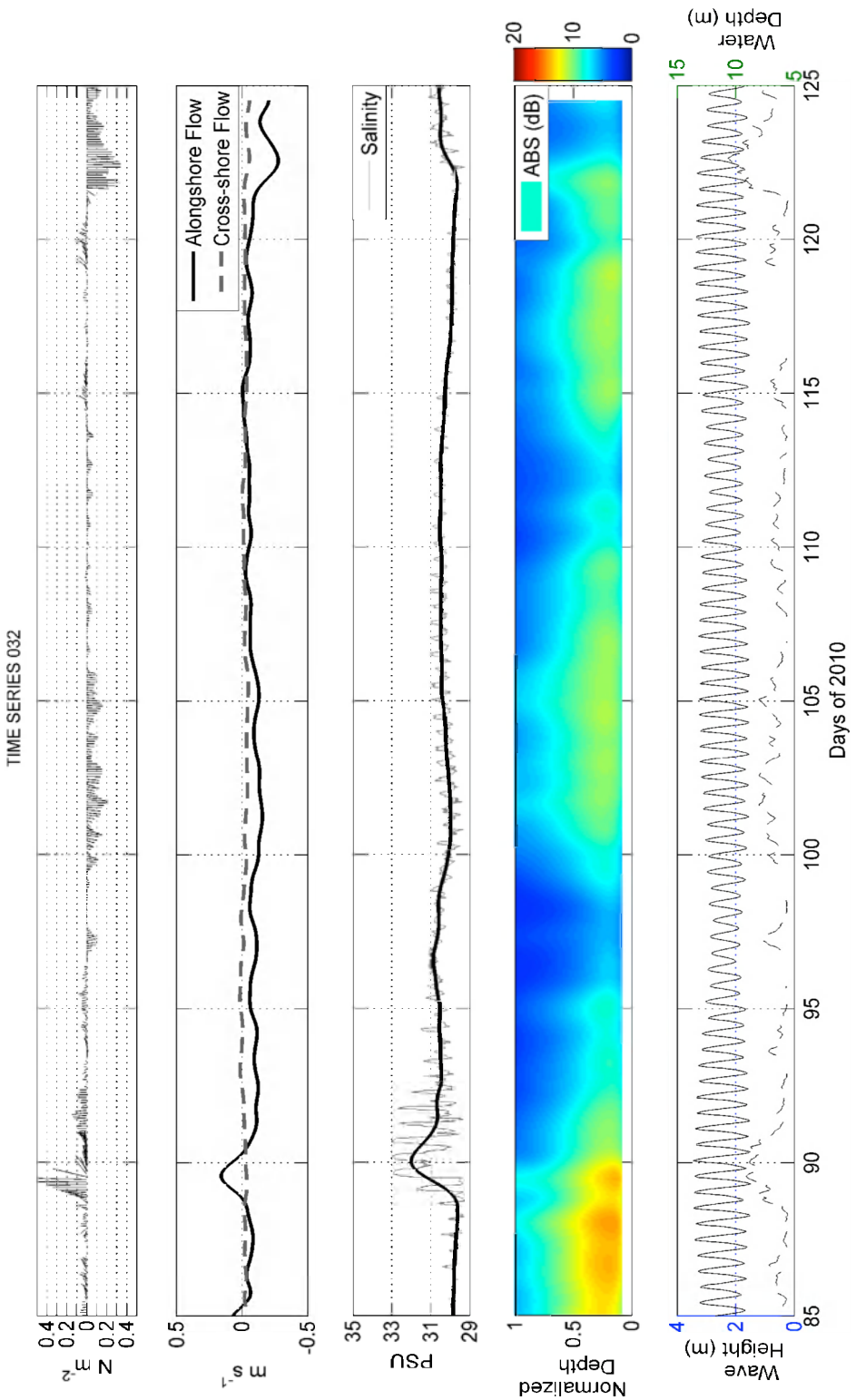

Figure 4.5 *Time-series of wind, flow, salinity, ABS, wave and tidal elevation parameters in 2010*

MODIS images. The coastal turbidity has an average SPM concentration at MOW1 of about 50 mg l^{-1}, which is significantly higher than the 30 mg l^{-1} found in the yearly averaged image (Fig. 4.1).

4.5. Discussion

4.5.1. Subtidal flows

At the measuring location (MOW1), tidal residual flows are always directed towards the southwest under weak (<0.1 N m^{-2}) wind stress conditions. Evidence from hydrodynamic modelling shows that the measuring site is influenced by the Westerscheldt estuary, counterbalancing the northeast-directed residual transport which is generally found in the coastal zone of the southern Bight (Lacroix et al 2004, Fettweis et al. 2007). Our data confirm thus the significant influence of the Westerscheldt estuary on the hydrodynamic circulation up to at least Zeebrugge and MOW1. During weak SW wind periods, there is inertia against this circulation, directed to the SW (e.g. 2007/300-301 and 2010/119-120). However, a north-northeast wind enhances these flows.

4.5.2. Transport of sediment suspensions

Bottom stress under the influence of currents and waves was computed, and correlated with depth-averaged SPM concentration from BM-ADCP deployment of 2006. SPM concentrations during the ebb are slightly higher than during flood (Fig. 4.9 a). A good correlation between bottom shear stress and SPM concentration should be expected if SPM concentration is mainly due to re-suspension by bottom shear stress. This is not the case (R^2=0.50) pointing to other influencing factors such as the availability and consolidation degree of the cohesive sediments and the fluctuations in horizontal advective flux of fine sediments (e.g. Dyer 1994). In this perspective, the alongshore advection is considered (Fig. 4.9 b). Ebb coincides with higher SPM concentrations for both positive and negative subtidal flow regimes. The observed hysteresis is due to sediment entrainment and settling, and the advection of the sediment concentration gradient. The correlation between the depth-averaged, low-pass filtered SPM concentration and bed shear stress yields a good positive relationship regarding the negative flow regime (R^2=0.74) since the spring-neap variation is not really overprinted by meteorological forcing, unlike the positive flow regime case (R^2=0.40). Periods with stronger low-pass filtered negative flow are correlated with higher SPM concentration due to local re-suspension and advection. The tidally- and wind-driven motion of coastal waters is reflected in the salinity. Under southwest winds, the oceanic saline water is pushed through the Strait of Dover into the Belgian coastal zone. On the other hand, northern winds tend to spread out riverine, freshwater from the Scheldt-Rhine-Meuse estuaries along the Belgian coast (Yang 1998, Lacroix et al. 2004, Arndt et al. 2011). It is suggested that the negative flow will also advect sediments from the estuary towards the southwest, explaining R^2=0.74. Since sediments present in the lower Scheldt are marine (Verlaan and Spanhoff 2000), an episodic buffering of sediments under prolonged periods of southwest winds was suggested (Terwindt 1977, Van Alphen 1990, Baeye et al. 2011). SPM will then subsequently be released under changing hydro-meteorological conditions (N and NE winds). In addition, the freshwater discharge (measured at 50 km upstream) was evaluated during the ADCP deployments, and continuous but low discharging (~80 m^3 s^{-1}) indicate that riverine SPM output events were not likely to be measured in the BM-ADCP time-series.

4.5.3. Vertical mixing of suspended sediments

Meteorological conditions have also an influence on the vertical mixing of SPM in the water column; this depends on the settling velocities and on the vertical mixing processes (Pleskachevsky et al. 2011). Vertical mixing is calculated as the ratio between near-surface to near-bed SPM concentrations (Fig. 4.7 d). The data show that a good vertical mixing (high ratio) is associated with the major southwest wind events occurring in the first part of the 2006 time-series (blue highlights).

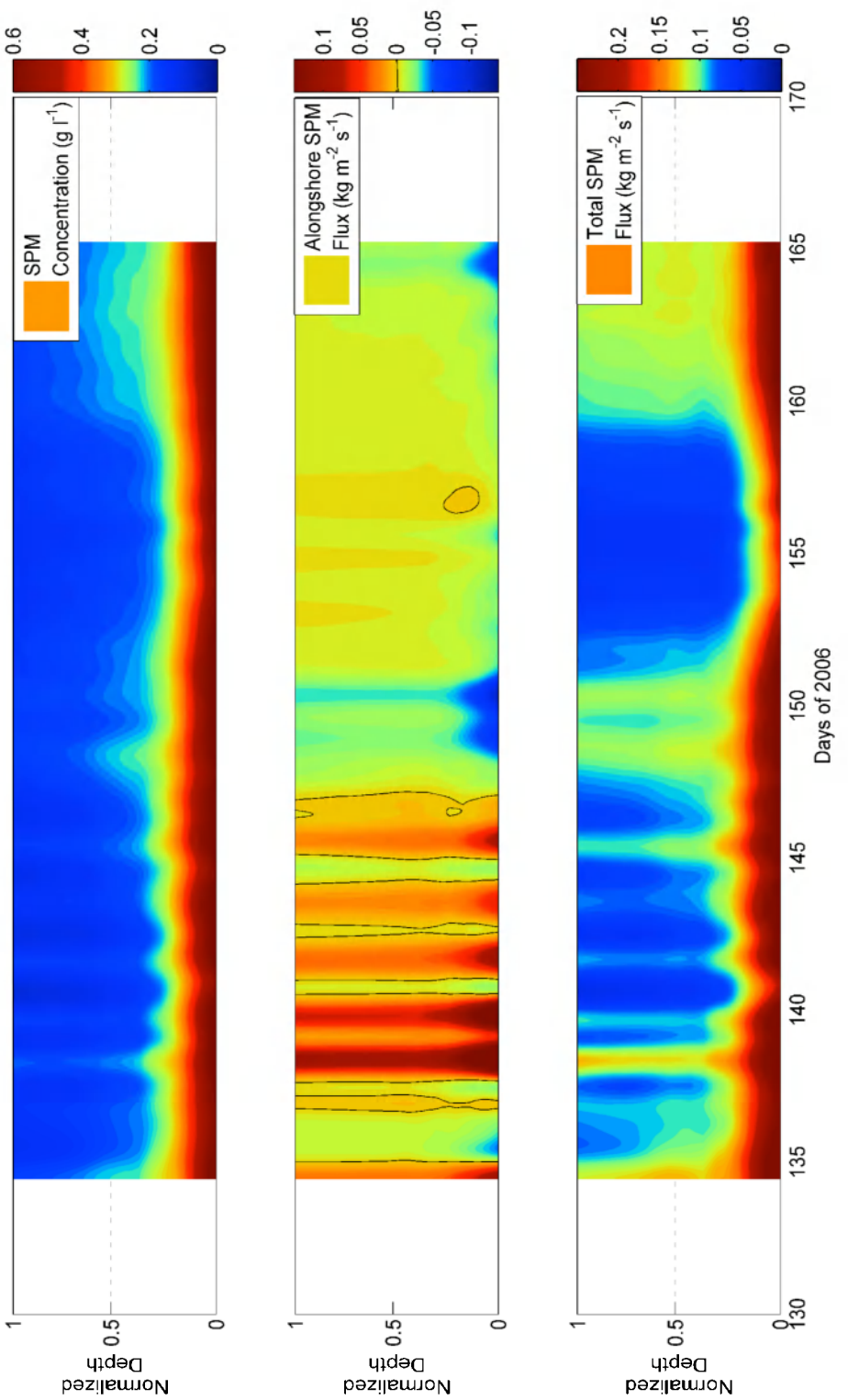

Figure 4.6 *BM-ADCP time-series 2006 from* ***top*** *to* ***bottom*** *SPM concentration, alongshore sediment flux and total sediment flux, respectively*

In between these events, less energetic conditions increase SPM settling out of the water column and accordingly the near-bed SPM concentration. Under these wind (SW) conditions, a positive correlation exists between vertical mixing parameter and the low-pass filtered bed shear stress (R^2=0.64). However, during negative alongshore flow (red highlight) a negative correlation (R^2= - 0.45) was found pointing to no relationship between good mixing and increased bed shear stress (like the positive flow regime). Possibly, prominent near-bed processes, such as the formation of high-concentrated mud suspension and fluid mud layers also exist during strong negative flow hydrodynamics. The overall degree of vertical mixing under negative flow conditions remains high, and is explained by the associated particle size spectrum that is now dominated by finer (silt-size) particles requiring less energy (necessary) to be in re-suspension. The particles during northeast-directed flows are typically coarser, implying rapid settling of the particles (fine sands) during less energetic phases. HCMSs are most important towards vertical mixing capacity of the water column when considering the sediment transport in tidal time domains; since the cyclic (quarter-diurnal) HCMS occurrences will be mostly filtered out in the subtidal signal. Fig. 4.10 (top) shows the seabed evolution (ADV altimetry) with the short-term occurrence of HCMSs, especially under southwest-directed flows (2006 from doy 146 on). HCMSs reach the ADV sampling volume, in which currents are measured, indicating HCMS layers of at least 20 cm thick.
Satellite images will always underestimate SPM concentration and transport due to the strong vertical gradients in SPM concentration (Fettweis and Nechad 2011). This means also that the surface CTM zone as observed in satellite images is generally less extended than the near-bed CTM. Figs. 4.1 and 4.8 show the mixing, as observed at the surface, for average conditions (based on wind climate) and for storm conditions (winds with northern component, and waves >1.5 m). Under averaged conditions (Fig. 4.1), the navigational channels have lower surface SPM concentration than its surroundings. This is explained by the deeper water depth in the channels than in the surroundings (15 vs. 10 m MLLWS); water depth being a controlling factor in the vertical sediment distribution (e.g. Hommersom et al. 2010). Under northerly storms, however, the SPM concentration is high in the whole area. Fettweis et al. (2010) have argued that the soft mud deposits in the navigational channels are re-suspended during such storm conditions. The latter is thus confirmed by satellite images (Fig. 4.8 vs. Fig. 4.1). The seabed evolution, derived from the ADV (Fig. 4.10) was plotted together with the wave-induced bottom stress (Fig. 4.10, bottom). The 2-days lasting northern storm (2006/149-150) resulted in seabed erosion of at least 5 cm. After the storm the SPM was settling again resulting in formation of HCMS (or fluid mud) layers of almost 10 cm, these layers remained until the end of the deployment. Bed erosion also occurred under southwestern wind events. The short term HCMS layers (up to 20 cm) occur in association with these events (vertical white lines); though it manifests on a more regular basis in the negative flow regime (Fig. 4.10 from 2006/147 onwards). The CTM, under the negative flow regime, is therefore more likely related to the formation of HCMS layers with a thickness of more than 20 cm (on fluid mud); these occur typically during slack tides (see Chapters 2 and 6). It is known from literature (Mehta 1989, Winterwerp and van Kesteren 2004) that fluid mud is hard to entrain, and tends to dampen turbulent energy. This possibly also contributes to the negative correlation between the mixing parameter and the bed shear stress for this flow condition.

4.5.4. Disposal of mud

Subtle fluctuations in depth-averaged sediment concentrations without any observed change in hydro-dynamical forcing have been observed in the data (see above, 4.4.2.). Possibly they are linked to small scale processes. Plausible mechanism for these variations is thought to be disposal of dredged material on a nearby disposal site (east off Zeebrugge), where between 60 x 10^3 and 120 x 10^3 tons of dry matter has been disposed during the BM-ADCP mooring in 2006. Disposal of fine-grained sediments result in an increase of SPM concentration in a larger area (Van den Eynde 2004, Fettweis et al. 2011). However, based on the current BM-ADCP time-series no direct evidence of impact of disposal of dredged material could be established.

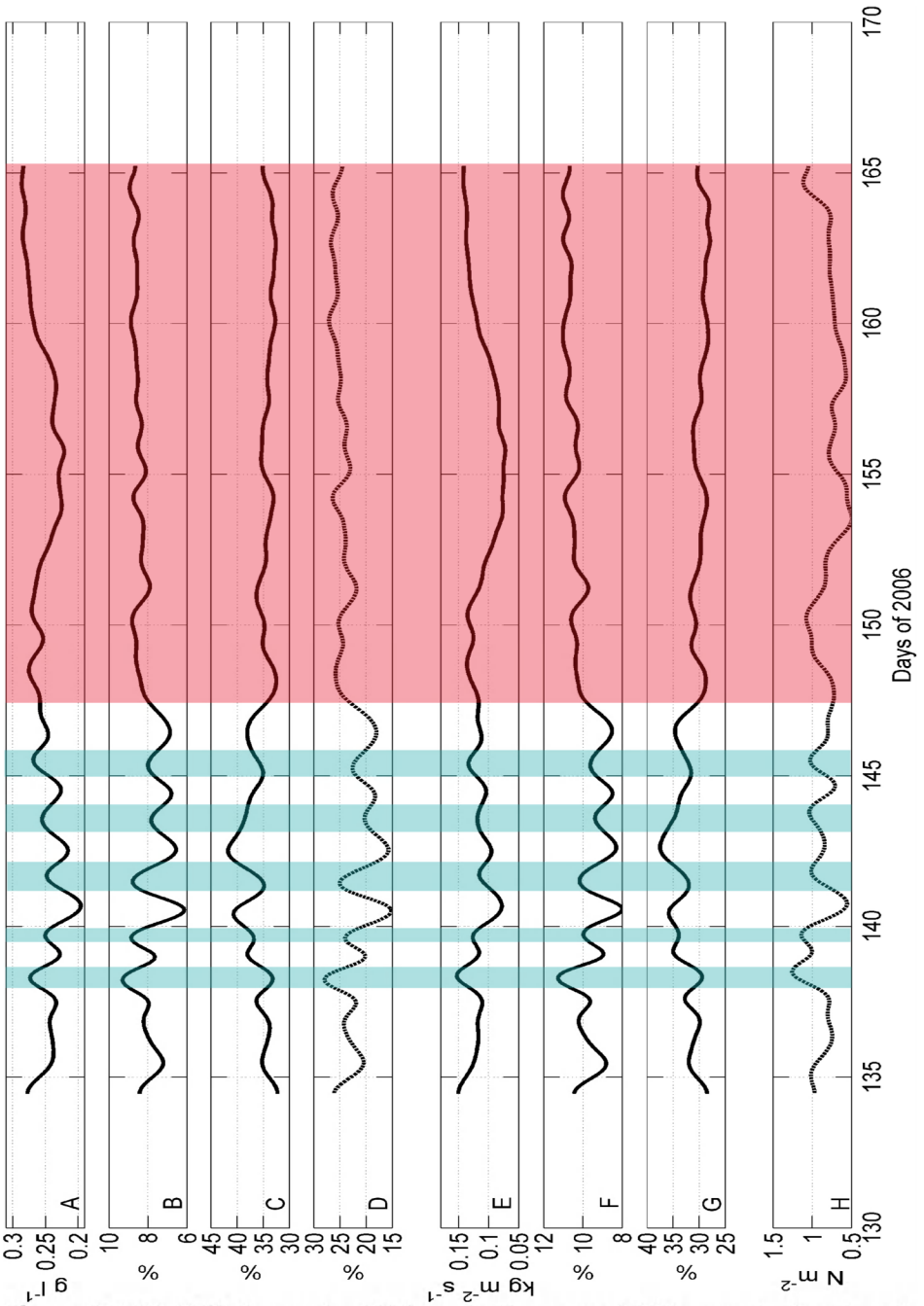

Figure 4.7 *BM-ADCP time-series 2006;* ***a****, depth-averaged SPM concentration;* ***b****, ratio (%) SPM concentration near-surface to the total SPM concentration;* ***c****, ratio (%) SPM concentration near-bed to the total SPM concentration (in %);* ***d****, ratio SPM concentrations near-surface to near-bed (mixing ratio);* ***e****, depth-averaged total SPM flux;* ***f,*** *upper sediment flux to total SPM flux (%);* ***g****, near-bed SPM flux to the total flux (%); h, low-pass filtered (residual) bed shear stress (Pa). Blue highlight refers to the enhanced positive (NEW) flow regime phases, and red is the negative flow regime*

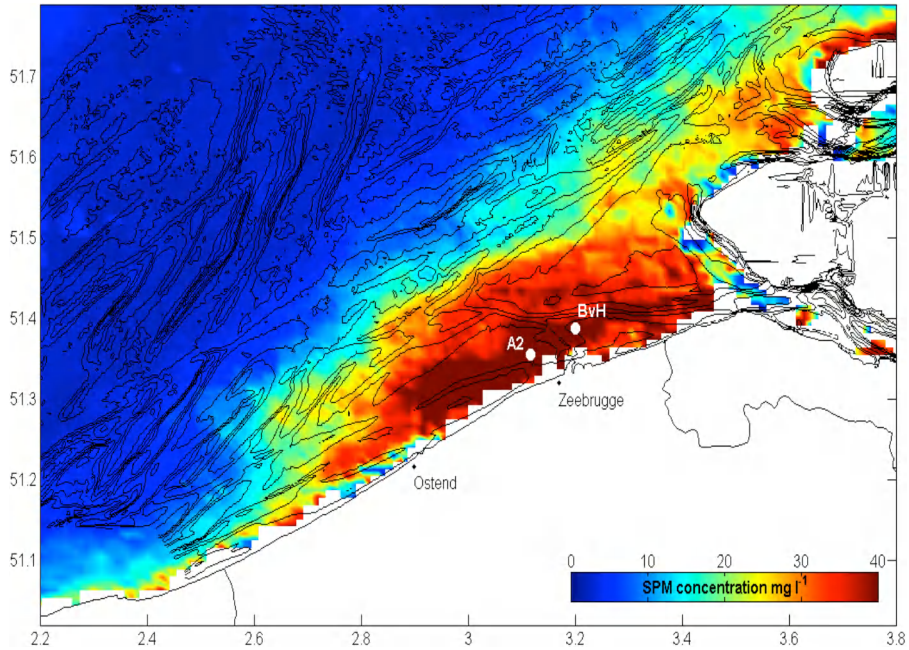

Figure 4.8 *SPM concentration composite maps derived from MODIS Aqua satellite during northern storm wave conditions (winds with north component and significant wave height >1.5 m). A2 and BvH are MOW1 and MOW3, respectively. Vertical and horizontal axes are latitude and longitude (in degree), respectively*

4.6. Conclusions

Wind-driven flows were quantitatively investigated, and considered to be important in the study area. Time-series (40 days each) of BM-ADCP current profiles, as well as acoustic backscatter data were studied in terms of sediment transport (fluxes). An approximation of full water column SPM fluxes through combined use of ADP and BM-ADCP was realised. Based on the alongshore flow direction, two flow regimes were characterised in terms of sediment flux and vertical mixing. The negative flow regime (SWW Case; towards France) corresponds to decreased salinity and increased turbidity (higher SPM concentration). The nature of SPM is cohesive and the water column is vertical mixed; however, this mixing is not hydrodynamically controlled. Linked to this flow direction, storm waves (from the north) result in the largest extent of the coastal turbidity maximum as observed at water surface. Enhanced erosion of the seabed and mixing capacity are the main responsible mechanisms. The positive flow regime (NEW Case; towards the Netherlands) readily shows increased salinity, but decreased turbidity. This regime is characterized by vertical mixing of the water column, and high SPM fluxes. The long-term evolution of the system is therefore dependent on the mutual occurrence of the flow regimes, and thus on the wind climate.

4.7. Acknowledgements

I want to acknowledge the crew of RV Belgica, Zeearend and Zeehond for their skilful mooring and recuperation of the tripod and BM-ADCP. Measurements would not have been possible without technical assistance of A. Pollentier, J-P. De Blauwe, and J. Backers (Measuring Service of MUMM, Oostende).

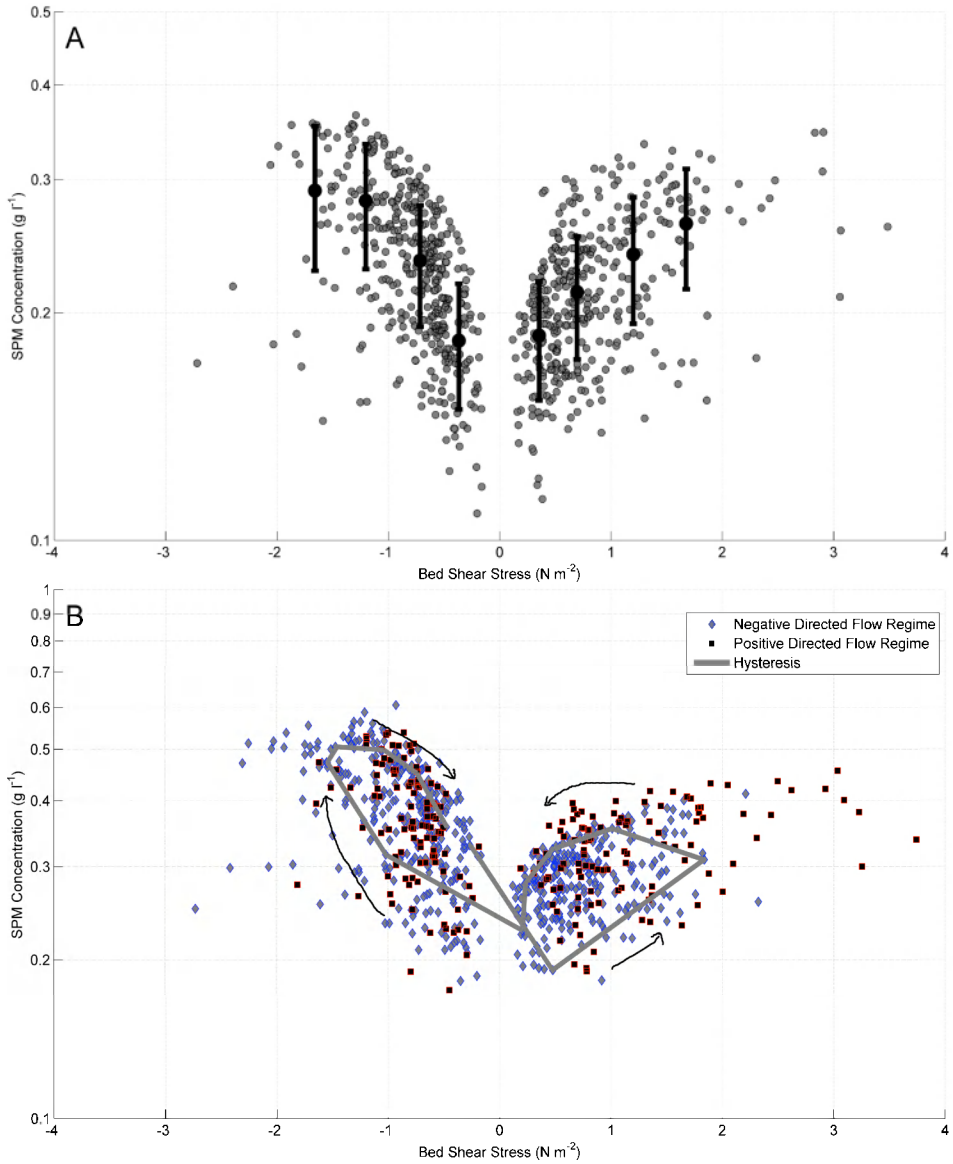

***Figure 4.9 a**, Bed Shear Stress – depth-averaged SPM concentration with vertical error bars; **b,** Bed Shear Stress vs. SPM concentration at 2 m above bed (for the negative 'diamonds' and positive 'squares' flow regime). BM-ADCP period 2006*

4.8. References

Arndt S, Lacroix G, Gypens N, Regnier P, Lancelot C (2011). Nutrient dynamics and phytoplankton development along an estuary-coastal zone continuum: A model study, 49-66. In Journal of Marine Systems 84 (3-4).

Baeye M, Fettweis M, Voulgaris G, Van Lancker V (2011). Sediment mobility in response to tidal and wind- driven flows along the Belgian inner shelf, southern North Sea. Ocean Dynamics 61(5), 611-622.

Beardsley RC, Limeburner R, Rosenfeld LK (1985). Introduction to the CODE-2 moored array and large-scale data report, in CODE-2: Moored Array and Large-Scale Data Report, edited by R. Limeburner, Tech. Rep. WHOI-85–35, 234 pp., Woods Hole Oceanogr. Inst., Woods Hole, Mass.

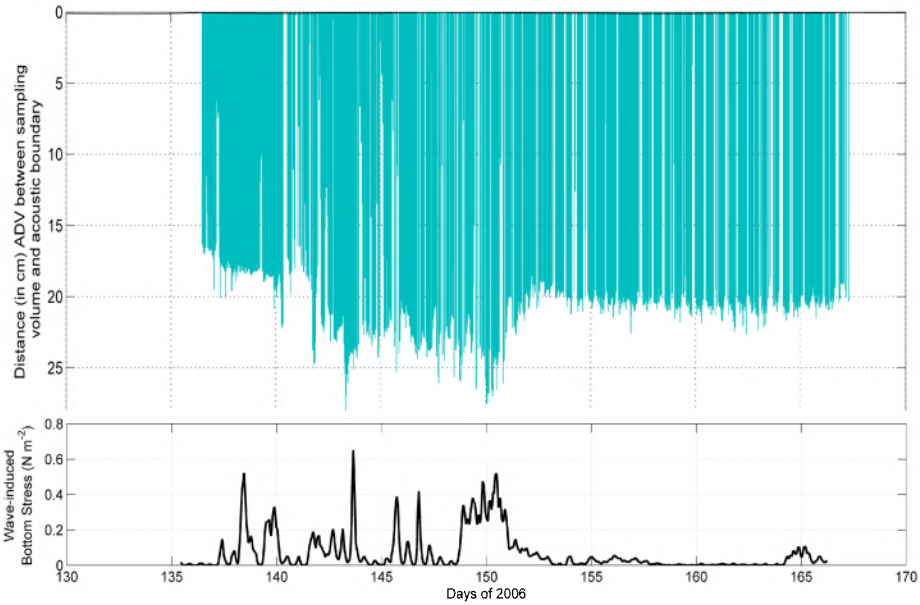

***Figure 4.10 Top**, bed evolution (ADV altimetry) and **bottom**, wave-induced bed shear stress*

Creed EL, Pence AM, Rankin KL (2001). Inter-Comparison of Turbidity and Sediment Concentration Measurement from an ADP, an ABS-3, and a LISST, in: Proceedings of Oceans 2001 MTS/IEEE Conference Proceedings, Honolulu, HI, 2001, (3) 1750-1754.

Deines KL (1999). Backscatter estimation using broadband acoustic Doppler current profilers, in: Proceedings of the IEEE Sixth Working Conference on Current Measurements, San Diego, CA, March 11-13, 1999, pp. 249-253.

Delhez EJM, Carabin G (2001). Integrated modelling of the Belgian coastal zone Estuarine, Coastal and Shelf Science 53(4), 477-491.

de Ruijter WPM, Postma L, Kok JMD (1987). Transport Atlas of the Southern North Sea Rijkswaterstaat, The Hague. 33 pp.

Downing J (2006). Twenty-five years with OBS sensors: The good, the bad, and the ugly. Continental Shelf Research 26, 2299-2318.

Downing A, Thorne PD, Vincent CE (1995). Backscattering from a suspension in the near field of a piston transducer. Journal of the Acoustical Society of America 97 (3), 1614-1620.

Du Four I, Van Lancker V (2008). Changes of sedimentological patterns and morphological features due to the disposal of dredge spoil and the regeneration after cessation of the disposal activities. Marine Geology 255(1-2), 15-29

Dyer KR (1994). Estuarine sediment transport and deposition. In: Pye, K. (ed.) Sediment Transport und Depositional Processes. Blackwell Scientific Publications, Oxford, 193-218.

Fettweis M, Nechad B (2011). Evaluation of in-situ and remote sensing sampling methods of SPM concentration, Belgian continental shelf (southern North Sea) Ocean Dynamics 61(2-3), 157-171.

Fettweis M, Du Four I, Zeelmaeker E, Baeteman C, Francken F, Houziaux J-S, Mathys M, Nechad B, Pison V, Vandenberghe N, Van den Eynde D, Van Lancker V, Wartel S (2007). Mud Origin, Characterisation and Human Activities (MOCHA). Final Scientific Report, D/2007/1191/28. Belgian Science Policy Office, 59 pp.

Fettweis M, Francken F, Van den Eynde D, Verwaest T, Janssens J, Van Lancker V (2010). Storm influence on SPM concentrations in a coastal turbidity maximum area with high anthropogenic impact (southern North Sea). Continental Shelf Research 30, 1417-1427.

Fettweis M, Van den Eynde D (2003). The mud deposits and the high turbidity in the Belgian-Dutch coastal zone, Southern bight of the North Sea. Continental Shelf Research, 23, 669-691.
Fewings MR, Lentz SJ (2009). A momentum budget for the inner continental shelf south of Massachusetts. Journal of Geophysical Research 115 C12.
Grasmeijer BT, Kleinhans MG (2004). Observed and predicted bed forms and their effect on suspended sand concentrations. Coastal Engineering 51, 351-371.
Gullentops F, Moens M, Ringele A, Sengier R (1976). Geologische kenmerken van de suspensie en de sedimenten. In: Nihoul, J., Gullentops, F. (Eds.), Project Zee-Projet Mer., vol. 4. Science Policy Office, Brussels, Belgium, pp. 1–137.
Gutierrez BT, Voulgaris G, Work PA (2006). Cross-shore variation of wind-driven flows on the inner shelf in Long Bay, South Carolina, United States, Journal of Geophysical Research 111, C03015.
Gutierrez BT, Voulgaris G, Thieler ER (2005). Exploring the persistence of sorted bedforms on the inner-shelf of Wrightsville Beach, North Carolina: Continental Shelf Research 25 (1), 65-99.
Grant WD, Madsen OS (1986). The Continental-Shelf Bottom Boundary Layer Annual Review of Fluid Mechanics 18, 265-305.
Hoitink AJF, Hoekstra P (2005). Observations of suspended sediment from ADCP and OBS measurements in a mud-dominated environment. Coastal Engineering 52(2), 103-118.
Hommersom A, Wernand MR, Peters S, Boer de J (2010). A review on substances and processes relevant for optical remote sensing of extremely turbid marine areas, with a focus on the Wadden Sea. Helgoland Marine Research 64(2), 75-92.
Lacroix G, Ruddick KG, Ozer J, Lancelot C (2004). Modelling the impact of the Scheldt and Rhine/Meuse plumes on the salinity distribution in Belgian waters (southern North Sea). Journal of Sea Research 52, 149-163.
Large WG, Pond S (1981). Open Ocean Momentum Flux Measurements in Moderate to Strong Winds. Journal of Physical Oceanography 11, 13.
Lauwaert B, Bekaert K, Berteloot M, De Backer A, Derweduwen J, Dujardin A, Fettweis M, Hillewaert H, Hoffman S, Hostens K, Ides S, Janssens J, Martens C, Michielsen T, Parmentier K, Van Hoey G, Verwaest T (2009). Synthesis report on the effects of dredged material disposal on the marine environment (licensing period 2008-2009). Report by BMM, ILVO, CD, aMT and WL BL/2009/01. 73 pp.
Lentz (1995). The Amazone River Plume during AMASSEDS: Subtidal current variability and the importance of wind forcing: Journal of Geophysical Research 100 C2, 2377-2390.
Lentz SJ, Guza RT, Elgar S, Feddersen F, Herbers THC (1999). Momentum balances on the North Carolina inner shelf. Journal of Geophysical Research 104, 18205–18226.
Lynch JF, Gross TF, Sherwood CR, JD Irish, Brumley BH (1997). Acoustical and optical backscatter measurements of sediment transport in the 1988-1989 STRESS experiment Continental Shelf Research 17 (4), 337-366.
Medwin H, Clay CS (1998). Fundamentals of Acoustical Oceanography, Academic Press. 712 pp.
McNinch JE, Luettich RA (2000). Physical processes around a cuspate foreland headland: implications to the evolution and long-term maintenance of a cape-associated shoal. Continental Shelf Research, 20 (17), 2367-2389.
Mehta AJ (1989). On estuarine cohesive sediment suspension behavior. Journal of Geophysical Research 94 C10, 14303-14314.
Nihoul J (1975). Effect of tidal stress on residual circulation and mud deposition in the southern Bight of the North Sea. Review of Pure and Applied Geophysics 113, 577–591.
Nielsen P (1986). Suspended sediment concentrations under waves. Coastal Engineering 10, 23–31.
Pawlowicz R, Beardsley B, Lentz S (2002). Classical tidal harmonic analysis with errors in matlab using t-tide. Computers & Geosciences 28, 929–937.

Pietrzak JD, de Boer GJ, Eleveld MA (2011). Mechanisms controlling the intra-annual mesoscale variability of SST and SPM in the southern North Sea. Continental Shelf Research 31(6), 594-610.
Pleskachevsky A, Dobrynin M, Babanin A, Günther H, Stanev E (2011). Turbulent mixing due to surface waves indicated by remote sensing of suspended particulate matter and its implementation into coupled modelling of waves, turbulence, and circulation. Journal of Physical Oceanography 41, 708–724.
Sanay R, Voulgaris G, Warner JC (2007). Tidal asymmetry and residual circulation over linear sandbanks and their implication on sediment transport: A process-oriented numerical study, Journal of Geophysical Research 112, C12015 15 pp.
Stanev EV, Dobrynin M, Pleskachevsky A, Grayek S, Günther H (2009). Bed shear stress in the southern North Sea as an important driver for suspended sediment dynamics. Ocean Dynamics 59(2), 183-194.
Soulsby RL (1983). The bottom boundary layer of shelf seas. In Physical Oceanography of Coastal and Shelf Seas, ed. B. Johns, pp. 189-266. Amsterdam: Elsevier. 470 pp.
Soulsby (1997). Dynamics of Marine Sands, Thomas Telford, London, pp. 249.
Terwindt JHJ (1977). Mud in the Dutch Delta area. Geologie en Mijnbouw 56 (3), 203-210.
Urick RJ (1983). Principles of underwater sound, 3rd ed. New York: McGraw-Hill 423 pp.
Verlaan PAJ, Groenendijk FC (1993). Long term pressure gradients along the Belgian and Dutch coast. MAST G8M report DGW-93.045, Rijkswaterstaat Tidal Waters Division.
Van Veen J (1936). Onderzoekingen in de Hoofden in verband met de gesteldheid der Nederlandse Kust, Nieuwe Verhandelingen van het Bataafse Genootschap voor Proefondervindelijke Wijsbegeerte te Rotterdam, 2e reeks, IIe deel, 252 pp.
Van Lancker V, Du Four I, Verfaillie E, Deleu S, Schelfaut K, Fettweis M, Van den Eynde D, Francken F, Monbaliu J, Giardino A, Portilla J, Lanckneus J, Moerkerke G, Degraer S (2007). Management, Research and Budgetting of Aggregates in Shelf Seas related to End-users (Marebasse). Belgian Science Policy: Brussels, 139 pp.
Van Alphen JS (1990). A mud balance for Belgian–Dutch coastal waters between 1969 and 1986. Netherlands Journal of Sea Research 25, 19–30.
Verfaillie E, Van Lancker V, Van Meirvenne M (2006). Multi-variate geostatistics for the predictive modelling of the surficial sand distribution in shelf seas Continental Shelf Research 26(19), 2454-2468.
Van den Eynde D (2004). Interpretation of tracer experiments with fine-grained dredging material at the Belgian Continental Shelf by the use of numerical models. Journal of Marine Systems 48, 171-189.
Verlaan PAJ, Spanhoff R (2000). Massive sedimentation events at the mouth of the Rotterdam waterway. Journal of Coastal Research 16, 458-469.
Winterwerp JC, Van Kesteren WGM (2004). Introduction to the physics of cohesive sediment in the marine environment. Developments in Sedimentology 56, (Elsevier, Amsterdam). 576 pp.
Wright LD (1989). Benthic boundary layers of estuarine and coastal environments. Reviews in Aquatic Sciences 1(1), 75-95.
Yang L (1998). Modelling of hydrodynamic processes in the Belgian Coastal Zone, Applied Mathematics. Catholic University of Louvain, Leuven, pp. 204.
Zeelmaekers E (2011). Computerized qualitative and quantitative clay mineralogy: introduction and application to known geological cases. PhD Thesis. Katholieke Universiteit Leuven. Groep Wetenschap en Technologie: Heverlee. ISBN 978-90-8649-414-9. XII, 397 pp.

Hydro-meteorological influences and multimodal suspended particle size distributions in the Belgian nearshore area*

Michael Fettweis[1], Matthias Baeye[2], Byung Joon Lee[3], Peihung Chen[4], Jason C.S. Yu[4]

[1]*Royal Belgian Institute of Natural Science, Management Unit of the North Sea Mathematical Models, Gulledelle 100, 1200 Brussels, Belgium*

[2]*Ghent University, Renard Centre of Marine Geology, Krijgslaan 281 (S8), 9000 Gent, Belgium*

[3]*Katholieke Universiteit Leuven, Hydraulics Laboratory, Kasteelpark Arenberg 40, 3001 Heverlee, Belgium*

[4]*National Sun Yat-Sen University, Department of Marine Environment and Engineering, Lien-Hai Road 70, 80424 Kaohsiung, Taiwan*

*published in Geo-Marine Letters (Springer)

M. Baeye helped writing the manuscript, helped interpreting all datasets (hydro-meteorological data, LISST, SPM, altimetry), and made figures 5.2, 5.3, 5.4 and 5.6. Also, the acoustic-optics interpretation in relation to particle composition was realised by M. Baeye; as well as the LISST ensemble-averaging based on subtidal flow direction.

Abstract

Suspended particulate matter (SPM) concentration and particle size distribution (PSD) were assessed in a coastal turbidity maximum area (southern North Sea) during a composite period of 37 days in January–April 2008. PSDs were measured with a LISST 100X and classified using entropy analysis in terms of subtidal alongshore flow. The PSDs during tide-dominated conditions showed distinct multimodal behaviour due to flocculation, revealing that the building blocks of flocs consist of primary particles (<3 µm) and flocculi (15 µm). Flocculi comprise clusters of clay minerals, whereas primary particles have various compositions (calcite, clays). The PSDs during storms with a NE-directed alongshore subtidal current (NE storms, Case NEW) are typically unimodal and characterised by mainly granular material (silt, sand) re-suspended from the seabed. During storms with a SW-directed alongshore subtidal current (SW storms, Case SWW), by contrast, mainly flocculated material can be identified in the PSDs. The findings emphasise the importance of wind-induced advection, alongshore subtidal flow and high-concentrated mud suspensions (HCMSs) as regulating mechanisms of SPM concentration, as well as other SPM characteristics (cohesiveness or composition of mixed sediment particles) and size distribution in a high-turbidity area. The direction of subtidal alongshore flow during SW storm events results in an increase in cohesive SPM concentration, HCMS formation, and the armouring of sand; by contrast, there is a decrease in cohesive SPM concentration, no HCMS formation, and an increase in sand and silt in suspension during NE storms.

Keywords: Suspended particulate matter; particle size distribution; statistical handling; coastal turbidity maximum; wind impact; seabed variations

5.1. *Introduction*

Knowledge of the size distribution of suspended particulate matter (SPM) is needed to understand and predict sediment dynamics (Eisma 1986, van Leussen 1994, Curran et al. 2007, Mikkelsen et al. 2007, Winter et al. 2007, Bowers et al. 2009, Lee et al. 2011). Natural SPM comprises many different substances with time- and site-specific concentrations and can be subdivided into inorganic and organic fractions. The inorganic fraction consists mainly of clay minerals as well as carbonates and other non-cohesive minerals (Berlamont et al. 1993, Fettweis 2008); the organic fraction of SPM is prevalently made of micro-organisms and their metabolic products, as well as the remains of dead organisms and faecal pellets (Mari and Burd 1998, Hamm 2002, Bhaskar et al. 2005). Sediments in coastal areas generally consist of sand and mud. The mud–sand ratio influences the transition between cohesive and non-cohesive behaviour, and has a major influence on erosion, SPM concentration, SPM composition and benthic ecological properties (Williamson and Torfs 1996, Panagiotopoulos et al. 1997, van Ledden et al. 2004). In such areas, SPM reflects the bed composition and may consist of a mixture of cohesive and non-cohesive mineral particles (Manning et al. 2010). Close to a sandy seabed, SPM is likely to also contain re-suspended mineral grains, whereas higher in the water column or in muddy environments SPM occurs typically in the form of flocs composed of aggregates of mainly clay minerals, organic matter and water. Mud and sand can be deposited as alternating layers when mud and sand settle either separately from independent suspension or simultaneously. The latter implies segregation due to settling of sand grains through the non-consolidated mud layer (van Ledden et al. 2004).

Flocs vary in size on short time-scales (ebb–flood), as they are formed by collisions due to differential settling of smaller particles with cohesive properties in low-turbulence regimes, and are ruptured by shear in high-turbulence regimes (Lick et al. 1993, van Leussen 1994, Winterwerp 1998). With increasing turbulent shear, breakage of flocs generates smaller particles/flocs but re-suspension of bigger deposited minerals can generate larger particles and flocs in suspension. SPM is therefore likely to have a multimodal particle size distribution (Mikkelsen et al. 2007, Mietta et al. 2010, Lee et al. 2011, Verney et al. 2011), which reflects the fast temporal changes in floc sizes due to variation in turbulent shear as well as the overlapping distributions of flocs and mineral grains in mixed sediment environments under strongly varying shear stresses.

Under laboratory conditions, Manning et al. (2010) have shown that flocculation influences the deposition and settling of sand–mud mixtures. Little data are, however, available that deal with re-suspension of sand, mud and sand–mud mixtures in natural environments. The aim of this work is therefore to present in-situ measurements in an area with mixed bed sediments and to examine the influence of tides, wind and wave effects on the particle size distributions (PSDs) of flocs and granular particles. Furthermore, the potential for mud and sand fractions to occur simultaneously in suspension is discussed, as this can contribute to knowledge on the long-term evolution of a system, notably in terms of conceptual and mathematical models. Understanding of sediment mobility in such environments requires the use of multi-parametric observations supported by mathematical methods. The observations should account for the mutual interaction of sand and mud in suspension as a function of bed armouring, sheltering and exposure effects, erosion and re-suspension, and flocculation dynamics (Wiberg et al. 1994, Wallbridge et al. 1999, Wu et al. 2003). The fragility of flocs makes them difficult to sample, and measurements of floc properties should rely on high-resolution in-situ techniques employing, for example, LISST, floc cameras and holographic cameras (van Leussen 1994, Agrawal and Pottsmith 2000, Manning et al. 2006, Mikkelsen et al. 2006, Benson and French 2007, Graham and Nimmo-Smith 2010).

With this scope in mind, in-situ measurements of SPM concentration, PSDs, and also of currents were carried out in Belgian coastal waters (southern North Sea) by means of optical and acoustical sensors. PSDs provide essential information on floc and particle dynamics, as emphasised by Mikkelsen et al. (2006). In the present study, statistical methods (entropy analysis, fitting of PSDs with summed log-normal functions) and ensemble-averaging have therefore been applied to classify PSDs and to establish links with the underlying processes. Similar measuring approaches (e.g. Fugate and

Friedrichs 2002, Thorne and Hanes 2002, Voulgaris and Meyers 2004, Hoitink and Hoekstra 2005), statistical methods (Jonasz and Fournier 1996, Mikkelsen et al. 2007) and averaging (Murphy and Voulgaris 2006) have been successfully adopted in various marine environments.

5.2. *Study site*

Measurements were carried out in the Belgian nearshore zone (Fig. 5.1) in the southern bight of the North Sea, characterised by bottom sediments varying from pure sand to pure mud (Verfaillie et al. 2006) and by highly turbid waters. Nearshore SPM concentration ranges between 0.02–0.07 g l^{-1} and reaches 0.1 to >3 g l^{-1} near the bed; lower values (<0.01 g l^{-1}) occur offshore (Fettweis et al. 2010).

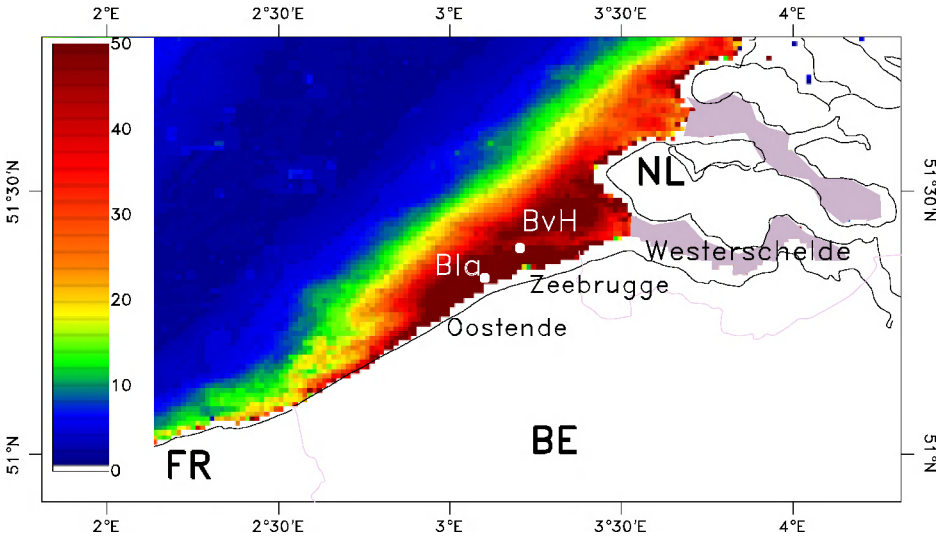

Figure 5.1 *Map of the Belgian coastal area (southern North Sea), showing yearly averaged surface SPM concentration (mg dry wt l^{-1}) derived from moderate resolution imaging spectroradiometer (MODIS) images of 2002–2009 (extracted from Nechad et al. 2010), the tripod measurement station at Blankenberge (Bla) and the wave measurement station at Bol van Heist (BvH); coordinates are in °N latitude and °E longitude*

The tidal regime is semi-diurnal, and the mean tidal range at Zeebrugge is 4.3 and 2.8 m at spring and neap tide, respectively. The tidal current ellipses are elongated in the nearshore area and become gradually more semi-circular towards the offshore. The current velocities near Zeebrugge (nearshore) vary from 0.2–1.5 m s^{-1} during spring tide and 0.2–0.6 m s^{-1} during neap tide. Ebb currents are directed towards the southwest and flood currents towards the northeast.
South-westerly winds dominate the overall wind climate, followed by winds from the NE sector. Maximum wind speeds coincide with the south-westerly winds; nevertheless, the highest waves are generated under north-westerly winds. Salinity varies between 28 and 34 PSU in the coastal zone, due to wind-induced advection of water masses and river discharge (Lacroix et al. 2004, Fettweis et al. 2010).
The effect of hydro-meteorological forcing (tide- and wind-induced flows) on SPM transport and the formation of high-concentrated mud suspensions (HCMSs) has been investigated by Baeye et al. (2011) for the Belgian nearshore area. They report that winds blowing from the N-NE increase and those (however no storm winds) from the SW decrease the overall SPM concentration at the measurement site. The latter is related to advection of less turbid English Channel water, inducing a shift of the turbidity maximum towards the NE and the Westerscheldt estuary. Under these conditions, marine mud is imported into the estuary. Under protracted NE winds,

HCMSs are formed and can persist during several tidal cycles.
The measurement station Blankenberge is situated about 5 km SW of the port of Zeebrugge, in the eastern part of a shoreface-connected sand ridge (Wenduine Bank) at about 1 km from the shore (Fig. 5.1). The water depth varies between about 6 and 10 m at this location. Sediment samples near Blankenberge show variable sediment characteristics with a median grain size of about 150 µm.

5.3. *Materials and methods*

5.3.1. *Instrumentation and deployment*

Data were collected between January and April 2008 over a composite period of 37 days, using a tripod to measure currents, salinity as well as SPM concentration and PSD (see Table 5.1, and figure captions for dates). The instrumentation suite consisted of a 5 MHz SonTek Acoustic Doppler Velocimeter (ADV Ocean-Hydra), a 3 MHz SonTek Acoustic Doppler Profiler (ADP), two D&A optical backscatter point sensors (OBSs), a Sea-bird SBE37 CT and a Sequoia Scientific LISST (laser in-situ scattering and transmissometry) 100 X type C. All data (except LISST) were stored in two SonTek Hydra data logging systems.
The LISST was mounted at 2 meters above the bed (hereafter referred to as mab) and the OBSs at 0.2 and 2 mab. ADV velocities were measured at 0.2 mab, while the ADP profiler was attached at 2.3 mab and down-looking, measuring current and acoustic intensity profiles with a bin resolution of 0.25 m. Mean values were obtained every 10 minutes for the OBS, LISST and ADV, while the ADP was set to record a profile every 1 minute; subsequent averaging was performed at a 10-minute interval to match the sampling interval of the other sensors. The long deployments ensured accurate assessments of conditions over complete neap and spring tides, and included a variety of meteorological events.

Table 5.1 *Modal size (µm) and volumetric fractions (%) of primary particles (PP), flocculi, microflocs and macroflocs for the entropy groups of the two deployments (cf. Fig. 5.5). Mode 1 (PP) and mode 2 (flocculi) have a fixed size of 3 and 15 µm respectively*

	PP	Flocculi	Microflocs	Macroflocs
Group 1	6%	43%	46 µm, 47%	230 µm, 4%
Group 2	2%	25%	58 µm, 68%,	271 µm, 5%
Group 3	1%	16%	87 µm, 80%	360 µm, 3%
Group 4	1%	15%	119 µm, 69%	339 µm, 16%

5.3.2. *SPM concentration, HCMSs and turbulence*

The OBS and ADP backscattered signals were used to estimate SPM concentration. OBS voltage readings were converted into SPM concentration by calibration against filtered water samples during several field campaigns (Fettweis et al. 2006). A linear relationship was assumed between all OBS signals and SPM concentrations from filtration. After conversion to decibels, the ADP backscattered acoustic signal strength was corrected for geometric spreading and water attenuation. Furthermore, an iterative approach (Kim et al. 2004) was used to correct for sediment attenuation. The highest OBS-derived SPM concentration estimates were used to empirically calibrate the ADP's first bin. As variations in SPM composition and size were not taken into account, the ADP backscatter signal was calibrated in terms of 'average' SPM.
Limitations associated with optical and acoustic instruments have been addressed by Thorne et al. (1991), Hamilton et al. (1998), Bunt et al. (1999), Fugate and Friedrichs (2002), Voulgaris and Meyers (2004) and Downing (2006). In general, acoustic

backscattering is affected by sediment type, size and composition. All these parameters are difficult to quantify by single-frequency backscatter sensors (Hamilton et al. 1998). OBSs have primarily been designed to be most sensitive to SPM concentration; size effects are an order of magnitude lower than those of concentration, and flocculation effects are even smaller (Downing 2006). Compared to optical devices, acoustic devices are more sensitive to coarser grain sizes and thus produce better estimates of the mass concentration of the coarser granular fraction. Briefly, when SPM composition changes from very fine material to silt- or sand-sized grains without changes in concentration, then the SPM concentration derived from acoustic and optical backscattering will differ. An ADP calibrated for fine material will have a stronger backscattering and, thus, it produces an apparently higher concentration when the SPM becomes coarser. By contrast, under these circumstances the optical backscatter signal will decrease, resulting in an apparent decrease in SPM concentration.
Besides the time-series of current velocities and acoustic amplitude, the ADP was also configured to measure and store the distance between sensor and seabed (Baeye et al. 2011). The altimetry of the ADP was used to detect variation in bed level, and also for the identification of deposition and re-suspension of fine-grained sediments. For the study site, decreasing distance between the probe and the bed boundary can correspond to the presence of HCMSs acting as an acoustic reflector.
The high-frequency ADV measurements (measuring rate of 25 Hz) were used to decompose the velocity in terms of a mean and a fluctuating part. The variance of velocity fluctuations served to calculate the turbulent kinetic energy (TKE), this being a measure of turbulence intensity (Pope et al. 2006).

5.3.3. Classification of PSDs

Two methods for the classification of particle size spectra were applied. The one uses the flow data to separate the LISST records into different groups corresponding to different hydrodynamic forcing. The collected time-series were filtered for the tidal signal using a low-pass filter for periods less than 33 h, and decomposed into along- and cross-shore components. The alongshore low-pass flow served to characterise the tidal cycle in terms of wind-driven flow. Three cases were identified, one corresponding to pure tidal flow (Case 0) and two to periods with significant influence of wind-driven flows: case SW (or Case SWW cf. Chapter 2) has winds from the NW–NE resulting in residual alongshore currents directed towards the SW; case NE (or Case NEW cf. Chapter 2) has winds from the SW and residual alongshore currents directed towards the NE. Moreover, each tidal cycle was classified as neap or spring depending on the particular tidal range. This classification has resulted in a total of six categories of tidal cycles, where each category represents both tidal and wind forcing. Tidal cycles from each category were ensemble-averaged to create a representative tidal cycle for each case (cf. Murphy and Voulgaris 2006, Baeye et al. 2011 for a more detailed description of the method).
The other method of classification entails entropy analysis to evaluate the randomness of an event (such as a particle size distribution) and to assign the event to a group with similar characteristics. Applied to PSDs, entropy analysis allows grouping the size spectra without assumptions about the shape of the spectra and is therefore suited for analysis of unimodal, bimodal as well as multimodal distributions (Woolfe et al. 1998). Entropy analysis has been successfully applied to grain size distributions from sedimentary deposits (Forrest and Clarke 1989, Woolfe and Michibayashi 1995, Woolfe et al. 1998, Orpin and Kostylev 2006) and to LISST particle size distributions of suspended matter (Mikkelsen et al. 2007, Krivtsov et al. 2011). Our analysis was carried out with the FORTRAN routine of Johnston and Semple (1983) extended with a module to calculate the optimal number of groups using the Calinski-Harabasz pseudo F-statistic (Orpin and Kostylev 2006, Stewart et al. 2009). The results are presented as an averaged and normalized PSD for each group.

5.3.4. Multimodal log-normal distribution function

Mathematical functions such as summed log-normal distribution functions can be used to describe PSDs. This approach was applied to decompose the averaged and

normalized PSDs from entropy analysis into a sum of four log-normal functions, in order to quantify the volumetric fraction of primary particles, flocculi, micro- and macro-flocs. This four-level ordered structure results from flocculation of clay minerals, as reported by van Leussen (1994). The multimodal log-normal distribution function can then be written as an integrated distribution function of four log-normal distribution functions (Whitby 1978, Jonasz and Fournier 1996, Sun et al. 2002, Hussein et al. 2005):

$$\frac{\mathrm{d}W}{\mathrm{d}D} = \sum_{i=1}^{4} \frac{\overline{W}_i}{\sqrt{2\pi}\ln(\sigma_i)} \exp\left[-\frac{1}{2}\left(\frac{\ln\left(D/\overline{D_i}\right)}{\ln(\sigma_i)}\right)^2\right]$$

where D is the particle diameter, W the volume concentration, $\overline{D_i}$ the geometric mean diameter, σ_i the geometrical standard deviation, and $\overline{W_i}$ the volumetric fraction of an ith unimodal PSD. The DistFit™ software (Chimera Technologies, Forest Lake MN, USA), which has been widely employed in analyzing aerosol particles, was used to generate the best fits, defined as the minimum errors between fitted and measured PSDs (Whitby 1978, Hussein et al. 2005). For two modal peaks, fixed sizes of 3 µm (lowest size class of the LISST) and 15 µm were chosen; the modal peaks of the bigger fractions were variable (15–200 and 200–500 µm). The standard deviations were allowed to vary between 1 and 2.5. The choice of parameters is based on assumptions and experiences (cf. Makela et al. 2000, Lee et al. 2011).

5.4. Results

5.4.1. Time-series

The SPM concentration derived from the ADP (2 mab) and OBS (2 and 0.2 mab), the median particle size derived from the LISST, the along- and cross-shore subtidal flow, and the seabed altimetry derived from the ADP are presented in Fig. 5.2 and 6.3 for the two deployments. Note that the alongshore flow is positive when it is directed towards the NE and negative towards the SW. Positive cross-shore flow is directed towards the shore.

Two storms were registered during the January–February 2008 deployment. The first occurred on days 30.5 to 32.5 (1–2 February) and had a significant wave height (H_s) of up to 2.8 m. The second was on days 35–37 (H_s=1.5 m; see Fig. 5.2). The wind direction during both storm events was variable from the SW to the W and NW at times of peak wave heights. The wind during and before these time periods was generally blowing from the SW–W, resulting in a positive subtidal alongshore flow; these are therefore called NE-ward storms (NE storms). During the rest of the deployment, the significant wave heights were lower (H_s<1.5 m) and the wind blowing mainly from the SW and W.

SPM concentration at 2 mab (OBS) varied between 0.01 and 1.5 g l^{-1} during the calmer periods, with distinct neap–spring tidal variations. The SPM concentration at both 0.2 and 2 mab (OBS) decreased to less than 0.1 g l^{-1} during the first storm (days 30.5–32.5). The SPM concentration derived from the ADP was generally lower than that of the OBS (2 mab), except during the onset of the storms when the 2-mab OBS signal decreased, whereas the backscattered ADP signal increased. The SPM concentration from the ADP during the first storm is significantly correlated with the wave height, and the tidal signal is hardly distinguishable.

The variations in median particle size (D50: 20 to >180 µm) during calm meteorological conditions were typically associated with the tidal current variations. Largest floc sizes occurred around slack water and smallest ones during maximum currents. The LISST data show significantly different median particle sizes and particle size variations during the storm periods.

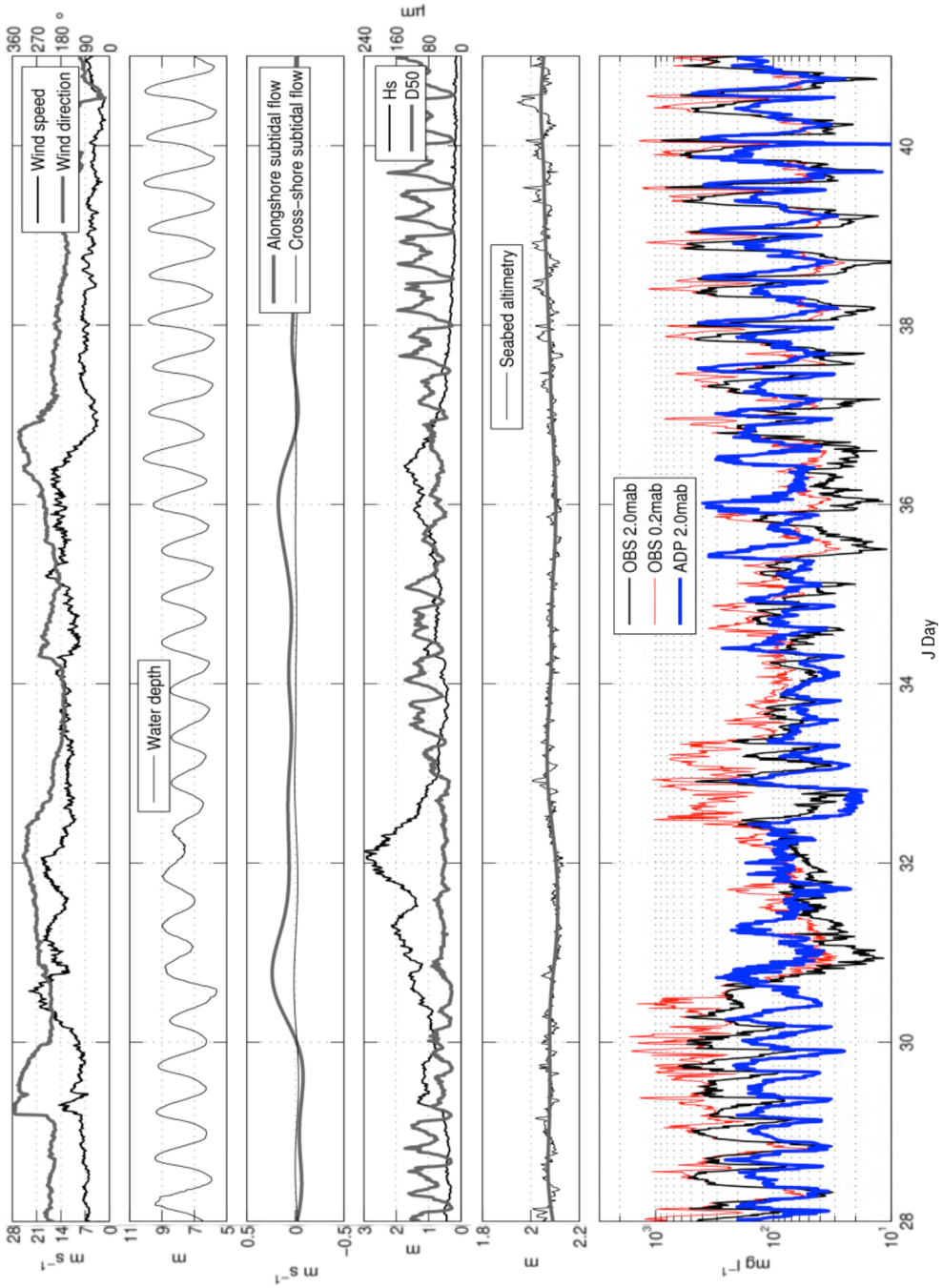

Figure 5.2 *January–February 2008 deployment (28/01 15:38 to 11/02 13:40): time-series of wind velocity and direction (wind from 0°=N, 90°=E, 180°=S, 270°=W) at Bol van Heist; water depth; subtidal alongshore (positive towards the NE, negative towards the SW) and cross-shore flow (positive onshore, negative offshore); significant wave height and D50 of particle size distribution; seabed altimetry; and SPM concentration from OBS (0.2 and 2 mab) and ADP (2 mab)*

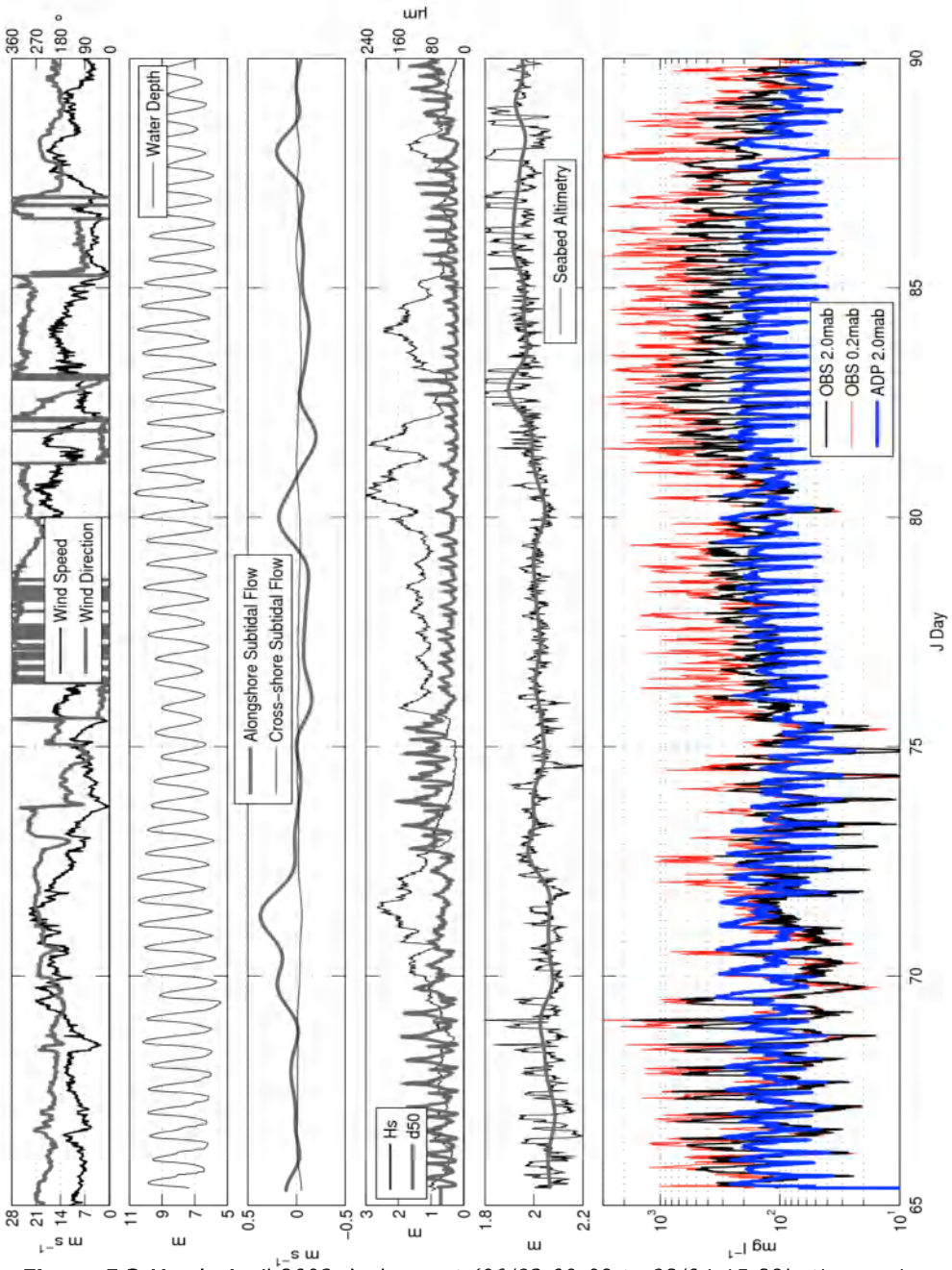

Figure 5.3 *March–April 2008 deployment (06/03 09:09 to 08/04 15:29): time-series of wind velocity and direction (wind from 0°=N, 90°=E, 180°=S, 270°=W) at Bol van Heist; water depth; subtidal alongshore (positive towards the NE, negative towards the SW) and cross-shore flow (positive onshore, negative offshore); significant wave height and D50 of particle size distribution; seabed altimetry; and SPM concentration from OBS (0.2 and 2 mab) and ADP (2 mab)*

The maxima of D50 were smaller and the minima bigger than during periods with mainly tidal forcing (D50: 30–60 µm on days 31–32.5, and 45–70 µm on days 35–37). The typical quarter-diurnal tidal signal in D50 has disappeared during the first NE

storm. The distance between the ADP and the seabed (altimetry) increased during both NE storms, and varied as a function of tides from day 38 on, when the weather was calm. The March–April 2008 deployment was characterised by generally stronger winds (see Fig. 5.3). Significant wave heights of up to 2.5 m were recorded between days 70 and 73 (10–13 March) during a period of SW wind turning towards the W. This storm and a short period around days 79–81 (19–21 March) are associated with positive subtidal alongshore flow and are also classified as 'NE storm'. Similar to the first two storms (days 31–32.5 and 35–37, Fig. 5.2), the SPM concentration at 2 mab derived from the OBS was lower than that from the ADP backscattered signal. The SPM concentration at 0.2 mab was also low. The altimetry increased during both NE storms. The next storms were all characterised by northerly wind directions (NE–N–NW). This type of wind direction generates a negative subtidal alongshore flow directed towards the SW and, therefore, these are called SW-ward storms (SW storms). They occurred on days 76–79 (16–19 March) and days 81–85 (23–25 March). The H_s reached values of 2 m (day 76), 3 m (day 81), 2.7 m (day 84) and 1.8 m (day 88).
The SPM concentration (OBS) was high during the whole period, especially around days 81–88, whereas the SPM concentration from the ADP was always lower (<0.25 g l^{-1}), which is in contrast with the observation made during the NE storms of February and March. The SPM concentration at 0.2 mab reached high values (>3 g l^{-1}), pointing to the occurrence of an HCMS. The latter is confirmed by the generally lower altimetry (and higher seabed) during the period. The data show also that periods with negative alongshore flows (SW storms) are related with decreasing altimetry; however, lowest altimetry was after the storm. The tidally averaged SPM concentration at 2 mab (OBS) varied between 0.6–1.0 g l^{-1} at 2 mab and between 1.6–3.0 g l^{-1} at 0.2 mab. The median particle size of the SPM during the SW storms was similar to that of the NE storms; smaller maxima and larger minima (20–60 µm) were observed than during the meteorological calm periods (15–150 µm). However, the median particle size during the NE storms (days 70–73 and day 32) was clearly different from that of the SW storms (days 81–85). The NE storm at the end of the time-series (day 88, 28 March) is different from the previous in the sense that ADP and OBS SPM concentrations show similar behaviour. The storm followed a period with prominent HCMS layers and evidently was too short for the flocs to be transported away from the site.

5.4.2. Classification of PSDs

The PSD groupings according to alongshore currents are shown in Fig. 5.4. As PSDs represent averages of large amounts of data, which show typical behaviour related to prominent hydro-meteorological conditions, the short-term events such as storms are filtered out. Multimodal distributions caused by formation of macroflocs occurred during ebb and were typically associated with case 0 (no wind) and case NE. They are more obvious during high-energy conditions (spring tide). Multi-modality due to the occurrence of a rising tail in the lowest size classes of the LISST or a peak in the distribution around 150 µm occurred at peak flood velocity (most obvious for SW spring tide).
Entropy analysis revealed that the optimal number of entropy groups was 4. The averaged PSDs per group are shown in Fig. 5.5, and the corresponding temporal distributions of the groups in Fig. 5.4. In contrast with the grouping based on alongshore currents (Fig. 5.4), the entropy-based grouping involves mathematical and not physical characteristics. Nevertheless, the results show that the entropy groups correspond with specific conditions during a tidal cycle and during storm periods, indicating a transition from unimodal distributions with rising tails in the lowest size classes towards multimodal distributions with gradually higher probabilities of occurrence of macroflocs. The shape of group 1 is convex for the lower size classes and concave for the larger sizes. The shape of the distributions in the next size classes becomes gradually more concave in the lower and more convex in the larger size classes. The different groups of particle size distributions obtained, using the entropy method, have been fitted with a sum of four log-normal functions. The volume fraction and geometric mean of the four modes are presented in Table 5.1 and Fig. 5.7. The finest particles represent 1–6% (primary particles) and 15–43% (flocculi) of the volume fraction, the microflocs have modes between 46–119 µm and represent 47–

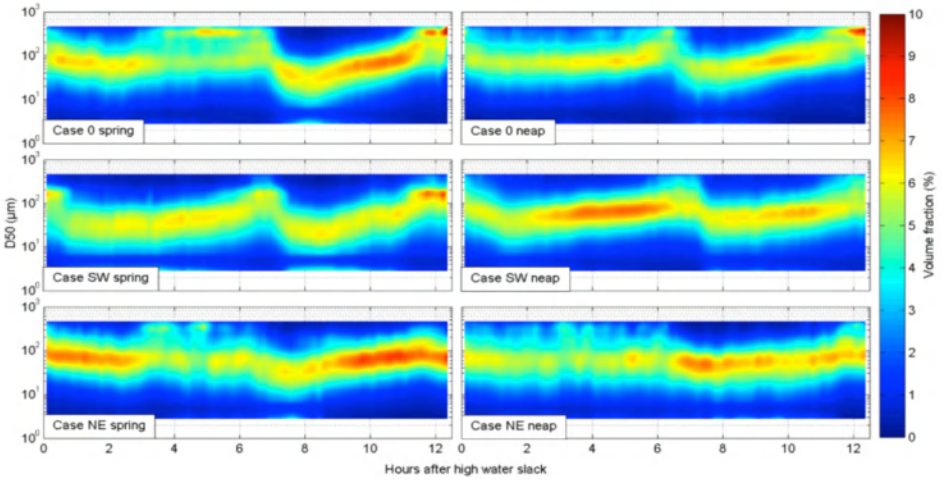

Figure 5.4 *Classification of PSD as a function of alongshore subtidal currents: averaged PSD during one tidal cycle at 2 mab for (**from top to bottom**) case 0 (no wind), case SW (SW-directed alongshore subtidal current) and case NE (NE-directed alongshore subtidal current) at (**from left to right**) spring and neap tide*

80% of the volume fraction, and the macroflocs have a mode of 230–360 µm and a volume fraction varying between 4–16%.

5.5. *Discussion*

The different entropy groups as well as the low-pass filtered tidal PSDs indicate a transition between bimodal distributions with rising tails in the lowest size classes and multimodal distributions with gradually bigger particle sizes when turbulence decreases. This behaviour is well described in the literature (e.g. Manning et al. 2006; Mikkelsen et al. 2007; Mietta et al. 2010; Verney et al. 2011) and is typically associated with tidal forcing. PSDs during storm conditions or other high-energy conditions (maximum flood currents during spring tide) are different and show unimodal or multimodal distributions. Below some points are discussed in more detail to explain these as a combination of flocculation processes and erosion events of non-cohesive sediments.

5.5.1. *Flocculation: primary particles, flocculi, flocs*

Several characteristic behaviours of the PSDs were identified by curve fitting analysis. The PSDs have a major modal peak of microflocs and additional peaks, such as a rising tail in the lowest size class (primary particles), and humps of small particles (flocculi) and macroflocs (Fig. 5.7). The data show that the macroflocs in the Belgian nearshore area have a geometric mean between 230–360 µm and the microflocs between 46–119 µm. Significant amounts of macroflocs occur only in group 4. The microfloc population was characterised by a gradual shift of the PSD towards bigger size classes at times of decreasing currents.

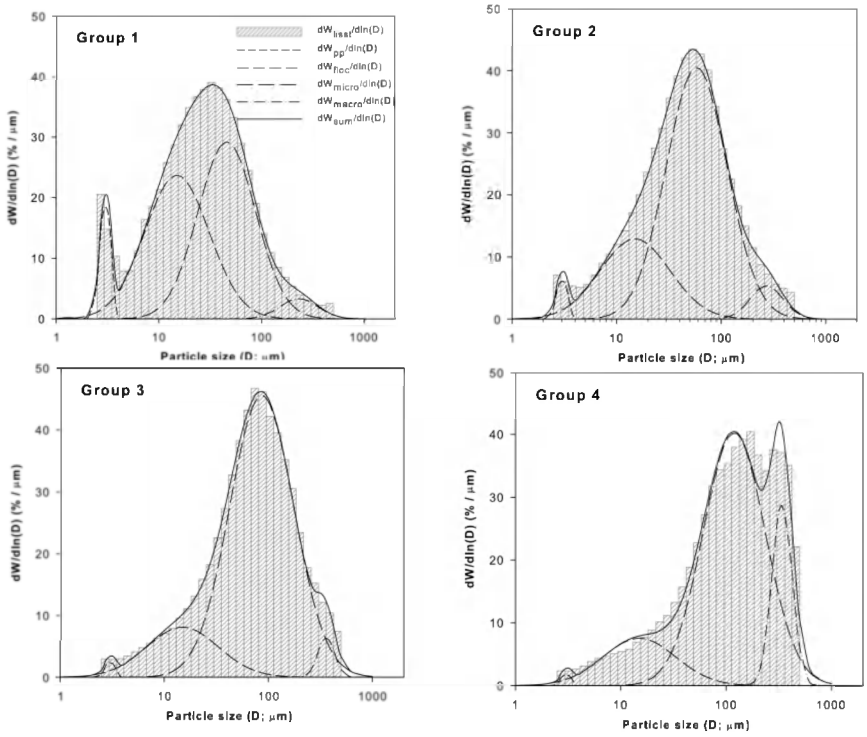

Figure 5.5 *January–February and March–April 2008 deployments: averaged PSD for the four entropy groups, $dW_{lisst}/dln(D)$, together with the fitted sum of the four log-normal functions, $dW/dln(D)$*

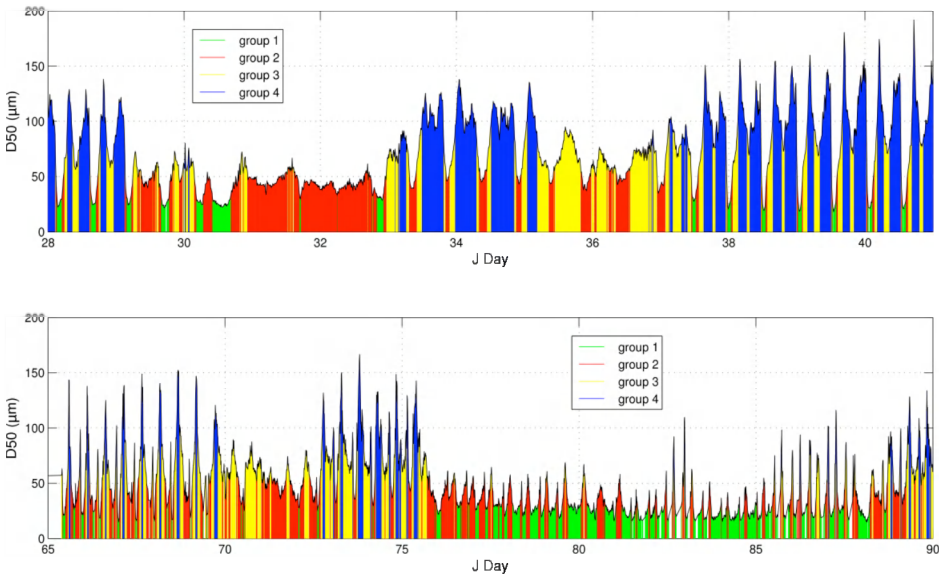

Figure 5.6 *January–February and March–April 2008 deployments: temporal distributions of the four entropy groups*

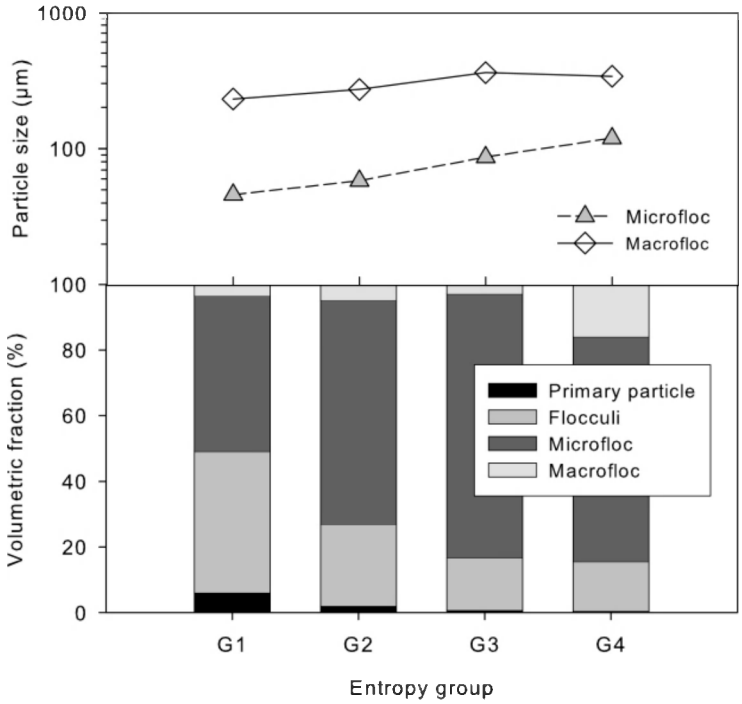

Figure 5.7 *Modal sizes and volumetric fractions of primary particles, flocculi, microflocs and macroflocs in the four entropy groups during both deployments*

The rising tail in the lowest size classes is due to the presence of particles up to 10 times smaller than the smallest size bin (i.e. 0.25–2.5 µm), as well as the occurrence of non-spherical particles (O.A. Mikkelsen, personal communication). Andrews et al. (2010) report that fine 'out of range' particles affect the entire PSD, with a significant increase in the volume concentration of the first two size classes of the LISST, a decrease in the next size classes and, surprisingly, a small increase in the largest size classes. 'Out of range' particles (<2.5 µm) cause an erroneous size distribution (Andrews et al. 2011). The rising tail in our data corresponds with very fine particles resulting from floc breakage. The curve fitting at the 3 µm mode is thus a relict of the inaccuracy of the LISST instrument for fine particles. The volume fraction calculated for this size distribution should therefore be interpreted as an indication for the presence of very fine particles or primary particles. Pre-treatment of fine sediments is needed in order to measure the grain size of individual clay particles (Huang 1989); this suggests that in marine waters clay minerals occur as clusters (with sizes of 15 µm) of a few crystals, as well as individual crystals. Chang et al. (2007) mention that only the fraction <8 µm (analysed after pre-treatment in the laboratory) is present in flocs. This, together with the fact that the median grain size of the SPM from the study area is about 2 µm (Fettweis 2008), confirms that our flocculi (15 µm) consist of clusters of clay minerals rather than silt-sized particles, which are hardly broken down to primary particles (clay minerals), even under high shear (Mietta 2010). The data show that primary particles of possibly different composition (calcareous particles, clay minerals) and flocculi occur as building blocks of the flocs. This could explain why fractal theory based on a single type of primary particle is not able to accurately describe flocculation (Kranenburg 1994, Fettweis 2008).

The PSDs are dominated by primary particles, flocculi and microflocs at maximum flood velocity, suggesting partially disruption of microflocs into primary particles and flocculi, and nearly complete disappearance of the fragile macroflocs (Fig. 5.4 and 5.7). The fact that macroflocs are still found at high current velocities (entropy groups 1 and 2) can possibly be explained by the occurrence of fine 'out of range' particles, as reported by Andrews et al. (2010); the actual volume concentration of macroflocs during these events is thus probably lower. The TKE as a function of median particle

size (D50) is shown in Fig. 5.8 for different situations. TKE is low during calm weather conditions (Fig. 5.8 a); the fact that a hysteresis relation is observed during ebb and flood indicates that floc size is primarily a function of turbulence and available residence time (Winterwerp 1998). Macroflocs are formed during slack water, when turbulence is low, but also during ebb, when currents are still significant but less so than during flood. The latter suggests that mild turbulence below a threshold favours collision and enhances flocculation. When turbulence becomes too high above the threshold, then flocs are disrupted.

5.5.2. Erosion: mixed sediments in suspension

The rising tail in the finest classes of the entropy spectra is associated with high-energy events (group 1 in Fig. 5.5, 5.6) and indicates floc breakage. It was therefore surprising to see that, during SW storm conditions, only a small rising tail was detected in the finest size classes of the LISST. The PSD was log-normally distributed, almost unimodal, and the main mode

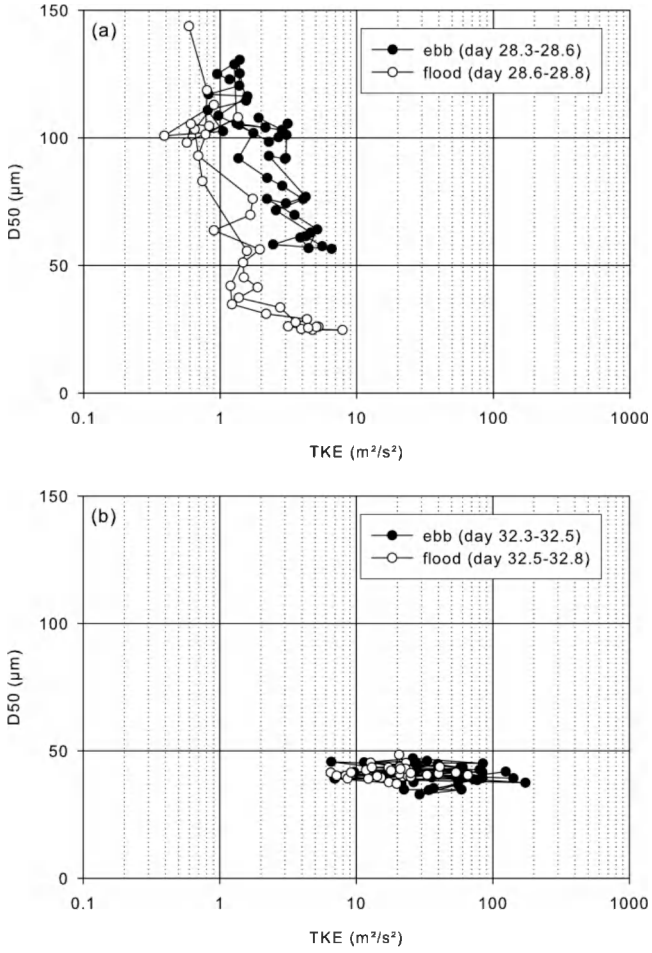

Figure 5.8 *Turbulent kinetic energy (TKE) as a function of median particle size:* ***a*** *neap tide (day 28),* ***b*** *NE storm (day 32)*

remained almost constant in size (D50≈50 µm; see entropy group 2 occurring dominantly around days 32 and 71; Fig. 5.5, 6.6). NE storms were characterised by lower SPM concentrations derived from the OBS than from the ADP at 2 mab (Fig. 5.2, 5.3), suggesting that the composition and size of the SPM has partially changed from

flocculated fine-grained material to silt-sized grains. The latter is confirmed by the distinctly different PSD measured during these events (Fig. 5.5, 5.6), as well as by the observation that TKE has almost no effect on particle size (Fig. 5.8 b, c), in contrast with calm weather (Fig. 5.8 a) and SW storm conditions (Fig. 5.8 d).

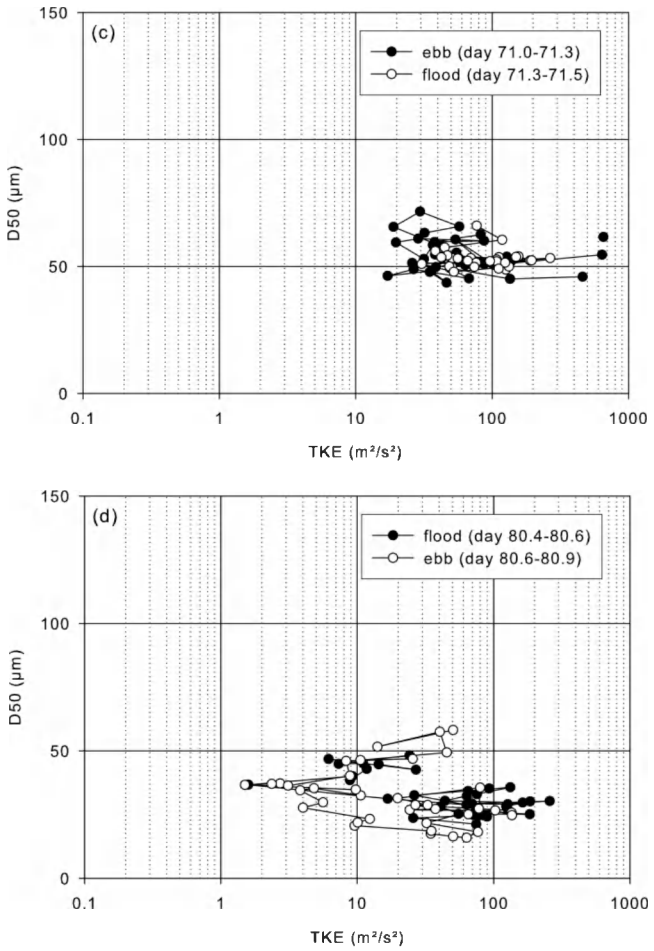

***Figure 5.8** (**continued**) Turbulent kinetic energy (TKE) as a function of median particle size: **c** NE storm (day 71) and **d** SW storm (days 80–81)*

Furthermore, the altimetry signal increased, pointing to erosion events and, thus, disappearance of fine-grained material. The low SPM concentration derived from the OBS during the NE storms is thus most probably caused by changes in the size and composition of SPM, explaining the apparent decrease in SPM concentration (Downing 2006). If composition would not have changed, then one would expect an increase in optical backscattering during high-energy events as flocs break up, resulting in an apparent increase in SPM concentration (Agrawal and Traykovski 2001). The fact that, during NE storms, PSDs and acoustical and optical backscatter signals varied differently can be explained only by a decrease in concentration of flocculated material and by changes in the composition of SPM due to wave-induced re-suspension of coarser bed material. Prevailing SW winds enhance NE-directed subtidal flow, which generally results in a decrease in SPM concentration at this site due to advection of low-turbidity, high-salinity water from the English Channel towards the measurement site (Baeye et al. 2011). The latter is confirmed by the increase in salinity observed during this period. The lower concentration of flocs explains the absence of a rising tail

in the PSD spectra (Fig. 5.9 a, b) during the storm, in contrast with the PSDs at times of maximum flood currents.
During SW storms (days 81–85, Fig. 5.3), a different behaviour was observed: SPM concentration derived from the OBS increased, whereas that derived from the ADP did not show significant changes. The PSDs during this storm were mostly characterised by a prominent rising tail in the smallest size classes (see dominance of group 1 in Fig. 5.6 around SW storms, and Fig. 5.9 c, d). The shape of the PSD during the SW storm varied from more convex in the lower size classes and more concave in the bigger sizes towards gradually more concave in the lower size classes and more convex in the higher size classes when currents decreased (see Fig. 5.9 c, d). This is typically associated with flocculation (Mikkelsen et al. 2007).
Compared to NE storms, the higher concentration of flocs observed during SW storms is related to different subtidal alongshore flow directions (see above). The observed increase in SPM concentration in the OBS signal at 0.2 and 2 mab is thus mainly caused by the advection of fine material into the study area. SW storm conditions are often associated with the occurrence of persistent HCMS layers (Fettweis et al. 2010). The latter is confirmed by the higher seabed level derived from ADP altimetry (Fig. 5.3); this is typically associated with HCMS formation, as reported by Baeye et al. (2011). These authors argue that they act as inverse armouring and prevent sand and silt from being eroded. Non-cohesive grains are detected only if the turbulence is high enough to lift the particles up to 2 mab. The seabed consists of sand and silt and is generally not covered by HCMSs during NE storm conditions, as SPM concentrations are generally lower due to the advection of less turbid English Channel water. It is under these conditions that sand and silt dominate the SPM (SW storm, Fig. 5.9 a, b).

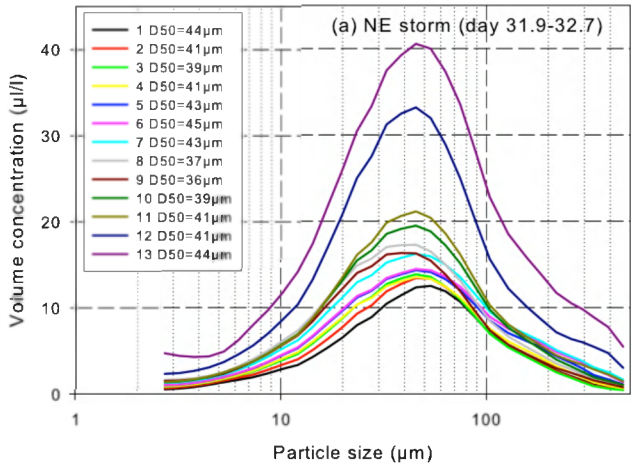

Figure 5.9 *Hourly PSD during a tidal cycle for two NE storms (**a, b**), and during flood (**c**) and ebb (**d**) for a SW storm*

5.5.3. Breaking waves and air bubbles

Air bubbles are inevitably linked with the presence of wind-driven sea waves. Individual bubble clouds are generated by breaking waves and persist for several minutes (Thorpe 1995). The size of bubbles varies strongly and can range between tens of µm up to a few cm (Deane and Stokes 2002); as such, it falls partially into the size range of the LISST. As the measurement site is situated in shallow waters (6 m MLLWS), the occurrence of air bubbles during storms could possibly influence the measurements. At a water depth of 6–10 m, waves start to break if the wave height divided by water depth is bigger than 0.78 (CEM 2003);
this occurs for wave heights >4.7 m and indicates that, during the recorded storms when the significant wave heights reached up to 3 m, the waves were only occasionally breaking around low water. It is therefore not very likely that air bubbles significantly influenced the volume concentration and size distribution of SPM.

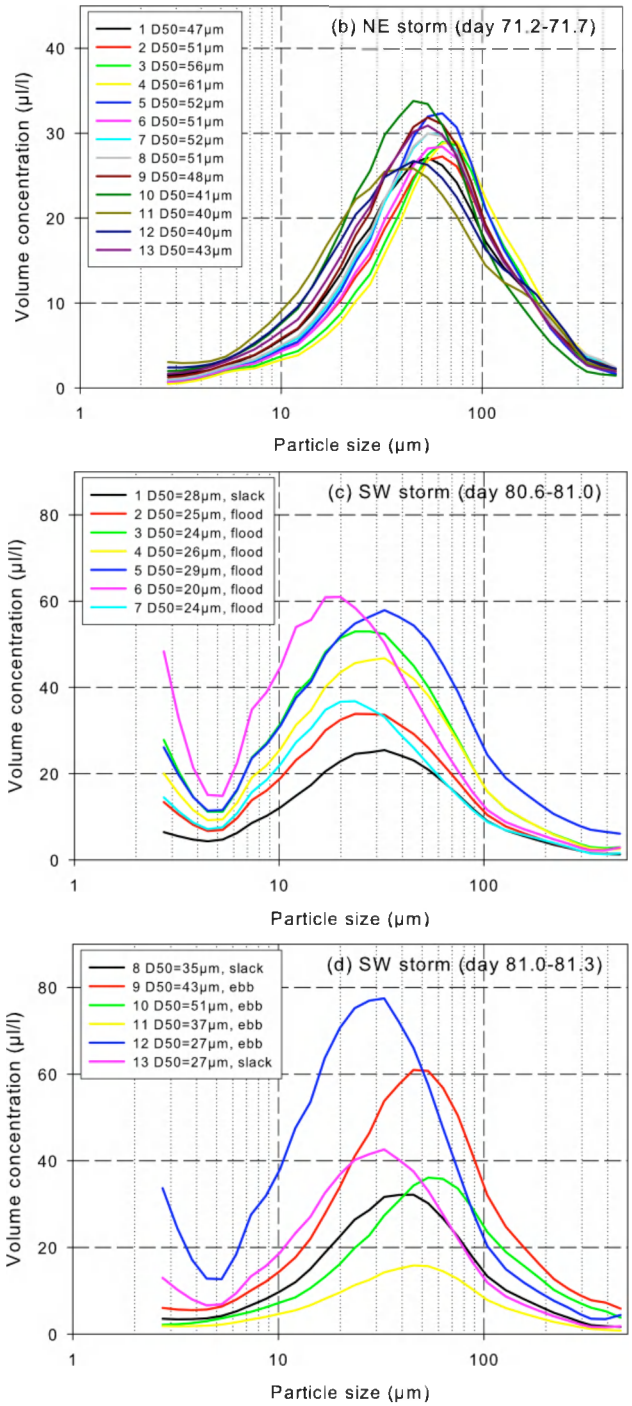

Figure 5.9 *(**continued**) Hourly PSD during a tidal cycle for two NE storms (**a, b**), and during flood (**c**) and ebb (**d**) for a SW storm*

The findings that two different types of storms with similar wave heights and periods produced different PSDs and that SPM concentration was high further suggest that erosion and flocculation processes, rather than air bubble entrainment, are dominating the observed PSDs.

5.6. Conclusions

Analysis of PSDs together with the interpretation of acoustically and optically derived SPM concentration and altimetry allowed identifying differences in SPM composition during storm conditions. The data show the importance of wind-induced advection, alongshore subtidal flow and HCMS formation as regulating mechanisms of SPM concentration, as well as other SPM characteristics (cohesiveness or composition of sediment particles) and size distribution in a high-turbidity area, rather than solely turbulence shear from currents and waves. The former is the clue to explain the different behaviour of SPM concentrations from ADPs and OBSs and the observed differences in PSDs during different storms. Wind direction and strength influences the subtidal alongshore flow and results in an advection of the coastal turbidity maximum. This is associated with an increase in cohesive SPM concentration, the formation of HCMSs and the armouring of sand during SW storms, or with a decrease in cohesive SPM concentration, no HCMS formation and an increase in sand and silt in suspension during NE storms.

Particle size distributions were generally multimodal and consisting of primary particles, flocculi, microflocs and macroflocs. During NE storms, however, PSDs were unimodal and consisting of mainly granular material (silt, sand) re-suspended from the seabed, whereas during SW storms flocculated material was still being identified in the PSDs. The data suggest that two populations of primary particles (<3 µm and flocculi 15 µm) coexist and are the building blocks of flocs. Flocculi consist of clusters of clay minerals, whereas primary particles are of various compositions (calcite, clays).

Mixed sediments were found in suspension at 2 mab at times of maximum flood currents at spring tide and during storms. At the measurement site, this occurs more prominently when the winds are blowing from the SW–W. The size distribution of the local bed sediments is thus influencing the SPM size distribution only when HCMSs are not present and when turbulence induced by currents (maximum flood currents) or waves is strong enough to bring sand or silt into suspension. Flocs are disappearing from the measurement site when winds are blowing from northerly directions (NW–NE), due to advection.

The study has shown that first estimates of SPM composition can be made using available sensors; the results remain nevertheless qualitative. Detailed analysis of the mineralogical and organic components is, however, necessary to understand SPM dynamics. Quantitative analytical techniques have been developed in the laboratory (Zeelmaekers 2011), but are not available for the collection of in-situ time-series. A new generation of detectors and sensors is needed, based on the different optical and acoustical properties of very heterogeneous SPM components. The study also underlines the necessity of developing common and standardized methodologies for processing acoustic and optical backscatter signals. This is especially needed for sound formulations and interpretations of long-term changes in SPM concentration and composition at a given locality, and in order to meaningfully compare data from different localities collected by emerging coastal and ocean observatories.

5.7. Acknowledgements

The study was partly funded by the Maritime Access Division of the Ministry of the Flemish Community (MOMO project) and by the Belgian Science Policy (Science for a Sustainable Development, QUEST4D, SD/NS/06A). M. Baeye acknowledges a specialisation grant from IWT (Agency for Innovation by Science and Technology, Flanders). B.J. Lee acknowledges financial support from the Flemish Science Foundation (FWO Vlaanderen) for funding the FWO project no. G.0263.08. G. Dumon (Ministry of the Flemish Community, Maritime Services, Coastal Division/Hydrography) made available wind and wave measurement data. We wish to acknowledge the crew of RV Belgica for their skilful mooring and recuperation of the tripod. Measurements would not have been possible without technical assistance of A. Pollentier and his team

(Measuring Service of MUMM, Oostende). The manuscript benefited from the constructive assessments of two anonymous referees.

5.8. References

Agrawal YC, Pottsmith HC (2000). Instruments for particle size and settling velocity observations in sediment transport. Marine Geology 168, 89–114.

Agrawal YC, Traykovski P (2001). Particles in the bottom boundary layer: concentration and size dynamics through events. Journal of Geophysical Research 106(C5), 9533–9542

Andrews S, Nover D, Schladow SG (2010). Using laser diffraction data to obtain accurate particle size distributions: the role of particle composition. Limnology Oceanography: Methods 8, 5074–526.

Andrews SW, Nover DM, Reuter JE, Schladow SG (2011). Limitations of laser diffraction for measuring fine particles in oligotrophic systems: pitfalls and potential solutions. Water Resources Research 47, W05523.

Baeye M, Fettweis M, Voulgaris G, Van Lancker V (2011). Sediment mobility in response to tidal and wind-driven flows along the Belgian inner shelf, southern North Sea. Ocean Dynamics 61, 611–622.

Benson T, French JR (2007). InSiPID: a new low-cost instrument for in-situ particle size measurements in estuarine and coastal waters. Journal of Sea Research 58, 167–188.

Berlamont J, Ockenden M, Toorman E, Winterwerp J (1993). The characterisation of cohesive sediment properties. Coastal Engineering 21, 105–128.

Bhaskar PV, Grossart H-P, Bhosle NB, Simon M (2005). Production of macro-aggregates from dissolved exopolymeric substances (EPS) of bacterial and diatom origin. FEMS Microbiology Ecology 53, 255–264.

Bowers DG, Braithwaite KM, Nimmo-Smith WAM, Graham GW (2009). Light scattering by particles suspended in the sea: the role of particle size and density. Continental Shelf Research 29, 1748–1755.

Bunt JAC, Larcombe P, Jago CF (1999). Quantifying the response of optical backscatter devices and transmissometers to variations in suspended particulate matter. Continental Shelf Research 19, 1199–1220.

CEM (2003). Coastal Engineering Manual, Chapter 4. Surf zone hydrodynamics. US Army Corps of Engineers, EM 1110-2-1100.

Chang TS, Flemming B, Bartholomä A (2007). Distinction between sortable silts and aggregated particles in muddy intertidal sediments of the East Frisian Wadden Sea, southern North Sea. Sedimentary Geology 202, 453–463.

Curran KJ, Hill PS, Milligan TG, Mikkelsen OA, Law BA, Durrieu de Madron X, Bourrin F (2007). Settling velocity, effective density, and mass composition of suspended sediment in a coastal bottom boundary layer, Gulf of Lions, France. Continental Shelf Research 27, 1408–1421.

Deane GB, Stokes MD (2002). Scale dependence of bubble creation mechanisms in breaking waves. Nature 418, 839–844.

Downing J (2006). Twenty-five years with OBS sensors: the good, the bad, and the ugly. Continental Shelf Research 26, 2299–2318.

Eisma D (1986). Flocculation and de-flocculation of suspended matter in estuaries. Netherlands Journal of Sea Research 20, 183–199.

Fettweis M (2008) Uncertainty of excess density and settling velocity of mud derived from in-situ measurements. Estuarine Coastal and Shelf Science 78, 426–436.

Fettweis M, Francken F, Pison V, Van den Eynde D (2006). Suspended particulate matter dynamics and aggregate sizes in a high turbidity area. Marine Geology 235, 63–74.

Fettweis M, Francken F, Van den Eynde D, Verwaest T, Janssens J, Van Lancker V (2010). Storm influence on SPM concentrations in a coastal turbidity maximum area with high anthropogenic impact (southern North Sea). Continental Shelf Research 30, 1417–1427.

Forrest J, Clark NR (1989). Characterizing grain size distributions: evaluation of a new approach using multivariate extension of entropy analysis. Sedimentology 36, 711–722.

Fugate DC, Friedrichs CT (2002). Determining concentration and fall velocity of estuarine particle populations using ADV, OBS and LISST. Continental Shelf Research 22, 1867–1886.
Graham GW, Nimmo-Smith WAM (2010). The application of holography to the analysis of size and settling velocity of suspended cohesive sediments. Limnology and Oceanography: Methods 8, 1–15.
Hamilton LJ, Z Shi, SY Zhang (1998). Acoustic backscatter measurements of estuarine suspended cohesive sediment concentration profiles. Journal of Coastal Research 14, 1213–1224.
Hamm CE (2002). Interactive aggregation and sedimentation of diatoms and clay-sized lithogenic material. Limnology and Oceanography 47, 1790–1795.
Hoitink AJF, Hoekstra P (2005). Observations of suspended sediment from ADCP and OBS measurements in a mud-dominated environment. Coastal Engineering 52, 103–118.
Huang SL (1989). The influence of disaggregation methods on X-ray diffraction of clay minerals. Journal of Sedimentary Research 59, 997–1001.
Hussein T, dal Maso M, Petäja T, Koponen IK, Paatero P, Aalto PP, Hämeri K, Kulmala M (2005). Evaluation of an automatic algorithm for fitting the particle number size distributions. Boreal Environmental Research 10, 337–355.
Johnston RJ, Semple RK (1983). Classification using information statistics. Concepts and Techniques in Modern Geography 37. GeoBooks, Norwich.
Jonasz M, Fournier G (1996). Approximation of the size distribution of marine particles by a sum of log-normal functions. Limnology and Oceanography 41, 744–754.
Kim HY, Gutierrez B, Nelson T, Dumars A, Maza M, Perales H, Voulgaris G (2004). Using the acoustic Doppler current profiler (ADCP) to estimate suspended sediment concentration. University of South Carolina, Columbia (USA), Tech Rep CPSD 04-01.
Kranenburg C (1994). On the fractal structure of cohesive sediment aggregates. Estuarine Coastal and Shelf Science 39, 451–460.
Krivtsov V, Mikkelsen OA, Jones SE (2011). Entropy analysis of SPM patterns: case study of Liverpool Bay. Geo-Mar Letter.
Lacroix G, Ruddick K, Ozer J, Lancelot C (2004). Modelling the impact of the Scheldt and Rhine/Meuse plumes on the salinity distribution in Belgian waters (southern North Sea). Journal of Sea Research 52, 149–163.
Lee BJ, Toorman E, Molz FJ, Wang J (2011). A two-class population balance equation yielding bimodal flocculation of marine or estuarine sediments. Water Research 45, 2131–2145.
Lick W, Huang H, Jepsen R (1993). Flocculation of fine-grained sediments due to differential settling, Journal of Geophysical Research 98, 10279–10288.
Makela JM, Koponen IK, Aalto P, Kulmala M (2000). One-year data of submicron size modes of tropospheric background aerosol in southern Finland. Journal of Aerosol Science 31, 595–611.
Manning AJ, Bass SJ, Dyer KR (2006). Floc properties in the turbidity maximum of a mesotidal estuary. Marine Geology 235, 193–211.
Manning AJ, Baugh JV, Spearman J, Whitehouse RJS (2010). Flocculation settling characteristics of mud: sand mixtures. Ocean Dynamics 60, 237–253.
Mari X, Burd A (1998). Seasonal size spectra of transparent exopolymeric particles (TEP) in a coastal sea and comparison with those predicted using coagulation theory. Marine Ecology Progress Series 163, 63–76.
Mietta F (2010). Evolution of the floc size distribution of cohesive sediments. PhD Thesis, Delft University of Technology, The Netherlands.
Mietta F, Chassagne C, Verney R, Winterwerp JC (2010). On the behavior of mud floc size distribution: model calibration and model behavior. Ocean Dynamics 61, 257–271.
Mikkelsen OA, Hill PS, Milligan TG (2006). Single-grain, microfloc and macrofloc volume variations observed with a LISST-100 and a digital floc camera. Journal of Sea Research 55, 87–102.
Mikkelsen OA, Hill PS, Milligan TG (2007) Seasonal and spatial variation of floc size, settling velocity, and density on the inner Adriatic Shelf (Italy). Continental Shelf Research 27, 417–430.

Murphy S, Voulgaris G (2006). Identifying the role of tides, rainfall and seasonality in marsh sedimentation using long-term suspended sediment concentration data. Marine Geology 227, 31–50.
Nechad B, Ruddick KG, Park Y (2010). Calibration and validation of a generic multisensor algorithm for mapping of total suspended matter in turbid waters. Remote Sensing of Environment 114, 854–866.
Orpin AR, Kostylev VE (2006) Towards a statistically valid method of textural sea floor characterization of benthic habitats. Marine Geology 225, 209–222.
Panagiotopoulos I, Voulgaris G, Collins MB (1997). The influence of clay on the threshold of movement of fine sandy beds. Coastal Engineering 32, 19–43.
Pope ND, Widdows J, Brinsley MD (2006). Estimation of bed shear stress using the turbulent kinetic energy approach - A comparison of annular flume and field data. Continental Shelf Research 26, 959–970.
Stewart LK, Kostylev VE, Orpin AR (2009) Windows-based software for optimising entropy-based groupings of textural data. Computers & Geosciences 35, 1552–1556.
Sun D, Bloemendal J, Rea DK, Vandenberghe J, Jiang F, An Z, Su R (2002). Grain-size distribution function of polymodal sediments in hydraulic and aeolian environments, and numerical partitioning of the sedimentary components. Sedimentary Geology 152, 263–277.
Thorne PD, Hanes DM (2002). A review of acoustic measurement of small-scale sediment processes. Continental Shelf Research 22, 603–632.
Thorne PD, Vincent CE, Hardcastle PJ, Rehman S, Pearson ND (1991). Measuring suspended sediment concentrations using acoustic backscatter devices. Marine Geology 98, 7–16.
Thorpe SA (1995). Dynamical processes of transfer at the sea surface. Progress in Oceanography 35(4), 315–352.
van Ledden M, van Kesteren WGM, Winterwerp J (2004). A conceptual framework for the erosion behaviour of sand-mud mixtures. Continental Shelf Research 24, 1–11.
van Leussen W (1994). Estuarine macroflocs and their role in fine-grained sediment transport. PhD Thesis, University Utrecht, The Netherlands.
Verfaillie E, Van Meirvenne M, Van Lancker V (2006). Multivariate geostatistics for the predictive modelling of the surficial sand distribution in shelf seas. Continental Shelf Research 26, 2454–2468.
Verney R, Lafite R, Brun-Cottan JC, Le Hir P (2011). Behaviour of a floc population during a tidal cycle: laboratory experiments and numerical modelling. Continental Shelf Research 31, S64–S83.
Voulgaris G, Meyers S (2004). Temporal variability of hydrodynamics, sediment concentration and sediment settling velocity in a tidal creek. Continental Shelf Research 24, 1659–1683.
Wallbridge S, Voulgaris G, Tomlinson BN, Collins MB (1999). Initial motion and pivoting characteristics of sand particles in uniform and heterogeneous beds: experiments and modeling. Sedimentology 46, 17–32.
Whitby K (1978). The physical characteristics of sulfur aerosols. Atmosperic Environment 41, S25–S49.
Wiberg PL, Drake DE, Cacchione DA (1994). Sediment re-suspension and bed armoring during high bottom stress events on the northern California inner continental shelf: measurements and predictions. Continental Shelf Research 14, 1191–1219.
Williamson H, Torfs H (1996). Erosion of mud/sand mixtures. Coastal Engineering 29, 1–25.
Winter C, Katoshevski D, Bartholomä A, Flemming BW (2007). Grouping dynamics of suspended matter in tidal channels. Journal of Geophysical Research 112, C08010.
Winterwerp JC (1998). A simple model for turbulence induced flocculation of cohesive sediment. Journal of Hydraulic Research 36, 309–326.
Woolfe KJ, Michibayashi K (1995). "Basic" entropy grouping of laser-derived grain-size data: an example from the Great Barrier Reef. Computers & Geosciences 21, 447–462.

Woolfe KJ, Fielding CR, Howe JA, Lavelle M, Lally JH (1998). Laser-derived particle size characterisation of CRP-1, McMurdo Sound, Antarctica. Terra Antarctica 5, 383–391.

Wu B, Molinas A, Shu A (2003). Fractional transport of sediment mixtures. International Journal of Sedimentary Research 18, 232–247.

Zeelmaekers E (2011). Computerized qualitative and quantitative clay mineralogy – Introduction and application to known geological cases. PhD Thesis, Katholieke Universiteit Leuven, Belgium. ISBN 978-90-8649-414-9. XII, 397 pp.

Mine burial in the seabed of high-turbidity area (Belgian coastal zone) - findings from a first experiment*

Matthias Baeye[1], Michael Fettweis[2], Sebastien Legrand[2], Yves Dupont[3], Vera Van Lancker[2]

[1]*Department of Geology and Soil Science,*
Renard Centre of Marine Geology (RCMG), Ghent University,
Ghent 9000, Belgium

[2]*Management Unit of the North Sea Mathematical Models*
(MUMM), Royal Belgian Institute of Natural Sciences,
Brussels 1200, Belgium

[3]*Naval Logistics (DIRNAVLOG),*
Belgian Defence, Marine Basis,
Zeebrugge 8380, Belgium

*accepted for publication in Continental Shelf Research (Elsevier)

M. Baeye processed and interpreted the datasets, wrote the manuscript and made all figures (except for Fig. 6.14). Co-authors helped by reviewing the manuscript and/or providing the datasets. S. Legrand was responsible for the 3D model (OPTOS-BCZ) results.

Abstract

The seabed of the North Sea is covered with ammunition dating back from World Wars I and II. With increasing human interference (e.g. fisheries, aggregate extraction, harbour related activities), it forms a threat to the safety at sea. In this study, test mines were deployed on a sandy seabed for three months to investigate mine burial processes as a function of hydrodynamic and meteorological conditions. The mine experiment was conducted in a shallow (9 m), macrotidal environment characterized by highly turbid waters (yearly and depth-averaged suspended particulate matter concentration of 100 mg l^{-1}). Results showed some variability of the overall mine burial, which corresponded with scouring processes induced by a (sub-) tidal forcing mechanism. The main burial events however were linked to storm-related scouring processes, and subsequent mine roll into the resulting pit. Two storms affecting the mines during the 3-month experiment resulted in enduring increases in burial volume to 60% and 80%, respectively. More cyclic and ephemeral burial and exposure events appear to be linked to the local hydrodynamic regime. During slack tides, suspended sediment settles on the seabed, increasing the burial volume. In between slack tides, sediment is re-suspended, decreasing the burial volume. The temporal pattern of this never reported burial mechanism, as measured optically, mimics the cyclicity of the suspended sediment concentration as recorded by ultrasonic signals at a nearby benthic observatory. Given the similarity in response signals at the two sites, we hypothesize that the formation of high-concentrated mud suspensions (HCMS) is a mechanism causing short-term burial and exposure of mines. This short-term burial and exposure increase the chance that mines are 'missed' during tracking surveys. Test mines contribute to our understanding of the settling and erosion of HCMS, and thus shed a light on generic sedimentary processes.

Keywords: Mine burial experiment; scouring; suspended particulate matter; high-concentrated mud suspension; slack tides

6.1. *Introduction*

World War I and II-era explosives are scattered over the seabed of the North Sea and form a threat to the safety at sea. A wide variety of warfare ammunition may be encountered and exposed with increasing human activities at sea (e.g. fisheries, dredging, harbour construction and wind-farm development). Mine detection is a priority in French, Belgian and Dutch waters. However, mines are usually not detected when they are completely covered with sediment, thus remaining a potential risk associated with all activities that disturb the seabed (NRC 2003).
Mine burial processes are commonly categorized into the following two groups: impact and post-impact burial (Wilkens and Richardson 2007). Burial by impact is well-known from literature (Mulhearn 1995, Chu et al. 2002, Abelev et al. 2007, Aubeny and Han 2007), and occurs when the mine (or object) falls freely through the water column. As the amount of burial is dependent on the bearing strength of the seabed sediment, burial by impact occurs mostly in areas with poorly consolidated muddy sediments. Post-impact mine burial is typically occurring in sandy bottoms and is mainly associated with sand-water-object interactions. As such, burial by scour is well-known in the fields of mine detection (e.g. Jenkins et al. 2007), maritime archaeology (e.g. Saunders 2005, Quinn, 2006) and marine engineering, such as seabed pipelines (e.g. Akoz et al. 2010). Scour occurs due to disturbance in the wave- or tide-induced flow caused by presence of obstacles such as pipelines. It typically manifests itself at the upstream face of the object (Saunders 2005, Garcia et al. 2009), and diminishes downstream of the obstacle, where scour-related depressions grade into depositional features (Inman and Jenkins 2005). The impact of waves on exposed mines accounts for most mine burial (e.g. Plager 2000, Voropayev et al. 2003, Hay and Speller 2005, Cataño-Lopera and Garcia 2006 a, Friedrichs and Trembanis 2006, Geurts et al. 2007, Grilli 2007, Traykovski et al. 2007, Trembanis et al. 2007, Wever and Luehder 2007). It forces the rollover of mines into scour pits, especially during storms. A second post-impact burial mechanism is related to migration of megaripples, causing periodical burial and exposure of object (Wever 2003, Cataño-Lopera and Garcia 2006 b, Cataño-Lopera et al. 2007, Wever and Luehder 2007, Garcia et al. 2009). This type of process occurs irrespective of the presence of the object, and also results from other changes in the (overall) seabed morphology, such as those resulting from seasonal changes in wave climate (Richardson and Briggs 2000, Jenkins et al. 2007). Additional burial mechanisms discussed in the literature are burial by fluidization associated with wave-induced failure in the sediment surrounding the mine (e.g. Brandes and Riggs 2002, 2004), and biological activity (Richardson and Briggs 2000).
The present study focuses on mine burial processes and on the predictability of mine burial in high-turbidity areas. A mine experiment was conducted in a mainly sandy seabed environment situated in Belgian coastal area (southern North Sea). The area is also characterised by the occurrence of high-concentrated mud suspensions (HCMS) (IMDC and WL 2007, Baeye et al. 2011). The latter are responsible for the short-term burial of the test mine, a mechanism that has to our knowledge never been described before. In the paper a detailed analysis is given of the daily patterns of mine burial and exposure by the formation and erosion of HCMSs superimposed on the longer-term burial controlled by storm waves. The paper also suggests that test mines can be used as an alternative instrumentation to study the dynamics of HCMS in high-turbidity areas.

6.2. *Environmental conditions*

The Belgian coastal zone is shallow (0-15 m below Mean Lower Low Water Spring (MLLWS)) with seabed sediments varying from pure sand to pure mud (Verfaillie et al. 2006). Highly turbid, coastal waters occur between Nieuwpoort and the Westerscheldt river mouth (Fig. 6.1). Suspended particulate matter (SPM) originates mainly from import from the Dover Strait and from erosion of Holocene mud layers in the coastal zone (Fettweis and Van den Eynde 2003). SPM concentrations may reach >3.0 g l^{-1} close to the bed. Mean tidal range at Zeebrugge is 4.3 m (2.8 m) at spring (neap) tide and maximum current velocities exceed 1.0 m s^{-1}. Tidal ellipses are commonly well-aligned with the coastline orientation. Typically, tides are responsible for more than 90% of the total variance observed in the time-series data of tidal elevation. The

associated amplitudes of the M2 and S2 dominant and semi-diurnal constituents are 1.8 and 0.5 m, respectively (Mouchet 1990). The rest of the total variance is explained by the occurrence of wind-induced flows. Significant sea set-up occurs with prevalent winds blowing from NW, and sea set-down occurs with SE winds. Wind forcing tends to bias the residual flow pattern (Yang 1998), and the SPM circulation along the Belgian coast (Fettweis et al. 2006, Fettweis et al. 2007, Baeye et al. 2011). Southwest winds are associated with recurring low-pressure weather systems (depressions) moving from the Atlantic Ocean towards Europe. High wind speeds may occur throughout the year; however, significant storms are abundant in the period October until March. Thus, significant wave heights are typically largest during fall and winter months in the southern North Sea. Salinity (range of 28-34 in the nearshore) varies with tides and wind forcing, and is fortnightly modulated (Lacroix et al. 2004). Winds blowing from the NE-E wind sectors coincide with decreasing salinity, as the influence of the Westerscheldt estuary increases. On the other hand, salinity increases under SW winds, when less turbid, open-Atlantic waters enter the study area through the English Channel.

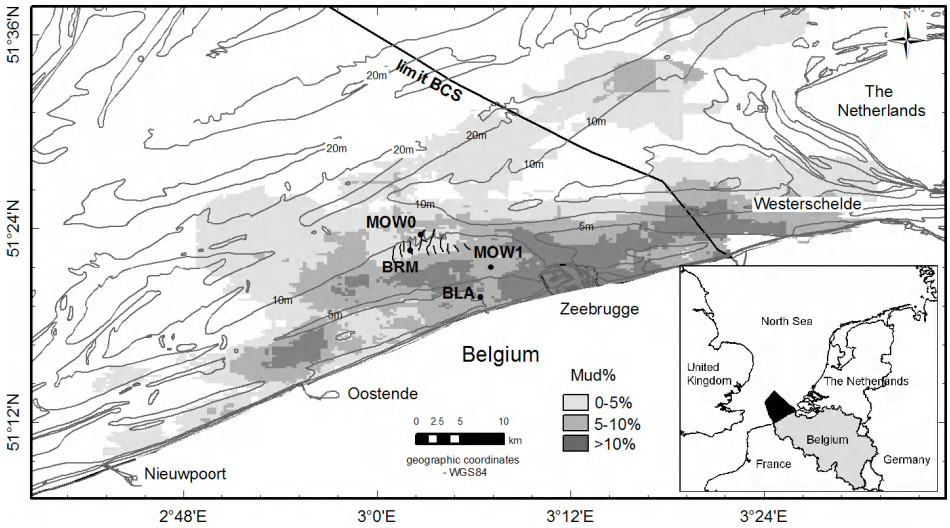

Figure 6.1 *Location of the mine experiment (BRM) in the southern Bight of the North Sea. The bathymetry (MLLWS) and mud content of the sandy seabed samples are given for the Belgian Coast. zone. Other monitoring stations in the area at the time of the experiment were MOW0 (Oceanographic station), MOW1 (benthic observatory) and BLA (investigated site in Baeye et al. 2011 - Chapter 2)*

6.3. *Methodology for data collection and analysis*

6.3.1. Mine burial experiment (BRM)

A mine burial experiment was conducted using test mines developed by the Forschungsanstalt der Bundeswehr für Wasserschall-und Geophysik (FWG, Fig. 6.2). The test mines have a diameter (D) of 0.47 m, are 1.7 m in length and weigh 509 kg (apparent weight in water 238 kg). Mine motion (pitch and roll) is recorded via a built-in, three-axis accelerometer. The mines were designed with three rings consisting of 24 optical sensor pairs (LED bridges). These are equally spaced around the mine at 15° intervals, both in the middle and at either end; this results in a range of vertical burial resolution or vertical bed evolution variations between 0.2 and 3 cm. The LED bridges rely on optical light transmission over a short path of 4 cm. "1" recordings

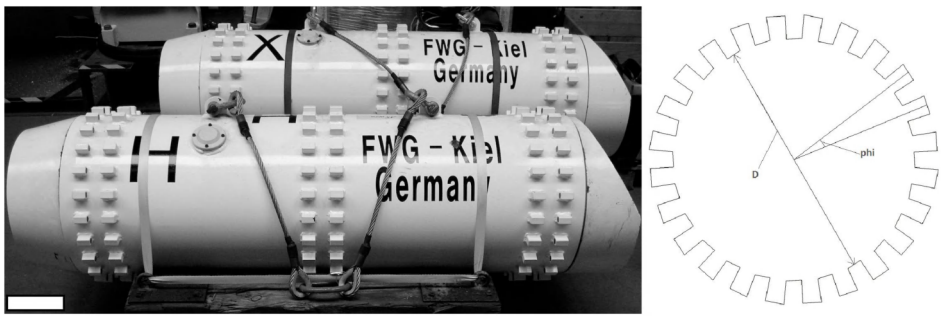

***Figure 6.2** (**left**) Pre-deployment photo of the test mines. The white bar in the lower left corner represents 20 cm. (**right**) BRM cross-section with D (47 cm), diameter, and phi, the angle between two successive LED housings. Mine burial diameter refers to the height of the mine (or mine ring) buried with respect to the lowest LED pair*

correspond to sediment hindering light propagation, whereas "0" recordings correspond to proper light propagation. The conceptual model of recording mines in sandy environments is based on the presence of bedforms (ripples, megaripples) that would cover the mine partially or completely, and temporally (dependent on the migration speed of the (mega-) ripples). On the other hand, hydrodynamics (tidal currents, storm waves) will also affect the burial stage of the mine, i.e. by scour. The signal per ring corresponds to the bed evolution measured vertically. When a sequence of burial and exposure is read in the signal from the three different rings, then typically one may state that ripples are passing the mine. The recording interval of 15 min in this experiment sets the limit of the time resolution. Variations occurring at periods less than 15 min are not fully characterized, and per 15 min interval, only the final result of pitch, roll and the number of buried sensor pairs is recorded (Wever and Luehder 2007). Mine burial is given either by the diameter B (per ring), or by the total mine burial volume (in %) taking into account all rings. The burial diameter is calculated as follow:

$$B = \frac{D}{2}\left(1 - \cos\left(\frac{n\varphi}{2}\frac{\pi}{180}\right)\right)$$

with n, the number of buried sensors ("1" recordings) and φ the angle interval of 15° (Fig. 6.2, right). Time-series data of mine burial were low-pass filtered to analyze longer-term (>33 hours) variability (see also 6.3.2). No "bad" recordings, caused by bio-fouling, were observed. The mines were deployed on a sandy seabed in water depths of 9 m -MLLWS. At the experiment's onset (September 25th, 2008 or year day 269), sonar imagery of the seabed revealed that both mines were oriented 115° True North (Fig. 6.3). The mine records lasted 104 days until January 6th, 2009.

6.3.2. *Meteorological, Oceanographic station and wave buoy (MOW0)*

During the mine experiment, current data were collected at MOW0, a measuring pole located about 1 km from the BRM site and in water depths of 10 m -MLLWS. An upward-looking Doppler current meter (Aanderaa®, DCM-12, 600 kHz) records burst data at 10-minute sampling intervals, with a ping rate of 4 Hz. The time-series was low-pass filtered to remove trends (i.e. tides) occurring at periods less than 33 hours (Beardsley et al. 1985). Each point was replaced with a weighted average of 33 hours on either side of the central point. Further, the two horizontal current components were rotated into a long- and cross-shore orthogonal coordinate system. The positive cross-shore axis is directed landward (T°155), and the positive longshore axis is northeastward (T°65). Wind speed and directions (meteorological convention) were recorded at 25 m above MLLWS at MOW0, and converted following the oceanographic convention. Wind shear stresses were estimated using the adjusted wind data for 10 m above MLLWS (U_{10}) and by introducing a neutral drag coefficient (C_{DN}) (Large and Pond 1981):

$$C_{DN} = 1.2\ 10^{-3}, \text{ for } 4 \text{ m s}^{-1} \leq U_{10} \leq 11 \text{ m s}^{-1},$$

$$C_{DN} = \left(0.49 + 0.065\, U_{10}\right) 10^{-3}, \text{ for } 11 \text{ m s}^{-1} < U_{10} \leq 25 \text{ m s}^{-1}.$$

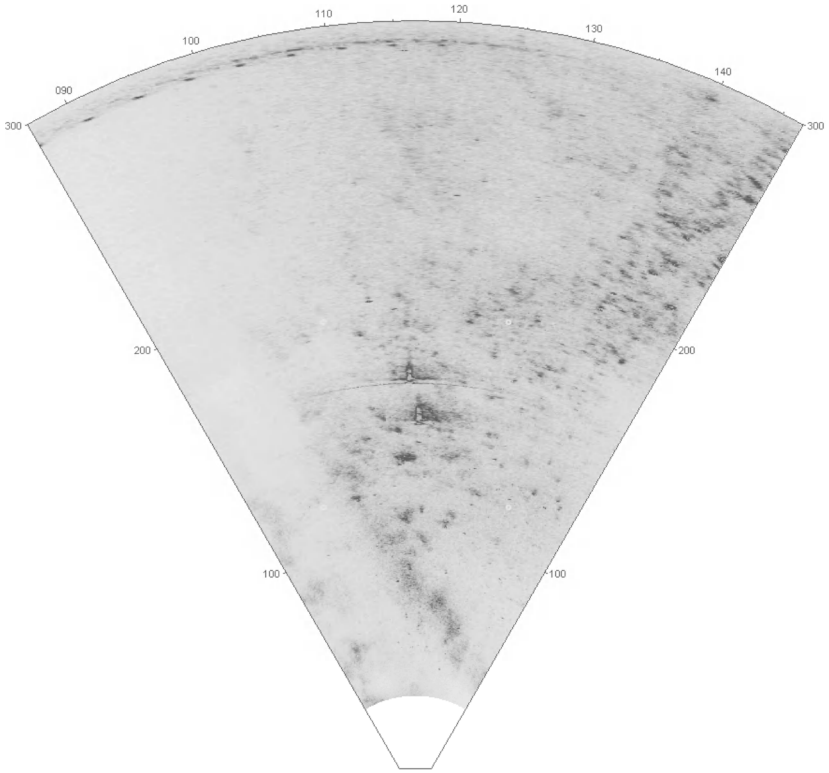

Figure 6.3 *Image of the test mines on the seabed, as obtained by MCMV (mine counter measure vessel) hull-mounted sonar. Both mines are oriented 115° true north (toward the top of the page), and they are situated about 150-200 meters from the sonar*

6.3.3. Benthic observatory

During part of the mine experiment, a benthic tripod was deployed at a more inshore location (MOW1, see Fig. 6.1) with same water depth (9 m –MLLWS) for a time period of 25 days (days 322 – 347). A SonTek® 3 MHz Acoustic Doppler Profiler (ADP) (2.25 mab), a SonTek® 5 MHz Acoustic Doppler Velocimeter (ADV) (0.35 mab) and two D&A® Optical Backscatter Sensors (OBS) (2.25 & 0.25 mab) recorded on the tripod (http://www.mumm.ac.be/EN/Monitoring/Belgica/tripod.php). All time-series data were stored in two SonTek® Hydra data logging systems. Calibration of the OBS's was carried out for several tidal cycles in the nearshore area; a linear regression between OBS-NTU and SPM concentrations from water sample treatment was obtained (cf. Fettweis 2008). In addition to the currents, the ADV also measured continuously the distance between the sensor and the top of the 5 MHz acoustic detection layer. However, when HCMSs near the bed (eventually fluid mud) reach the ADV measuring volume, both the current measurements and boundary layer detection may become erroneous. Defining the acoustic boundary layer is known to perform well for a sandy seabed (Velasco and Huhta 2010); however, recently it was also used successfully in delineating the upper boundary of a poorly defined mud beds (Baeye et al. 2011).

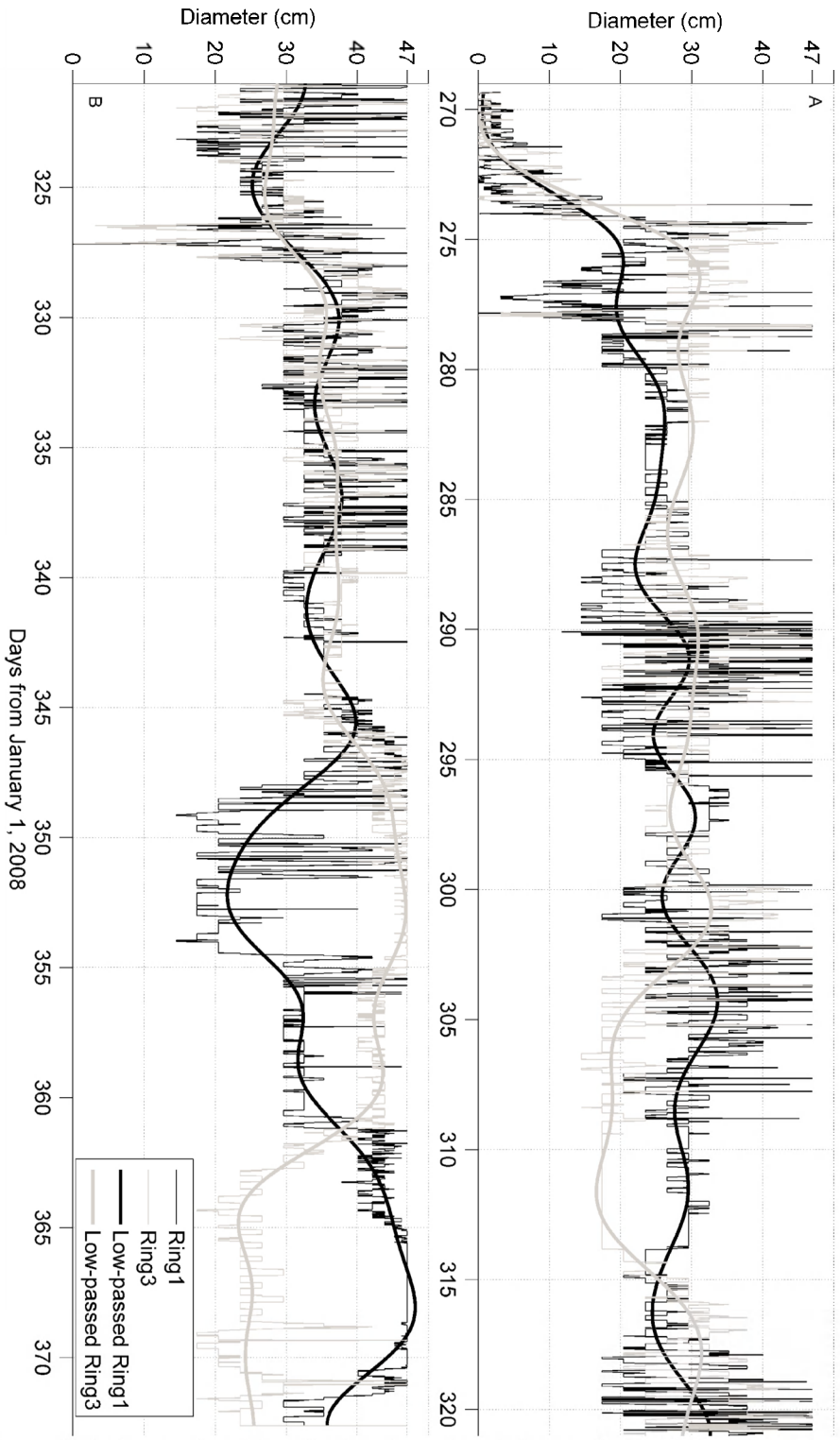

Figure 6.4 *Time-series data of mine rings 1 and 3, together with their low-passed filtered curves for days 269-321 (**a**), and for days 321-373 (**b**)*

It is difficult to detect this type of boundary because it is a strong concentration gradient (lutocline) rather than a sharp water-sediment interface. To overcome the issue of failing ADV boundary detections, Baeye et al. (2011) used a technique based on the ADP backscatter intensity. It considers the first high return in the backscattered signal (i.e. beam has hit the boundary), then it selects 5 bin values on either side of the maximum value, and fits a quadratic equation to them. The location of the maximum value found, represents the top of the 3 MHz acoustic detection layer. Further, a classification of 40 tidal cycles was realized for a mean tidal range of 3.6 m and distinguishing neap tides and spring tides.

6.3.4. *Acoustic surveys*

Repeated surveys were conducted to monitor the changing seabed morphology, and to visualize the mine burial stage and heading of the mines. Different instruments were used: an automated underwater vehicle (AUV-REMUS100 with 900 kHz frequency sonar), a pole-mounted multi-beam system (EM1002s, 100 kHz) and towed side-scan sonar (KLEIN 3000 series, 100 and 500 kHz).

6.3.5. *Hydrodynamic numerical model*

The currents, surface elevation and turbulent kinetic energy were modelled using an implementation of the COHERENS V2.0 hydrodynamic model to the Belgian Continental Shelf. This 3D model (OPTOS-BCZ) solves the continuity and momentum equations on a staggered sigma coordinate grid with an explicit mode-splitting treatment of the barotropic and baroclinic modes. A description of the COHERENS model can be found in Luyten et al (1999) and Luyten (2011). OPTOS-BCZ covers an area between 51°N and 51.92°N and between 2.08°E and 4.2°E. The horizontal resolution is 0.71' (longitude) and 0.41' (latitude), corresponding to a grid size of about 800 m. Boundary conditions of water elevation and depth-averaged currents for this model were provided by the operational models OPTOS-NOS (covering the North Sea) and OPTOS-CSM (covering the North-West European Continental Shelf) of the Management Unit of North Sea Mathematical Models (see www.mumm.ac.be). Pison and Ozer (2003) and Dujardin et al (2010) validated the current velocities of OPTOS-BCZ using ADCP measurements. The bottom shear stress for currents alone was determined using the calculated current velocity in the lowest layer of the model and using a bottom roughness length of 0.35 cm. The latter is based on the most significant seabed ripples or dunes (i.e. interact most with the flow). Therefore, the roughness length is given by the ratio between the square of the dunes height and their wavelength. The aim of using the model is estimating the hydrodynamics at the mine site, since no in-situ recordings of currents were realized.

6.4. *Results*

6.4.1. *Mine burial*

The time-series data derived from mine rings 1 and 3 (outer end rings) recordings show high variability over time (Fig. 6.4). Their low-passed signals show an opposite burial behaviour indicating opposing trends of increased burial and exposure occurring at the mine ends. The shorter-term (intra-tidal) variations are more easily observed in Fig. 6.5, which shows only four tidal cycles with corresponding near-bed current components. At maximum ebb and flood (see highlights in Fig. 6.5), one signal corresponds to more exposure and the other with increase in burial. This pattern occurs for almost 75% of the time, corresponds with relative bed-level changes of 10-15 cm around the mine.

6.4.2. *Meteorological influence*

SSW-SW winds were the strongest and most abundant during the experiment, followed by winds blowing from the NW sector. NE and E winds were weaker and less common. The wind changed direction frequently, with drops in pressure and low sea

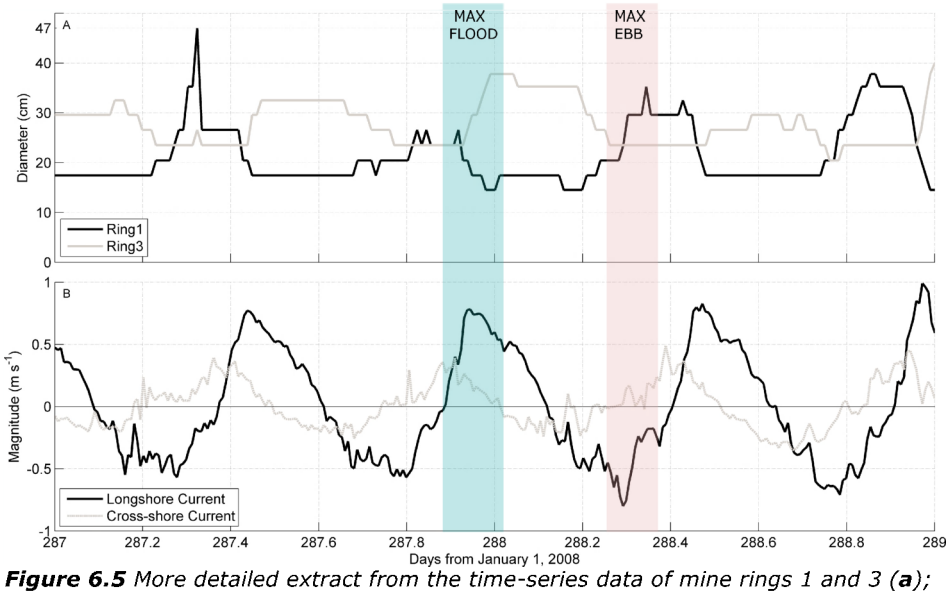

Figure 6.5 *More detailed extract from the time-series data of mine rings 1 and 3 (**a**); and the corresponding longshore and cross-shore currents (**b**) for a period of 2 days (~4 tidal cycles). The currents were recorded at 3 meters above bed*

surface levels corresponding to periods with southerly winds. Meteorological observations show evidence of two storms that forced sizable short-term increases in sea level and significant wave height (figs. 6.6, 6.7). During these storms, which represent only 1% of the monitoring time, the significant wave height (averaging 0.8 m with a mean period of 4 s) increased to more than 2.5 m.
Significant mine burial is associated with the passage of these storms. A first storm impacted the area in October 2008 (days 275-277), generating significant wave heights of more than 2.5 m (Fig. 6.8). Minor mine roll was recorded, together with increased mine burial. In addition, a reorientation was likely to be induced by the storm action (as observed in sonar images between both storms). A second storm event, with wave heights of up to 3.5 m, hit the area in November 2008 (days 326-328). As a result, the mine rolled 90°. During both storms, short-term formation of scour pits and the associated exposure of the outer ends of the mines were followed by the mines rolling into the pits. They settle at a greater depth relative to the seabed. Increased burial followed when the wave energy returned to fair-weather values and the scour pit quickly filled up with sediments.
When comparing low-passed mine behaviour to wind-stress measurements, it is clear that wind direction is one of the parameters governing longer-term mine burial (Fig. 6.9). During periods of E-NE winds (wind stress toward the W-SW) ring 1 was buried deeper than ring 3. During periods of prevailing SW winds, the opposite was true. Therefore, meteorological conditions may explain the contribution of wind forcing to mine burial behaviour on the longer term.

6.4.3. Suspended particulate matter (SPM)

The acoustic layer detection derived from the acoustics on the benthic tripod show good agreement with the mine burial data (Fig. 6.10). The ADV signal is hard to read, since its time-series is discontinuous, explained by either attenuation of the acoustic signal and/or an increase in HCMS thickness reaching and disturbing the ADV sampling volume. Although the match is far from perfect, the three signals show synchronous periodic rises and falls of the top of the boundary layer. The rises correspond with SPM settling out of the water column during ebb slack tide (i.e. slack water after high water, red highlights in Fig. 6.10) and flood slack tide (i.e. slack water after low water, blue highlights in Fig. 6.10). This is observed under both spring and neap tide phases (Figs. 6.11 and 6.12).

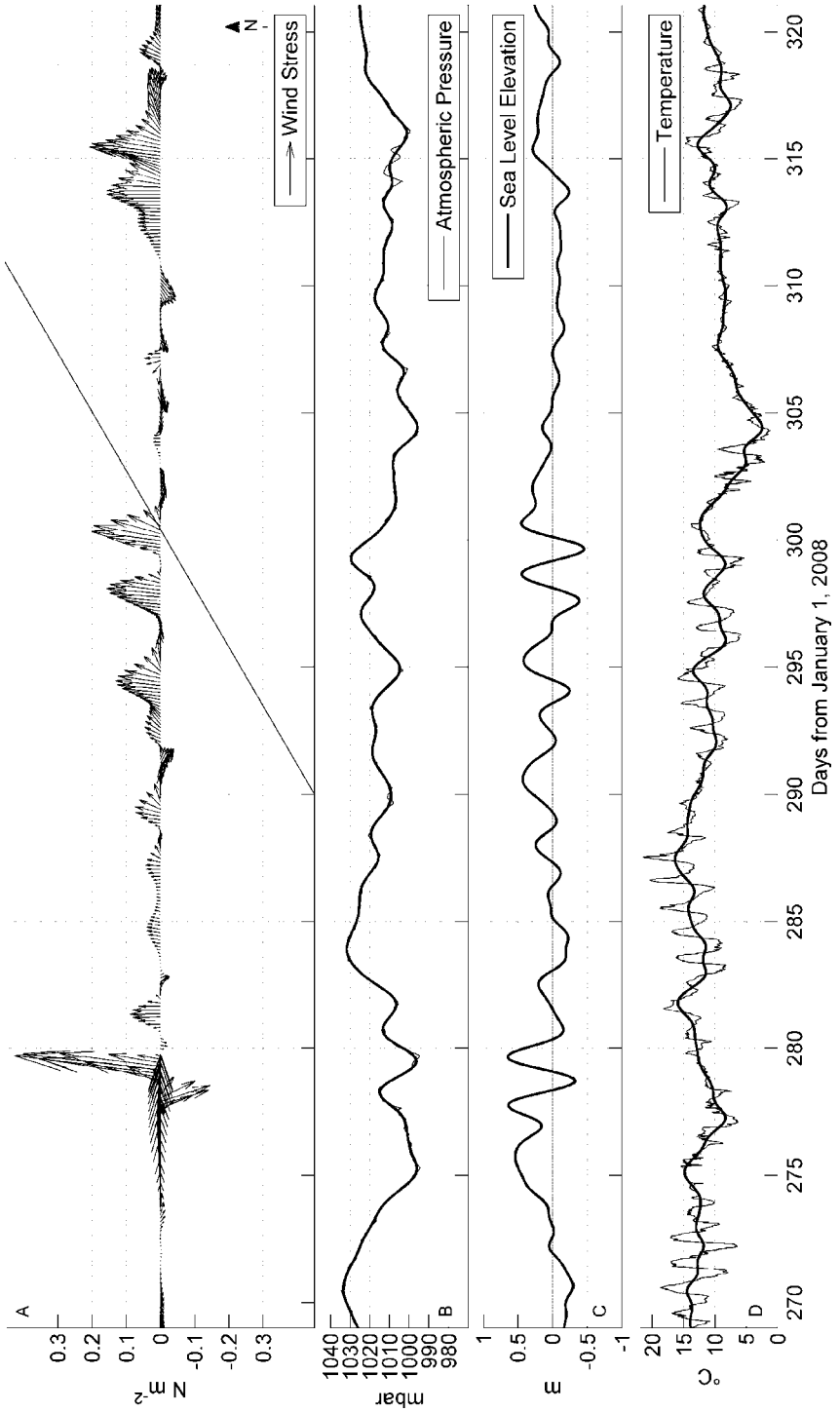

Figure 6.6 *Meteorological records for days 269-321: (**a**) wind stress; (**b**) atmospheric pressure; (**c**) sea level and (**d**) temperature. In the wind stress time-series, north is indicated with arrow*

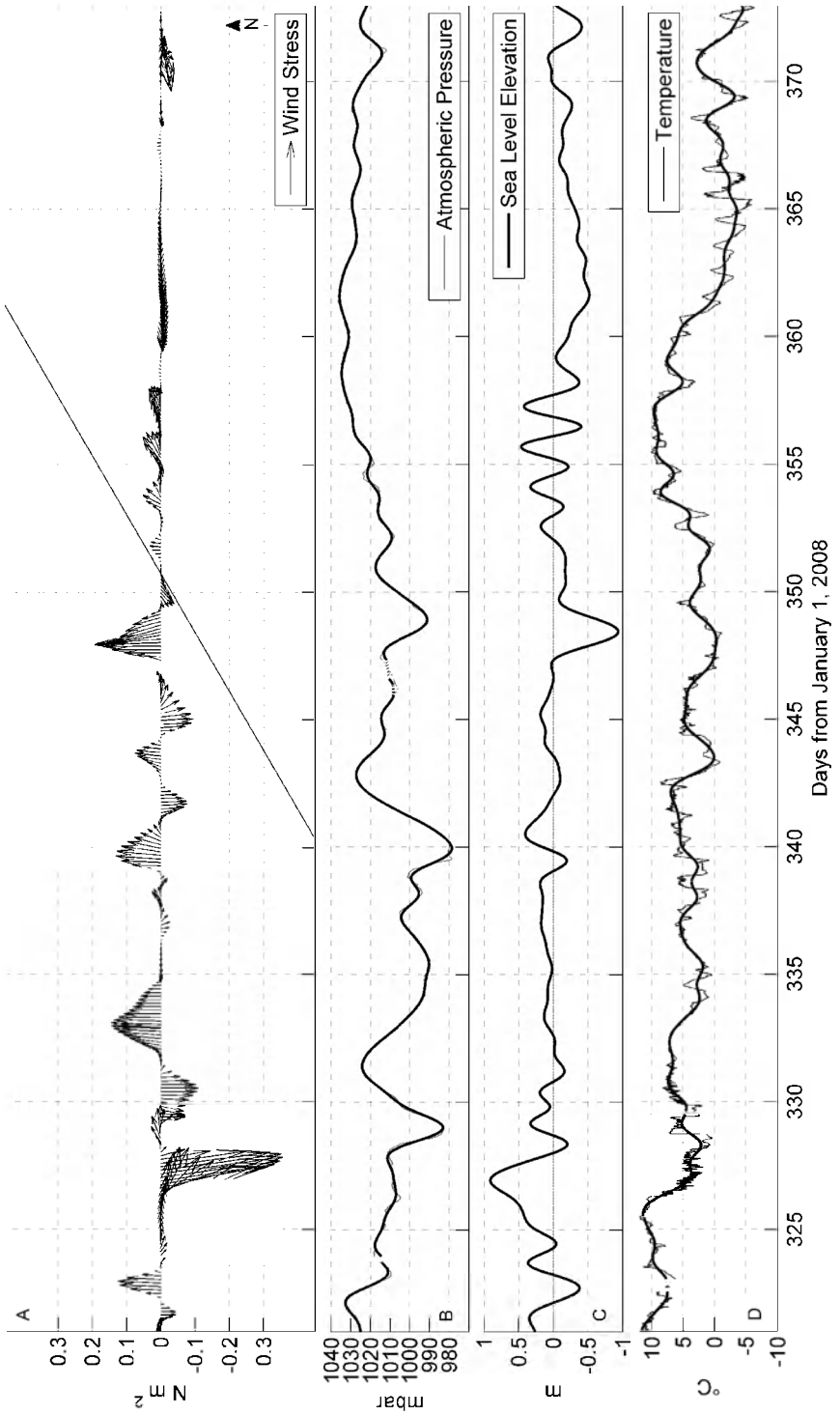

Figure 6.7 *Meteorological records for days 269-321: (**a**) wind stress; (**b**) atmospheric pressure; (**c**) sea level and (**d**) temperature. In the wind stress time-series, north is indicated with arrow*

Generally, SPM concentration (2 mab) is in line with the tidal forcing, with re-suspension peaks at maximum ebb and maximum flood, and SPM settling during slack tide. The observed rises of the boundary layer reach up to 25 cm around ebb slack tide and up to 7 cm at flood slack tide. SPM concentrations at 2 mab are significantly different from those at 0.2 mab; the latter also reflecting the boundary layer rises and falls.

6.4.4. Seabed characteristics

The mine experiment was conducted 9 km off the coast where large, N-S oriented sand dunes define the overall underwater landscape. These bed forms are several meters in height and hundreds of meters in length (see black lines for mapped sand waves in Fig. 6.1 near "BRM"). Smaller dunes (megaripples) with a maximum height of 0.5 m and wave length of a few meters are superimposed on these dunes. No-well defined bed forms were visible on the acoustic data collected during the mine experiment. However, a survey conducted after the mine stopped recording when its battery died (January 2009) showed megaripples of up to 30 cm in height and up to 7 m in wave length. Seabed samples collected with a box-corer in the proximity of the mine and by divers directly around the mine. Sand (with intercalations of mud) and compacted mud (Holocene) was sampled, often covered with fresh mud. Rather coarse sands (550 µm), compared with the medium-grained sand (450 µm) away from the mine, were found in the divers' samples at the mine site. Also, a secondary silt-grain size modus was found in the samples.

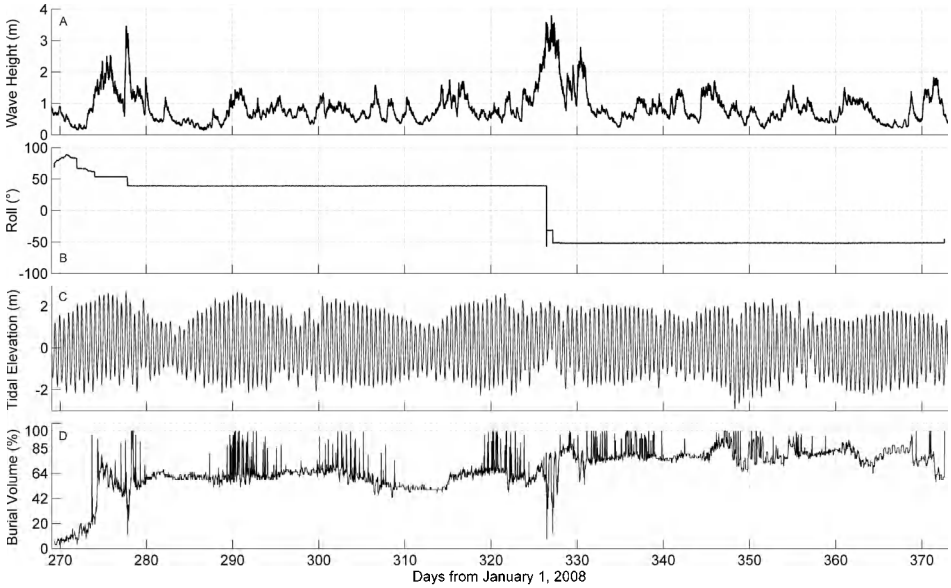

Figure 6.8 *Meteorological records for days 269-321: (**a**) wind stress; (**b**) atmospheric pressure; (**c**) sea level and (**d**) temperature. In the wind stress time-series, north is indicated with arrow*

6.5. Discussion

In literature, mine burial is linked to several processes (cf. Wilkens and Richardson 2007). On a sandy seabed, the most important one is burial by scour as a result of sand-water-object interactions. Our data show that SPM dynamics is also a possible mine burial driver. This process, which has not been linked to mine burial before, may be very important in high-turbidity environments with thick HCMSs. Table 6.1 summarizes all three types of burial processes (i.e. by HCMS, by scour, by storm waves) regarding their occurrences and maximum burial potentials during the monitoring period.

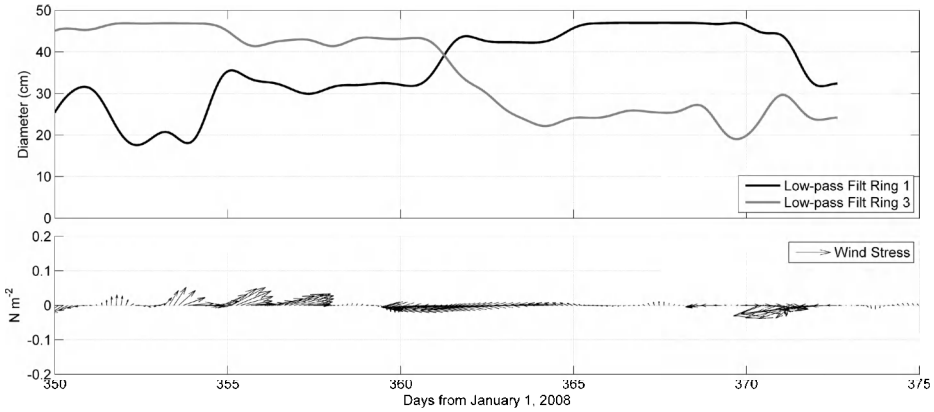

Figure 6.9 *Extract from the mine burial time-series (days 350-372).* ***Below****, wind stress; and* ***above****, two burial rings (at mine ends)*

Table 6.1 *Mine burial behaviour (occurrences and burial volumes) for the three types of mine burial*

	occurrence (time)	max burial (cm)
by scour	75%	15
by HCMS	10%	15
by storm	2%	30

6.5.1. Mine burial by scour-and-deposition cycles

Wave-induced scour and subsequent deposition in scour pits are responsible for most of the mine burial, especially on sandy seabeds. The signal of the mine burial volume is dominated by 2 main stages that are related to high-energy wave events: (1) 60% burial was reached after the first storm, which impacted the area a few days after the mine was placed on the seabed; (2) 80% mine burial was reached after a second, more severe storm. In this respect, (Cataño-Lopera and Garcia 2006 a) remarked the importance of the angle of attack. In our case, the initial angle of 115°T (Fig. 6.3) changed during the first storm to 65°T as revealed from the acoustic imagery of the seabed. This alignment was in correspondence with the storm waves propagating towards the S-SE under the N-NW wind conditions. This new orientation was practically parallel to the principal axis of the tidal current ellipse; as such no further alignments of the mines were observed afterwards. This leads to symmetrical conditions of the flow and sediments around the mine, similar to the observations of (Cataño-Lopera and Garcia 2006 a, Cataño-Lopera et al. 2007). It is known that tidal forcing affect the mine ends with scour and deposition cycles on a quarter-diurnal basis (Brandes 1999, Brandes and Riggs 2004). Our data show that for most of the time no substantial changes in the total mine burial volume occurred. However, variations in the burial volume were observed when a wind-driven flow was sustained. As a result, enhanced scouring on one mine end occurred over several days (Fig. 6.9). As similar with tidal forcing, flow vortices in the upstream end of the mine object increase scouring (Richardson and Briggs 2000, Saunders 2005, Friedrichs and Trembanis 2006). Because of bedload transport and seabed erosion, winnowing of finer sand (and silt/clay) fractions is likely to occur (Friedrichs and Trembanis 2006). This might explain the rather coarse sands (550 µm) in the divers' samples at the mine site, collected prior to mine recovery.
Based on seabed images (e.g. Fig. 6.3), no megaripples were observed in the very direct proximity of the mine during the experiment. However, the area might show the presence of this type of bedforms; as such, this burial mechanism cannot be just ruled out. Nonetheless, megaripple migration cannot account for short-term burial pattern because it is a process unrelated to semi-diurnal slack-time periodicity.

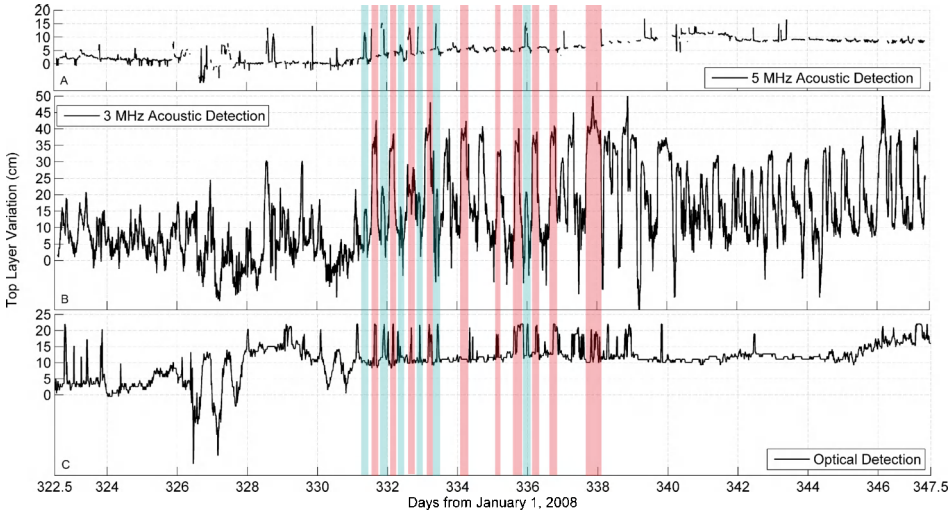

Figure 6.10 *Time-series of vertical seabed changes by means of ADV (**a**), ADP (**b**) and BRM (**c**). a, b are recordings at MOW1, and c at BRM (nearby MOW0). Optical and acoustic instruments detect HCMS layer formation. ADV shows many gaps, and the ADP shows high rises up to 25 cm. Near-synchronicity of the main peaks strongly suggests that HCMS formation and disintegration played a role in the burial and exposure of the test mine. Blue and red highlights show flood and ebb slack tides, respectively*

6.5.2. Mine burial by transient HCMSs

Wave-induced scour and subsequent deposition in scour pits are responsible for most of the mine burial, especially on sandy seabeds. The signal of the mine burial volume is dominated by 2 main stages that are related to high-energy wave events: (1) 60% burial was reached after the first storm, which impacted the area a few days after the mine was placed on the seabed; (2) 80% mine burial was reached after a second, more severe storm. In this respect, (Cataño-Lopera and Garcia 2006 a) remarked the importance of the angle of attack. In our case, the initial angle of 115°T (Fig. 6.3) changed during the first storm to 65°T as revealed from the acoustic imagery of the seabed. This alignment was in correspondence with the storm waves propagating towards the S-SE under the N-NW wind conditions. This new orientation was practically parallel to the principal axis of the tidal current ellipse; as such no further alignments of the mines were observed afterwards. This leads to symmetrical conditions of the flow and sediments around the mine, similar to the observations of (Cataño-Lopera and Garcia 2006 a, Cataño-Lopera et al. 2007). It is known that tidal forcing affect the mine ends with scour and deposition cycles on a quarter-diurnal basis (Brandes 1999, Brandes and Riggs 2004). Our data show that for most of the time no substantial changes in the total mine burial volume occurred. However, variations in the burial volume were observed when a wind-driven flow was sustained.
As a result, enhanced scouring on one mine end occurred over several days (Fig. 6.9). As similar with tidal forcing, flow vortices in the upstream end of the mine object increase scouring (Richardson and Briggs 2000, Saunders 2005, Friedrichs and Trembanis 2006). Because of bedload transport and seabed erosion, winnowing of finer sand (and silt/clay) fractions is likely to occur (Friedrichs and Trembanis 2006). This might explain the rather coarse sands (550 μm) in the divers' samples at the mine site, collected prior to mine recovery.
Based on seabed images (e.g. Fig. 6.3), no megaripples were observed in the very direct proximity of the mine during the experiment. However, the area might show the presence of this type of bedforms; as such, this burial mechanism cannot be just ruled out. Nonetheless, megaripple migration cannot account for short-term burial pattern because it is a process unrelated to semi-diurnal slack-time periodicity.

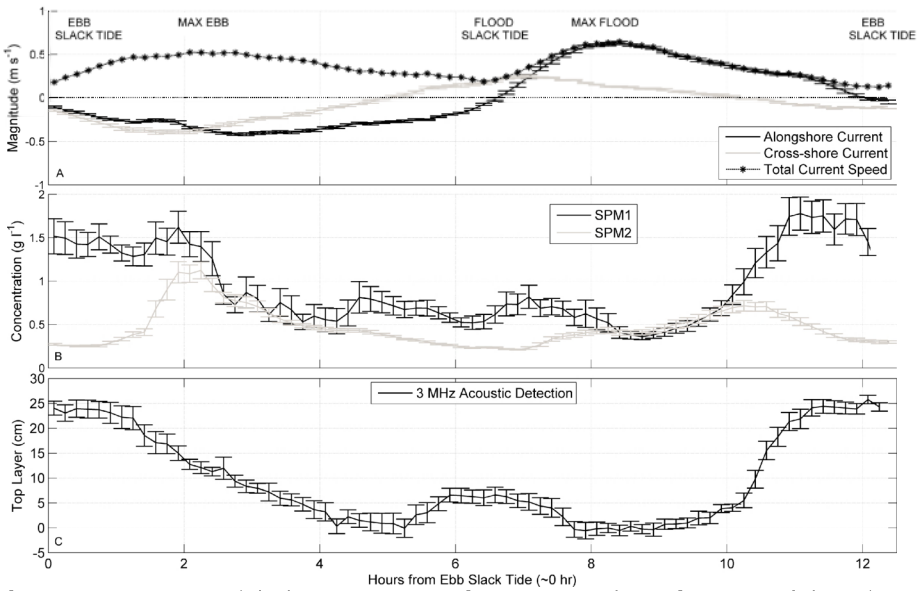

Figure 6.11 *Spring tidal-phase averages of time-series data of currents (**a**), sediment suspension (**b**), and HCMS dynamics (**c**). SPM1 and SPM2 are for 0.2 and 2 mab, respectively*

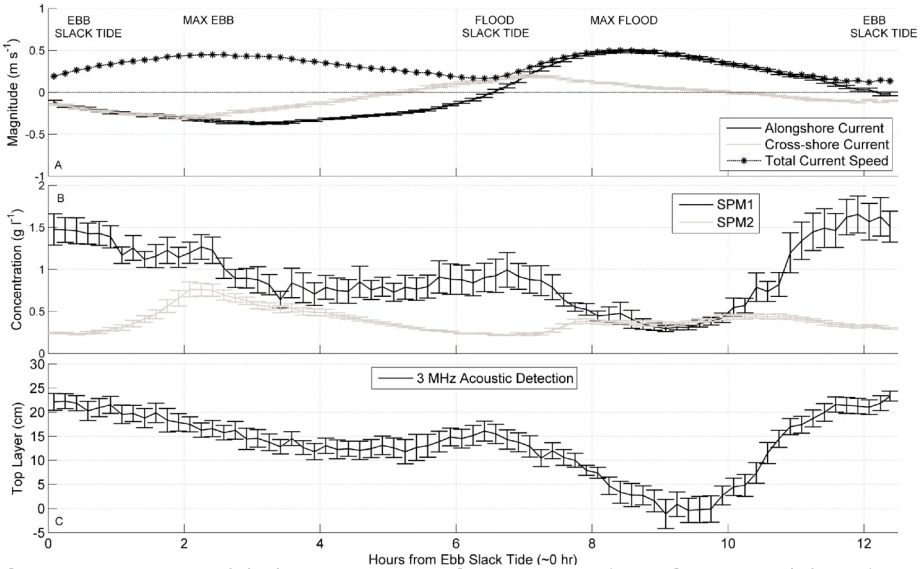

Figure 6.12 *Neap tidal-phase averages of time-series data of currents (**a**), sediment suspension (**b**), and HCMS dynamics (**c**). SPM1 and SPM2 are 0.2 and 2 mab, respectively*

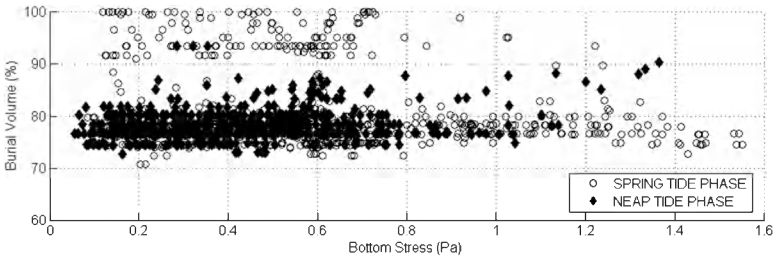

Figure 6.13 *Hydrodynamic model results (mine site) of bottom stress plotted against the mine burial volume indicate that phases with 90-100 % of mine burial coincide with slack tides (bottom stresses <0.7 Pa) during spring tide phases. Neap tide phases do not show any increased burial*

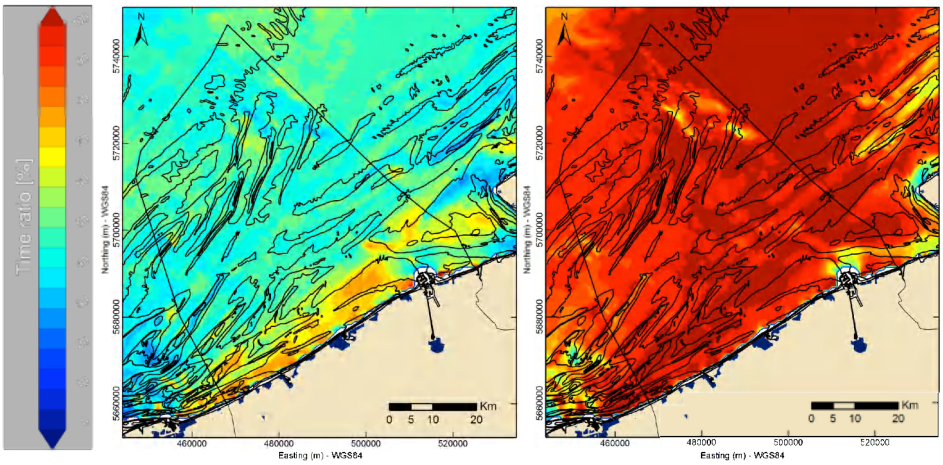

Figure 6.14 *Model results of slack tide ratio over two tidal cycles (neap tide,* ***right*** *and spring tide,* ***left****). Slack tide is here defined as when bottom shear stresses are less than 0.7 Pa; this is in accordance with erosion resistance measurements of bed samples taken in the study area (Fettweis et al. 2010). Blue is 0% and red 100% time ratio. Figure illustrates the high temporal variability (contrast between neap and spring) in hydrodynamics and in the potential of mine burial by HCMS as such*

6.6. Conclusions

Time-series data recorded by a test mine has been analyzed in combination with hydrodynamic and meteorological recordings, and a shorter time-series data of suspended sediment concentration. Nearby the port of Zeebrugge, the study area is characterized by highly turbid waters. However, the sandy seabed seems to be responsible for a well-known burial process that is related to scour by storm waves. This process accounts for most of the mine burial volume (60 and 80%). Tidal forcing will also account for some scour of the seabed around the mine. Furthermore, the hydrodynamic pattern present in the study area can be biased by changing wind conditions. As a result, subtidal flow forcing is acting on the mine as well.
Superimposed on the mine burial by scour signal, a more cyclic (quarter-diurnal) burial signal occurred preferably during spring tide phases. Benthic observations of SPM concentration and changing seabed evolution have shown that during slack tides, the mine is covered with HCMS layer. An acoustic (3 MHz) detection method reveals these bed boundary level changes (up to 25 cm), in accordance to what is observed by the optics-based test mine measurements. The potential of the test mine detecting HCMS layers has been proven by the authors, and mine burial by transient HCMS is introduced. The latter has implications towards mine hunting strategies. In order to assess the possibility that mines in HCMS areas are missed during tracking surveys,

additional experiments will have to be conducted in areas with mud suspensions of various thickness and stability. Areas and circumstances where HCMSs are relatively persistent should be monitored and analyzed in detail as part of follow-up studies. For Belgium, the areas with highest risk are closest to shore during neap tides, when burial is potentially the most prolonged.

6.7. *Acknowledgments*

The presented results were obtained thanks to the cooperation between the Bundesamt für Wehrtechnik und Beschaffung - Forschungsanstalt der Bundeswehr für Wasserschall-und Geophysik (BWB - FWG, Germany), the Belgian Naval Defence - Direction Générale Material Resources (DGMR) and the Management Unit of the North Sea Mathematical Models (MUMM). The first author (M. Baeye) acknowledges a specialization grant from IWT (Agency for Innovation by Science and Technology, Flanders). Research at MUMM was partly funded by the Maritime Access Division of the Ministry of the Flemish Community (MOMO project) and by Belgian Science Policy (Science for a Sustainable Development, QUEST4D project, SD/NS/06A). T. Wever and R. Lühder (FWG) are thanked for their assistance on the preparation and deployment of the FWG burial recording mines. L. Vigin (MUMM) is thanked for her assistance on creating the GIS figure 6.14. The captains and their crews of Belgian Navy's minehunters Lobelia and Primula are acknowledged for the skilful deployment and recuperation of the test mines. G. Dumon (Ministery of the Flemish Community, Maritime Services, Coast. Division/Hydrography) made available wind and wave measurement data. We also want to acknowledge the crew of RV Belgica for mooring and recuperation of the tripod; and, A. Pollentier and L. Naudts and their team (Measuring Service of MUMM, Oostende) for technical support. The two reviewers are thanked for their constructive remarks.

6.8. *References*

Abelev, A.V., Valent, P.J., Holland, K.T., 2007. Behavior of a Large Cylinder in Free-Fall through Water. Oceanic Engineering, IEEE Journal 32, 10-20.

Akoz, M.S., Sahin, B., Akilli, H., 2010. Flow characteristic of the horizontal cylinder placed on the plane boundary. Flow Measurement and Instruments 21, 476-487.

Aubeny, C.P., Han, S., 2007. Effect of Rate-Dependent Soil Strength on Cylinders Penetrating Into Soft Clay. Oceanic Engineering, IEEE Journal of 32, 49-56.

Baeye, M., Fettweis, M., Voulgaris, G., Van Lancker, V., 2011. Sediment mobility in response to tidal and wind-driven flows along the Belgian inner shelf, southern North Sea. Ocean Dynamics, 1-12.

Beardsley, R.C., Limeburner, R., Rosenfeld, L.K., 1985. Introduction to the CODE-2 moored array and large-scale data report, in: Limeburner, R. (Ed.), CODE-2: Moored array and large-scale data report. WHOI, Massachusetts, p. 234.

Brandes, H.G., 1999. Mine Burial due to Wave-induced Liquefaction and Other Processes, 9th Int. Offshore and Polar Eng. Conf., Brest, France, p. 568:574.

Brandes, H.G., Riggs, H.R., 2002. Modeling of Seabed Liquefaction and Other Processes Responsible for Mine Burial. ASME Conf. Proc. 2002, 455-462.

Brandes, H.G., Riggs, H.R., 2004. Modeling of Sediment Mechanics for Mine Burial Prediction. University of Honolulu, p. 11.

Cataño-Lopera, Garcia, M.H., 2006 a. Burial of Short Cylinders Induced by Scour under Combined Waves and Currents. Journal of Waterway, Port, Coastal, and Ocean Engineering 132, 11.

Cataño-Lopera, Y.A., Demir, S.T., Garcia, M.H., 2007. Self-Burial of Short Cylinders Under Oscillatory Flows and Combined Waves Plus Currents. Oceanic Engineering, IEEE Journal 32, 191-203.

Cataño-Lopera, Y.A., García, M.H., 2006 b. Geometry and migration characteristics of bedforms under waves and currents. Part 1: Sandwave morphodynamics. Coastal Engineering 53, 767-780.

Chu, P.C., Smith, T.B., Haeger, S.D., 2002. Mine Impact Burial Prediction Experiment, J. of Counter-Ordnance Technology, p. 10.

Dujardin, A., Van den Eynde, D., Vanlede, J., Ozer, J., Delgado, R., Mostaert, F., 2010. BOREAS – Belgian Ocean Energy Assessment: A comparison of numerical tidal models of the Belgian part of the North Sea. Version 2_0. WL Rapporten, 814_03. Flanders Hydraulics Res., Soresma & MUMM: Antwerp, Belgium. BELSPO contract SD/NS/13A

Fettweis, M., 2008. Uncertainty of excess density and settling velocity of mud flocs derived from in-situ measurements. Estuarine, Coastal and Shelf Sciences 78, 426-436.

Fettweis, M., Francken, F., Pison, V., Van den Eynde, D., 2006. Suspended particulate matter dynamics and aggregate sizes in a high turbidity area. Marine Geology 235, 63-74.

Fettweis, M., Francken, F., Van den Eynde, D., Verwaest, T., Janssens, J., Van Lancker, V., 2010. Storm influence on SPM concentrations in a coastal turbidity maximum area with high anthropogenic impact (southern North Sea). Continnetal Shelf Research 30, 1417-1427.

Fettweis, M., Nechad, B., Van den Eynde, D., 2007. An estimate of the suspended particulate matter (SPM) transport in the southern North Sea using SeaWiFS images, in-situ measurements and numerical model results. Continental Shelf Research 27, 1568-1583.

Fettweis, M., Van den Eynde, D., 2003. The mud deposits and the high turbidity in the Belgian-Dutch coastal zone, southern bight of the North Sea. Continental Shelf Research 23, 669-691.

Friedrichs, C.T., Trembanis, A.C., 2006. Forecasting Scour Related Mine Burial Using a Parameterized Model. School of Mar. Sci., Virginia Institute of Mar. Sci., Gloucester Point, VA, p. 12.

Garcia, M.H., Cataño-Lopera, Y.A., Landry, B.J., 2009. Mine Burial by Local Scour and Sand Waves. Illinois, Urbana Dept of Civil and Environmental Engineering, pp. 11.

Geurts, B.J., Clercx, H., Uijttewaal, W., Voropayev, S., Testik, F., Fernando, H., Balasubramanian, S., 2007. Sediment transport, ripple dynamics and object burial under shoaling waves, Particle-Laden Flow, pp. 15-27.

Grilli, S.T., 2007. Wave Induced Mine Burial and Sediment Transport in Coastal Environment: Wave and Sediment Transport Modeling Studies. Dept of Oceanic Engineering, Kingston, Rhode Island, p. 12.

Hay, A.E., Speller, R., 2005. Naturally occurring scour pits in nearshore sands. Journal Geophysical Research 110, 15.

Inman, D.L., Jenkins, S.A., 2005. Scour and Burial of Objects in Shallow Water, in: Schwartz, M.L., Kearney, M., Stevenson, J. (Eds.), North America, Coast. Ecology. Encycl. Coastal Sciences pp. 714-721.

IMDC; WL (2007). Langdurige monitoring van zout/zoet-verdeling in de haven van Zeebrugge en monitoring zoutconcentratie slibconcentratie en hooggeconcentreerde slibsuspensies in de Belgische kustzone. Waterbouwkundig Laboratorium: Borgerhout. International Marine and Dredging Consultants Rep.

Jenkins, S.A., Inman, D.L., Richardson, M.D., Wever, T.F., Wasyl, J., 2007. Scour and Burial Mechanics of Objects in the Nearshore. Oceanic Engineering, IEEE Journal 32, 78-90.

Lacroix, G., Ruddick, K., Ozer, J., Lancelot, C., 2004. Modelling the impact of the Scheldt and Rhine/Meuse plumes on the salinity distribution in Belgian waters (southern North Sea). Journal of Sea Research 52, 149-163.

Large, W.G., Pond, S., 1981. Open Ocean Momentum Flux Measurements in Moderate to Strong Winds. Journal of Physical Oceanography 11, 13.

Luyten, P. J., Jones, J. E., Proctor, R., Tabor, A., Tett, P., Wild-Allen, K. 1999. COHERENS, a coupled hydrodynamical-ecological model for regional and shelf seas: User Documentation. MUMM report, Brussels, Belgium. 911 pp. http://www.mumm.ac.be/coherens.

Luyten P.J., 2011. COHERENS — A Coupled Hydrodynamical-Ecological Model for Regional and Shelf Seas: User Documentation. Version 2.0. RBINS-MUMM Report, Royal Belgian Institute of Natural Sciences.

Mouchet, 1990. Analysis of tidal elevation and currents along the Belgian Coast, Tech. Rep. G.H.E.R. University of Liège Sart Tilman, Liège.

Mulhearn, P.J., 1995. Experiments on Mine Burial or Impact - Sydney Harbour, Technical Note. Aeronautical and Maritime Res. Laboratory, Melbourne, p. 18.
NRC, 2003. Environmental Information For Naval Warfare. National Academies Press.
Pison, V., Ozer, J. 2003. Operational products and services for the Belgian coastal waters. In: Building the European capacity in operational modeling, Proc. 3rd Int. Conf. on EuroGOOS (Dahlin, H., Flemming, N.C., Nittis, K., Petersson, S.E., eds.). Oceanic Seriers 69, 503-509.
PIANC, 2008. Minimizing harbour siltation, p. 75.
Plager, W.L., 2000. Mine Burial in the Surf Zone, Naval Postgraduate School Monterey, CA, p. 66.
Quinn, R., 2006. The role of scour in shipwreck site formation processes and the preservation of wreck-associated scour signatures in the sedimentary record evidence from seabed and sub-surface data. Journal of Archaeological Sciences 33, 14.
Richardson, M., Briggs, K., 2000. Seabed-Structure Interaction in Coastal Sediments. Office Navy Res. Rep., Arlington, VA, p. 18.
Saunders, R.D., 2005. Seabed Scour Emanating from Submerged Three-dimensional Objects: Archaeol. Case Studies, Dept Civil and Environmental Engineering University of Southampton, UK, p. 207.
Schrottke, K., Becker, M., Bartholomä, A., Flemming, B., Hebbeln, D., 2006. Fluid mud dynamics in the Weser estuary turbidity zone tracked by high-resolution side-scan sonar and parametric sub-bottom profiler. Geo-Marine Letters 26, 185-198.
Traykovski, P., Geyer, R., Sommerfield, C., 2004. Rapid sediment deposition and fine-scale strata formation in the Hudson estuary. Journal of Geophysical Research 109, 20.
Traykovski, P., Richardson, M.D., Mayer, L.A., Irish, J.D., 2007. Mine Burial Experiments at the Martha's Vineyard coastal observatory. Oceanic Engineering, IEEE Journal
32, 150-166.
Trembanis, A.C., Friedrichs, C.T., Richardson, M.D., Traykovski, P., Howd, P.A., Elmore, P.A., Wever, T.F., 2007. Predicting Seabed Burial of Cylinders by Wave-Induced Scour: Application to the Sandy Inner Shelf Off Florida and Massachusetts. Oceanic Engineering, IEEE Journal 32, 167-183.
Uncles, R.J., Stephens, J.A., Law, D.J., 2006. Turbidity maximum in the macrotidal, highly turbid Humber Estuary, UK: Flocs, fluid mud, stationary suspensions and tidal bores. Estuarine Coastal Shelf Sciences 67, 30-52.
Velasco, D.W., Huhta, C.A., 2010. Experimental verification of acoustic Doppler velocimeter (ADV) performance in fine-grained, high sediment concentration fluids, SonTek/YSI Appl. Note.
Verfaillie, E., Meirvenne, M.V., Lancker, V.V., 2006. Multivariate geostatistics for the predictive modelling of the surficial sand distribution in shelf seas. Continental Shelf Research 26, 15.
Voropayev, S.I., Testik, F.Y., Fernando, H.J.S., Boyer, D.L., 2003. Burial and scour around short cylinder under progressive shoaling waves. Oceanic Engineering 30, 1647-1667.
Wever, T., 2003. Speed of Migrating Bedforms on the Sea Floor - A Review, FWG-Report. Forschungsanstalt der Bundeswehr für Wasserschall und Geophysik, pp. 20.
Wever, T.F., Luehder, R., 2007. Mine Burial Observations During the 2003-2004 U.S. Office of Naval Research Experiment. Oceanic Engineering, IEEE Journal 32, 184-190.
Wilkens, R.H., Richardson, M.D., 2007. Mine Burial Prediction: A Short History and Introduction. Oceanic Engineering, IEEE Journal 32, 3-9.
Winterwerp, J.C., 2002. On the flocculation and settling velocity of estuarine mud. Continental Shelf Research 22, 1339-1360.
Yang, L., 1998. Modelling of hydrodynamic processes in the Belgian Coastal Zone, Appl. Math. Catholic University of Louvain, Leuven, p. 204.

Monitoring the effects of disposal of fine sediments from maintenance dredging on suspended particulate matter concentration in the Belgian nearshore area*

Michael Fettweis[1], Matthias Baeye[2], Frederic Francken[1], Brigitte Lauwaert[1], Dries Van den Eynde[1], Vera Van Lancker[1], Chantal Martens[3], Tinne Michielsen[3]

[1]*Royal Belgian Institute for Natural Science (RBINS), Management Unit of the North Sea Mathematical Models (MUMM), Gulledelle 100, 1200 Brussels, Belgium*

[2]*Ghent University, Renard Centre of Marine Geology, Krijgslaan 281 (S8), 9000 Gent, Belgium*

[3]*Ministry of Public Works and Mobility, Maritime Access Division, Tavernierkaai 3, 2000 Antwerp, Belgium*

*published in Marine Pollution Bulletin (Elsevier)

M. Baeye was responsible for the analysis of HCMS dynamics (SPM and ADV altimetry) and for the interpretation in relation to disposal activity.

Abstract

The impact of continuous disposal of fine-grained sediments from maintenance dredging works on the suspended particulate matter concentration in a shallow nearshore turbidity maximum was investigated during dredging experiment (port of Zeebrugge, southern North Sea). Before, during and after the experiment monitoring of SPM concentration using OBS and ADV altimetry was carried out at a location 5 km west of the disposal site. A statistical analysis, based on the concept of populations and sub-sampling, was applied to evaluate the effect. The data revealed that the SPM concentration near the bed was on average more than 2 times higher during the dredging experiment. The disposed material was mainly transported in the benthic layer and resulted in a long-term increase of SPM concentration and formation of fluid mud layers. The study shows that SPM concentration can be used as an indicator of environmental changes if representative time-series are available.

Keywords: Dredged material disposal; dredging; fluid mud; SPM concentration; suspended sediments; monitoring

7.1. *Introduction*

The Water Framework Directive (2000/60/EC) and recently adopted EU Marine Strategy Framework Directive (2008/56/EC) (see e.g. Borja 2005, Devlin et al. 2007) identifies human induced changes in the concentration of suspended particulate matter (SPM) as one of the main pollutants. Disposal of fine-grained dredged material at sea has a varying impact on the marine environment (Nichols 1988, Bray et al. 1996, Hill et al. 1999, O'Connor 1999, Smith and Rule 2001, Lohrer and Wetz 2003, Simonini et al. 2005, Lee et al. 2010) and constitutes an important problem in coastal zone management (OSPAR 2008). Dredging activities can be classified as either maintenance or capital dredging. Maintenance dredging typically involves the periodic or continuous removal of sediments deposited in navigation channels and harbours as a result of natural processes. Capital dredging is associated with deepening or with construction activities and consists thus of civil engineering works limited in time. Very often, ports and navigation channels are situated in coastal or estuarine turbidity maximum areas and suffer from rapid sedimentation of fine-grained material (PIANC 2008), necessitating frequent maintenance dredging and disposal operations. The effect of increased turbidity due to disposal operations on the ecosystem are well documented in low-turbidity (<10 mg l^{-1}) waters (e.g. Orpin et al. 2004); but less obvious in coastal and estuarine areas where suspended particulate matter (SPM) concentration is high as well differences between minima and maxima. Dredging and disposal effects are site-specific (Ware et al. 2010) and require the understanding of the site-specific dynamics in order to evaluate environmental impact of dredging and disposal works. In case of mainly non-cohesive material is the impact of disposal of dredged material at sea most significant at the seabed (Du Four and Van Lancker 2008, Okada et al. 2009) and the impact on the environment may remain near-field and short-term (Fredette and French 2004, Powilleit et al. 2006). When cohesive sediments are disposed then significant increases in turbidity may occur in the water column (Hossain et al. 2004, Van den Eynde 2004, Wu et al. 2006) depending on the mode, timing, quantity, frequency of the disposal activity (Bolam et al. 2006).

The SPM dynamics control processes such as sediment transport, deposition, re-suspension, primary production and the functioning of benthic communities (McCandliss et al. 2002, Murray et al. 2002). It varies as a function of seasonal supply of fine-grained sediments, the interaction between cohesive and non-cohesive sediments, biological activity, remote or local availability of fine sediments, advective processes, erosion, deposition, storms, and human activities (Velegrakis et al. 1997, Bass et al. 2002, Schoellhamer 2002, Le Hir et al. 2007, Fettweis et al. 2010). Deepening of channels and construction of ports increases deposition of fine-grained sediments and has as consequence an increase of maintenance dredging and thus an increase of SPM concentration in and around the disposal site (Truitt 1988, Collins 1990, Wu et al. 2006). During slack water and after storm periods fluid mud layers may be formed by settling of suspended matter or fluidization of cohesive sediment beds (Maa and Mehta 1987, van Kessel and Kranenburg 1998, Li and Mehta 2000). Massive sedimentation of fine-grained sediments in harbours and navigation channel is often related to the occurrence of fluid mud layers (Fettweis and Sas 1999, Verlaan and Spanhoff 2000, Winterwerp 2005, PIANC 2008, Van Maren et al. 2009, De Nijs et al. 2009). Fluid mud is a high concentration aqueous suspension of fine-grained sediment with SPM concentrations of tens to hundreds of grams per litre and bulk densities of 1080 to 1200 kg m^{-3}; it consists of water, clay-sized particles, and organic materials; and displays a variety of rheological behaviours ranging from elastic to pseudo-plastic (Mac Anally et al. 2007).

The aim of this paper is to present and discuss the impact of continuous disposal of fine-grained sediments on the SPM concentration and on the fluid mud dynamics in a shallow nearshore turbidity maximum area during a one month dredging experiment. The experiment took place in the port of Zeebrugge (Belgian coastal area, southern North Sea) in the framework of studies conducted by the Flemish Ministry of Public Works and Mobility to develop more cost effective methods for dredging fluid mud. Monitoring of the effects on SPM concentration was required as the dredged matter was disposed at sea at a location closer to the shore and the port compared to the existing disposal sites. Previous studies have used numerical simulations to investigate the spatial distribution of material disposed of in the sea (e.g. Gallacher and Hogan

1998, Bai et al. 2003, Van den Eynde 2004), but even with recent progress in sediment transport modelling (e.g. Sanford 2008) limitations related to accurately simulating the dynamics of fluid mud layers and the interaction between the bed and the water column remain. In situ monitoring provides a good opportunity for investigating the impact of fine-grained matter dispersal behaviour and its fate due to disposal operations. In situ measurements of SPM concentration before, during and after the dredging experiment have been carried out at about 5 km from the disposal site together with sediment density and bathymetrical surveys at the dredging location and the disposal site. As the heterogeneity and complexity of the SPM concentrations are high, due to their natural high variability, statistical methods have been used to characterize temporal SPM concentration variation in a way that it can be used as indicator for changes induced by human activities.

7.2. *Study area*

The Belgian-Dutch nearshore area (southern North Sea, cf. Fig. 1.2, Fig. 2.1 b) is shallow (<10 m Mean Lower Low Water Springs, MLLWS) and characterised by sediment composition varying from pure sand to pure mud (Verfaillie et al. 2006). SPM forms a turbidity maximum between Ostend and the mouth of the Westerscheldt (cf. Fig. 4.1). Measurements indicate variations in SPM concentration in the nearshore area of 20–70 mg l^{-1}; reaching 100 to 3000 mg l^{-1} near the bed; lower values (<10 mg l^{-1}) occur in the offshore (Fettweis et al. 2010). The most important sources of SPM are the French rivers discharging into the English Channel, coastal erosion of the Cretaceous cliffs at Cap Gris-Nez and Cap Blanc-Nez (France) and the erosion of nearshore Holocene mud deposits (Fettweis et al. 2007). Tides are semi-diurnal with a mean tidal range at Zeebrugge of 4.3 m at spring and 2.8 m at neap tide. The tidal current ellipses are elongated in the nearshore area and become gradually more semi-circular further offshore. The current velocities near Zeebrugge (nearshore) vary from 0.2–1.5 m s^{-1} during spring tide and 0.2–0.6 m s^{-1} during neap tide; more offshore they range between 0.2-0.6 m s^{-1} during spring tide and 0.1-0.3 m s^{-1} during neap tide. Flood currents are directed towards the Northeast and ebb currents towards the Southwest. Winds blow predominantly from the southwest and the highest waves occur during north-westerly winds. Significant wave heights in the nearshore area exceed 1.5 m during 10% of the time. The strong tidal currents and the low fresh water discharge of the Westerscheldt estuary (yearly average is 100 m^3 s^{-1} with minima of 20 m^3 s^{-1} during summer and maxima of 600 m^3 s^{-1} during winter) result in a well-mixed water column with very limited salinity and temperature stratification.
On average 4.46×10^6 ton dry matter (tdm) is dredged annually in the port of Zeebrugge to maintain navigation depth; this represents about 60% of the total amount of maintenance dredging in the Belgian nearshore area (Lauwaert et al. 2009). The dredged matter consists of muddy sediments and is disposed on the disposal sites S1 (47%), Zeebrugge Oost (44%) and S2 (9%), see Fig 7.1. The sedimentation rate in the outer port of Zeebrugge is, on average, about 1.7 tdm m^{-2} per year. In 2007 and 2008, respectively, 0.7×10^6 tdm and 0.3×10^6 tdm of sediments were dredged in the Albert II dock (Fig. 7.1).

7.3. *Material and Methods*

7.3.1. *Dredging experiment*

Dredging with trailer hopper suction dredgers and open water disposal of the dredged material at designated locations, is inefficient for fluid mud and incur substantial costs (PIANC 2008). An automatic method to intercept and pump away fluid mud using stationary pumping system was evaluated by Berlamont (1989) for mud from the port of Zeebrugge. A similar approach was adopted for the dredging experiment, except that a cutter suction dredger was used instead of stationary pumping systems. The experiment took place in the Albert II dock situated in the outer port of Zeebrugge between 5 May and 2 June 2009 (Fig. 7.1). The dredger continuously dredged for periods of a few days up to a week at a fixed location and a fixed depth before being moved to another location. The dredged matter was pumped using floating pipelines over the harbour breakwater into the sea (see Fig. 7.1). The pumping capacity was

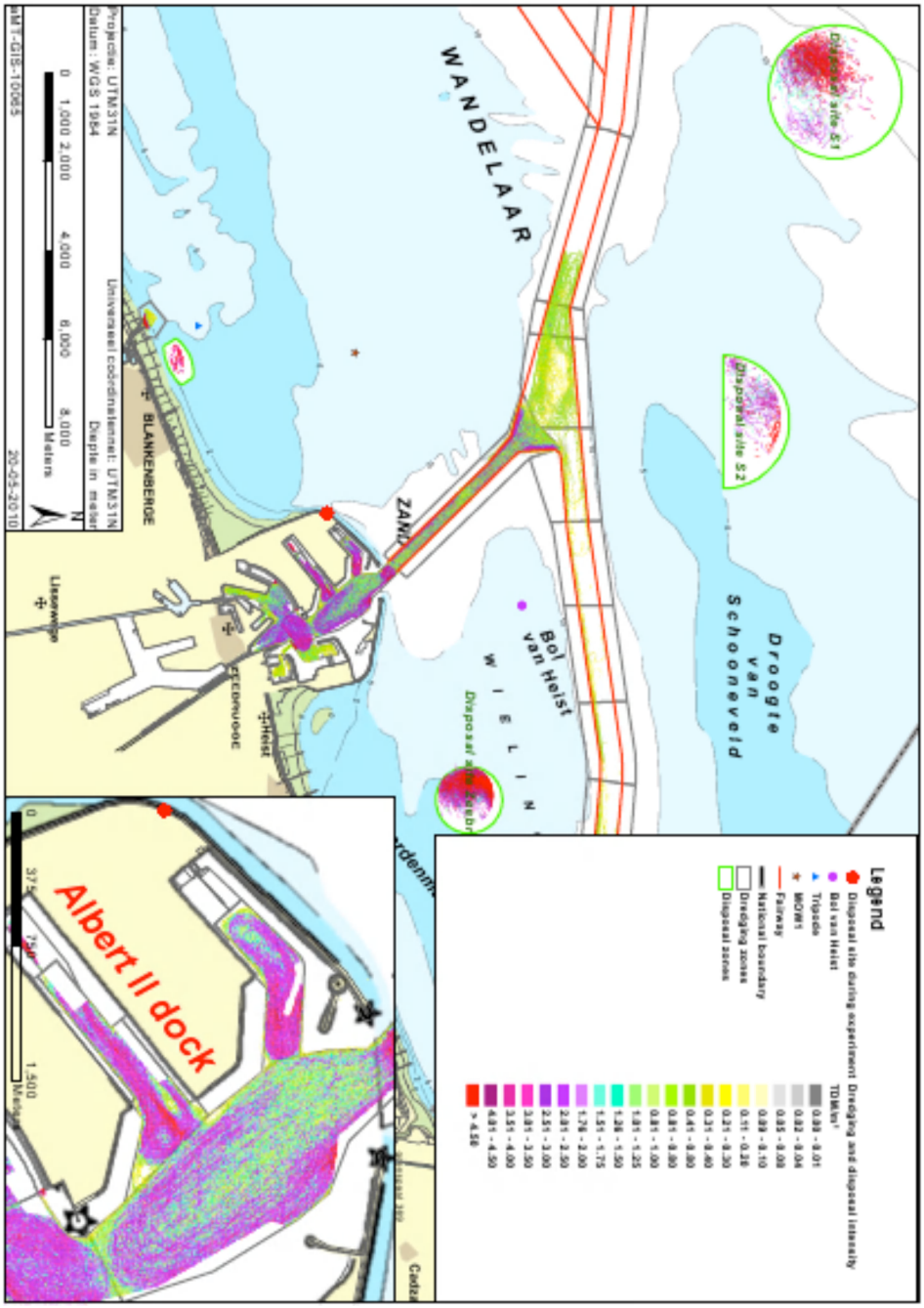

Figure 7.1 *Detail of the Zeebrugge area showing the measurement station at Blankenberge blue triangle), the wave measurement station at Bol van Heist (purple dot), the location of the disposal site during the field experiment (red dot), the MOW1 site (brown star), the Albert II dock and the existing disposal sites (green circles or half-circles). The background consist of bathymetry and of the dredging and disposal intensity (scale is from 0 to >4.5 tdm m^{-2}) for 2008 (in ton dry matter TDS)*

3000 m^3 h^{-1}, resulting thus –using the average density of the pumped matter (including salt and sediment) of 1.055 t m^{-3} – in 60×10^3 tdm of sediments that have been disposed during the duration of the experiment. As the density recordings of the dredge material were inaccurate, this should be seen as an estimate. The aim of the experiment was to investigate whether the thickness of the fluid mud layer with a density lower than 1200 kg m^{-3} could efficiently be reduced. This density is derived from ship manoeuvrability studies that aided in the redefinition of the level of dredging required (Delforterie et al. 2005, PIANC 2008).

7.3.2. In-situ monitoring

The monitoring during the disposal experiment is divided in near and far field measurements. The near field measurements consisted of bathymetrical surveys in the dock and at the disposal site and weekly mud density surveys in the Albert II dock (Fig. 7.1). Density profile measurements were carried out in situ using a gamma-ray densitometer that was pushed in the mud layer. Bathymetrical surveys were performed daily with 33/210 kHz echo sound measurements along fixed transects and weekly with multibeam.
The far field monitoring was carried out at a fixed location near Blankenberge (51.33°N 3.11°E) situated about 1 km offshore and 5 km west of the disposal site (Fig. 7.1) using a tripod which was developed for collecting time-series (up to 50 days) of SPM concentration and current velocity. The water depth at the site is about 6 m MLLWS and the seabed consists of fine sand (D50 = 150 µm) with ephemeral mud patches on top. The tripod was deployed for 240 days during 6 measuring periods before, during and after the experiment, see Table 7.1. 17% of the data have been collected during or shortly after the field experiment. A SonTek 5 MHz Acoustic Doppler Velocimeter (ADV) Ocean, a Sea-Bird SBE37 CT system and two D&A OBS3 sensors were mounted on the frame, one at about 0.2 and the other one 2 m above bottom (mab). Field calibration of the OBS sensors have been carried out during several tidal cycles carried out in the nearshore area in order to obtain SPM concentration. A Niskin bottle was closed every 20 minutes, thus resulting in about 40 samples per tidal cycle. Three sub samples were filtered on board of the vessel from each water sample, using pre-weighted filters (Whatman GF/C). After filtration, the filters were rinsed once with Milli-Q water (±50 ml) to remove the salt, and dried and weighted to obtain the SPM concentration. A linear regression between all OBS signals and SPM concentrations from filtration was assumed. The measuring volume of the ADV was situated at 0.2 mab. The altimetry of the ADV was used to detect variation in bed level due to the occurrence of fluid mud layers. Decreasing distance between probe and bed boundary may correspond with the presence of fluid mud acting as an acoustic reflector. However, the boundary detection may also fail, due to attenuation of the signal before reaching the bottom (Velasco and Huhta, App. Note SonTek).

7.3.3. Statistical analysis

Variation in SPM concentration at Blankenberge is related to tides, storms, seasonal changes and human impacts. SPM concentration can be defined as a statistical population. We can consider the measured SPM concentration time-series as sub-samples that are characterised by statistical properties, such as median, geometrical mean, standard deviation and probability density distribution. Fettweis and Nechad (2010) have shown that SPM concentration has a log-normal distribution. The probability density distributions of the different sub-samples, consisting of the different time-series or other sub-samples, were therefore fitted using log-normal distributions, and the X^2 test probability calculated to assess how well the distribution fits a log-normal one. By doing so statistical properties can be calculated so that inferences or extrapolations from the sub-sample to the population can be made. E.g. if the data series collected during different periods have similar log-normal distributions, geometric means and standard deviations, then we could conclude that - within the range of natural variability and measuring uncertainties - these data series represent similar sub-samples of the whole SPM concentration population. Consequently, if disposal of dredged material has a significant impact on SPM concentration then this should be detectable in the differences between the statistical parameters of the sub-

sample collected during the dredging experiment and of the whole population.
It is well known that waves have an important impact on cohesive sediment transport processes on continental shelves (e.g. Green et al. 1995, Cacchione et al. 1999, Traykovski et al. 2007, Fettweis et al. 2010). In order to assess this effect, sub-samples of the SPM concentration data have been selected based on bottom wave orbital velocities. The wave orbital velocity at the bottom was calculated from significant wave height measured at the station "Bol van Heist" (Fig. 7.1), the measured water depth and the JONSWAP spectrum of waves (Soulsby 1997). Sub-sampling of the data series allows filtering out the effects of random storms from the harmonic SPM concentration variations caused by tides. The statistical properties of sub-samples representing weather conditions can thus be calculated and the SPM concentrations can be correlated with sea state conditions.

Table 7.1 *Tripod deployments at Blankenberge and the median and maximum significant wave height (H_s) during the measurement period. Period 6a corresponds with the dredging experiment*

	Start (dd/mm/yyyy hh:mm)	End ((dd/mm/yyyy hh:mm)	Duration (days)	Median (max) H_s (m)
1	08/11/2006 14:30	15/12/2006 08:30	36.7	0.83 (2.76)
2	18/12/2006 10:47	07/02/2007 13:17	50.1	0.79 (2.96)
3	28/01/2008 15:38	24/02/2008 13:18	26.9	0.44 (2.82)
4	06/03/2008 09:09	08/04/2008 15:29	33.7	0.76 (3.03)
5	15/04/2008 08:58	05/06/2008 07:48	51.0	0.46 (1.69)
6	04/05/2009 09:59	15/06/2009 11:49	41.9	0.57 (1.89)
6a	05/05/2009 12:00	02/06/2009 07:00	27.8	0.55 (1.89)
6b	09/06/2009 00:00	15/06/2009 11:49	7.5	0.42 (1.12)

The statistical analysis is based on the assumption that the data collected before and after the dredging experiment (periods 1-5 and 6b in Table 7.1) are representative for the SPM concentration at this location. 15%, 38% and 47% of the measurements are situated in autumn, winter and spring, respectively.
As the SPM concentration is highest during autumn and winter and lowest during spring and summer (Fettweis et al. 2007, Dobrynin et al. 2010), the measurements are well distributed over the high and low SPM concentration periods. The median significant wave height (H_s) during the tripod measurements (measured at the wave station "Bol van Heist", Fig. 7.1 b) was 0.54 m, with 0.50 m, 0.61 m and 0.53 m during spring, autumn and winter, respectively. These values correspond well with the median H_s during the period 2006-2009 of 0.50 m (whole the period), 0.48 m (spring), 0.62 m (autumn) and 0.60 m (winter), supporting thus the assumption of representativeness.

7.4. Results

7.4.1. Near field monitoring

The dredging effort caused rapid (order of hours) formation of cone formed craters centred on the cutter head location (Fig. 7.2), which disappeared again after relocation of the cutter. Influx of sediment related to shipping activities and spring tide caused at some occasions the filling-up of the crater during a short period. The dredging caused a local deepening of the 1200 kg m^{-3} density surface, however the influence remained local and did not significantly changed the depth of the fluid mud density field in the dock, therefore the evaluation of the dredging experiment was negative in terms of efficiently reducing the thickness of the fluid mud layer (see Lauwaert et al. 2009).

7.4.2. Far field monitoring

The time-series for periods 1, 5 and 6 are shown in Fig. 7.3, 7.4 and 7.5. Generally, the SPM concentration signal is dominated by quarter-diurnal variations due to ebb-flood. The data show that the maximum SPM concentrations during a tidal cycle were sometimes up to 50 times higher than the minimum concentrations. The spring-neap tidal signal is often overprinted by wave effects and can only be identified clearly during calm meteorological conditions. The very high SPM concentrations measured near the bed during winter and autumn are related to storms and suggest that high concentrated benthic suspension layers have been formed that may stay for a few days. The ADV altimetry data show quarter-diurnal variations in bed level during periods with SPM concentration; this is explained as formation and re-suspension of fluffy layers during slack waters.

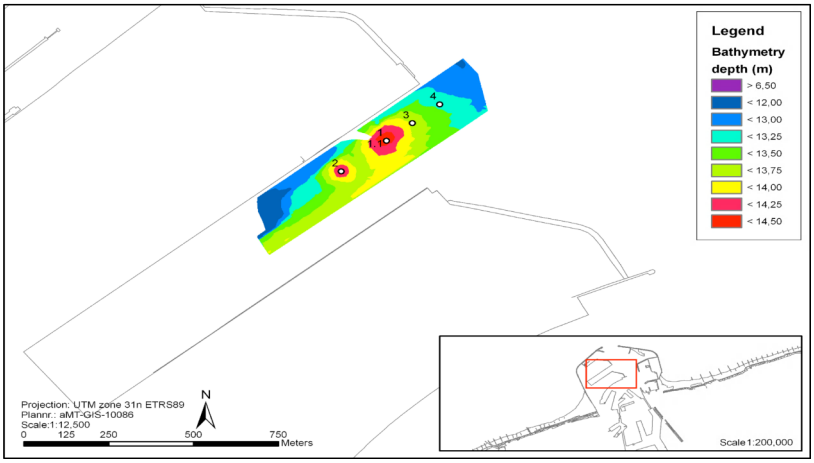

Figure 7.2 *Bathymetrical map of the 210 kHz echo soundings in the Albert II dock and the successive position of the cutter suction dredger (1-4) during the experiment. The bathymetrical survey was carried out when the dredger was operating in position 2. In position 1 a relict dredging crater is visible*

Period 1 is characterized by the occurrence of different storms (Fig. 7.3). On 12-13 November (day 316-317), a NW storm (winds blowing from NW) generated significant wave heights of about 2.8 m. The highest SPM concentrations were registered only about one day after the storm by the OBS at 0.2 mab and about two days after by the OBS at 2 mab (Fig. 7.3). The OBS data at 0.2 mab are characterised by very high minima in SPM concentrations (>0.8 g l^{-1}). The OBS at 2 mab measured an increase in SPM concentration only during a short period after the storm. This indicates that vertical mixing was limited. ADV altimetry shows a vertical rise of the acoustic reflective boundary after the storm (day 317 to 321) indicating the formation of a fluid mud. Its appearance coincided with low wave activity and decelerating currents associated with neap tide. The fluid mud layer disappeared around day 321 due to higher wave activity and accelerating currents. The altimetry signal shows then a bed boundary fluctuating with the quarter-diurnal tidal currents; the change in altimeter height on day 336 is probably caused by erosion of the sandy bed. During the deposition event on day 344, the sea floor as detected by the ADV altimetry raised about 10 cm, due to formation of fluid mud.
Period 5 (April – June 2008) was characterised by low meteorological disturbances. SPM concentration follows tidal and neap-spring tidal signal with higher SPM concentration around days 108-114, 124-130 and 142-144 (Fig. 7.4). A clear shift between the signal of the OBS at 0.2 mab and at 2 mab is observed from day 132 on (May 2008). The highest SPM concentrations occur at 0.2 mab during neap tide, whereas at 2 mab the highest values are around spring tide, indicating that SPM was deposited during neap tide and re-suspended during spring tide.

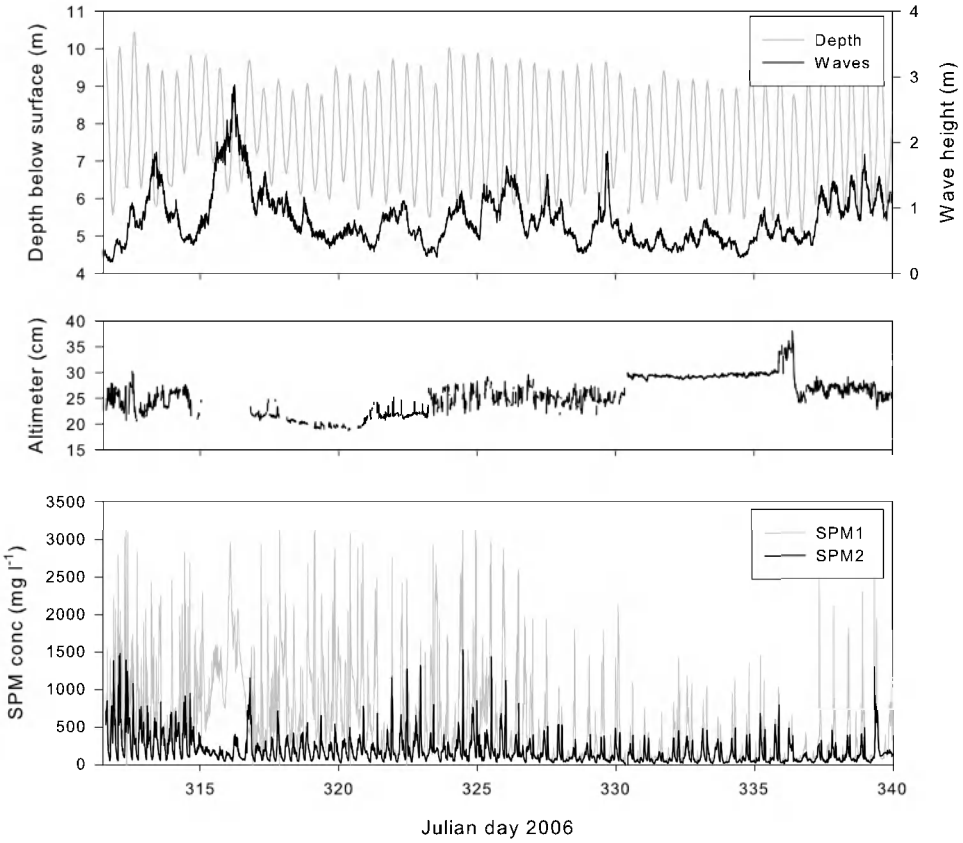

Figure 7.3 *Tripod measurements of 8 November - 6 December 2006 (part of measuring period 1). From* ***up*** *to* ***down****: depth below water surface (m) and significant wave heights at Bol van Heist; ADV altimetry; and SPM concentration derived from OBS at 0.2 mab (SPM1) and 2 mab (SPM2). Saturation of the OBS is at 3.2 g* l^{-1}

The acoustic bed boundary remained at the same distance after stabilization of the tripod at the beginning of the deployment. Deposition and consecutive re-suspension occurs as temporal events coinciding with the ebb-flood tidal signal during neap tides and the availability of SPM. During the deposition events, the sea floor as detected by the ADV altimetry raised on average by 10 cm, due deposition of mud. From day 140 on SPM concentration decreased, resulting in no increase of the acoustic bed boundary. May 2009 was marked by alternating W-SW and E-NE and relatively high wave conditions as compared to a similar period in May 2008 (Table 7.1, Fig. 7.4 and 7.5). During the experiment the SPM concentration at 0.2 mab was strikingly high, with tide-averaged values ranging from 0.3-1.6 g l^{-1}. These high values remained until one week after the end of the dredging experiment before decreasing to tide averaged values lower than 0.5 g l^{-1}. The high SPM concentrations in May 2009 are only partially due to higher waves. SPM concentration at 2 mab differs from the near-bed one, and reveals a dynamic controlled by tidal and neap-spring tidal variation, whereas near the bed high concentrated mud suspension or fluid mud layers have dominated the sediment dynamics. The ADV altimetry revealed also the decrease in acoustic bed boundary of 8-10 cm during neap tide (for day 134-139 and 153-159). For both periods mud was deposited because favourable hydro-meteorological conditions prevailed (i.e. low wave activity and decelerating currents); the mud layers remained during several days. After cessation of the disposal operations, the SPM concentrations at 0.2 mab remained still very high during 1 week and disappeared together with the fluid mud layer.

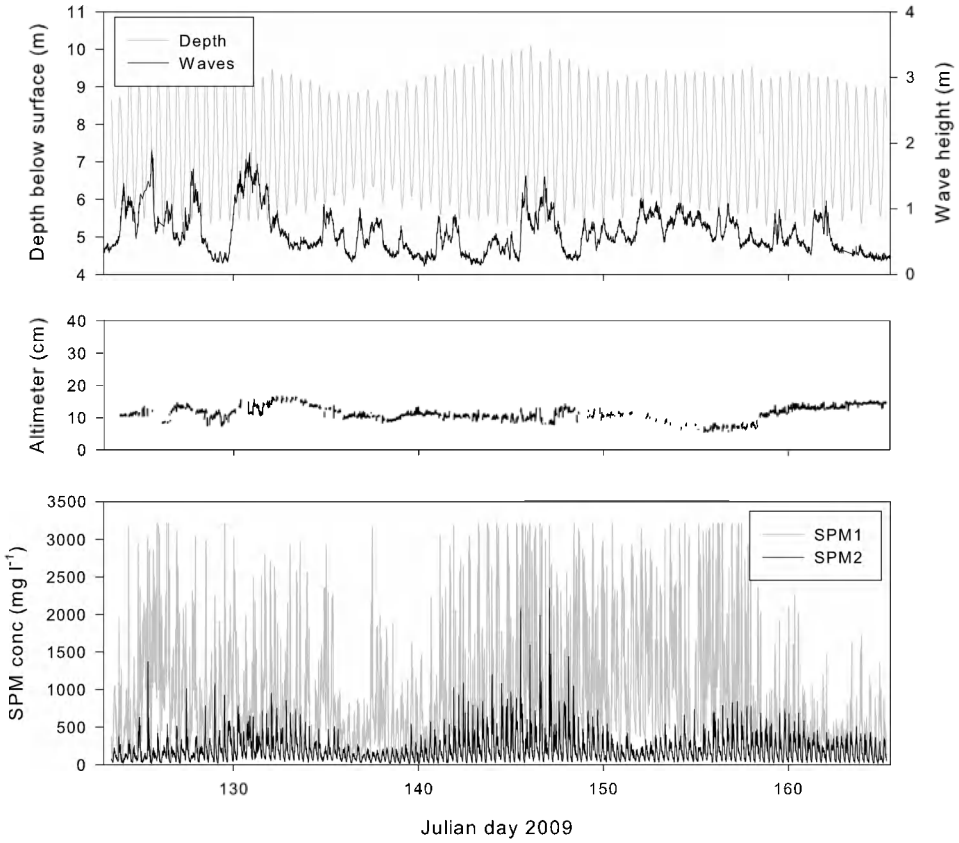

Figure 7.4 *Tripod measurements of 15 April – 23 May 2008 (part of measuring period 5). From* ***up*** *to* ***down****: depth below water surface (m) and significant wave heights at Bol van Heist; ADV altimetry; and SPM concentration derived from OBS at 0.2 mab (SPM1) and 2 mab (SPM2). After day 142, no SPM1 data are available. Saturation of the OBS is at 3.2 g* l^{-1}

7.4.3. Statistics of SPM concentration

For each of the 6 measuring period probability distributions were constructed for SPM concentration at 0.2 and 2 mab together with fitted lognormal distributions. The geometric mean (x*), median (D50) and multiplicative standard deviation (s*) of these distributions, together with the X^2 test results is shown in Table 7.2, some of the distributions are presented in Fig. 7.6. If the X^2 test probability is low ($p<0.05$), then the distribution would not correspond with a log-normal one. The results confirm that all distributions are log-normally distributed. The results show that the mean SPM concentration during autumn and winter (periods 1, 2, 3, 4) is generally higher than during spring (period 5). The mean and median SPM concentration at 0.2 mab during the field experiment (period 6 a) is significantly higher than during any of the other periods, whereas at 2 mab the same order of magnitude is observed than during a winter situation (periods 1, 2 and 3). During the field experiment (5 May – 2 June) the mean increased to 612 mg l^{-1} (0.2 mab), i.e. more than twice the mean value before and after the experiment; but remained nearly similar at 2 mab (150 mg l^{-1} vs. 128 mg l^{-1}).

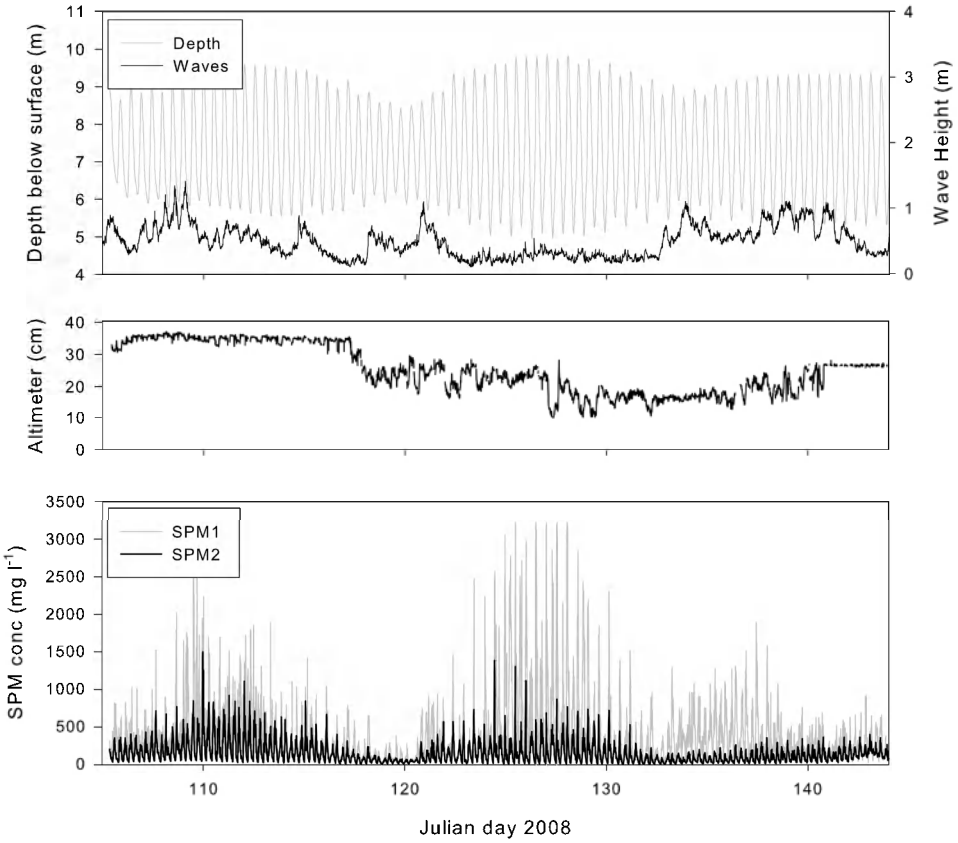

Figure 7.5 *Tripod measurements of 4 May – 15 June (measuring period 6). The field experiment lasted from 5 May until 2 June. From* ***up*** *to* ***down****: depth below water surface (m) and significant wave heights at Bol van Heist; ADV altimetry; and SPM concentration derived from OBS at 0.2 mab (SPM1) and 2 mab (SPM2). Saturation of the OBS is at 3.2 g* l^{-1}

Table 7.2 *Median (D50) and geometric mean SPM concentration (x*) in mg* l^{-1} *during the 6 deployments (Table 7.1) together with the* X^2 *test probability (p) compared with a lognormal distribution and the multiplicative standard deviation (s*). 1-5, 6b corresponds with all the data before and after the dredging experiment (6a)*

	0.2 mab								2 mab							
data	1	2	3	4	5	6a	6b	1-5,6b	1	2	3	4	5	6a	6b	1-5,6b
D50	341	288	199	321	280	672	345	281	137	143	116	150	106	150	158	131
x*	340	308	183	290	258	612	319	279	144	149	105	150	102	150	135	128
s*	2.9	3.0	2.4	3.0	2.7	2.6	2.2	2.9	2.3	2.3	2.5	2.5	2.4	2.3	2.3	2.4
p	1.00	0.57	0.77	0.96	0.82	0.99	0.37	0.93	0.93	0.94	0.59	0.99	0.94	0.99	0.12	0.99

The results of sub-sampling the SPM concentration data using as selection criterion a bottom wave orbital velocity (U_w) smaller than 0.03 m s^{-1} and bigger than 0.3 m s^{-1} are shown in Tables 8.3-8.4, respectively. The X^2 test probability is for some periods lower than 0.05, this is due to the fact that the sub-sample does not contain sufficient data. An U_w of 0.03 m s^{-1} (0.3 m s^{-1}) corresponds to a significant wave height of about 0.5 m (1.5 m) in 8 m water depth.

Table 7.3 *Median (D50) and geometric mean SPM concentration (x*) in mg l^{-1} during the 6 deployments (Table 7.1) and wave orbital velocities U_w < 0.03 m/s. Also shown is the X^2 test probability (p) of the distributions compared with a lognormal one and the multiplicative standard deviation (s*). 1-5, 6b corresponds with all the data before and after the dredging experiment (6a)*

	0.2 mab								2 mab							
data	1	2	3	4	5	6a	6b	1-5,6b	1	2	3	4	5	6a	6b	1-5,6b
	184	310	206	217	259	559	306	250	91	209	137	126	113	141	130	134
x*	221	341	181	203	239	470	269	237	103	196	116	127	103	142	121	124
s*	2.7	2.5	2.3	3.3	3.1	3.0	2.2	2.8	2.5	2.1	2.5	2.8	2.6	2.4	2.3	2.6
p	0.02	1.00	0.49	0.59	0.84	0.99	0.38	0.95	0.18	0.66	0.32	0.83	0.70	0.99	0.11	0.86

The results show that the mean SPM concentration at 0.2 mab is generally lower during low wave activity, except for period 2 and 3, whereas at 2 mab no clear relation can be observed. Before and after the field experiment, lower wave influence is not significantly changing the mean SPM concentration at 2 mab. The low mean SPM concentration during measuring period 3 is the result of calm weather (H_s = 0.46 m). The correlation between median SPM concentration and SPM concentration during higher wave action (U_w > 0.3 m s^{-1}) is only obvious for periods 1 and 6 (Table 7.4). For the other periods, the mean has similar values (period 4 and 5) or is even lower than the mean for all data (Table 7.2).

Table 7.4 *Median (D50) and geometric mean SPM concentration (x*) in mg l^{-1} during the 6 deployments (see table 1) and wave orbital velocities U_w > 0.3 m s^{-1}. Also shown is the X^2 test probability (p) of the distributions compared with a lognormal one and the multiplicative standard deviation (s*). 1-5, 6b corresponds with all the data before and after the dredging experiment (6a). For period 5 and 6b, not enough data correspond with these wave conditions to give statistical meaningful values*

	0.2 mab								2 mab							
data	1	2	3	4	5	6a	6b	1-5,6b	1	2	3	4	5	6a	6b	1-5,6b
D50	763	197	98	303	-	595	-	244	178	117	57	167	-	177	-	130
x*	609	237	115	288	-	651	-	270	197	114	61	162	-	169	-	129
s*	2.5	2.6	2.2	2.5	-	2.1	-	2.8	2.0	1.8	2.0	2.1	-	2.2	-	2.1
p	1.00	0.09	0.07	0.98	-	0.99	-	0.52	0.13	0.40	0.08	0.37	-	0.46	-	0.91

The cumulative frequency distributions of SPM concentration are shown in Fig. 7.7. The probability to have a SPM concentration at 0.2 mab higher than the median SPM concentration during the field experiments is on average 0.21 (periods 1-5, 6b), with 0.06 (period 4) and 0.30 (period 1) being the two extreme probabilities. At 2 mab the probabilities are on average higher (0.43: periods 1-5, 6b) and the extreme values are closer together (period 5: 0.32 – 0.52: period 6b).

7.5. Discussions

In this study, the results based on time-series measurements at a fixed location before, during and after an experimental disposal of dredged matter, indicated a significant higher SPM concentration during the disposal. Below we argue that the increase is not due to natural variability. The probability of having a SPM concentration higher than the median SPM concentration at 0.2 mab during the field experiment is low.

7.5.1. Wave influence

SPM transport on many shelves is mainly controlled by currents and waves and high concentrated mud suspensions or fluid mud layers are formed in wave-dominated areas (Li and Mehta 2000). The correlation between median SPM concentration and

SPM concentration during higher wave action (U_w > 0.3 m s^{-1}) is only obvious for periods 1 and 6a (Table 7.4). For the other periods, the median has a similar value (period 4) or an even lower value than the median for all wave conditions (Table 7.2). This is in contrast with observations made at MOW1 (Fig. 7.1) situated about 7 km offshore and at a water depth of about 10 m MLLWS, where the median SPM concentration was clearly correlated with wave orbital velocity (Fettweis and Nechad 2010). The differences in median SPM concentrations as a function of wave orbital velocity cannot be explained by the further offshore location and thus lower wave influence (Harris and Wiberg 2002) or differences in wave climate during the measurements. It points to our opinion to a time-lag occurring between waves and SPM concentrations at Blankenberge and thus to mainly advection of suspended matter from elsewhere as SPM source rather than local erosion. The mainly non-local sediment availability together with the fact that the median SPM concentration during the dredging experiment (period 6a) was always higher (also for the sub-samples with U_w > 0.3 and U_w < 0.03, see Table 7.2-7.4) than during the other periods, strengthen the argument that the high SPM concentration during this period was caused significantly by the disposal of dredged material.
As the median H_s during the dredging experiment (period 6a) was higher than during the same season in 2008 (Table 7.1) we could explain the high SPM concentrations during May 2009 (Fig. 7.5) as being partially due to higher wave activity. Increase in SPM concentrations remained, however, limited to the near bed, suggesting that vertical mixing due to waves was low. Fettweis et al. (2010) report that wave effects on SPM concentration are starting to become significant when H_s exceeds 2 m as the thick packages of Holocene and recent muddy sediments, found in the area, are then eroded. It is therefore not very likely that the May 2009 storms (maximum H_s < 1.8 m) have eroded sufficient sediments to explain the increase in SPM concentrations.

7.5.2. Ebb-flood dynamics

During a tidal cycle, several peaks in SPM concentration are observed; generally, two peaks occurred during ebb and one during flood. The first ebb peak is generally lower and occurred when the increasing current velocity has reached a critical value for re-suspending the fluffy layer. The second one occurred at the end of ebb and is a consequence of settling. This is confirmed by the fact that the SPM concentration peak at 0.2 mab is generally observed after the peak at 2 mab. Maxima in SPM concentration during flood occurred generally after slack water and point thus to re-suspension; the SPM concentration at 2 mab occurred after the peak at 0.2 mab. The mean of the SPM concentration maxima during a tide was at least 1.7 times higher during the dredging experiment than during the other periods (0.2 mab: 2670 mg l^{-1} vs. 1566 mg l^{-1}; 2 mab: 941 mg l^{-1} vs. 552 mg l^{-1}), whereas the mean of the minima was similar (0.2 mab: 109 mg l^{-1} vs. 99 mg l^{-1}; 2 mab: 35 mg l^{-1} vs. 40 mg l^{-1}). These processes of re-suspension and rapid deposition have also been identified in the ADV altimetry data. The OBS measurements indicated that the SPM concentration was generally higher during ebb at 0.2 mab, whereas at 2 mab it was generally higher during flood. This was more pronounced during measuring period 6a, where the highest peaks at 0.2 mab occurred more frequently during ebb than flood. The SPM during the disposal experiment was thus concentrated in the near bed layer rather than being well mixed in the water column, as was also observed by others (e.g. Wu et al. 2006, Siegel et al. 2009). The ebb-dominance of the near-bed SPM concentration indicates that SPM transport of fine sediments was from the disposal site towards the measurement location; the measurement location is situated in ebb direction of the disposal site. The SPM concentration and altimetry data both suggest that a lutocline or benthic plume was formed during the field experiment and that the fate of the fluid mud layer was controlled by the differences in bottom shear stress during neap and spring tidal periods.

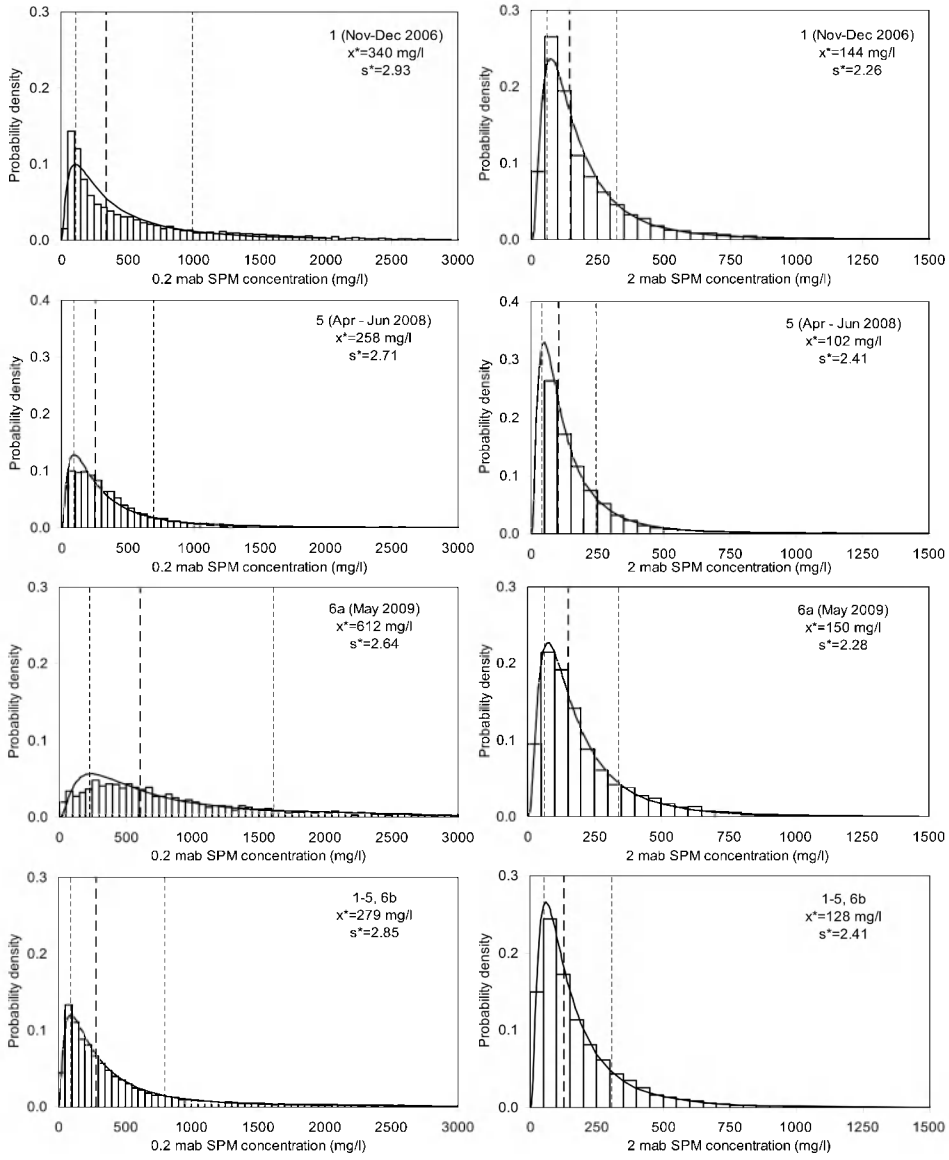

Figure 7.6 *Probability density distribution of the SPM concentration data at 0.2 mab (left) and 2 mab (right) for periods 1, 5, 6a (during dredging experiment) and all data except those during the dredging experiment (1 to 5 and 6b) and the corresponding log-normal probability density functions (periods 2-4 are not shown), see Table 1. The data are binned in classes of 50 mg* l^{-1}*, the dashed lines correspond to the geometric mean x* times/over the multiplicative standard deviation s**

7.5.3. Impact of disposal

The natural variability of SPM concentration in the area is very high, which is indicated by the high multiplicative standard deviations of the probability distributions (Table 7.2). Orpin et al. (2004) argue that the natural variability of the system could be used to define the limits of acceptable turbidity levels during dredging or disposal operations. Such an approach assumes that a short-term increase (several hours) that falls within the range of natural variability will not have any significant ecological effect. Orpin et al. (2004) developed this strategy for coral communities, which are

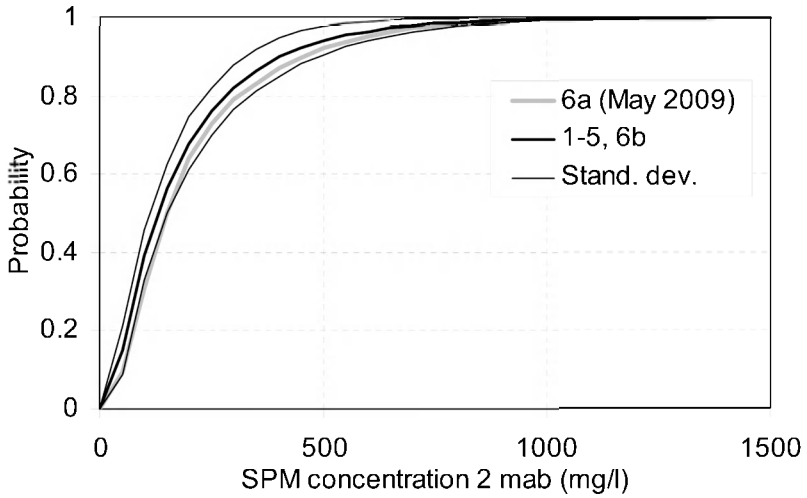

Figure 7.7 *Cumulative probability distribution of SPM concentration measured at 2 mab and 0.2 mab. The black line (1 to 5, 6b) shows the data not collected during the field experiment ± one standard deviation (thin black lines) and the grey one during the field experiment (6a), see Table 7.1*

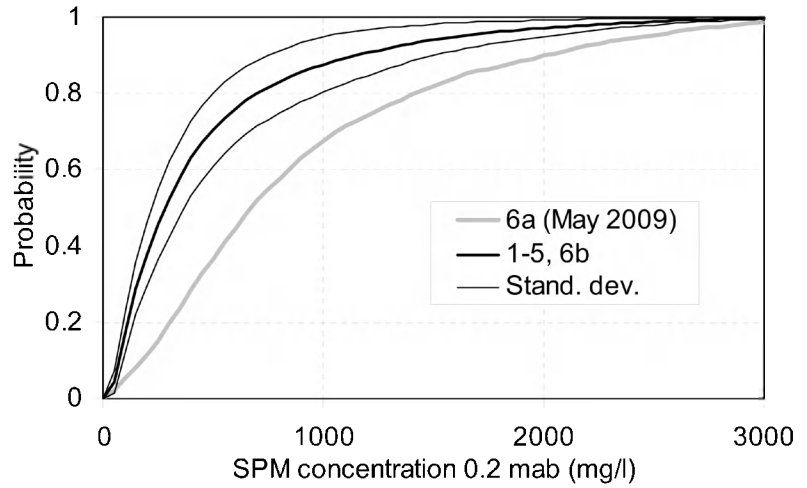

Figure 7.7 (continued) *Cumulative probability distribution of SPM concentration measured at 2 mab and 0.2 mab. The black line (1 to 5, 6b) shows the data not collected during the field experiment ± one standard deviation (thin black lines) and the grey one during the field experiment (6a), see Table 7.1*

much more sensitive to turbidity than the *Macoma balthica* community found in the high-turbidity area of the study site (Degraer et al. 2008). Changes in species density or faunal community may be attributable to changes in sediment composition and increased SPM concentration. Nevertheless, applying the same trigger to indicate acceptable upper limits of SPM concentration in the water column (2 mab) indicates that the increase is within natural variability of the system. However, we found that the cumulative frequency of SPM concentration at 0.2 mab during the dredging experiment was not included within one standard deviation of the curve for all the data not collected during the field experiment (Fig. 7.7), showing that significant change in turbidity and possibly bed sediment composition over a large area occurred. The results suggests that if the site would be used as permanent disposal site for maintenance dredging work then the SPM concentration in the near bed layer together

with deposition of mud would increase and might thus negatively affect the macrobenthos of a larger area. Van Hoey et al. (2010) report that on the disposal site Zeebrugge Oost (Fig. 7.1), situated west of the port, lower macro-benthos and epibenthos densities were found than elsewhere in the area.

7.6. Conclusions

Harbour authorities worldwide are obliged to dredge their major shipping channels, and subsequently to dispose the dredged spoil offshore. In this study an analysis method, based on the concept of statistical populations, was applied to evaluate the effects of disposal operations on SPM concentration in the Belgian nearshore area. The method provides a tool to account for the complexities associated with natural dynamics and the need to evaluate quantitatively human impact. SPM concentration can be used as an indicator of environmental changes if sufficiently long time-series are available that are representative of the natural variability. The major site-specific conclusions of the study are: the area has a very high natural variability of SPM concentration (min-max: 10 - 3300 mg l^{-1}); the SPM concentration near the bed (0.2 mab) was exceptionally high (median was more than 2 times higher) during the dredging experiment. Waves were not identified as being responsible for the high SPM concentrations; the disposal site was situated in ebb-direction of the measuring location. During the experiment, a generally higher SPM concentration near the bed during ebb and at 2 mab during flood was observed, suggesting that the disposed material was mainly transported in the benthic layer. The time-lag between high wave heights and high SPM concentration suggests further that the SPM has been advected towards the measuring location rather than eroded locally; the disposal results in a long-term increase of SPM concentration near the bed at the measuring location. This together with ADV altimetry suggest that fluid mud layers have been formed during whole the disposal experiment rather than being limited to neap tidal or storm conditions as observed during the other periods.

7.7. Acknowledgements

This study was funded by the Maritime Access Division of the Ministry of the Flemish Community in the framework of the MOMO project and by the Belgian Science Policy within the framework of the QUEST4D (SD/NS/06A) project. G. Dumon (Coastal Service, Ministry of the Flemish Community) made available wave measurement data. We want to acknowledge the crew of the RV Belgica, Zeearend, Zeehond and DN23 for their skilful mooring and recuperation of the tripod. The measurements would not have been possible without A. Pollentier and his team (measuring service of MUMM, Ostend).

7.8. References

Bai Y, Wang Z, Shen H (2003). Three-dimensional modelling of sediment transport and the effects of dredging in the Haiha Estuary. Estuarine Coastal Shelf Science 56, 175-186.

Bass SJ, Aldridge JN, McCave IN, Vincent CE (2002). Phase relationships between fine sediment suspensions and tidal currents in coastal seas. Journal of Geophysical Research 107(C10), 1-14.

Berlamont J (1989). Pumping fluid mud: Theoretical and experimental considerations. Journal of Coastal Research 5, 195-205.

Borja A (2005). The new European Marine Strategy Directive: Difficulties, opportunities, and challenges. Marine Pollution Bulletin 52, 239-242.

Bolam SG, Rees HL, Somerfield P, Smith R, Clarke KR, Warwick RM, Atkins M, Garnacho E (2006). Ecological consequences of dredged material disposal in the marine environment: A holistic assessment of activities around the England and Wales coastline. Marine Pollution Bulletin 52, 415-426.

Bray RN, Bates AD, Land JM (1996). Dredging and the Environment. In: Dredging: A Handbook for Engineers, Elsevier, 371-387.

Cacchione DA, Wiberg PL, Lynch JF, Irish JD, Traykovski P (1999). Estimates of suspended-sediment flux and bedform activity on the inner portion of the Eel continental shelf. Marine Geology 154, 83-97.
Collins M (1990). The behaviour of cohesive and non-cohesive sediments. In: Alzieu C, Galenne B (Eds.), Proc. Int. Seminar Environment. Asp. Dredging Act. Port Autonome de Nantes Saint-Nazaire, Nantes, pp. 15–32.
Degraer S, Verfaillie E, Willems W, Adriaens E, Vincx M, Van Lancker V (2008). Habitat suitability modelling as a mapping tool for macrobenthic communities: An example from the Belgian part of the North Sea. Continental Shelf Research 28, 369-379.
Delefortrie G, Vantorre M, Eloot K (2005). Modelling navigation in muddy areas through captive model tests. Journal of Marine Science and Technology 10, 188-202.
De Nijs MAJ, Winterwerp J, Pietrzak JD (2009). On harbour siltation in fresh-salt water mixing region. Continental Shelf Research 29, 175-193.
Devlin M, Bets M, Haynes D (2007). Implementation of the Water Framework Directive in European marine waters. Marine Pollution Bulletin 55, 1-2.
Dobrynin M, Gayer G, Pleskachevsky A, Günther G (2010). Effect of waves and currents on the dynamics and seasonal variations of suspended particulate matter in the North Sea. Journal of Marine Systems 82, 1-20.
Du Four I, Van Lancker V (2008). Changes of sedimentological patterns and morphological features due to the disposal of dredge spoil and the regeneration after cessation of the disposal activities. Marine Geology 25, 15-29.
Fettweis M, Sas M (1999). On the sedimentation of mud in access channels to the harbour of Antwerp. PIANC Bulletin 101, 53-59.
Fettweis M, Nechad B, Van den Eynde D (2007). An estimate of the suspended particulate matter (SPM) transport in the southern North Sea using SeaWiFS images, in situ measurements and numerical model results. Continental Shelf Research 27, 1568-1583.
Fettweis M, Francken F, Van den Eynde D, Verwaest T, Janssens J, Van Lancker V (2010). Storm influence on SPM concentrations in a coastal turbidity maximum area with high anthropogenic impact (southern North Sea). Continental Shelf Research 30, 1417-1427.
Fettweis M, Nechad B (2010). Evaluation of *in situ* and remote sensing sampling methods for SPM concentrations, Belgian continental shelf (southern North Sea). Ocean Dynamics 61, 157-171.
Fredette TJ, French GT (2004). Understanding the physical and environmental consequences of dredged material disposal: history in New England and current perspectives. Marine Pollution Bulletin 49, 93-102.
Gallacher PC, Hogan PJ (1998). Hydrodynamical dispersion of dredged materials sequestered on the abyssal seafloor. Journal of Marine Systems 14, 305–318.
Green MO, Vincent CE, McCave IN, Dickson RR, Rees JM, Pearson ND (1995). Storm sediment transport: observations from the British North Sea shelf. Continental Shelf Research 15, 889-912.
Harris CK, Wiberg PL (2002). Across-shelf sediment transport: Interaction between suspended sediment and bed sediment. Journal of Geophysical Research 107 (C1) 8-1, 8-12.
Hill AS, Veale LO, Pennington D, Whyte SG, Brand AR, Hartnoll RG (1999). Changes in Irish Sea benthos: possible effects of 40 years of dredging. Estuarine, Coastal and Shelf Science 48, 739-750.
Hossain S, Eyre BD, McKee LJ (2004). Impacts of dredging on dry season suspended sediment concentration in the Brisbane River estuary, Queensland, Australia. Estuarine Coastal Shelf Science 61, 539–545.
Lauwaert B, Bekaert K, Berteloot M, De Backer A, Derweduwen J, Dujardin A, Fettweis M, Hillewaert H, Hoffman S, Hostens K, Ides S, Janssens J, Martens C, Michielsen T, Parmentier K, Van Hoey G, Verwaest T (2009). Synthesis report on the effects of dredged material disposal on the marine environment (licensing period 2008-2009). MUMM, ILVO, CD, aMT, WL report BL/2009/01, 73 pp.

Lee D-I, Eom K-H, Kim G-Y, Baeck G-W (2010). Scoping the effective marine environmental assessment of dredging and ocean disposal of coastal sediments in Korea. Marine Policy 34, 1082-1092.
Le Hir P, Monbet Y, Orvain F (2007). Sediment erodability in sediment transport modelling: can we account for biota effects? Continental Shelf Research 27, 1116–1142.
Li Y, Mehta AJ (2000). Fluid mud in the wave-dominated environment revisited. In: McAnally WH, Mehta AJ (Eds.), Coastal and Estuarine Fine Sediment Dynamics. Proceedings Marine Science 3, 79–93.
Lohrer AM, Wetz JJ (2003). Dredging-induced nutrient release from sediments to the water column in a southeastern saltmarsh tidal creek. Marine Pollution Bulletin 46, 1156-1163.
Maa P-Y, Mehta AJ (1987). Mud erosion by waves: a laboratory study. Continental Shelf Research 7, 1269–1284.
McAnally WH, Friedrichs C, Hamilton D, Hayter EJ, Shrestha P, Rodriguez H, Sheremet A, Teeter A (2007). Management of fluid mud in estuaries, bays, and lakes. Present state of understanding on character and behavior. Journal of Hydraulic Engineering 133, 9-22.
McCandliss RR, Jones SE, Hearn MR, Latter RJ, Jago CF (2002). Dynamics of suspended particles in coastal waters (southern North Sea) during a spring bloom. Journal of Sea Research 47, 285-302.
Murray JMH, Meadows A, Meadows PS (2002). Biogeochemical implications of microscale interactions between sediment geotechnics and marine benthos: A review. Geomorphology 47, 15-30.
Nichols MM (1988). Consequences of dredging. In: Kjerfve B (Ed.), Hydrodynamics of Estuaries. CRC Press, Florida, 89–99.
Nechad B, Ruddick K, Park Y (2010). Calibration and validation of a generic multisensor algoritm for mapping of total suspended matter in turbid waters. Remote Sensing of Environment 114, 854-866.
O'Connor TP (1999). A wider look at the risk of ocean disposal of dredged matter. Marine Pollution Bulletin 38, 760-761.
Okada T, Larcombe P, Mason C (2009). Estimating the spatial distribution of dredged material disposed of at sea using particle-size distributions and metal concentrations. Marine Pollution Bulletin 58, 1164-1177.
Orpin AR, Ridd PV, Thomas S, Anthony KRN, Marshall P, Oliver J (2004). Natural turbidity variability and weather forecasts in risk management of anthropogenic sediment discharge near sensitive environments. Marine Pollution Bulletin 49, 602-612.
OSPAR (2008). Assessment of the environmental impact of dredging for navigational purposes, OSPAR Commission, Publication nr 366/2008, 17 pp.
PIANC (2008). Minimising harbour siltation, Report No 102, 75 pp.
Powilleit M, Kleine J, Leuchs H (2006). Impacts of dredged material disposal on a shallow, sublittoral macrofauna community in Mecklenburg Bay (western Baltic Sea). Marine Pollution Bulletin 52, 386-396.
Sanford LP (2008). Modeling a dynamically varying mixed sediment bed with erosion, deposition, bioturbation, consolidation, and armoring. Computers & Geosciences 34, 1263-1283.
Schoellhamer DA (2002). Variability of suspended-sediment concentration at tidal to annual time scales in San Francisco Bay, USA. Continental Shelf Research 22, 1857–1866.
Shi JZ, Gu W-J, Wang D-Z (2008). Wind wave-forced fine sediment erosion during slack water periods in Hangzhou Bay, China. Environmental Geology 55, 629-638.
Siegel H, Gerth M, Heene T, Ohde T, Rüss D, Kraft H (2009). Hydrography, currents and distribution of suspendedmatter during a dumping experiment in the western Baltic Sea at a site near Warnemünde. Journal of Marine Systems 75, 397-408.

Simonini R, Ansaloni I, Cavallini F, Graziosi F, Iotti M, Massamba N'Siala G, Mauri M, Montanari G, Preti M, Prevedelli D (2005). Effects of long-term dumping of harbor-dredged material on macrozoobenthos at four disposal sites along the Emilia-Romagna coast (Northern Adriatic Sea, Italy). Marine Pollution Bulletin 50, 1595-1605.

Smith SDA, Rule MD (2001). The effects of dredge-spoil dumping on a shallow water soft-sediment community in the Solitary Islands Marine Park, NSW, Australia. Marine Pollution Bulletin 42, 1040-1048.

Soulsby R (1997). Dynamics of marine sands. Thomas Telford Publications, London. 249 pp.

Traykovski P, Wiberg PL, Geyer WR (2007). Observations and modeling of wave-supported sediment gravity flows on the Po prodelta and comparison to prior observations from the Eel shelf. Continental Shelf Research 27, 375-399.

Truitt CL (1988). Dredged material behaviour during open water disposal. Journal of Coastal Research 4, 389–397.

Van den Eynde D (2004). Interpretation of tracer experiments with fine-grained dredging material at the Belgian Continental Shelf by the use of numerical models. Journal of Marine Systems 48, 171-189.

Van Hoey G, Hostens K, Parmentier K, Robbens J, Bekaert K, De Backer A, Derweduwen J, Devriese L, Hillewaert H, Hoffman S, Pecceu E, Vandendriessche S, Wittoeck J (2009). Biological and chemical effects of the disposal of dredged material in the Belgian Part of the North Sea (period 2007-2008). ILVO-report, Ostend (Belgium), pp. 97.

van Kessel T, Kranenburg C (1998). Wave-induced liquefaction and flow of subaqueous mud layers. Coastal Engineering 34, 109–127.

Van Maren DS, Winterwerp JC, Sas M, Vanlede J (2009). The effect of dock length on harbour siltation. Continental Shelf Research 29, 1410-1425.

Velasco DW, Huhta CA. Experimental verification of acoustic Doppler velocimeter (ADV) performance in fine-grained, high sediment concentration fluids. Application Note SonTek/YSI.

Velegrakis AF, Gao S, Lafite R, Dupont JP, Huault MF, Nash LA, Collins MB (1997). Re-suspension and advection processes affecting suspended particulate matter concentrations in the central English Channel. Journal of Sea Research 38, 17-34.

Verlaan PAJ, Spanhoff R (2000). Massive sedimentation events at the mouth of the Rotterdam waterway. Journal of Coastal Research 16, 458-469.

Ware S, Bolam SG, Rees HL (2010). Impact and recovery associated with the deposition of capital dredging at UK disposal sites: Lessons for future licensing and monitoring. Marine Pollution Bulletin 60, 79-90.

Winterwerp JC (2005). Reducing harbour siltation I: Methodology. Journal of Waterway, Port, Coastal and Ocean Engineering 131, 258–266.

Wu J, Liu JT, Shen H, Zhang S (2006). Dispersion of disposed dredged slurry in the meso-tidal Changjiang (Yangtze River) Estuary. Estuarine Coastal Shelf Sciences 70, 663-672.

Synthesis - new insights in the dynamics of sediment suspensions, associated with the coastal turbidity maximum, Belgian-Dutch coastal zone

A synthesis and discussion are provided on the understanding of suspended particulate matter (SPM) dynamics in the Belgian-Dutch nearshore zone. A coastal turbidity maximum (CTM) characterizes this area; still different processes control its dynamics. A particular phenomenon is the formation of high-concentrated mud suspensions (HCMS), impacting on near-bed processes.

Main questions are:

(1) What is the temporal variability of SPM concentration within the CTM zone?

(2) What is the spatial variability of the extent of the CTM zone?

(3) When and how are HCMSs formed? What is there influence on near-bed processes?

(4) Can acoustic and optical sensors be used to estimate the composition of SPM, especially in case of mixed (sand-mud) sediments?

(5) Can anthropogenically-induced changes in SPM concentration, due to e.g. disposal activities, be distinguished from the natural variability?

These five questions are addressed in four topics. A first topic relates to the natural SPM dynamics in the CTM zone. A second topic is on the formation of HCMS, with a focus on near-bed processes. A third topic is on the mixed-sediment environment in the CTM zone, and the implications on optical and acoustic measurements of turbidity. Finally, in a fourth topic, SPM concentrations and HCMS layers are proposed as indicators of environmental changes.

8.1. Natural variability of sediment suspensions

In the Belgium-Dutch coastal zone high SPM concentrations occur that are highly variable in time. The natural variability is related to overall SPM dynamics (re-suspension, settling), as well as to CTM-associated processes (advection), both acting on different time-scales:

- Intra-tidal (tides)
- Sub-tidal (meteorological, spring-neap, seasonal)
- Long-term climatic influence (NAO)

The knowledge of these processes is critical to understand the CTM system, to reveal natural trends, and to distinguish those from turbidity increases, induced by human-related activities. Long-term observations are available in the vicinity of Zeebrugge harbour allowing investigation of this variability. It is well-known that advection of water masses influences physical parameters such as salinity and SPM concentration in front of the Belgian coast (e.g. Lacroix et al. 2004). Both parameters are proxies for describing the horizontal distribution of different water masses as was shown in Baeye et al. (2011) (Chapter 2), Fettweis et al. (2010), and Chapter 4.
The marine waters from the English Channel that enter the North Sea through the Dover Strait have high salinity (>34) and generally low SPM concentrations. The coastal zone includes the region of freshwater influence from the Scheldt river (and Rhine-Meuse), which is characterized by lower salinity (28-32) and high SPM concentrations. These water masses can be advected under the influence of wind and tides. Therefore our data showed that high SPM concentrations are often more closely related to advection (Velegrakis et al. 1997, Blewett and Huntley 1998), rather than to instantaneous bed shear stress (Stanev et al. 2009). On a longer term, 2 periods, i.e. a high turbidity (late fall until early spring) and a low turbidity period (late spring until early fall) can be distinguished, corresponding to high-energy seasons (more storm activity) and low-energy periods (less storm activity). Other processes (water temperature and biological activity, river runoff and sediment load) are correlated with seasons, but they are of minor importance. Group-averaging procedures and entropy

analysis (statistical treatment) were used taking into account classification parameters that incorporate variability induced by:

- subtidal flow direction and strength;
- alongshore and cross-shore wind components (local wind field);
- North Atlantic Oscillation Index (NAOwi) (contrasting winters); and
- storminess (linked to winds with north component)

All 4 parameters are related to the wind climate, but correspond to different time-scales. Regarding the first 2 parameters, two cases are considered, based on differences in advection (northeast- against southwest-ward alongshore flow regime). Briefly, one can state that the northeast-ward flow corresponds to sustaining southwest winds, resulting in an overall decreased SPM concentration background. Further, major southwest wind events re-suspend bottom sediments (combined wave and current interaction) showing peaks in SPM concentration. Under these hydrodynamic conditions, in-situ re-suspension of mixed sediments (cohesive sediments and fine sands) can occur, and the CTM is extended more towards the Dutch coastal zone (entropy based analysis of MODIS-Aqua derived SPM maps in Chapter 3). The southwest-ward flow regime, typically under winds blowing from the N to NE sectors, tends to decrease the spatial extent of the CTM, but increases the SPM concentration. Here, it was observed that the advective sediment flux is the major process. The role of the Westerscheldt river on SPM input is considered as minor, since freshwater outflow is low (Fettweis et al. 2007a). Several authors have suggested that the estuary acts as a temporary sink of fine-grained (marine) sediments, rather than being a significant source of fine-grained (fluvial) sediments (Terwindt 1977, Van Alphen 1990, Verlaan and Spanhoff 2000). Arndt et al. (2011) studied the Westerscheldt estuary freshwater plume dynamics; they concluded that during prevailing winds with north component (SW-ward flow regime) the fresher water region extends maximal towards the SW; whereas under sustained SW winds the plume is much reduced, and retreated in the estuary. The synoptic SPM concentration maps regarding the two regimes are thus not linked to the observed freshwater Scheldt river 'plume'. In addition, the CTM zone extent under the SW ward flow regime is not connected with the Scheldt river mouth. Therefore, the CTM is not a typical river plume system, but is rather governed by the local hydrodynamics along the coast.
The storminess affecting the study area is also an important contributor for sediment re-suspension (Fettweis et al. 2010). Storminess is related to the NAO index which explains most of the variability in wind climate during December to March (NAO winter index = NAOwi Hurrell (1995)) providing the following synthesis:

- Sustained negative phases in the winter index are generally associated with dry and calm weather, with observations of weaker and more variable winds; and
- Positive phases: wetter, stormier weather over Europe, with increased abundance of southwesterly winds.

Variation in the NAOwi index (- or +) can be a proxy to explain the variation in the spatial distribution of SPM along the coast. In chapter 3, it was found that the influence of contrasting NAO conditions during two winters has a striking effect on the spatial extension of the CTM zone. Further, the storminess in the North Sea will also result in the development of high waves travelling from the North (large fetch). These waves are energetic, and will easily stir up bottom sediments. These meteorological events are the most extreme conditions for the Belgian-Dutch coastal zone, with a maximal CTM spreading and SPM concentrations (see Chapter 4).
Over the last decades, trend analyses of wind directions show an increase of southwesterly winds (Siegismund and Schrum 2001, Van den Eynde et al. 2011) in the southern North Sea. The geographical extension of the CTM during the last decades was thus more often spreading towards the mouth of the Westerscheldt estuary/Dutch waters as before, with a buffering of SPM into the river system (e.g. Terwindt 1977).

8.2. *HCMS appearances in the coastal turbidity maximum*

Direct evidence of high-concentrated mud suspensions (HCMS) was found in bottom samples. However, this study allowed identifying HCMS in the coastal turbidity maximum, through a combination of different instrumentation:

- optically (Optical Backscatter Sensor (OBS), Burial Recording Mine (BRM))
- acoustically (Acoustic Doppler Velocimeter (ADV), Acoustic Doppler Profilers (ADP))

The water column is typically characterized by high near-bed SPM concentrations decreasing towards the sea surface. Evidence derived from OBS points to the existence of HCMS. This study showed that the optical-based BRM is also able to measure HCMS. With nowadays acoustic instrumentation bottom detection routines have become available that are able to track bed evolution. Good bottom boundaries, such as hard bottoms (sand, concrete), generate well-defined peaks, in contrast to HCMS or fluid mud providing gradual transitions in their density gradient. Still, it is possible that a layer of higher concentration sediment is developing and triggers the peak-finding routine (pers. communication Velasco). In Chapter 2, it was suggested that a strong vertical sediment-induced density gradient acts as an acoustic reflector associated to the presence of HCMS. The generation of very high SPM concentrations near the bed implies that significant amounts of fine-grained sediments have to be re-suspended and/or eroded (see Chapters 3, 4 and 6). Spatial variability in the extension of the CTM zone, as well as in the SPM concentration, controls the extension, formation and the duration of HCMS occurrence. HCMS are related to different time-scales:

1. random events, such as storms;
2. low-energy conditions (e.g. neap tides; overall weak (land) wind conditions (typically <0.1 N m^{-2}); and
3. slack water phases

Waves may fluidize and erode cohesive mud beds (Maa and Mehta 1987, De Wit and Kranenburg 1997, Li and Mehta 2000, Silva-Jacinto and Le Hir 2001). In the Belgian nearshore area, it was found that during or after a storm, the SPM concentration increases significantly and HCMS are formed (evidence from OBS on benthic tripod).
HCMS types 2 and 3 differ from each other in terms of the duration of the HCMS occurrence (days vs. hours); HCMS layers formed during neap tides tend to last several days and are called semi-permanent HCMS layers in Chapter 2. In the much smaller time window of slack waters, transient or rapid HCMS may occur if SPM concentration is sufficiently high. The latter is typically associated with settling and re-suspension cycles occurring on a quarter-diurnal time scale. The characteristics of the near-bed current ellipse will determine the time of settling and re-suspension. In the nearshore area (CTM zone), the tidal ellipses are elongated, with more pronounced slack waters. The circular ellipses, typically occurring offshore, have less pronounced slack water phases. The altimetry of the ADV was configured to measure the vertical variations in seabed level, used to detect deposition and re-suspension of fine-grained sediments, and more specifically the presence of HCMS. Often a failure of the bottom boundary detection of the ADV was observed, that was explained by attenuation of the acoustic signal due to too high SPM concentration. Therefore the total attenuation of the signal or the failure of the bottom detection in the ADV indicates HCMS occurrence. In Fig. 8.1, time-series of ADV 5 MHz attenuated signal of bed detection is correlated with wind data, tidal range and current velocities. This particular time-series comprises the different types of HCMS favouring conditions, and corresponds in 52% of the time to the occurrence of HCMS. At about day 308, a HCMS occurred associated with a southwesterly storm. During neap tide, around days 300-306, a long-term HCMS layer (~fluid mud) was perceived under sustained southerly, weak winds (eventually backing to easterly winds and weak northern winds). During this period, the ADV currents measurements failed, as also the measuring volume was situated in the HCMS, which was at least 20 cm thick (20 cm corresponds to the distance of the

measuring volume of the ADV above the bed). Short-term slack water HCMS occurrences are observed throughout the first 6 days.
Table 8.1 lists up the percentage of time that the ADV failed in sensing the bottom for all benthic tripod moorings (at sites nearby the harbour of Zeebrugge - BLA and MOW1). HCMSs were present about 10% of the time at both mooring stations. Further, HCMS layers occurred throughout the year. When seasonality of the SPM concentration time-series is considered, HCMS layers occur in about 12 % of the time during the high-energy season, and in about 5 % during the low-energy season. The latter indicates the highly reduced SPM availability under those conditions, as also the lack of storm periods.
HCMS formation may be responsible for fast and massive siltation of the navigation channels, the access channel to the port of Zeebrugge (Pas van het Zand), and the port of Zeebrugge itself. Massive siltation is often observed during or after storm events. Indeed, soft mud deposits may be re-suspended from the navigation channels during stormy periods (see Chapter 4, Fettweis et al. 2009, 2010). This release of fine-grained sediments contributes to the formation of HCMS layers in the adjacent areas and to massive siltation after the storm in the dredging areas. The measurements carried out in the framework of an alternative disposal of dredged material practice revealed another HCMS formation (Chapter 7). The disposal of mud caused a long-term and significant increase in SPM concentration in the benthic layer. Evidence from ADV boundary detection (at least 32% of the mooring period) strengthens the idea of HCMS layers formed during the disposal of mud.
HCMS processes have an influence on object and mine burial applications (Chapter 6). From the test mine burial experiment, conducted at a site at the offshore edge of the CTM zone, a cyclic burial signal was found that was associated with HCMS formation during slack tide (1-2 hours). The study suggested that longer-term burial of the object by HCMS may occur, depending on the location (or local hydrodynamics). Hydrodynamic modelling has shown that most of the CTM zone is considered as a risk area for periodic mine burial by HCMS layers (Legrand et al. 2011).

8.3. *Cohesive and non-cohesive sediment dynamics in the CTM zone*

8.3.1. *Combined-use of acoustic and optical instruments*

A suite of optical and acoustic sensors, mounted on various platforms (tripod, bottom-mounted), was used to study sediment processes in the coastal turbidity maximum zone. By combining all available data sets, it was possible to improve the understanding of the behaviour of cohesive and non-cohesive sediments and their dynamics, and to monitor the occurrence of HCMS layers. It is suggested that cohesive and non-cohesive SPM dynamics may occur simultaneously in the study area under storm and enhanced flood phase conditions. Consequently, particle fraction separation, due to differential settling, may lead to an alternation of sand and mud layers. Indeed, seabed cores showed often that thin sand layers overtop Holocene mud layers, but also that HCMS or fluid mud layers occur on top of sand layers. This has implications towards erosion, as shown by e.g. van Ledden et al. (2004) and Le Hir et al. (2007).
Storm-induced waves, and associated sediment mobilization, lead to deposition of sand-dominated layers (storm deposits). As a result, the sand layer may act as a reservoir for fine-grained material (Chapter 2). On the other hand, HCMS may also protect the sand from being eroded in the CTM zone, due to inverse armouring. The particle size distribution (PSD) of the SPM is discussed in Chapters 2, 4 and 5. Different classification techniques (entropy, group-averaging) revealed a distinct (multi-modal) behaviour in PSD during tide-dominated and major wind (or storm) conditions. Particle size class spectra are dominated by micro-flocs with a rising tail in the lower size classes during maximum flood currents, suggesting partial disruption of micro-flocs into primary particles. Surprisingly, in the case of sustained winds (or storm-induced winds) blowing from the southwest (typically associated with increased wave action, and most abundant wind sector for the study area), it was found that the Laser In-Situ Scatter- and Transmissometer (LISST-100), or in-situ particle sizer, revealed the absence of primary particles. Particle size distributions were log-normal and shifted towards the silt to fine sand range. The OBS-3 systematically showed reduced SPM concentrations under these conditions, whereas increased SPM

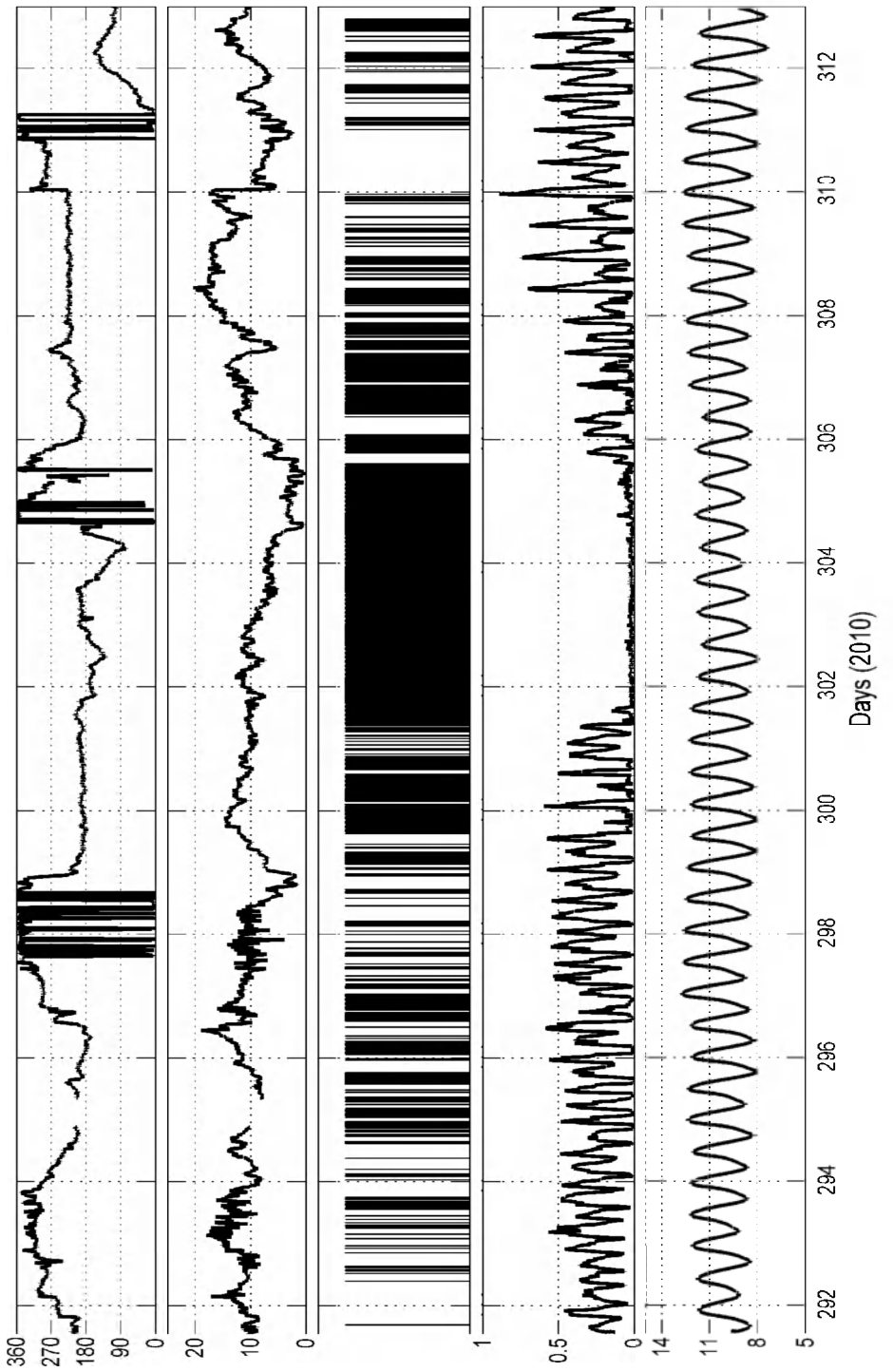

Figure 8.1 *Time-series of wind direction (meteorological convention, °), wind strength (m s^{-1}), ADV failures in detecting the seabed (= HCMS appearances), ADV currents (m s^{-1}), water depth (m- MLLWS), from* ***top*** *to* ***bottom*** *respectively*

Table 8.1 *(**left**) MOW1 moorings with percentage of time with expected HCMS occurrence, and (**right**) BLA moorings*

deployment start	deployment end	% of Time Failed Bottom Detection
07/02/05	08/02/05	6%
04/04/05	15/04/05	23%
22/06/05	12/07/05	14%
22/11/05	05/12/05	28%
13/02/06	27/02/06	7%
15/05/06	15/06/06	29%
10/07/07	19/07/07	2%
17/11/08	12/12/08	29%
09/02/09	19/03/09	24%
26/03/09	29/04/09	4%
06/11/09	08/12/09	9%
11/12/09	25/01/10	22%
25/01/10	25/03/10	16%
25/03/10	20/05/10	9%
20/05/10	23/07/10	6%
18/10/10	17/11/10	52%
17/11/10	15/12/10	27%
15/12/10	11/01/11	27%
31/01/11	21/03/11	23%

deployment start	deployment end	% of Time Failed Bottom Detection
08/11/07	15/12/07	20%
28/01/08	24/02/08	8%
06/03/08	08/04/08	20%
15/04/08	05/06/08	7%
04/05/09	15/06/09	32%

concentrations were derived from the ADP. These results are compared to independent observations from the LISST-100, revealing a shift in the particle size spectrum towards the sand fraction. Optical and acoustic sensors are indeed sensitive to changes in the particle size distribution (Thorne et al. 1991, Lynch 1997, Hamilton et al. 1998, Creed et al. 2001, Fugate and Friedrichs 2002, Voulgaris and Meyers 2004, Downing 2006). Generally, acoustic back-scatterance is more sensitive for larger solid particles than the OBS. The sensitivity of the instruments (OBS-3, ADCP) for different particle sizes was investigated. First results are presented in Chapter 4 where, the corrected backscatter, derived from the bottom-mounted ADCP, was correlated with the LISST. It was found that particle sizes, ranging between 40 and 100 µm, are most accurately measured by the ADCP. This is in agreement with the theory indicating that acoustic signals are most sensitive for $ka \sim 1$, k being the frequency of the acoustic signal and a the particle diameter (e.g. Lynch et al. 1997). A similar analysis was performed by comparing the OBS-3 output voltage to the different particle sizes measured by the LISST-100 (Fig. 8.2). A maximum (R^2 >0.90) is obtained for the particle sizes 25 to 80 µm, but decreases significantly for sizes larger than 80 µm. Subsequently, three individual size classes of the LISST are plotted against OBS-3 voltage and remarkably, the higher size classes correspond readily to 2-phase response curves (i.e. two different volume concentration population curve) (Fig. 8.3). This also explains the decrease in correlation degree, and pleads for cohesive sediment dynamics. Flocculation will lead to increasing volume concentration of the flocs. On the other hand, the lower curve (less steep slope) agrees with the presence of fine-grained material (fine sands) that is in suspension at 2 mab. Acoustics better estimate mass concentration since it is insensitive to density and size of flocs (Gibbs and Wolanski 1992, Bunt et al. 1999, Fugate and Friedrichs 2002, Hatcher et al. 2011). The acoustic backscatter-concentration is based on the mass concentration of the smaller constituent primary particles.

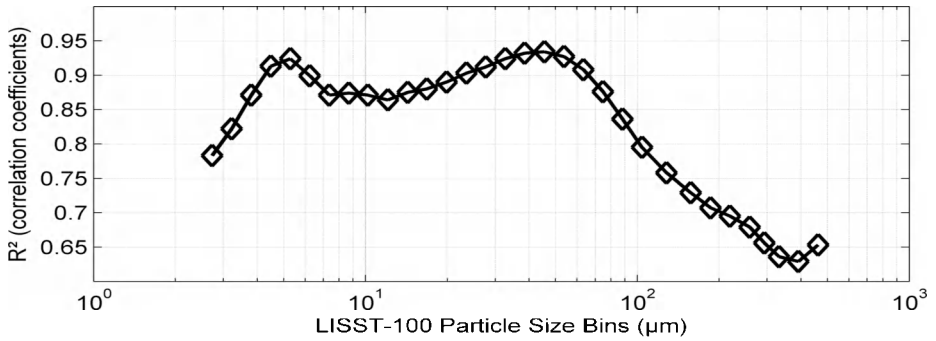

Figure 8.2 *Correlation between OBS output voltage and LISST volume concentration for each particle size class (total of 32 classes, ranging between 2.5 and 500 µm)*

8.3.2. Conceptual nearshore sediment transport

An extract from a spring-neap cycle time-series has been selected to show the different situations that are representative for the processes occurring in the CTM zone (Fig. 8.4). Most of the findings described above and in previous chapters are briefly schematized regarding SPM behaviour (concentration and nature) and HCMS occurrences:

Event I (day 28-30) & **V** (day 37-42): coastal waters; low energetic conditions (wind speeds < 10 ms^{-1}); spring tidal excursion (see large salinity and transmission oscillations); cycles of ebb floc formation and flood floc breakup; wide multi-modal particle size spectrum (or multiple particle size populations); slack water HCMS; long ebb phase allowing cohesive particles to floc together up to sizes of 500 µm.

Event II (day 30-31): more oceanic water input (increase in salinity); strong south-westerly winds; fine sands and decrease in (total) volume concentration (sand has higher density); decrease in the OBS-3 response; increase in acoustic backscatter; increased uni-modal particle size distribution (note that the particle size distribution is measured 2 mab); vertical segregation in the sand fraction; the higher in the water column the smaller the sand particles; absence of cohesive sediments; flocs are broken, and transported away from the measuring locations by wind-induced flows (SW winds).

Event III (day 32-33): storm event (winds with north component); increased SPM concentration; fine sands in suspension (since cohesive sediments were broken up and largely transported towards the northeast during event II); the cohesive sediment layer becomes exposed and fluidized as HCMS.

Event IV (day 33-36): medium energetic conditions (wind speeds ~10ms^{-1}); neap tidal signal in the cohesive SPM dynamics is less pronounced; post-storm HCMS formation during neap tide (day 34).

8.4. SPM concentration and HCMSs as indicators to detect environmental changes

Environmental changes are often inferred from changes in benthic communities (Dauer et al. 2000, Dauvin et al. 2007). SPM may be a driver of such change since it carries a major part of the food resources, though high concentrations may interfere with species filtering and respiratory systems (Rodriguez-Palma 2011). However, SPM concentration is known for its high spatial and temporal variability. Hence, it remains utmost challenging to distinguish naturally- from anthropogenically-induced disturbances. From long-term change analysis of the spatial distribution and relative abundance of macrobenthic species within the Belgian part of the North Sea, SPM was

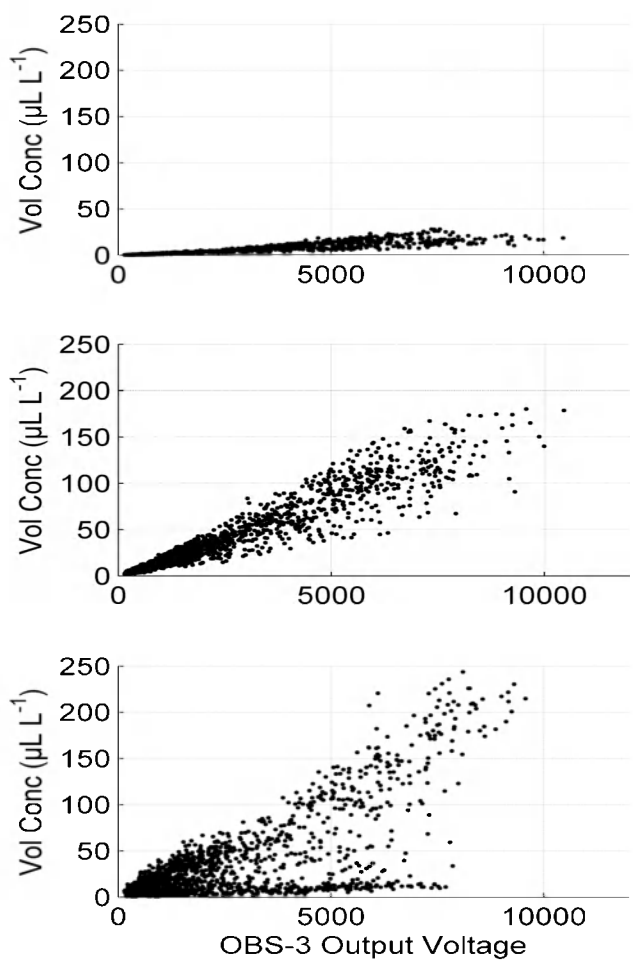

Figure 8.3 *Scatter plots for three different LISST-100 bins and OBS output signal; from* ***top*** *to* ***bottom*** *~5 µm, ~45 µm, ~150 µm, respectively*

indeed hypothesized as being a main driver of environmental change (Van Lancker et al. 2011). Comparing the periods 1899-1908 and 1994-2008, it was shown that bivalves, tolerant to higher mud contents, expanded, whilst bivalves typically thriving in clean sands, reduced significantly in their distribution and relative abundance. These findings agreed well with the suggestion of a human-induced increase of turbidity, which has likely resulted in transient deposition of higher amounts of surficial mud (Fettweis et al. 2009, Houziaux et al. 2011). Macrobenthos analyses pointed also to a higher amount of species contributing more evenly to bivalve species richness, as compared to the historical situation. A probable effect of eutrophication of the area, during the second half of the 20th century was hypothesized, as also the influence of NAO cyclicity. The latter was investigated in relation to the Westerscheldt river discharge, but no significant correlation could be found (Van Lancker et al. 2011).

The human-induced increase in turbidity was attributed mainly to increasing port and dredging works altering the fine-grained sediment dynamics (Fettweis et al., 2009). However, data, presented in chapter 3, suggest also that the CTM zone has become more significant (i.e. increased spatial extension and SPM concentration), due to an increasing frequency of occurrence of SW winds (Van den Eynde et al. 2011). As such, human-induced changes in SPM concentration are further influenced by changes in natural conditions.

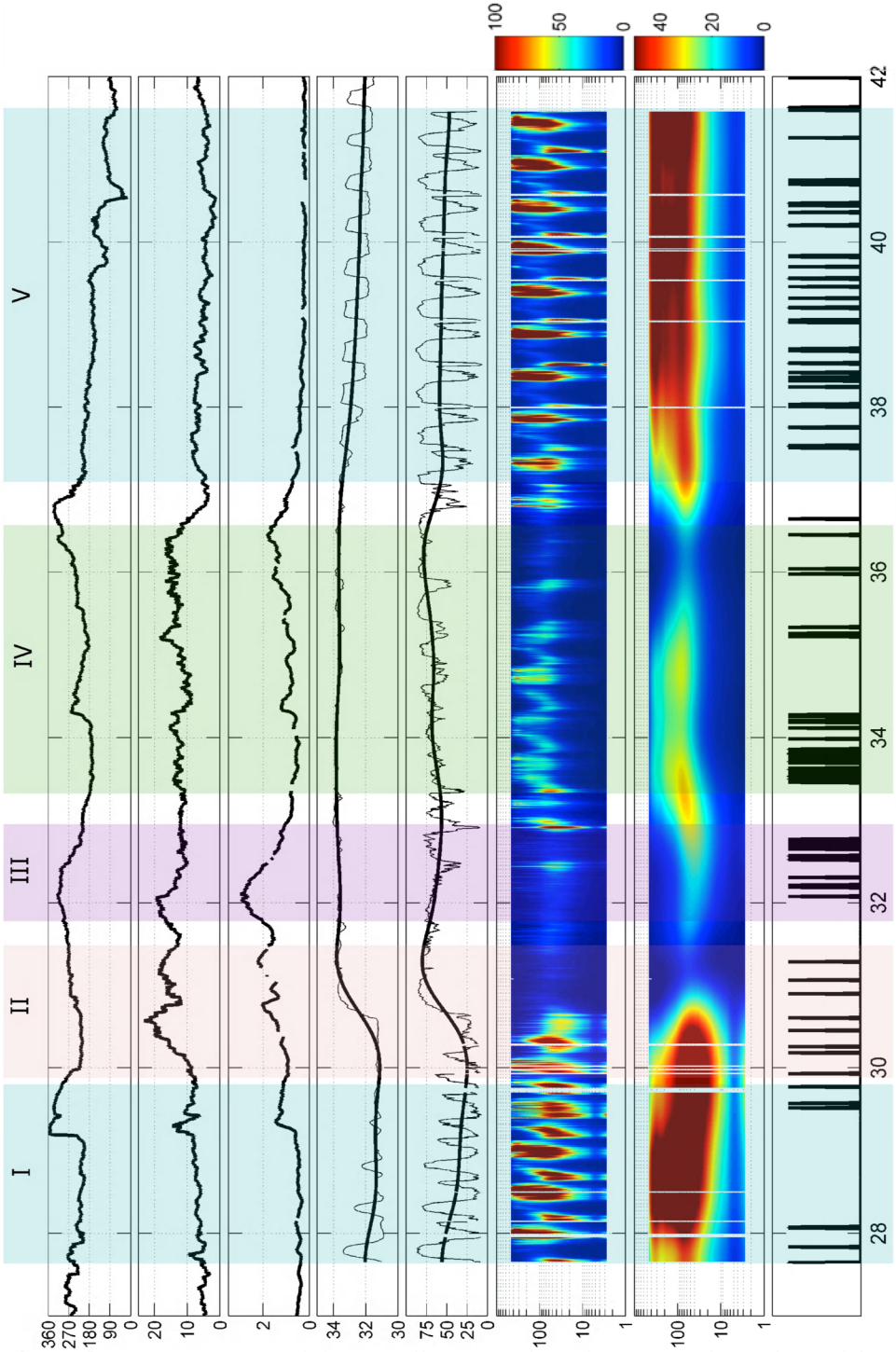

Figure 8.4 *Time-series: wind direction (°, meteorological convention), wind speed (m s^{-1}), wave height (m), salinity (PSU), LISST-100 turbidity (in %), LISST-100 particle size distribution (PSD) (in µL L^{-1}), low-pass filtered LISST-100 PSD (in µL L^{-1}), ADV-derived HCMS occurrences (spikes)*

For assessing natural from human-induced variability in SPM concentration (e.g. dredging-disposal activities for harbour accessibility or marine aggregate extraction) sufficiently long (monthly basis) time-series of SPM concentration in the CTM zone are needed that cover the highly spatial and temporal variability of the natural SPM concentration. A technique was introduced (Chapter 7) that analysed SPM concentration, at a specific station, as a statistical population. Therefore, the observational time-series (or subsamples) could be considered as subsamples of the total population. Fettweis and Nechad (2011) showed that SPM concentrations are log-normally distributed, and by considering such sub-populations as a log-normal distribution function, conclusions could be drawn concerning the representativeness of the sub-population. Using long-term tripod data, we were able to quantify the effect of disposal activities during a dedicated experiment (Chapter 7) within the CTM zone.
From the previous section, it was observed that salinity (low-pass filtered signal in figure 8.4) and turbidity (low-pass filtered transmission LISST-100) correlated significantly (R^2=0.90). It is therefore suggested that long-term salinity observations may act as a reference of the natural variability. Human-induced episodic influences in the SPM concentration time-series are expected to diverge from the salinity time-series trend line. To evaluate this oceanographic parameter as potential proxy for natural changes, hence linked to water mass distribution only, further research is needed.
In addition to the SPM concentration in the water column, near-bed processes associated with HCMS layers, whether or not related to disposal of dredged material, may also affect the habitat and benthos population. Physical properties of the seabed (such as grain size, porosity ...) characterize the substrate which is known to be a driver of patterns in diversity, function and integrity of benthic communities (Cardoso et al. 2010).
Therefore, it is expected that (massive) siltation (with HCMS layers) of the seabed may result in the presence of more opportunistic species in an area.
In summary, it is recommended to further evaluate SPM concentration and HCMS layers as drivers of habitat and benthos changes. If their importance is confirmed, these aspects should be considered also when optimizing disposal operations of fine-grained material from maintenance dredging and deepening works. If relationships can be established with changes in ecosystem structure and functioning, they have a high potential to become indicators of good environmental status for seafloor integrity within Europe's Marine Strategy Framework Directive (Van Lancker et al. 2011 b, Rice et al. 2012).

8.5. References

Arndt S, Lacroix G, Gypens N, Regnier P, Lancelot C (2011) Nutrient dynamics and phytoplankton development along an estuary-coastal zone continuum: A model study. Journal of Marine Systems 84 (3-4), 49-66.

Blewett J, Huntley DA (1998). Measurement of suspended sediment transport processes in shallow water off the Holderness Coast, UK. Marine Pollution Bulletin 37, 134–143.

Bunt JAC, Larcombe P, Jago CF (1999). Quantifying the response of optical backscatter devices and transmissometers to variations in suspended particulate matter. Continental Shelf Research 19, 1199-1220.

Cardoso AC, Cochrane S, Doerner H, Ferreira JG, Galgani F, Hagebro C, Hanke G, Hoepffner N, Keizer PD, Law R, Olenin S, Piet GJ, Rice J, Rogers SI, Swartenbroux F, Tasker ML, van de Bund W (2010). Scientific support to the European Commission on the Marine Strategy Framework Directive. Management group report, March 2010. Prepared under the Administrative Arrangement between JRC and DG ENV (no 31210 – 2009/2010), the Memorandum of Understanding between the European Commission and ICES managed by DG MARE, and JRC's own institutional funding, 65pp.

Creed EL, Pence AM, Rankin KL (2001). Inter-Comparison of Turbidity and Sediment Concentration Measurement from an ADP, an ABS-3, and a LISST, in: Proceedings of Oceans 2001 MTS/IEEE Conference Proceedings, Honolulu, HI, 2001, (3) 1750-1754.

Dauer DM, Ranasinghe JA, Weisberg SB (2000). Relationships between benthic community condition, water quality, sediment quality, nutrient loads, and land use patterns in Chesapeake Bay. Estuaries 23, 80-96.

Dauvin J-C, Ruellet T, Thiebaut E, Gentil F, Desroy N, Janson A-L, Duhamel S, Jourde J, Simon S (2007). The presence of Melinna palmata (Annelida: Polychaeta) and Ensis directus (Mollusca: Bivalvia) related to sedimentary changes in the Bay of Seine (English Channel, France). Cahiers Biologie Marine 48, 391-401.

de Wit PJ, Kranenburg C (1997). The wave-induced liquefaction of cohesive sediment beds. Estuarine, Coastal and Shelf Science 45, 261-271.

Downing J (2006). Twenty-five years with OBS sensors: The good, the bad and the ugly. Continental Shelf Research 26, 2299-2318.

Fettweis M, Du Four I, Zeelmaeker E, Baeteman C, Francken F, Houziaux J-S, Mathys M, Nechad B, Pison V, Vandenberghe N, Van den Eynde D, Van Lancker V, Wartel S (2007). Mud Origin, Characterisation and Human Activities (MOCHA). Final Scientific Report, D/2007/1191/28. Belgian Science Policy Office, 59 pp.

Fettweis M, Houziaux J-S, Du Four I, Van Lancker V, Baeteman C, Mathys M, Van den Eynde D, Francken F, Wartel S (2009). Long-term influence of maritime access works on the distribution of cohesive sediments: analysis of historical and recent data from the Belgian nearshore area (Southern North Sea) Geo-mar Letters 29(5), 321-330.

Fettweis M, Francken F, Van den Eynde D, Verwaest T, Janssens J, Van Lancker V (2010). Storm influence on SPM concentrations in a coastal turbidity maximum area with high anthropogenic impact (southern North Sea). Continental Shelf Research, 30, 1417-1427.

Fettweis M, Nechad B (2011). Evaluation of in situ and remote sensing sampling methods of SPM concentration, Belgian continental shelf (southern North Sea) *Ocean Dynamics 61(2-3)*, 157-171.

Fettweis M, Houziaux J-S, Du Four I, Van Lancker V, Baeteman C, Mathys M, Van den Eynde D, Francken F, Wartel S (2009). Long-term influence of maritime access works on the distribution of cohesive sediments: analysis of historical and recent data from the Belgian nearshore area (Southern North Sea) Geo-marine Letters 29(5), 321-330

Fugate DC, Friedrichs CT (2002). Determining concentration and fall velocity of estuarine particle populations using ADV, OBS and LISST. Continental Shelf Research 22, 1867-1886.

Gibbs RJ, Wolanski E (1992). The effect of flocs on optical backscattering measurements of suspended material concentration. *Marine Geology* 107, 289-291.

Hatcher A, Hill P, Grant J (2001). Optical backscatter of marine flocs. *Journal of Sea Research* 46, 1-12.

Hamilton LJ, Z Shi, SY Zhang (1998). Acoustic backscatter measurements of estuarine suspended cohesive sediment concentration profiles. Journal of Coastal Research 14, 1213-1224.

Houziaux J-S, Fettweis M, Francken F, Van Lancker V (2011). Historic (1900) seafloor composition in the Belgian-Dutch part of the North Sea: A reconstruction based on calibrated visual sediment descriptions. Continental Shelf Research 31(10), 1043-1056.

Hurrell JW (1995). Decadal Trends in the North Atlantic Oscillation: Regional Temperatures and Precipitation. Science 269, 676-679.

Lacroix G, Ruddick KG, Ozer J, Lancelot C (2004). Modelling the impact of the Scheldt and Rhine/Meuse plumes on the salinity distribution in Belgian waters (southern North Sea). Journal of Sea Research 52, 149-163.

Legrand S, Baeye M, Fettweis M, Van Lancker V (2011). Towards the emergence of dedicated and specific operational oceanographic downstream services: the example of burried objects retrieval. The Future of Operational Oceanography, October 25-27, Hamburg (Germany).

Le Hir P (1997). Fluid and sediment integrated modelling application to fluid mud flows in estuaries. Cohesive Sediments, proc. INTERCOH '94.

Li Y, Mehta AJ (2000). Fluid mud in the wave-dominated environment revisited. In: Coastal and Estuarine Fine Sediment Dynamics. (McAnally WH, Mehta AJ eds.), Proceedings in Marine Science 3, 79-93.

Lynch JF, Gross TF, Sherwood CR, JD Irish, Brumley BH (1997). Acoustical and optical backscatter measurements of sediment transport in the 1988-1989 STRESS experiment Continental shelf research 17 (4), 337-366.

Maa P-Y, Mehta AJ (1987). Mud erosion by waves: a laboratory study. Continental Shelf Research 7, 1269–1284.

Rice J, Arvanitidis C, Borja A, Frid C, Hiddink JG, Krause J, Lorance P, Ragnarsson SÁ, Sköld M, Trabucco B (2012). Indicators for Sea-floor Integrity under the European Marine Strategy Framework Directive. Ecological Indicators 12, 174-184.

Rodriguez-Palma O (2011). The role of suspended particulate matter in the distribution and structure of macrobenthic communities in the Belgian part of the North Sea. MSc Thesis. University Brussels. pp. 56.

Siegismund F, Schrum C (2001). Decadal changes in the wind forcing over the North Sea. Climate Research 18, 39-45.

Silva Jacinto R, Le Hir P (2001). Response of stratified muddy beds to water waves. In: McAnally, W.H., Mehta, A.J. (Eds.), Coastal and Estuarine Fine Sediment Processes, Proceedings in Marine Science 3, 95–108.

Stanev EV, Dobrynin M, Pleskachevsky A, Grayek S, Gunther H (2009). Bed shear stress in the southern North Sea as an important driver for suspended sediment dynamics. Ocean Dynamics 59, 183–194.

Terwindt JHJ (1967). Mud transport in the Dutch Delta area and along the adjacent coastline Journal of Sea Research Netherlands 3 (4) 505-531.

Thorne PD, Vincent CE, Hardcastle PJ, Rehman S, Pearson ND (1991). Measuring suspended sediment concentrations using acoustic backscatter devices. Marine Geology 98, 7-16.

Van Alphen JS (1990). A mud balance for Belgian–Dutch coastal waters between 1969 and 1986. Netherlands Journal of Sea Research 25, 19–30.

Van den Eynde D, De Sutter R, De Smet L, Francken F, Haelters J, Maes F, Malfait E, Ozer J, Polet H, Ponsar S, Reyns J, Van der Biest K, Vanderperren E, Verwaest T, Volckaert A, Willekens M (2011). Evaluation of climate change impacts and adaptation responses for marine activities. Final Report - Draft. Brussels : Belgian Science Policy, pp. 114.

Van Lancker V, Baeye M, Du Four I, Degraer S, Fettweis M, Francken F, Houziaux JS, Luyten P, Van den Eynde D, Devolder M, De Cauwer K, Monbaliu J, Toorman E, Portilla J, Ullman A, Liste Muñoz M, Fernandez L, Komijani H, Verwaest T, Delgado R, De Schutter J, Janssens J, Levy Y, Van lede J, Vincx M, Rabaut M, Vandenberghe H, Zeelmaekers E, Goffin A (2012). QUantification of Erosion/Sedimentation patterns to Trace the natural versus anthropogenic sediment dynamics (QUEST4D). Final Report. Science for Sustainable Development. Brussels: Belgian Science Policy, 97 pp. + Annexes.

Van Lancker V, Houziaux J-S, Fettweis M, Degraer S, Vanaverbeke J, Braeckman U, Rabaut M, Vincx M, Van Hoey G (2011b). MSFD Descriptor 6 on Seafloor Integrity (D6). Status of knowledge and Ways Forward in Belgium. Internal Report Marine Strategy Framework Directive Working Group Belgium, 22 pp.

van Ledden M, van Kesteren WGM, Winterwerp J (2004). A conceptual framework for the erosion behaviour of sand-mud mixtures. Continental Shelf Research 24, 1-11.

Velegrakis AF, Gao S, Lafite R, Dupont JP, Huault MF, Nash LA, Collins MB (1997). Re-suspension and advection processes affecting suspended particulate matter concentrations in the central English Channel. Journal of Sea Research 38, 17–34.

Verlaan PAJ, Spanhoff R (2000). Massive sedimentation events at the mouth of the Rotterdam waterway. Journal of Coastal Research 16, 458-469.

Voulgaris G, Meyers S (2004). Temporal variability of hydrodynamics, sediment concentration and sediment settling velocity in a tidal creek. Continental Shelf Research 24, 1659-1683.

Conclusions and future research perspectives

9.1. *Conclusions*

Data from quasi-continuous multi-sensor benthic measurements increased the knowledge of the natural variability of SPM processes for three stations in the Belgian coastal zone. Together with findings obtained from analysis of surface SPM concentration maps, spatial dynamics of the coastal turbidity maximum (CTM) zone were then captured. Analysis of the different data sets (benthic frame and tripod, satellite and vessel), in combination with hydro-meteorological information, resulted in reaching the following conclusions:

The alongshore flow direction was considered to categorize flow regimes induced by winds. An overall good correlation was found between alongshore winds and flows. It was observed that sustaining winds with a north component (N-NE winds) induce a subtidal flow towards the southwest (towards France). This wind sector accounts for 15% of the time, and its magnitude is on average 7.1 m s^{-1} (± 3.3 m s^{-1}). The opposite subtidal flow regime (towards the Netherlands) is mainly triggered by winds from the west-southwest (23%), and are generally stronger (9.5 ± 4.3 m s^{-1}). A northeast-directed flow regime is characterized by increased salinity and reduced SPM concentration. This is because of the advection of Atlantic waters (through the English Channel and Strait of Dover) co-mingling with the coastal waters in the study area. However, these winds can persist and are strong enough to generate waves (average significant wave height of 0.85 m), resulting in increased combined (wave and current) shear stresses acting on the soft cohesive deposits. In addition, synoptic SPM concentration maps under these meteorological conditions show an extension of the coastal turbidity maximum zone towards the Dutch waters. Also, the freshwater 'plume' of the River Scheldt is influenced by these meteorological conditions. However, in this regime the extension of the plume is limited (although freshwater discharge is high); hence there is no link between the CTM zone and the freshwater plume. The Scheldt river system is known not to generate a classical river (turbidity) plume, as found elsewhere in the southern North Sea (e.g. Humber, Thames, Elbe etc.). Further, transport of marine fine matter into the River Scheldt is expected.
During major west-southwest wind events (or storms), it was observed and concluded that cohesive sediment and the primary particles and flocculi (larger flocs are destroyed) are transported away towards the northeast, and that fine sands dominate the particle size distribution. This has implications towards the used instrumentation: the OBS-3 (optical backscatter sensor) systematically showed reduced SPM concentrations under these conditions; whereas, the acoustic response (from the acoustic Doppler velocimeter) becomes dominant since the instrument-specific properties (e.g. frequency of output signal) are more sensitive to a uni-modal particle size distribution in the coarse silt – fine sand range and to solid particles rather than flocs.

Regarding the southwest-directed flow regime, the coastal waters are less affected by Atlantic waters resulting in lower salinities. Freshwater from the Scheldt (and Rhine-Meuse) is more pushed towards the south. Again, the CTM zone is not linked with the freshwater plume, since the CTM zone is not connected with the river mouth. The CTM zone itself covers now a much smaller area close to the shore. In the CTM zone, it was found that SPM background concentrations are generally higher. It was suggested that a release of fine sediments from the Scheldt River mouth contributes to the turbidity. Multi-modal particle size distributions are observed and are related to the cohesive sediment dynamics, with flocculation and disaggregation processes being more important. Because of these dynamics, the OBS-3 will perform well, since no sands in suspension interfere. Nevertheless, flocculation will affect the optical response in a negative way, and obtained SPM concentrations will be less accurate.
It is concluded that the study area is subdued to different hydrodynamic controls (different flow regimes), which on their turn will affect SPM nature and concentration. The SPM concentration is mainly associated with the advection of water masses, and hence salinity and SPM concentration may be considered as co-variables.

Storminess is mostly present during the high-energy season (winter), and is expressed by the manifestation of gravity waves affecting the shallow study area. Highest waves

occur with winds from the north (+2 m waves). Aforementioned, the northeast-ward flow regime also includes major southwest storm events, and the associated waves have a wave period of about 4 s. It is observed that the northerly winds may generate somewhat longer-period waves, because of the larger fetch (open North Sea). They impact on the seabed significantly, because of the larger wave orbital velocities. As a result, more fine matter is resuspended and the CTM zone extends spatially and witness the highest surface SPM concentrations. It is further suggested that the consolidated cohesive (Holocene) muddy sediments of the large mud plate in the coastal zone, and the soft mud deposits in the navigational channels, are eroded under these meteorological conditions.

More significant alongshore displacement in CTM position towards the Dutch coastal waters is observed in winter months with stronger-than-average southwesterly winds. Winter periods also exist in which southwesterly winds are less abundant, resulting in different spatial patterns of the CTM. The latter is based on the climatological index, North Atlantic Oscillation (winter), even substantially influencing CTM position for longer periods (4 months).
Towards near-bed processes, the study revealed the occurrence and importance of high-concentration mud suspensions (HCMS) layers. These suspensions have concentrations up to a few g l^{-1}. It is concluded that they may correspond to different time-scales:

- intra-tidal (slack tide)
- associated to storm events
- neap tides

The first HCMS type is common in the CTM zone and is observed on a regular basis (quarter-diurnal), especially when current ellipses are elongated; thus with long phases of slack tide (i.e. reduced turbulent energy). The gravitational settling of SPM, out of the water column, on the sea bed is further enhanced by flocculation. The larger the flocs, the faster they will settle. The second type has been observed to occur when wave-induced shear stresses fluidize the cohesive and muddy bed, resulting in HCMS layers. Also, post-storm phases with HCMS layers were observed and were explained by the massive amount of SPM available in the water column. The sediments from the navigation channels contribute to this type of HCMS formation. The last type is associated with reduced turbulent energy conditions under neap tide in which SPM settles down and covers the seabed with HCMS (and eventually fluid mud), until the subsequent spring tide will resuspend it again. Worldwide, HCMS are associated with rapid and massive siltation in harbour basins and navigation channels. As a consequence, intensive dredging-disposal cycles are necessary to ensure the accessibility to the harbours. An experiment of alternative ways of disposal of dredged material included the disposal of mud over the breakwater of Zeebrugge harbour. It has been statistically proven that also the disposal activities induced the formation of HCMS layers, and possibly fluid mud, at some distance away from the disposal site. The statistical method allowed accounting for the complex natural dynamics and showed the need to evaluate human impact quantitatively. Ultimately, SPM concentration can be used as an indicator of environmental changes. Therefore the natural variability must be known fully, pleading for long data series covering consecutive hydro-meteorological conditions. Ultimately, a study on mine burial in the CTM zone revealed the importance of occurrences of HCMS (fluid mud) towards the detection of sea mines or other objects. Optics-based burial-registration mines can be used to detect HCMS layers; this, in combination with acoustics from benthic observatories, opens up new avenues in the research on the behaviour of HCMS. All types of ammunition will potentially (periodically) be buried and exposed cyclically when suspended sediment is abundantly present, regardless of shape, density and orientation. The danger of missing ammunition during tracking surveys is greatest in areas and under circumstances where and when HCMS are relatively persistent. The latter should be monitored and analysed in detail as part of follow-up studies. For Belgium, the highest risk for mine burial is within the CTM zone during neap tides. Burial is then potentially the most prolonged.

9.2. *Future research perspectives*

SPM dynamics in the coastal area including the influence of the Westerschelde estuary:

- Consequences of the (long-term) variations in the spatial extension of the CTM (coastal turbidity maximum) zone should be further completed by targeted analyses, e.g. how is the SPM budget of the Westerscheldt estuary varying with meteorology/climate and freshwater discharge; has the SPM budget of the estuary changed?
- Shorter temporal (several tides) variations in the alongshore position and extent of the CTM, and advection of suspension clouds should be investigated with gradient-wise (alongshore and/or cross-shore) deployment of several identical tripod systems. Also, in relation with the functioning of the Westerscheldt (temporal storage of SPM, and followed by SPM release) this measuring strategy could be considered.
- Organic matter and biological particles (plankton) have a strong influence on flocculation and thus SPM transport. Future research should focus on the interaction of biological and mineralogical induced flocculation and on the effects of variations in organic matter concentration due to e.g. algae bloom on the SPM dynamics. Is deposition of SPM enhanced during these periods of high organic matter concentration and what is their influence on the carbon cycle? What and how have algae blooms, which are caused by eutrophication of coastal waters from human activities, changed the SPM dynamics and thus the ecosystem?
- Up to know, the HCMS and fluid mud dynamics were investigated in a few locations, however density of these layers could not be assessed with the instrumentation used. The mapping of the geographical extension and of the occurrence of HCMS or fluid mud layers along the Belgian coast (CTM) will provide information on the SPM dynamics in the area. This is especially of importance to understand the siltation of navigation channels and harbours as a function of environmental and meteorological conditions; and will allow improving measures to reduce dredging volumes. The mapping could be carried out using free-fall penetrating density probe. During tidal cycles, the penetrometer measurements could also reveal how fluid mud (or HCMS) built up and erodes in relation to the local hydrodynamics. The measurements may further reveal the density of the different mud suspensions/layers allowing to estimate the concentration of the suspensions and thus to calculate which part of the total SPM transport occurs in the benthic layer.
- Further studies on object/mine burial by HCMS/fluid mud should include simultaneous benthic tripod measurements together with research (BRM) mines. Then, multivariate statistical approaches must be considered and following parameters must then be integrated: tidal range, wind speed and direction, subtidal flow strength and direction, wave boundary layer, salinity, and flocculation in order to identify and predict burial as a function of various parameters.
- Towards anthropogenic activities such as disposal of dredged mud (and associated suspended sediment plumes), field campaigns should be organized with hull-mounted ADCP transects measurements nearby or across the disposal site(s). This data must evaluate and support the existing modelling results on the dispersal/dispersion of the disposed sediments (sediment plume).

Improving measurement techniques and accuracy:

- Standardized methods for the processing of acoustic and optical backscatter signals should be developed. The latter is requested to formulate sound conclusions on long-term changes in SPM concentration and composition at a single location, collected by the emerging coastal or sea observatories.
- Towards accuracy of OBS sensors, it is further suggested to deploy OBS sensors that are calibrated in different ranges, since significant changes in suspended concentrations occur in the CTM zone. This will allow better

estimating sediment fluxes during future deployments. Or calibrate directly from OBS signal (voltages) to SPM concentration in order to achieve an improved standard error in SPM concentration conversions.

- Varying particle size spectra and their influence on measurements of turbidity (OBS, AD(C)P) are often related to flocculation processes but are also linked to the mineralogical characteristics. It is suggested that a combination of different sensors (optics, acoustics, particle sizer) is necessary in order to understand the nature of suspensions. Dependent on system frequency, range in particle size for optimal detection by the sensor must be further studied (e.g. two-phase diagrams obtained from correlation study with particle size data and acoustic backscatter).
- Measurements in laboratory and in-situ are required in order to define acoustically the top of sediment suspension layers (i.e. lutoclines related to fluid mud or HCMS layers) as a function of the acoustic frequency of the instrument and the composition of the SPM/HCMS. The in-situ measurements can be carried out using e.g. free-fall penetrating density sensors.
- A combination of different measuring techniques, such as hull-mounted ADCP together with ferry-box data (e.g. the AUMS system on board of the R/V Belgica) collected while the vessel is navigating, will result in extended data sets that have been proven to be useful in other areas.